# Security Strategies In Wireless Sensor Networks

James Robert Harbin

PhD

University of York

Electronics

September 2011

# Abstract

This thesis explores security issues in wireless sensor networks (WSNs), and network-layer countermeasures to threats involving routing metrics. Before WSNs can mature to the point of being integrated into daily infrastructure, it is vital that the sensor network technologies involved become sufficiently mature and robust against malicious attack to be trustworthy.

Although cryptographic approaches and dedicated security modules are vital, it is important to employ defence in depth via a suite of approaches. A productive approach is to integrate security awareness into the network-layer delivery mechanisms, such as multihop routing or longer-range physical layer approaches. An ideal approach would be workable within realistic channel conditions, impose no complexity for additional control packets or sentry packets, while being fully distributed and scalable.

A novel routing protocol is presented (disturbance-based routing) which attempts to avoid wormholes via their static and dynamic topology properties. Simulation results demonstrate its avoidance performance advantages in a variety of topologies. A reputation-based routing approach is introduced, drawing insights from reinforcement learning, which retains routing decisions from an earlier stabilisation phase. Results again demonstrate favourable avoidance properties at a reduced energy cost.

Distributed beamforming is explored at the system level, with an architecture provided allowing it to support data delivery in a predominantly multihop routing topology. The vulnerability of beamforming data transmission to jamming attacks is considered analytically and via simulation, and contrasted with multihop routing. A cross-layer approach (physical reputation-based routing) which feeds physical-layer information into the reputation-based routing algorithm is presented, permitting candidate routes that make use of the best beamforming relays to be discovered.

Finally, consideration is given to further work on how cognitive security can save energy by allowing nodes to develop a more efficient awareness of their threat environment.

# Contents

# List of Figures

# List of Tables

# Acknowledgements

Firstly, I am extremely grateful to my supervisor Dr Paul Mitchell for his invaluable contributions and advice throughout my PhD. Dr Dave Pearce also provided considerable support for the early development of my ideas, and I would also like to thank him for his insights too.

I am grateful to everyone in the Group for the interesting intellectual and social environment provided. Dr David Grace provided advice in the production of my transfer report and a productive transfer report viva, and Professor Alister Burr helped with ideas regarding distributed beamforming ideas.

For the friends I made in York over the course of my Masters and PhD, Paul, Sarah, Tom, Jodie, Matthew, Keith, Edgar, Davita and no doubt many others, I am also especially thankful for your companionship.

I must mention again Matthew for being a supportive flatmate and graciously tolerating my excesses during the final stages of producing of the thesis.

Lastly, my family for advice and support throughout the PhD, particularly my mother for her proofreading, my father for his support and advice on structuring this thesis, and my sister for her encouragement.

# Declaration

All work presented in this thesis as original is so, to the best knowledge of the author. References and acknowledgements to other researchers have been given as appropriate.

Some of the research presented in this thesis has resulted in a number of publications, listed in the bibliography: [1] [2] [3] [4].

## List of Publications

Publications produced as a result of the work in this thesis are summarised below:

- J. Harbin, P. Mitchell, and D. Pearce, Security Of Self-Organizing Networks: MANET, WSN, WMN, VANET, ch. 19: ”Secure Routing Architectures Using Cross Layer Information for Attack Avoidance: With Case Study on Wormhole Attacks”, pp. 465-492. Taylor and Francis Group (CRC Press), 1st ed., Dec. 2010.
- J. Harbin, P. Mitchell, and D. Pearce, Wireless sensor network wormhole avoidance using disturbance-based routing schemes in ISWCS 2009: Proceedings of the Sixth International Symposium On Wireless Communication Systems, (Piscataway, NJ, USA), pp. 76-80, IEEE Press, Sept. 2009.
- J. Harbin, P. Mitchell, and D. Pearce, Wireless sensor network wormhole avoidance using reputation-based routing in ISWCS 2010: Seventh International Symposium on Wireless Communication Systems, pp. 521 - 525, Sept. 2010.
- J. Harbin and P. Mitchell, Reputation Routing To Avoid Sybil Attacks In Wireless Sensor Networks Using Distributed Beamforming ISWCS 2011: Eighth International Symposium on Wireless Communication Systems (accepted), Nov. 2011.

# Chapter 1

# Introduction

This thesis provides an introduction to wireless sensor networks (WSNs), their history and potential, previous deployments and engineering issues that concern them, and the security challenges that will have to be overcome before WSNs can be widely deployed. It proposes new low-overhead routing schemes to address their security concerns. The thesis then assesses the use of distributed beamforming, and particularly hybrid routing approaches that can discover the most stable and threat-free beamforming clusters to deliver data in a WSN.

The motivation for work in this area is the existence of a disconnect between the traditional homogeneous multihop routing structure assumed for the canonical WSN, and the more ad-hoc physical layer solutions employed to engineer real-world deployments. As an example, although the literature is normally based around the assumptions of homogeneous nodes of equal hardware capabilities and pure multihop routing, many topologies in real deployments have relied upon relaying mechanisms such as a dedicated backbone link between entities. Therefore, it is worth exploring how clusters of homogeneous nodes can function collaboratively and securely together to form a heterogeneous link, in the context of a multihop network.

Many security solutions for WSNs currently exist as external modules, separate from fundamental functions of the protocol stack. Some rely upon physical-layer features that would be impractical for direct deployment in a realistic network, or impose excessive overheads or computational complexity that would be insufficiently scalable.

Cryptography has been relied upon to protect confidentiality and integrity of message delivery, and authentication of peers to ensure only known devices can participate. However, the limited energy reserves upon nodes reduce the extent to which cryptography (particularly public-key cryptography) can be relied upon to secure WSN systems. Furthermore, it is not possible for cryptographic solutions to guarantee security in the presence of attacks with external devices that modify the topology. Attacks which involve distortions of the topology by external devices, such as the wormhole attack, cannot be prevented by encryption of transmitted data.

This motivates the investigation of security techniques that integrate more closely with the essential data delivery activity of the network, particularly the multihop routing phases that a large network must perform in order to secure data delivery. Focusing on routing away from a region of the network in which actual or anticipated threats exist is a viable mechanism to avoid exposure to threats. It also forms a useful line of defence as part of a defence in depth strategy, adding resilience at the routing level.

## 1.1 Scope

The first goal of the thesis is to explore the performance of novel routing schemes for avoidance of a standard security attack, the wormhole attack. Disturbance-based and reputation-based routing schemes are introduced and analysed. The wormhole attack is interesting for study as it involves an attacker with the advantage of heterogeneity, which in many real-world deployments has often been relied upon by the deployment authority to implement a workable system. The thesis describes these protocols for wormhole avoidance and the intuitions behind their method of operation. It then presents simulation results, demonstrating wormhole avoidance by these routing protocols under realistic scenarios and deployment topologies.

The second goal is to explore distributed beamforming approaches from a systems level, and assess one of their security properties versus multihop routing, specifically their resistance to signal jamming attacks. These distributed beamforming clusters (supernodes) will be considered as an opportunistic support to form final-stage links within a multihop routing network, and the previous techniques for reputation-based routing will be applied to adaptive selection of supernodes with consistent performance.

## 1.2 Thesis Structure

This section illustrates how best the thesis should be read. Figure 1, page 23 gives the structure of the core chapters of the thesis, illustrating any structural dependencies between its different chapters. Material from earlier chapters will be required in order to fully comprehend these chapters.

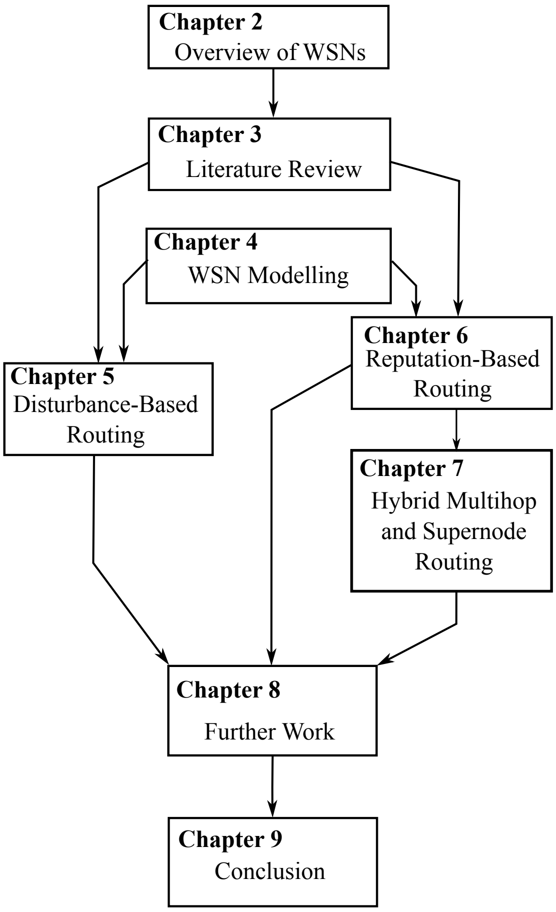

Figure 1: The structure of the thesis

### 1.2.1 Chapter 2

Chapter 2 provides a general overview of wireless sensor networks, and introduces the main engineering challenges they face, such as the importance of energy efficiency, and the potential for cross-layer protocols to improve performance. This is introduced by analysing previous sensor node platforms and deployments, and considering the essential characteristics that separate previous example deployments from typical research cases. This is used to motivate the work performed in the thesis.

### 1.2.2 Chapter 3

Chapter 3 presents a literature review which investigates in detail the security challenges facing wireless sensor networks. It presents motivations for potential attack in different application scenarios. It defines essential fundamental properties of security in a system, together with the specific challenges for security engineering in WSNs. For example, given the energy limitations under which conventional WSNs operate, any individual device introduced by an attacker can often access resources beyond the capabilities of an individual node.

Chapter 3 then presents a taxonomy of common attacks within WSNs, and approaches that the literature has employed to mitigate them. The shortcomings and drawbacks of these approaches for realistic WSN deployments are used to motivate the work in the forthcoming chapters.

### 1.2.3 Chapter 4

Chapter 4 explores a methodology to design protocols and implement practical WSN systems, and motivates simulation as important for the development of new network protocols, resulting from the high costs of deployments and the need for a consistent environment for testing. The simulation environments and specific software used for the production of results within the thesis are analysed and motivated.

The chapter then presents radio communication models that will be presented throughout the thesis in order to perform comparisons of different data transmission methodologies. A distributed beamforming transmission scheme is introduced and an architecture provided for coordinating transmission to the sink from the beamforming supernodes. Finally, standard topologies are specified and their connectivity properties analysed.

### 1.2.4 Chapter 5

Chapter 5 presents an analysis of the wormhole attack and how disturbance-based routing protocols can assist in avoidance of wormhole links. The wormhole attack is one of the most insidious attacks upon WSN systems, allowing an attacker with only a pair of physical devices to gain effective control over a distributed network.

Chapter 5 first classifies wormholes in terms of how they respond to neighbour discovery packets. It then introduces the concept of disturbance-based routing, a novel set of techniques that can provide robust routing in the presence of wormhole attacks. The disturbance-based scheme provides avoidance of wormholes either through their static or dynamic topology properties. Simulation results are presented to demonstrate their effectiveness.

### 1.2.5 Chapter 6

Chapter 6 introduces reputation-based routing, which incorporates techniques from reinforcement learning in order to provide robust avoidance of the wormhole attack. The intuition behind its logarithmic routing metric is explained and the metric equations defined. Simulation results are then presented to show that reputation routing is highly effective in avoiding the wormhole attack in cases in which there exists an early stabilisation period before the wormhole is introduced in the network.

### 1.2.6 Chapter 7

Chapter 7 examines the integration of distributed beamforming into a multihop network to assist multihop routing, with distributed beamforming clusters acting as a final-stage relay to reach the sink node. It extends the reputation-based routing approach employed in Chapter 7 with a cross-layer parameter of received signal-to-interference and noise ratio (SINR). Simulation results are presented to show that this modified physical reputation-based routing can adaptively discover the most secure and stable candidate structures for beamforming to use as the final stage of multihop routing to the sink.

### 1.2.7 Chapter 8

Chapter 8 considers how the techniques considered in the thesis can be integrated for deployment in an environment consisting of uncertain threats. An architecture for cognitive security, in which WSN nodes attempt to understand their security environment and deploy cross-layer countermeasures is motivated and presented. Open research questions for future development of cognitive security architectures are presented.

### 1.2.8 Chapter 9

Chapter 9 concludes the thesis and provides a summary of the issues involved in security engineering, particularly within the energy-constrained domain of WSNs. The criteria for deployment of the particular schemes developed in the thesis are considered. The novel contributions contained within the thesis are summarised and their context within the literature is explained.

# Chapter 2

# Overview of Wireless Sensor Networks

## 2.1 Introduction To Wireless Sensor Networking

A vision is emerging of the convergence of wireless communications, embedded sensing and processing devices with distributed algorithms into the field of wireless sensor networks (WSNs). The proponents of this emerging technology envision a future in which environments from nature reserves to cities are instrumented with disposable computing nodes, each with an onboard radio transceiver, battery, environmental sensors and processing capabilities.

Wireless sensor network research grew out of the distributed sensor networks project at the Defence Advanced Projects Research Agency (DARPA) [5], although the technology of the 1970s limited processing and communications and restricted the nodes to large form factors. With the exponential progress and cost reduction in microprocessing during the 1990s and 2000s, many new applications for WSN deployment emerged. The Amorphous Computing project [6] envisioned highly generic, cheap and indistinguishable miniature devices, operating by analogy to the individual cells of biological systems.

Since then, deployment of wireless sensor networks has been considered for diverse spectrum domains, including logistics [7], medicine [8], environmental monitoring [9] [10], military monitoring [11] and surveillance [12]. Surveys of WSN concepts and technology illustrate the directions taken in the literature [13] [14].

### 2.1.1 Fundamentals of WSN Architecture

The literature typically understands a wireless sensor network to refer to a large number (potentially several hundred or thousand) discrete integrated processing, communication and sensing devices, normally powered from a finite energy source such as a chemical battery and equipped with a radio transceiver for communication. Illustrating the influence of amorphous computing on the direction of the typical WSN, the majority of devices are assumed to be highly homogeneous: generic and broadly interchangeable in their capabilities [6].

These individual devices are known as WSN nodes. In the typical case, one or more privileged communication endpoints exist, known as the sink node(s) or base station(s). The function of sink nodes is to store and process received data, transfer information out of the network, or assist the nodes to organise collaborative behaviour. The sink, given its special role and assumption of wired connection to an outside network, is frequently better resourced in terms of processing and energy than other network nodes.

It is common for practical developments to exhibit a hierarchy of devices [15], some of which have enhanced capabilities [16]. Special capabilities possessed by these devices can include additional energy storage, increased transmission range [17] or data rates, or additional hardware such as global positioning system (GPS) receivers to bootstrap or support localisation protocols [18].

Upon activation, WSN nodes self-organise through execution of network protocols designed to achieve their deployment objectives. As well as their application-specific sensing tasks such as measuring temperature, humidity, or even sampling audio or video data, the network coordination duties of these protocols include:

**Neighbour discovery** To gain awareness of the immediate network environment

**Media access scheduling** To establish how to avoid interference and achieve efficient use of the shared wireless channel

**Time synchronisation** To timestamp received data and for smooth operation of other network protocols

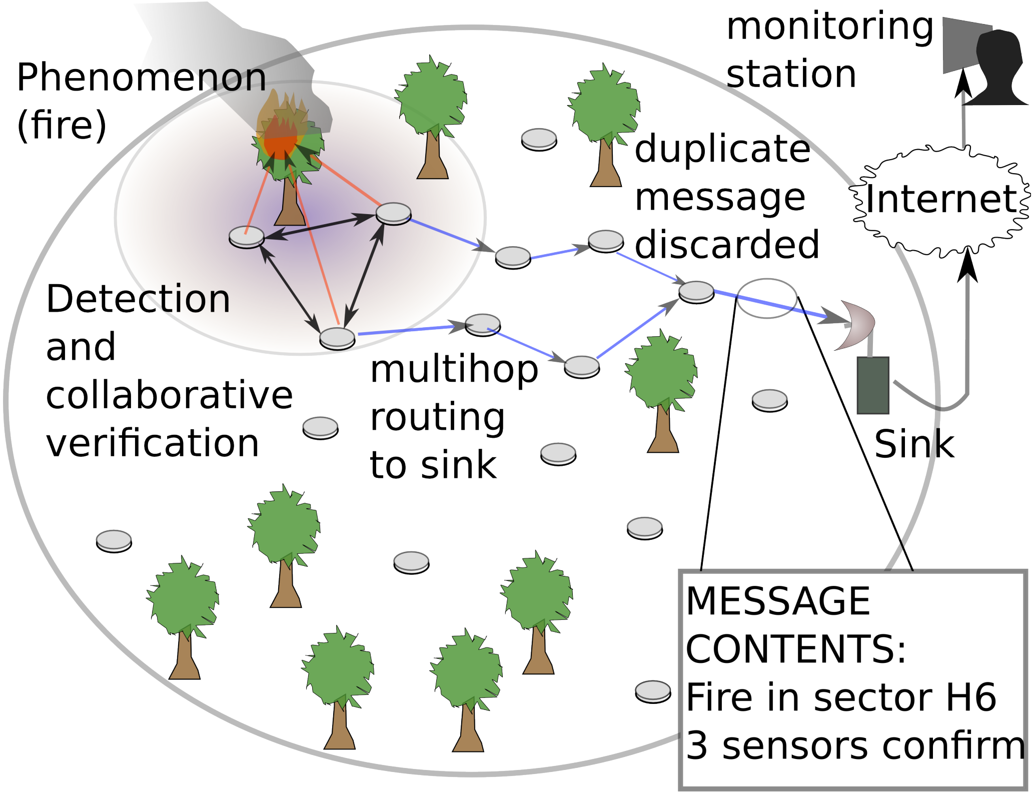

Figure 2: Diagram of a simple WSN, showing the interactions involved in detection of a forest fire

**Localisation** Discovering their geographic positions relative to the sink or to nearby peers

**Data aggregation or preprocessing** To verify sensed reports with peers and potentially combine data to save bandwidth and energy

**Routing** Discovering routes for relaying data through the network towards the sink node

Figure 2, page 29, demonstrates these concepts with a sensor network system giving early warning of a forest fire to a monitoring station. The example demonstrates initial detection of a phenomenon of interest, verification of the detection with multiple sensors, and the construction of multihop routes to relay the data obtained back to the sink node. Upon reaching the sink, the information is relayed out of the network, by mechanisms normally independent of the sensor networking problem domain such as a wired communications channel or out-of-band directional communications link. Human operators at a monitoring station can then arrange a response to extinguish the fire.

### 2.1.2 WSN Hardware Platforms

The previous section provided a general conceptual introduction to wireless sensor networking, and the conventional approach to solving the problems. It is important in a research field to remain creative with protocol design and explore how advanced application scenarios can be enabled through the use of custom hardware. In the meantime, WSN technology is not likely to be cost-effective for mass pervasive deployments. In "Wireless Sensor Networks: Deployments and Design Frameworks" [19], Elena Gaura states:

> "It is clear... that node cost is a constraining factor in many of the case studies presented in this book, showing that, in general, real life deployments are greatly affected by the amount of funds available for a given project."

Exponential progress in transistor density has been recorded through Moore's Law [20], which forecasts a doubling of price-performance at least every 18 months [21]. Although at the limits of raw performance this advantage is likely to face challenges [21]. However, given increased usage of microcontrollers and wireless transceiver technology, mass-production of cheap, almost disposable nodes with capabilities exceeding contemporary devices is likely by the end of the decade.

In this time, it is expected that not only more efficient protocols and deployment methodologies will exist, informed by iterative trials of designs, but that new generations of WSN nodes will offer improved capabilities in the domains of wireless communications (improved flexibility and increased data rates), onboard processing and technology. An example would be the potential for improved stability oscillators to enable groups of nodes to make distributed beamforming transmissions [22]. A surveying of the characteristics of the past and planned WSN hardware platforms will be extremely useful to illustrate trends in the design of future protocols.

#### 2.1.2.1 Hardware Capabilities

Although WSN technology is primarily a research topic and the current generation of nodes are still too expensive to be effectively disposable, it is important to

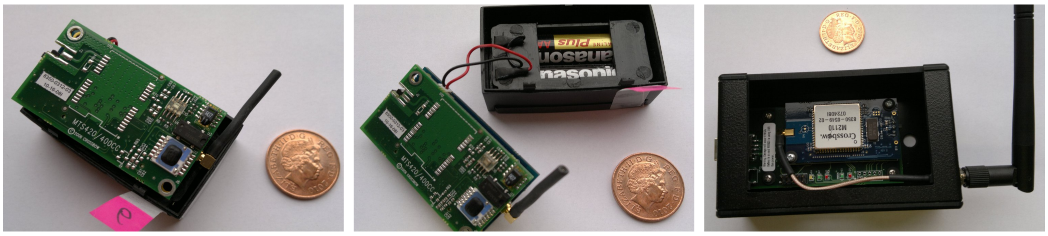

Figure 3: Mica nodes and their associated base station

examine typical features of node platforms. Platforms range from well-tested nodes manufactured on medium scale and used in test deployments over the last decade, current emerging node platforms (Jennic), to ambitious research visions (Smart Dust). A survey of some of these node families follows in order to discover their essential features, similarities and notable trends in the evolution of node hardware.

#### 2.1.2.2 Mica Nodes

The Mica2 (MPR400) [23] and MicaZ (MPR2400) [24] nodes (Figure 3, page 31), manufactured by Crossbow Technologies, are typical third-generation wireless sensor nodes. They are compatible with the open-source TinyOS embedded operating system [25] which provides a component-based protocol implemented in the nesC concurrent extension to the C language.

The Mica2 and MicaZ feature an Atmel ATmega128L 8-bit processor running at 7MHz. The modular design allows external sensor boards to be attached to a main processing and transceiver board, decoupling sensing and allowing application flexibility via the integration of custom sensors to meet specific scenario objectives. Power is supplied via either an external connector or onboard mounting for two AA batteries, which typically provide a current capacity of 2000 mAh, although lithium ion (Li-On) batteries can provide a maximum of 2800mAh. Figure 3, page 31 shows the Mica nodes, with attached battery connector, and an associated base station with power and connectivity to a management computer supplied over Universal Serial Bus (USB). The Chipcon CC1000 transceiver of the Mica2 operates on the 868/915 MHz band. Its data rate of 38.4 kbps provides for messaging applications such as that studied in Section 2.1.1, page 28, and the choice of simple and robust modulation techniques, such as frequency-shift keying (FSK) and on-off keying (OOK), giving good error tolerance and imposing little in terms of synchronisation and channel estimation demands, with consequent power efficiency.

The Chipcon CC2420 radio transceiver of the MicaZ operates on the 2.4 GHz Industrial, Scientific and Medical band, on which users may operate licence-free in the UK. It is compliant with the IEEE 802.15.4 standard [26], and operates at the increased data rate of 250kbps, with more complex modulation scheme of direct sequence spread spectrum (DSSS) with Offset Quaternary Phase-Shift Keying (O-QPSK). The increased data rate enables higher data rates from the end source, enabling continuous reporting scenarios that encroach upon the field of ad-hoc networking.

#### 2.1.2.3 Jennic Nodes

A more recent development in WSN technology is provided by the Jennic nodes from NXP Semiconductor (Figure 4, page 33). The JN5148 nodes provide a richer computing environment than the Mica nodes, with 32-bit RISC processors and 128 kB of RAM and ROM. Specialist physical interfaces also allow significantly more data to be sampled, with a digital audio interface allowing audio sampling for phenomena detection. Peak data rates of up to 500 kbps and 667 kbps [27] allow the potential for transmission of low-rate multimedia data such as audio and (with hardware assistance) video. The protocol environment employed is also focused upon enabling higher-layer solutions, with no direct official support for the de-facto standard TinyOS environment in favour of a custom JenNet suite.

Accordingly, the nodes and associated technologies are typically marketed at system integrator usage, for example, industrial applications, rather than for direct research. The JenNet protocols provide application integrators with custom higher layer abstractions built upon Zigbee. For example, routing is handled automatically via a tree-healing protocol, which implicitly assumes a relatively small and static network (theoretical maximum of 500 nodes with addressing scheme employed) directed by the sink as coordinator. There is also a centralised channel allocation scheme that selects a single channel for the entire network to use. This exemplifies a recent trend for commercial WSN nodes to offer low-configuration applications for logistical control applications. Out of the box, the nodes operate a demonstration application for local temperature monitoring to a base station.

With the Jennic nodes, it is possible to bypass the JenNet protocols and to operate directly upon IEEE 802.15.4 [26], providing significantly increased functionality, such as forming arbitrary mesh topologies and implementing custom MAC and routing protocols. This is important for the ability to implement research protocols upon the nodes.

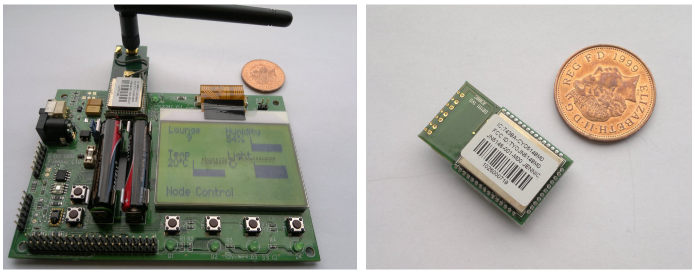

Figure 4: Photographs of the Jennic base station and an individual node

#### 2.1.2.4 Spec Motes - Smart Dust

An ultimate destination for WSN technology is provided by the Smart Dust project. The ambitious vision of Smart Dust is to build WSN concepts on a technology foundation of MEMS (micro-electro-mechanical systems). MEMS [28] postulates physical technologies for communication and power at the millimetre scale and below, allowing the extension of WSNs to encompass ultra-high resolution monitoring. Such approaches could include destructive stress testing of physical systems and industrial prototypes during breakdown, medical and military espionage applications. Figure 5, page 34, reproduced from the Smart Dust project, illustrates a prototype Smart Dust mote with a total volume within 10 cubic millimetres.

### 2.1.3 Importance of Energy Efficiency

Some wireless sensor network concepts have explored ideas for energy gathering from the environment, through mechanisms such as solar cells or piezoelectric charging [29]. However, the power source assumed for WSN devices is conventionally assumed to be a limited resource such as a non-rechargable chemical battery. Furthermore, it is often assumed that the environment for the application scenario is inaccessible or inhospitable, and therefore manual replacement of batteries is not feasible. Therefore, initial energy available at deployment normally limits the lifetime of WSN nodes, mandating the conservation of energy at all levels of the protocol stack where possible.

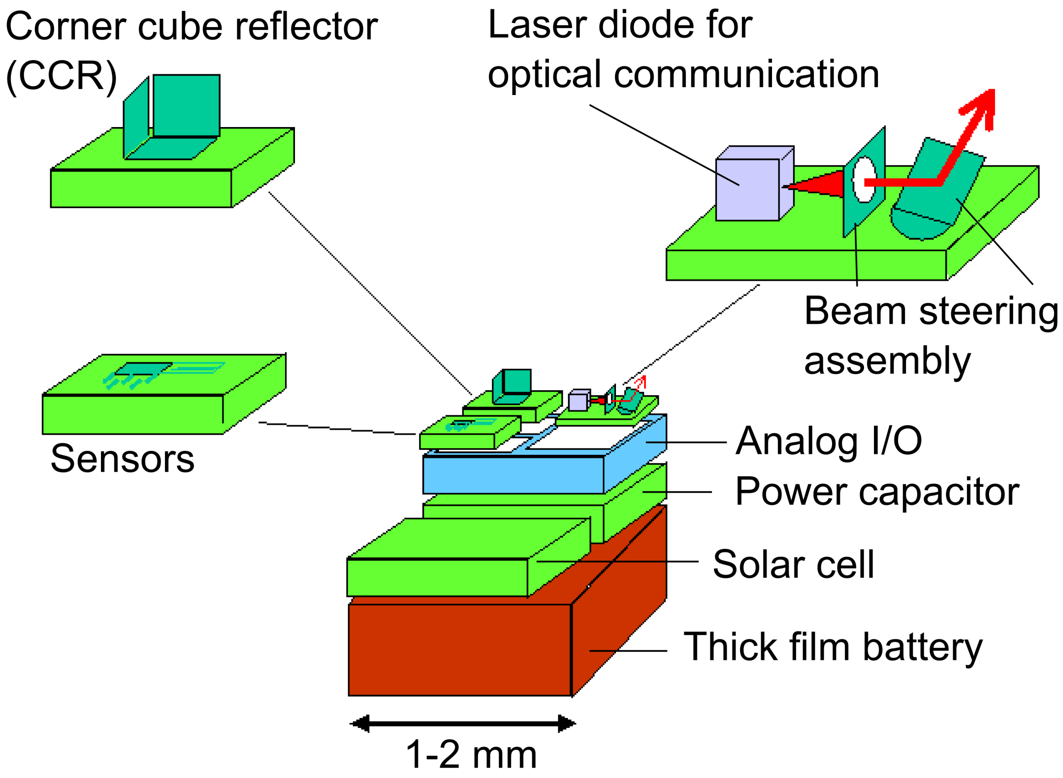

Figure 5: The Spec motes envisaged by the Smart Dust project
Adapted from: `http://robotics.eecs.berkeley.edu/~pister/SmartDust/figures/colormote.gif`

### 2.1.4 Energy Efficiency Via Cross-Layer Techniques

Traditional networking and inter-networking of wired devices developed out of a heterogeneous environment with many classes of devices with completely distinct design philosophies and transport technologies, which were united under a broader construct - specifically, the standardisation process of the layered Open System Interconnection (OSI) model to define network architecture [30], (Figure 6a). This abstraction and division provided scope for researchers and industry to divide and conquer the looming problems of networking research, and much research in emerging fields is still governed by these distinctions today. For example, research into the media access control (MAC) protocols attempts solely to coordinate transmission and reception in such a way as to minimise energy consumption [31].

Header and control information for the network layer would thus be opaque to such protocols, which would treat it merely as passive data to be relayed. In such an approach, it is evident that performance would be sub-optimal, due to the duplication of traffic for the coordination phases of both MAC layer activity and routing. In the development process of traditional wired networking, orthogonality and cleanliness of

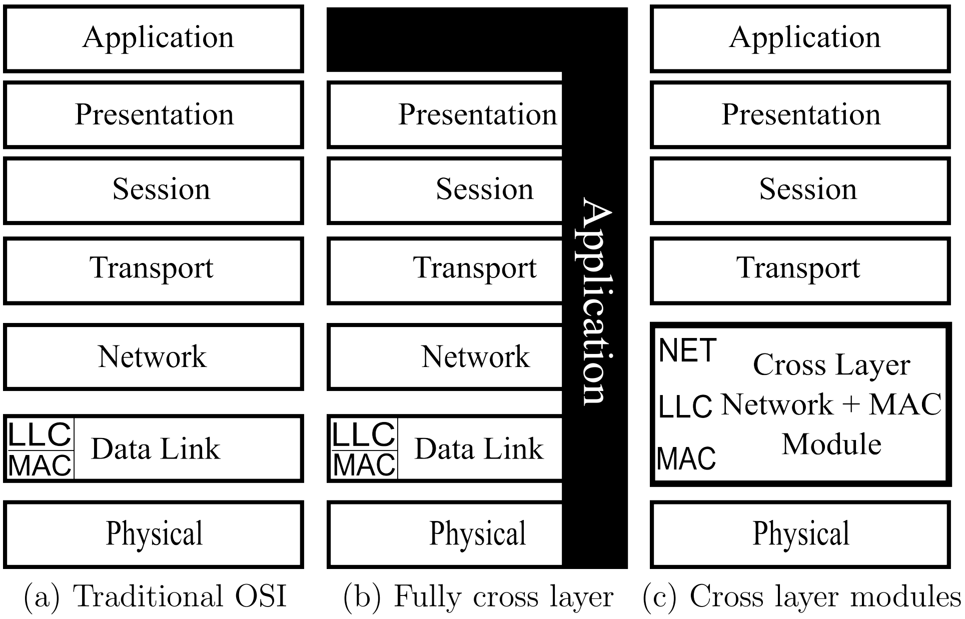

(a) Traditional OSI (b) Fully cross layer (c) Cross layer modules

Figure 6: The traditional OSI model and its variation by the use of cross-layer techniques

the network stack, which permitted component reuse, a heterogeneous market, and long-term stability of standardised interfaces was preferred over theoretical maximal performance.

However, a fundamental difference in the design goals and deployment architecture of WSN technology suggests relaxation of these constraints. WSN systems are normally envisaged to be deployed under a coordinated process by a single end user or system integrator. They are assumed to be subject to energy constraints that do not exist in wired communications where line power is available.

There is a wide variance in the estimation of the energy impact of communication relative to computation. As an example, one study found every bit transmitted has approximately the same energy cost as the execution of 800 instructions [32]. In addition, in a multihop network there exists a relaying burden [33] in which every intermediate node in a multihop routing chain incurs the energy and capacity costs of forwarding a packet towards the sink. These costs will involve the associated transmissions, receptions and retransmissions, in addition to the overheads of route acquisition phases. In a power-constrained environment dependant on chemical batteries, efficiency demands that any opportunity to share information needs to be considered whatever the impact on orthogonality or design purity of the protocol stack.

Therefore, in a sensor network, processing and energy constraints favour some departures from the formal purity of the traditional OSI model [34]. Dispensing entirely with any semblance of abstraction and layering, and allowing an end-user application to solve simultaneously all problems associated with dynamic networking through an ad-hoc application-specific approach (Figure 6b, page 35) would be likely to prove impractical as spiralling complexity would lead to system failures, escalating development costs and ultimately the loss of viability. However, blurring or adjusting the boundaries of the strict protocol stack in specific cases, or combining two adjacent layers into a single one, offers advantages that have begun exploration under cross-layer techniques.

Such cross-layer approaches permit, for example, decisions shared between the MAC and the routing layer (as illustrated in Figure 6c, page 35) to make routing decisions based upon MAC congestion information [35], or speed of response [36]. It is also possible to combine multiple conventional protocol layers into a single module, for example, making MAC and power control adjustments to optimise network-layer parameters such as overall network lifetime [37]. A cross layer approach will be explored in Chapter 7 to make a routing decision to optimise a security goal based on physical layer information.

## 2.2 Motivation For Work

This section presents a motivation for the work through considering characteristics of real deployments and how they relate to the typical WSN case presented in Section 2.1.1, page 28. It is important to give an overview of these since, ultimately, the judgement of a concept is in a proof-of-concept implementation, and surveying real implementations may reveal characteristics that are very instructive for future designs.

### 2.2.1 Practical Network Deployments

WSN deployment trials implemented in real research projects have shown clear differences in their architecture and methodology than the classical case in the literature. In this section the overall vision, hardware and protocols employed during real deployments will be contrasted with the typical case.

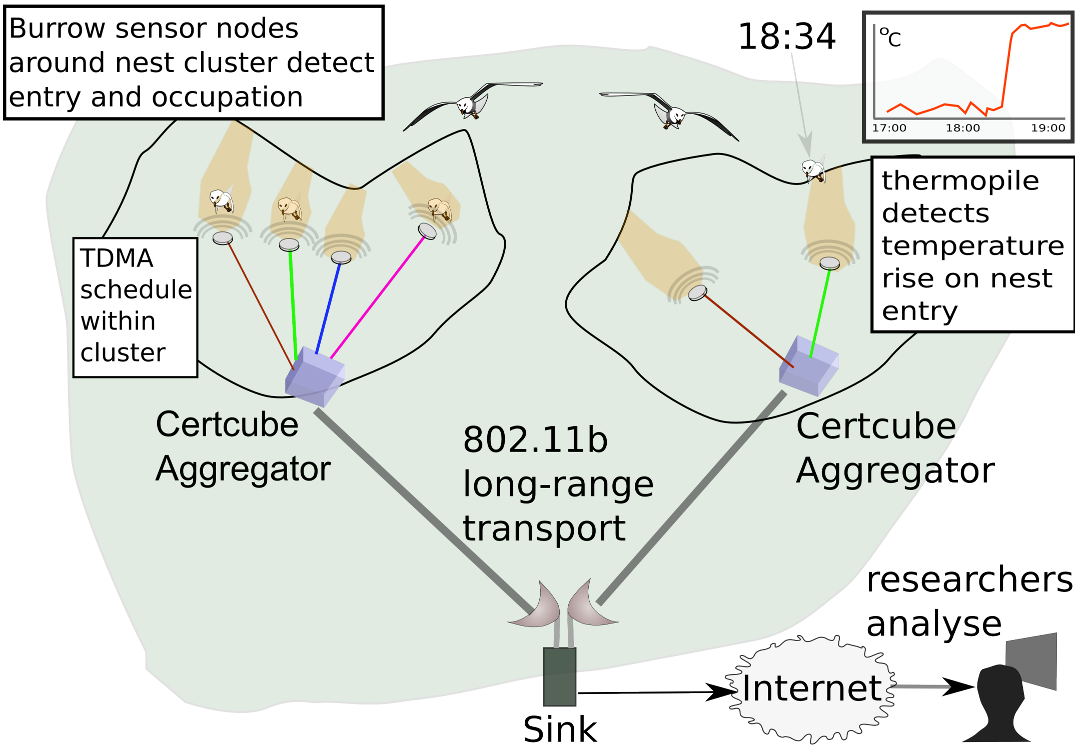
Burrow sensor nodes around nest cluster detect entry and occupation
18:34
°C
17:00
18:00
19:00
thermopile detects temperature rise on nest entry
TDMA schedule within cluster
Certcube Aggregator
802.11b long-range transport
Certcube Aggregator
researchers analyse
Internet
Sink

Figure 7: Diagram of the Great Duck Island scenario, showing clustering of the sensors around nesting sites and relaying from aggregation points

#### 2.2.1.1 Environmental Monitoring - Great Duck Island

The Great Duck Island monitoring project [10] was an early experiment employing WSN technologies to study the behaviour and habitat of a number of Storm Petrel seabirds upon an island off the coast of Maine, USA. Many of its characteristics are still in common use in recent deployments, particularly the use of multiple heterogeneous device classes as opposed to a single participating node.

In the Great Duck Island project, the desire for unobtrusive monitoring motivated the use of WSN technology. Sensors allowed the behaviour of the birds to be studied without human interference, which can lead to nest abandonment and therefore disruption to the ecology under study. Temperature and light sensors upon WSN nodes (deployed manually in advance) obtain data used to infer occupation patterns of bird burrows during the nesting season. The nodes communicated with CertCube aggregation points which buffer and act as central communications relays via wireless Ethernet 802.11b to the Great Duck Island computer and from there to the wider Internet (Figure 7, page 37).

The first major distinction from conventional WSN literature is the small number of nodes deployed (thirty-two), and the explicit heterogeneous hierarchy employed in the project. The depth of the protocol stack was limited; without a requirement for multihop routing algorithms, the main service required is media access control to coordinate transmissions within the range of a single centralised coordinator. The topology was effectively a traditional star and no multihop relaying was used by the end nodes. Instead the network relied upon a small enough number of nodes within direct transmission range of the central coordinator, and the establishment of a time-division multiple access (TDMA) schedule for coordinated transmission. Effectively, in terms of interference behaviour and operation, each monitoring cluster functioned as a separate sensor network.

In this case, the physical structure of the environment and the spatial clustering of the physical phenomena dictated the heterogeneous solution. With a number of closely clustered static phenomena of interest, it was much more cost-effective (in terms of both physical hardware and the attendant debugging and maintenance costs) to cluster sensors around the nests in which the birds would be studied and use heterogeneous links as a relaying backbone. By contrast, blanket coverage of the island with a sparse multihop sensor field would incur greater deployment cost for comparatively little gain in terms of the information delivered.

#### 2.2.1.2 Agricultural Monitoring - Vineyard Monitoring

User requirements of wireless sensor networks in an agricultural case study (specifically, vineyard monitoring) are explored in [38] (Figure 8, page 39). This environment is production-oriented rather than research-oriented: end-users do not have the technical competence or inclination to directly interpret low-level data or log reports, or to debug network connectivity problems. Instead, the network presents aggregate data on irrigation and pest control to operators via centralised graphical interfaces (touchpoints).

The authors also propose to use mobility for data collection, rather than multihop routing. They recommend the use of *data mules*, privileged nodes attached to the workers, to pick up data as they traverse the network. The standard self-organising multihop network deployment is mentioned as a possible solutions for data distribution. However, the standard deployment often assumes a sparse, security-sensitive or otherwise inaccessible terrain, in which the protocol overheads for multihop route formation are inevitable to overcome range limitations of the

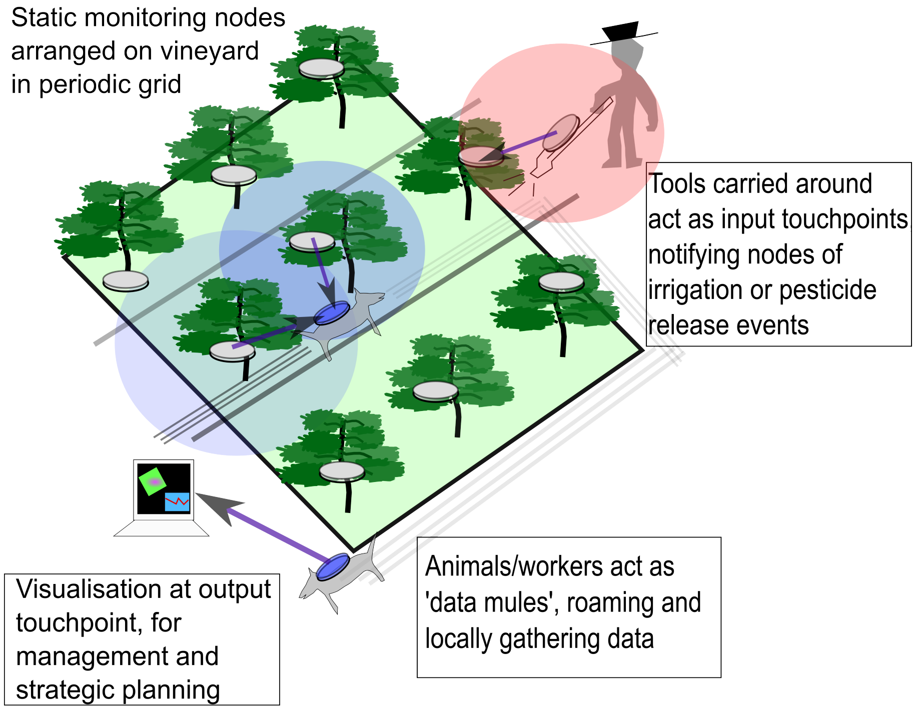
Static monitoring nodes arranged on vineyard in periodic grid
Tools carried around act as input touchpoints notifying nodes of irrigation or pesticide release events
Visualisation at output touchpoint, for management and strategic planning
Animals/workers act as 'data mules', roaming and locally gathering data

Figure 8: A diagram of the vineyard monitoring sensor network scenario

WSN transceivers. Since humans are working within this environment anyway, it is sensible to use their inherent mobility to collect data.

#### 2.2.1.3 Security Monitoring Scenario - ExScal

The DARPA Extreme Scale monitoring project (ExScal) [39] (Figure 9, page 40) demonstrated a large-scale sensor network deployment project closer to the canonical deployment case of nodes monitoring a large terrain, originally envisaged to be extensible to 10 square kilometres. The test deployment was intended for surveillance monitoring of a perimeter and employed 1200 devices to cover a 1km by 300 metre region. Nodes detect the presence of intruders via passive infra-red (PIR).

The project employed heterogeneity for data relaying, with an explicit hierarchy that formed a three tier network, with the sink as the top tier. The lowest and least resourced tier consisted of XSM (eXtreme Scale Motes), devices built around an 8-bit Atmel ATmega128L microcontroller and Chipcon CC1000 transceiver, as in the Mica motes Section 2.1.2.2, page 31. These nodes were supported by a second tier of XSS (eXtreme Scale Stargate) devices, consisting of a 32-bit Linux computer with 802.11 connectivity. The XSS devices have responsibility for managing a local cluster of 20 to 50 XSM nodes.

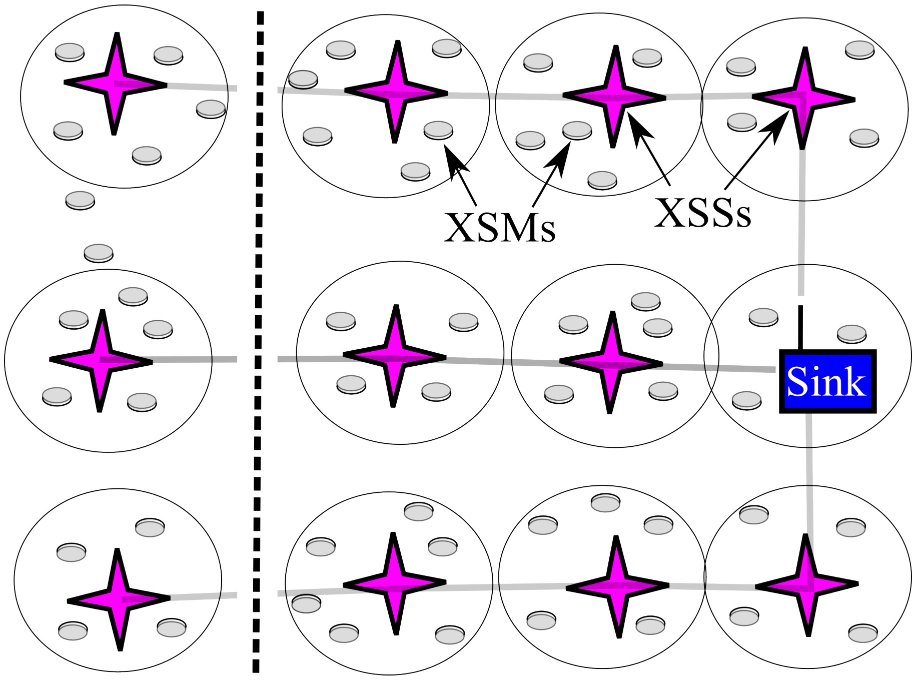

Figure 9: The ExScal monitoring project WSN design involving a three-level hierarchy

At the network layer, a redundant routing protocol is employed, Logical Grid Routing [40] which distributes data upon a grid to potential parents. This protocol was intended to spread traffic across potential parents, in order to cope with observed fluctuations in link performance and per-hop coverage. Therefore the routing layer effectively took upon the task of ensuring reliability at the MAC layer, coping with individual link failures by diversification at the routing protocol.

### 2.2.2 Deployment Versus Theory

It is important to consider the distinctions between the common deployments and the typical case in the literature for protocol design. As in the Great Duck Island and vineyard monitoring case, deployments have frequently involved explicit backbone links or mobile sinks rather than a homogeneous topology with hop-by-hop multihop routing. Privileged devices have been employed with additional hardware such as a GPS receiver.

The node count employed and terrain coverage has been small, with only the ExScal project touching the large deployments originally envisaged for economic reasons. A discrepancy in terms of scale could exist for economic reasons, with current node prices and experimental budgets not permitting a full deployment at the scale envisaged. Alternatively, the large-scale multihop routing design, with its attendant relaying burden, may not be the most efficient way to engineer a workable sensor network.

## 2.3 Importance Of Security

Early on in the development of wired network systems, it was common to assume an inherently friendly security environment, in which users are mutually trusting and without motivation to disrupt or attack systems. This assumption has broken down with the explosive expansion of networks via the Internet, to encompass a wider user community, who are mutually rivalrous with a variety of motivations to compromise security of networked systems.

Before wireless sensor networks can ever become part of widespread infrastructure, carry out tasks such as medical monitoring, or be deployed in aeronautical or avionics environments, it will be necessary to convince stakeholders that they can fulfil their deployment objectives, without suffering failure as a result of malicious attacks. The foundational application for sensor networks is a military network [11], in which as part of the scenario there exist adversaries motivated to destroy communications facilities and subvert network resources.

Even in situations less overtly hostile than a military scenario, motivations to attack and subvert the network may exist. In the ExScal system, intruders may be interested in crossing the monitoring perimeter without detection. In the agricultural monitoring example in Section 2.2.1.2, page 38, competitors or saboteurs could be interested in misrepresenting yields from the vineyard, or falsely signalling failures or pesticide contamination. If nodes are envisioned to be sufficiently generic as to be widely deployed, it must be anticipated that they will be cheap enough to be disposable, and so low-effort attacks against them will potentially become mainstream.

Chapter 3 provides an in-depth analysis of the security environment for wireless sensor networks, giving motivations for attack in common scenarios, a taxonomy of common attacks, responses to them, and a review of countermeasures adopted to these threats in the literature.

## 2.4 Hypothesis

There is a distinction between the canonical case in the literature, which is highly homogeneous, and between many real deployments. As explored, many deployments have relied upon the use of heterogeneous backbones to support a reliable large scale service. It is possible that in future sensor networks, security and performance advantages can be delivered by a combination of physical layer techniques such as distributed beamforming rather than multihop routing. By using distributed beamforming combined with self-organisation, it is possible to gain the advantages of heterogeneity from the self-organising interactions of homogeneous nodes, without requiring the deployment of special hardware in the field, or the manual adjustment of antennas in order to form long-range transmission links.

If a sufficient density of nodes is not available for beamforming to be a universal relaying mechanism, it is possible to use hybrid approaches, which combine multihop forwarding (assisted by adaptive routing algorithms) to assist with the transport of data to reach beamforming clusters. This approach inherently provides the useful fallback position of routing directly to the sink node. The option of using an adaptive protocol which combines multihop routing with beamforming can enhance security.

The hypothesis studied in this thesis is that there is considerable utility in a combination of data relaying approaches, using multihop routing with adaptive algorithms, supported by distributed beamforming as a final stage to provide a secure and dependable WSN. Investigation of the hypothesis will explore how multihop routing can be protected against attacks in which the attacker exploits heterogeneity (the wormhole attack), and how distributed beamforming provides resilience against signal jamming attacks. Finally, all the techniques will be combined to provide an adaptive routing protocol for a multihop network which is also robust against the sybil attack. Then consideration will be given to how system integrators can select the most useful techniques for a particular threat environment.

# Chapter 3

# Literature Review

## 3.1 Security Overview

Security is a key consideration in contemporary network environments. Early in the development of the Internet, protocols implicitly assumed a trusted and altruistic user base who would never attempt to snoop on routed traffic and pick up plaintext passwords, forge a sender address on an incoming email message, or attempt to subvert name services or end hosts. When a network or inter-network serves a single organisation, or small group of academic organisations with a common purpose and interest and united by a common ethic, this may be a workable assumption; when the network is extended into the physical world, including users with rivalrous ideologies and interests, such assumptions become questionable.

Although there may not be rivalry amongst the intended users of a WSN system (those responsible for deployment are usually the end users or an agent for them), there is ample opportunity for external attackers to interfere with traffic sent over inherently insecure multihop channels. In wired networks, external attackers would be required to compromise physical channels, which is likely to reveal their presence. For example, splicing a backbone cable involves visible attachments and potentially traceable impacts upon channel properties and reception. However, in a WSN, the deployment region is frequently sparsely populated, and any arbitrary external device with a transceiver is able to access the wireless channel. This creates vulnerability to malicious attack by external entities, and consequently a risk to system security.

The low-cost nodes envisaged for future deployment (Section 2.1.2, page 30) frequently operate using 8-bit microcontrollers. These nodes are assumed to be poorly resourced and therefore cryptographic approaches must be employed judiciously [41]. It is likely that economics will favour node cost reduction, increasing the scale of networks that can be deployed, over an increase in computation resources on board, particularly where such resource increases would have an inherent energy cost [42].

Therefore, the opportunities for a potential attacker over those present in richly-resourced wired environments are greatly increased, and even seemingly tenuous motives for attack are worthy of serious consideration. This chapter will analyse the security environment of a WSN, giving a taxonomy of common attacks and countermeasures to them. It will then analyse common security solutions and architectures and motivate the further work in the following chapters.

### 3.1.1 Motivations For Attack In Different Application Domains

In order to have an accurate conception of the threat environment, it is important to consider in advance the intentions of potential attackers. Studying the goals and motivations of attackers allows likely attacks to be anticipated and suitable countermeasures prepared. This section considers the different application domains in which a WSN is liable to face attack, analysing the motivations behind each system and how it influences likely patterns of attack.

#### 3.1.1.1 Military Networks

A military network is the key driver for WSN security, and much of the early research on sensor networks was funded by military agencies [5]. Military WSN Research is still ongoing via agencies such as the UK Ministry of Defence (MoD). A recent Competition of Ideas project considered the deployment of WSNs as part of a heterogeneous battlefield support environment [43].

Under their deployment assumptions, military networks are operating in areas in which there already exists an attacker of significant resources (potentially comparable to or greater than the deployment authority) whose direct interest is in disabling assets belonging to the operators. Damage to the network may be incidental, from the destruction of sensor and aggregation elements mounted in various assets, or may result from targeted attempts directed against the network itself.

An attacker confronting a military network could be extremely well-resourced, potentially an opposing army, with sufficient resources to inject targeted interference, examine protocol stacks offline to detect vulnerabilities, and deploy custom equipment to launch attacks, perhaps with equal or greater resources on board than any authorised network nodes.

#### 3.1.1.2 Logistics

WSN systems have been proposed for logistical tracking systems, both for delivery scheduling for customers and for business optimisation. They can also be used to assure regulatory compliance; SecuriFood [44] uses embedded sensors to provide an audit trail ensuring frozen or chilled food has had a sufficient cold chain throughout transit to the final retailer.

Several motivating cases for attack against logistical networks exist. Compromising network entities such as weight stations or consignment trackers could give competitors access to business-critical information. Forging temperature readings could cause food to be discarded unnecessarily, with associated wastage and costs. Although there is common administrative authority, there is a possibility for insider attacks by staff; cloning tracking sensors attached to valuable parcels could allow theft to go undetected for sufficiently long as to allow the perpetrators to escape.

#### 3.1.1.3 Vehicular Networks

WSN concepts have been proposed for integration into cars and roadside systems, as part of Vehicular Ad-Hoc Networks (VANETs) [45]. Potential applications for VANETs include traffic behaviour monitoring, road and congestion charging, and vehicle tracking and recognition.

A variety of motivations for attack against such networks exist. Subverting road charging mechanisms presents a direct financial advantage to attackers, and attempts to clone the identity of other vehicles could be very valuable to those intent upon impersonating others.

#### 3.1.1.4 Environmental Monitoring

Sensor networks have been proposed for a variety of environmental monitoring applications, for example soil quality analysis, or pollution monitoring within oceans, or to protect rare animals in desert terrain [46]. Given the sparse deployment and absence of assets of immediately obvious value, this scenario may appear to be one in which the motivation for attack is questionable.

However, the value of security in such scenarios is determined by economics, frequently depending on costs that may be unclear of intangible. For illustration, consider the case of a polluting company. If compliance with pollution regulations is sufficiently expensive, it may prove cheaper to hire an unscrupulous expert to cleverly deceive a monitoring network than to implement expensive pollution reduction measures.

### 3.1.2 Lessons For WSN Deployment

The lesson for current research on WSNs is therefore one of foresight and caution. It would be premature to deploy sensor networks without a thorough analysis of risks, threat models, and vectors of attack that an adversary may use against them. Failure to deal proactively with this risk may lead to a situation in which the critical infrastructure depends on fundamentally insecure technologies, upon which crippling attack can be easily mounted.

It is unlikely that sensor networks will ever achieve wide penetration if early leading-edge projects show well-publicised vulnerabilities. The more likely scenario is that the development of the sensor network field will be hampered by poor publicity. Attempts to couple the critical infrastructure tightly to speculative network technologies are likely to be met with stiff resistance if early security breaches lead to a loss of user confidence.

## 3.2 Nature of WSN Security

The broad goals of security engineering in the WSN, and indeed in any general communications system, typically involve the provision of a system with some combination of the following key properties [47]:

**Confidentiality** The ability to keep the contents of a message secret and prevent its disclosure

**Integrity** Protecting a message from alteration in transit

**Availability** Ensuring communication services cannot be denied or suppressed by attackers

**Authentication** Ensuring that communications come from the entity that they claim and not a malicious imposter

In a system of richly resourced entities such as a client-server network, security can often afford to be conservative; adopting longer key sizes than expected for future-proofing against cryptanalytic breakthroughs. It is also important to provide resilience via the concept of defence in depth [48]- the layering multiple orthogonal technologies to protect against failure of any individual component. For example, energy-efficient cryptography can be combined with security-sensitive routing that proactively steers traffic away from regions containing a threat, as explored in Chapter 5. A combination of techniques therefore protects against compromise of any one component.

Roman [49] identifies intrinsic security of the nodes, protocols and the communication protocols of the sink as data acquisition security, as distinguished from data dissemination security, which is concerned with the security of the access network and physical terminals on which users access the output data. Although security is limited by its weakest link and this would need to be considered in an end-user deployment, the security of the sink from external compromise is out of the scope of the work considered in this thesis.

In a distributed, energy-constrained system such as a wireless sensor network, security properties need not be universal at the finest levels of granularity. For example, if signal jamming is directed against a proportion of nodes, the implicit redundancy of the distributed system can retain availability of the network itself while tolerating the removal or disruption of a proportion of its elements. There is also the issue of aggregation and the criticality of information for network level objectives. As an example, data aggregation may mean that only some information (for example, final alert conditions) requires the most stringent protection on integrity and confidentiality, and low-level sensor readings from individual nodes may not be sufficiently meaningful to be worth protecting. This illustrates how energy can be saved by focusing resources intelligently on protecting specific entities.

It is important to recognise that perfect security, if it requires availability, is always unattainable in a wireless communication system even if energy and onboard processing were unlimited, as it is always possible to envisage a denial of service threat that defeats system availability. For example, a sufficiently powerful wideband jammer can always completely disable any wireless communications system including a WSN, by merely saturating a system with interference.

Ultimately a more practical goal of a well-designed system is that it continues to fulfil its network-level objectives under the range and severity of attacks assumed in its design specification and threat model. The availability property therefore becomes a level of fault tolerance [50], implying robustness or survivability on the network level. A well-engineered system should deliver graceful degradation in network performance, for example, proportion of data delivered, in proportion to the level of malicious attack launched.

### 3.2.1 Security Assumptions

#### 3.2.1.1 Variations In Capability

In order to analyse security in sensor networks effectively, it is important to consider common assumptions behind the capabilities of the attacker and the trust assumed between network entities. Doing so provides a clearer insight into the attacks and defences that are feasible. This section considers the capabilities of both attackers and defenders, exploring some foundational properties for security in WSNs.

Attackers effectively form a continuum in capabilities (Figure 10, page 49), with variability in the devices they can access to deploy. These malicious devices are considerably distinct in their onboard processing, energy reserves, antennas and transceiver capabilities.

Individual attacking devices thus range from subverted or reprogrammed nodes of the originally deployed network or equivalent platform, to more powerful devices with software radio and more powerful antennas capable of injecting additional jamming.

Ultimately the greatest threat is posed by laptop-class devices with considerably more power and heterogeneous links capable of mounting sophisticated attacks such as the wormhole attack, explored further in Section 3.5, page 56.

The attacking devices with limited range have the potential to be more subtle, only intercepting or influencing one region, but this limits the scope of damage that can be caused. To achieve wider disruption, such attacks generally have to concentrate higher up the protocol stack, for example, attempting to influence routing to get other nodes to unwittingly assist the attack. Alternatively, it is anticipated that a sophisticated attacker could deploy more individual devices, or perhaps employ remote reprogramming to compromise and change the function of a portion of network nodes. [51].

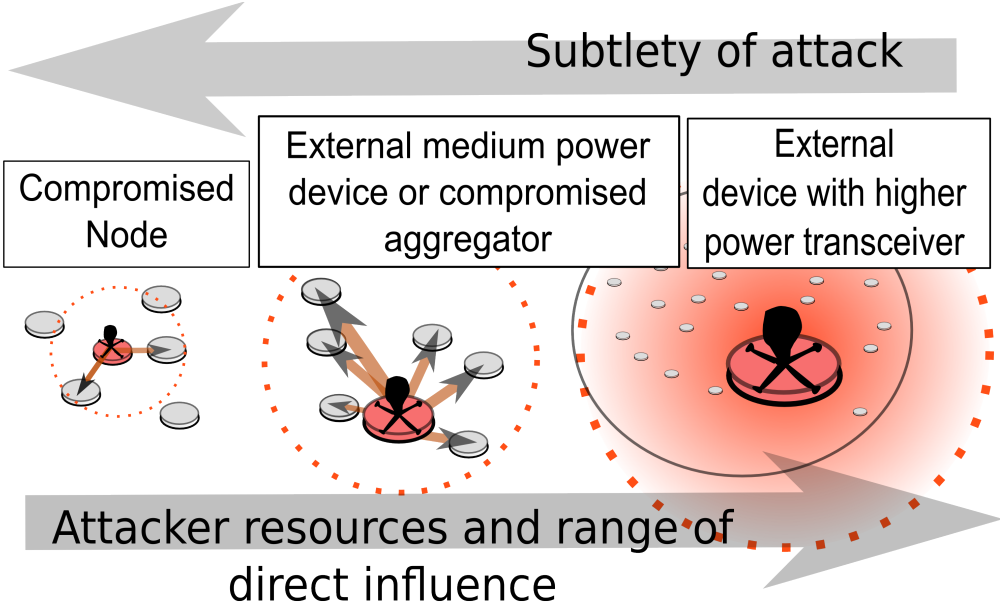
Subtlety of attack
Compromised Node
External medium power device or compromised aggregator
External device with higher power transceiver
Attacker resources and range of direct influence

Figure 10: The continuum of resource levels of potential classes of attacker

#### 3.2.1.2 Fundamental Assumptions

The following characteristics in the WSN security domain are assumed within this thesis, arising from the inherent limitations of the environment and its security challenges [41]. In an unprotected WSN running entirely upon plaintext transmission, the following assumptions hold regarding the security situation:

**Lack of channel confidentiality** The attacker can snoop on traffic, observe any messages injected into the channel, and buffer or copy such messages for later replay. This may occur via a compromised node or using custom equipment to passively observe and inject.

**Lack of availability on channel** The attacker can jam the channel, inject targeted interference in such a way as to overwhelm a receiver and prevent accurate reception. This attack is always possible to disable any network if sufficiently intense. In Section 4.9, page 101, its impact upon WSN systems is assessed, showing that with a high enough number of small jammers, network functionality can be disabled entirely.

**Lack of integrity on channel** The attack can distort a message in transit without the knowledge of the sender. This may not require accurate time synchronisation to break simultaneously into transmission in the middle of a message. An attacker with greater resources could achieve the objective by using a directional antenna to jam a message at a single recipient, and then injecting a fraudulent version of the message during the retransmission.

**Trusted base station** Compromise of the base station is normally assumed to be out of the scope of the network security policy, since the base station is assumed to have a connection to external systems such as the wired Internet, and therefore its interactions include elements outside the WSN.

**Possibility of node capture** Since sensor nodes are physically small and untethered, it is assumed that attackers may capture them. Using standard interfaces such as Joint Test Action Group (JTAG) connectors allow attackers to mount insider attacks by reprogramming or repositioning them, and thereby alter their protocol behaviour. Such reprogramming is a key enabler for many other attacks, since it allows behaviour of the network's own devices to be altered.

**Compromise of node key information** This refers to the removal of key information from a node, via physical removal of nodes from the network and analysis of their memory image. Although tamper resistant devices such as smartcards are widely used, they are not yet economically viable for use in a WSN, given the costs they add to node manufacture [52].

## 3.3 Threat Taxonomy and Common Attacks

The most insidious threats in a WSN are those which show an insight into the protocols comprising the active stack and operate upon its highest layers to put control undetected into the attacker's hands. Several attacks do not outwardly disrupt network functioning but make it possible for the attacker to gradually increase their level of control to enable a later attack. The seminal analysis of the WSN threat environment is Karlof and Wagner's paper [42], which provides an attack taxonomy concentrating on routing and network-layer attacks. In their analysis it is not considered the role of a routing protocol to provide explicit confidentiality, which is considered handled by other mechanisms, such as link-layer or end-to-end encryption. Instead they focus on the property of network robustness and how routing-level attacks can impact upon them.

### 3.3.1 Selective Forwarding

In a selective forwarding attack, nodes fail to keep up their obligations to relay traffic for other nodes, and instead some traffic is silently discarded. Although this may appear on first consideration indistinguishable from node failure, a selective forwarding attack is more subtle in that a node participates in route formation as usual but fails to complete delivery when requested by other nodes.

The effectiveness of selective forwarding to the attacker largely depends on where the compromised node is located and the volume of routed traffic that cross the compromised node. A useful modification from the perspective of the attacker is to compromise route formation, increasing the proportion of routes that use the malicious node.

In order to handle a selective forwarding attack, Marti et al. [53] provide two schemes in which nodes watch the behaviour of their neighbours for unexpected deviations, and assess the likely results of anomalous behaviour on the wider network. The watchdog is a protocol which compares expected behaviour of a peer to the observed, tracking deviations, and signalling potential misbehaviour if the deviation is significant. The protocol must be tolerant enough to cope with changing channel conditions and resulting failure to overhear, while vigilant enough to detect genuine attacks. The *pathrater* is a companion protocol which maps local trust ratings to influence on routing decisions, building up a rating for paths themselves.

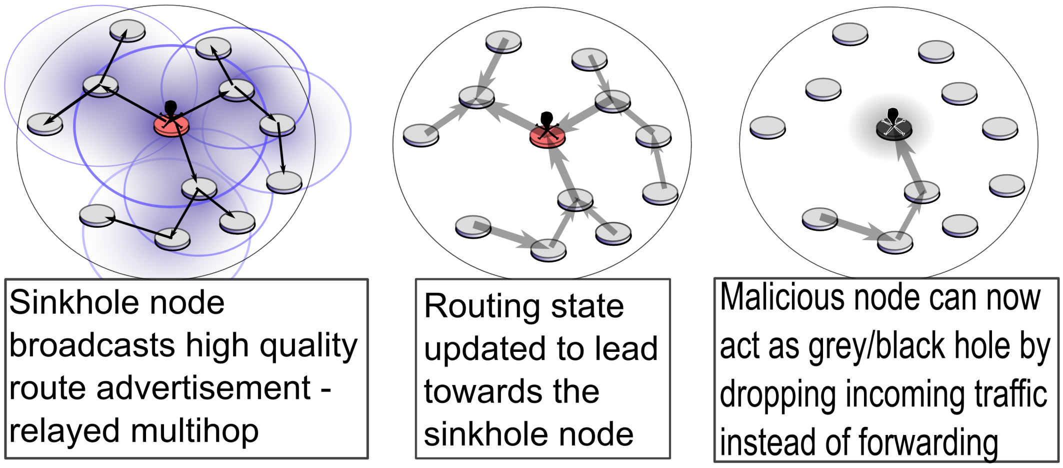
Sinkhole node broadcasts high quality route advertisement - relayed multihop
Routing state updated to lead towards the sinkhole node
Malicious node can now act as grey/black hole by dropping incoming traffic instead of forwarding

Figure 11: A blackhole or greyhole attack resulting from a sinkhole

### 3.3.2 Sinkhole

A sinkhole attack occurs when a node combines selective forwarding with route modification or fraudulent route formation; attempting to influence routing state held in other nodes so as to draw traffic into it. The sinkhole attack is illustrated in Figure 11, page 52. An attacker first pollutes routing state by advertising itself as a base station, or replying to route request messages advertising high quality route to a base station, thereby adjusting routes so as to draw in traffic from a region of the network. Secondly, the sinkhole can be converted into a blackhole by dropping the inbound traffic that has been drawn to the node. This leads to resource consumption (wasted power until alternative routes are found) or, if the routing is used, denial of service (failed delivery in the region).

In a more subtle variation of the attack, the greyhole attack, only some traffic is discarded. The attacker can select which traffic to discard, potentially dropping traffic of a certain type, or randomly discarding a certain proportion of packets to increase overall loss rates. A troublesome example would be a malicious node which delivered all low-priority traffic faithfully and kept up obligations sufficiently to maintain routes as active, but discarded notifications of a genuine emergency situation. This attempts to frustrate the detection of the greyhole, by making it difficult to reliably distinguish it from an unlucky node experiencing poor channel conditions and thus intermittent connectivity.

Subtle behaviour monitoring and reputation systems with a long history would be required to combat subtle greyhole attacks under real network conditions, but they require techniques for handling badmouthing attacks [54], in which nodes attempt to pollute the reputation state of other nodes with fraudulent reports of misbehaviour.

### 3.3.3 Sybil Attack

The Sybil attack [55] occurs when a single physical node impersonates additional identities (its sybil identities). For example, a malign node may forge randomly generated addresses in order to participate as multiple virtual nodes in routing or MAC protocols. It is a general problem in distributed systems, but especially severe in sensor networks since reliance on trusted parties to establish and vouch for identity is difficult due to the distance of nodes from a trusted authority such as the sink and the energy expense of dense party-to-party exchanges.

The sybil attack allows compromise of multihop routing protocols. Karlof and Wagner [42] find general routing vulnerabilities resulting from the sybil attack. If, for example, a multipath routing protocol diversifies a data flow to reduce the risk of compromise, the security benefits are lost if the attacker is using a Sybil attack; the node identities that the routing protocol has assumed all reduce to the single physical identity of the attacker.

The sybil attack allows compromise of multihop routing protocols, and the creation of an unexpected single point of failure. In a multihop network (Figure 12, page 54), this allows attackers to defeat the diversity provided by multihop routing. From the perspective of source S (Figure 12a), traffic is sent along several diverse multihop routes, which allows some routes to continue without disruption if an intermediate node fails. However, since one of malicious node M's sybil identities is included on all three paths, from the true view (Figure 12b), M has defeated the multipath protection and become a single point of failure, controlling all traffic in the network.

#### 3.3.3.1 Certification Solutions To Sybil Attack

Douceur [55] shows how the sybil attack can compromise voting and reputation systems, as well as attempts to build redundancy into protocols. The solution proposed is the use of a central certification authority to authenticate nodes and

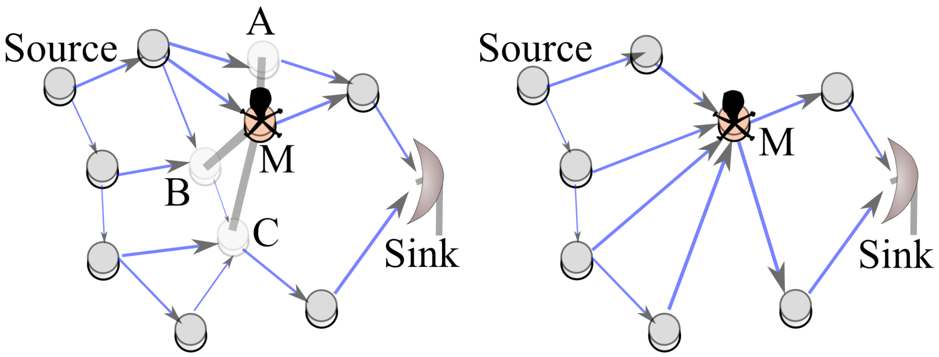

(a) Source perspective (b) True perspective

Figure 12: The sybil attack and its impact upon routing

verify their claimed identities, but the communication overheads of this become prohibitive in larger networks. Furthermore, it assumes that all nodes are known to or directly contactable by the sink, which may not be true in extremely large scenarios or those with mobility, in which nodes could move rapidly.

#### 3.3.3.2 Resource Testing Solutions To Sybil Attack

The most fundamental solution to directly verifying identity and detecting an ongoing Sybil attack involves the use of resource testing, taking advantage of limitations on communication, computation and storage within a restricted time-frame. A viable example for sensor networks involves communication. Since typical hardware has only one radio per node, a challenge involving sending packets simultaneously to multiple receivers could distinguish a sybil from two independent nodes.

Newsome et al. [56] analyse the Sybil attack specifically in sensor networks, dividing it further into attacks with stolen versus fabricated identities, and simultaneous versus non-simultaneous attacks. Non-simultaneous attacks are difficult to respond to well; Douceur's analysis shows they cannot be handled by resource testing, and generally, may not be easily distinguishable from mobility within the network itself.

The primary problem with WSN sybil detection via verification by peers is that it involves collaboration, in which other nodes are required to implement the detection protocols and vouch for each other. This is difficult in the presence of multiple malicious sybils in a region, as malicious nodes can mutually guarantee their false identities to generate still further fraudulent identities. Generally, there is always a trade-off between the intensity and overheads of testing and the likelihood of correct detection of the attack.

#### 3.3.3.3 Mobility Assessment Solutions To Sybil Attack

Mechanisms exist to detect the sybil attack in mobile networks, focusing on detecting mobility patterns. The sybil attack leads to correlations in connectivity patterns [57]; if the underlying sybil node moves, then all its Sybil identities nodes must move together. Solutions exist in the case of a mobile network which can distinguish a sybil from multiple moving nodes via analysis of MAC layer collisions [58]. However, all these detection approaches assume the presence of mobility to detect the presence of sybils; in the case of a static network, this detection mechanism is ineffective.

### 3.3.4 Resource Consumption and Denial of Service

Resource consumption attacks are those which attempt to exhaust physical or virtual limited resources such as battery power or security descriptors. An example would be the conceptsleep deprivation attack [59] in which unintended media-access control interactions are used to exploit protocol rules to deplete batteries earlier than intended.

A related attack is a denial-of-service (DOS) attack, which is an attack upon system availability. One example of resource consumption combining with denial of service in the pursuit of the attacker's goals occurs in the formation of routing loops. A routing loop is an anomalous condition in which route formation is subverted so that packets circulate endlessly, both denying the delivery service and wasting limited energy. If packets are not authenticated, then they can easily be created through sending fraudulent routing packets. For example, in a gradient-based routing protocol, if node A advertises to B that it is a suitable next hop and vice versa, then packets will circulate endlessly until they either expire or energy is exhausted. Although this trivial example is easily detected when there are only two nodes, it can be extended to a loop of any size.

In a geographic protocol which forwards packets by preferentially delivering to the hop closest to the sink, an adversary can create a routing loop by forging a location announcement. As presented in Figure 13, page 56, node B is physically closer to the sink than node A. However, by forging a position announcement to B claiming to be from A and placing node A closer, the malicious outsider M can trick B into forwarding back to A. This attack will cause packets to circulate endlessly until any time-to-live (TTL) counters expire or the nodes are exhausted.

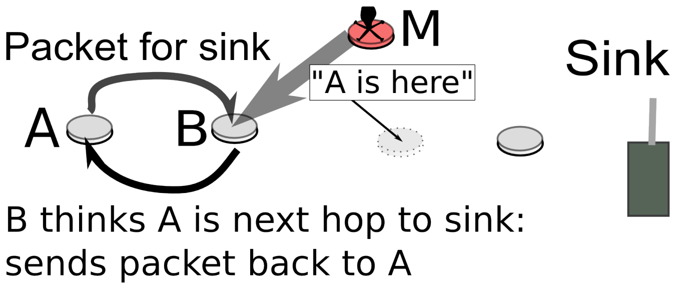

Figure 13: Resource consumption attack involving the formation of a routing loop in geographic protocols

## 3.4 Asymmetric Channel Attack

The HELLO flood attack [42] is a denial-of-service attack which can be mounted by an attacker with greater transmission range than network nodes. By using a powerful transceiver to globally broadcast a high-quality route advertisement proclaiming itself as a base station, recipients are tricked into sending packets to a neighbour which is unreachable, as the reverse channel is unavailable to the limited radio of a conventional mote. The attack is crippling against any protocols which trust all inbound announcements. However, protocols which involve an explicit handshake or other two-way communication with the receiver survive this, as they validate the presence and reachability of a peer in advance before using it for forwarding.

## 3.5 Wormhole Attack

The wormhole attack occurs when the attacker exploits heterogeneity to attack the network. It occurs in a network in which the attacker deploys a pair of malicious devices with a private out-of-band, low-latency, point-to-point channel between them. These devices tunnel all traffic received at one endpoint to the other and rebroadcast it at the remote endpoint. As a result, route request and response packets are tunnelled between the endpoints, reaching the sink via the shortcut link. The network is then dependent upon the wormhole link, and its disconnection by the attacker can sever the topology.

The attack is highly insidious in that it allows the network to function undisturbed as long as the attacker wishes, albeit with a distorted topology which does not match the physical placement of nodes. The use of multihop routing through a distributed field of nodes aims to avoid single points of failure, but the wormhole attack generates a new single point of failure under the attacker's control, and encourages a large proportion of network traffic to use it. Following this, the wormhole can become a greyhole or blackhole by discarding some or all of the traffic sent across the wormhole link.

In Figure 14, page 57, Node A's perception of the topology is that it is adjacent to the sink (since the wormhole tunnels routing notifications straight through without following the routing protocol) while in fact the true route is much longer. The wormhole attackers M1 and M2 are therefore now able to distort, observe or drop all traffic using the wormhole. Even if traffic is encrypted, analysis of traffic patterns can alert the attacker to ongoing phenomena or changes in network behaviour.

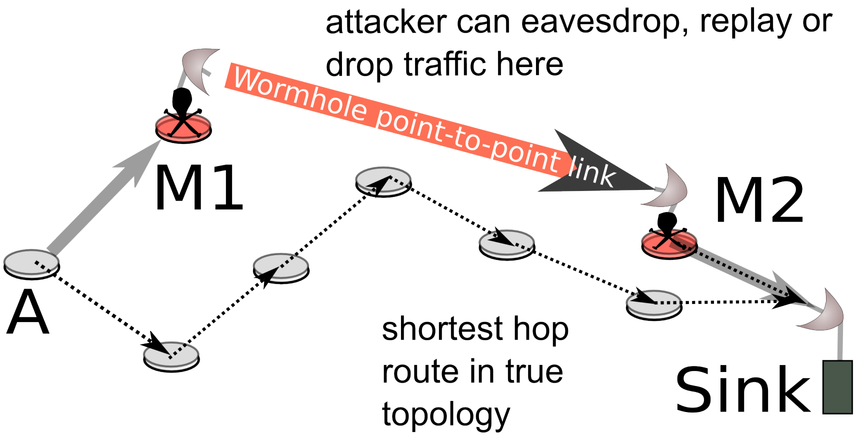
attacker can eavesdrop, replay or drop traffic here
Wormhole point-to-point link
M1
M2
A
shortest hop route in true topology
Sink

Figure 14: The wormhole attack, allowing a pair of malicious attackers to control a substantial proportion of network traffic

### 3.5.1 Packet Leashing Wormhole Countermeasures

An early and logical solution to the wormhole attack is packet leashing [60], which relies upon an insurmountable physical constraint which underlies communications; the speed of light limit. This approach specifies a security module which can be run periodically to bound transmission range between two nodes via interchange of a pair of specially designed sentry packets. The logic behind this approach is that the wormhole distorts the true topology via its private out-of-band channel, invisible to network entities. However, unlike a hypothetical wormhole in physics which may enable instantaneous interaction between distant regions, this wormhole cannot circumvent the speed of light limit and relay traffic instantaneously. Imposing a time limit for communications therefore serves to limit the length of the private channel, bounding the possible distance of interaction between two peers. By using a link range testing process regularly and excluding links in which the leashing test response packets arrive late at their original sender, use of an out-of-band channel can be detected before the pair of endpoints can participate maliciously in any network operations.

The most accurate approach to packet leashing is the temporal synchronisation variant. This approach ensures accurate time synchronisation exists via a global clock, and then makes a transmission from one node to another. By timing the return of the acknowledgement, it is possible to estimate a round-trip-time (RTT) and therefore the distance that was travelled by the packet. This allows wormhole links to be rejected, since the distance will be above a predefined threshold.

A major problem with the scheme is its reliance on the exact details of timing. The relatively small distances involved in sensor network communications mean that the time delay must be detected within extremely tight time constraints (e.g. within 134 nanoseconds to bound the remote peer distance to 20 metres). This is difficult to implement on a congested network given the analogue characteristics of low-cost sensor transceivers taking time to switch states, the drift of onboard oscillators and problems with maintaining clock synchronisation, and possible heavy contention for the surrounding channel. Furthermore, practical MAC protocols concerned with energy usage and minimising idle listening are unlikely to offer the instantaneous channel access for both request and response that would be needed to distinguish wormhole packets from directly transmitted ones.

A further problem with this technique is that it is troublesome to implement when multihop routing environments become heterogeneous such as in a majority of real deployments (such as in Section 2.2.1, page 36). This arises as a maximum transmission threshold distance must be defined, beyond which rejection of the link will occur. Therefore, it is difficult to introduce authorised heterogeneous devices such as long-distance bridging links which are under the control of the deployment authority. These will not deliver their intended benefits to the network as they will be indistinguishable from a wormhole and thus rejected as suspicious.

The geographic form of the packet leashing system verifies peer locations via processing information from a secure localisation protocol, and only requires loose time synchronisation to accomplish this. However, secure localisation is itself a non-trivial problem, which imposes additional hardware requirements [18]; normally at least a certain proportion of beacon devices, together with tight collaboration to detect devices attempting to forge such localisation approaches. Liu [61] presents an approach to assist with this secure localisation. If localisation is required by the application, then the coordination overheads of this additional layer of complexity may be acceptable.

### 3.5.2 Approaches Exploiting Additional Hardware

Another approach involves the introduction of extra hardware, for example, directional antennas upon nodes [62]. Packets are marked with their transmission direction (Figure 15, page 60), which can be extracted from the header and compared on reception to check that it is sensible. The diagram shows a transmission to the north-east quadrant which will be accepted by the receiver if it is received from the south-east antenna. Figure 15b, page 60, shows an example security situation in which traffic would be rejected. For example, if a packet is sent in the north-east quadrant and yet arrives at its receiver from a direction other than south-west, it is possible that a wormhole between them has rebroadcast it improperly. It is possible that a wormhole could exist in a region and simply adjust the direction markers embedded in packet headers, although presumably encryption would ensure the integrity of packets en-route. However, given that the wormhole's presence may impede even key-exchange, it is possible that a wormhole could take part in a man-in-the-middle style attack which interferes with key establishment and thus defeats this approach, altering traffic on rebroadcast to defeat the detection or perform any other malicious traffic alteration.

A major drawback regarding this approach concerns operation in realistic short-range propagation environments. Over the short range the topology is likely to be highly irregular, and the presence of obstacles in the topology and reflections could lead to non-direct signal paths. Although it may perform wormhole detection, it is therefore likely to have an unacceptably high false positive rate, rejecting a lot of safe links in realistic topologies.

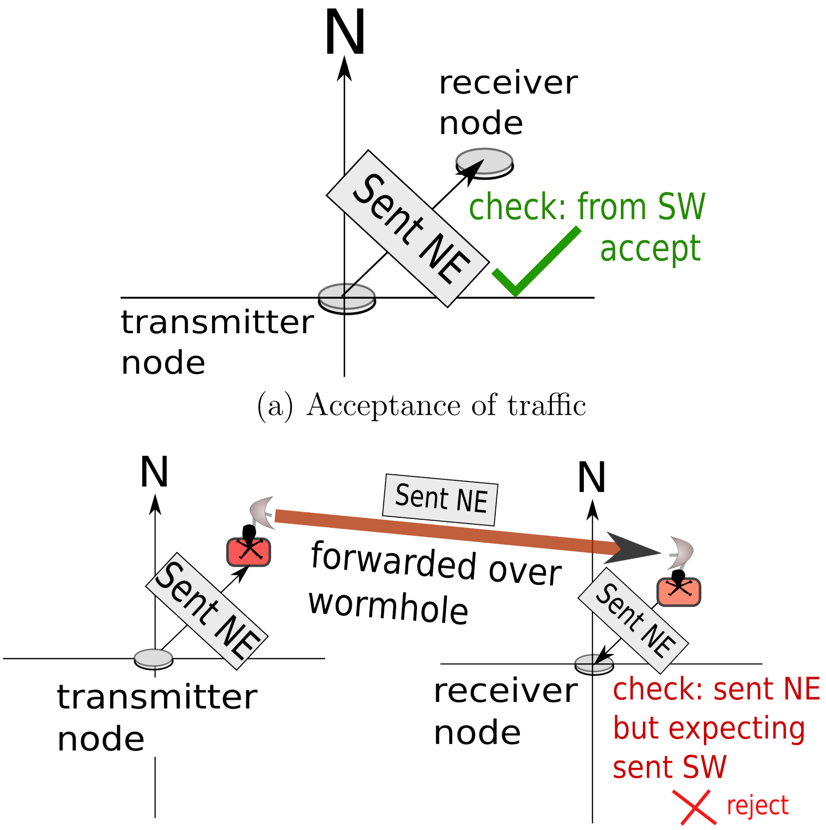

(a) Acceptance of traffic

(b) Rejection of traffic

Figure 15: The use of packet tagging and directional antenna approaches for wormhole detection

### 3.5.3 Graph-Theory Approaches

Another category of approaches use graph theory to reconstruct the topology and discover unusual properties of regions that could comprise a wormhole. For example, the graph-theoretic approach [63] attempts to discover unusual connectivity properties in a network, such as direct connectivity between nodes that would otherwise require several hops to reach. However, this approach bears a large coordination burden, and may fail in real-world cases in which obstructions create unusual connectivity topologies.

The visualisation approach [64] is conceptually similar, relaying upon global reconstruction of the entire topology, which carries an unacceptably high (cubic) time complexity. This would likely prove prohibitive for a future-proof algorithm for large-scale networks, but in segmented or hierarchical regions or on current test networks it could be viable.

Some approaches bring the responsibilities for detection to the network sink or endpoint at the routing level, rather than relying on distributed isolation at the link level. The Statistical Analysis of Multipath (SAM) [65] approach attempts to analyse an ensemble of multipath routes formed, and detect any single links appearing with greater frequency than expected in the distribution. With information on any heterogeneity used being known at the point of detection, this would allow the network to isolate suspicious links and instead choose safer ones that are less likely to be involved in wormhole activity. This would also have the advantage of improving performance by reducing the contention for busy links. This approach does make it difficult for the network to share any long-term information about the traffic levels that exist in the network, as the detection decisions are made entirely on the basis of a single routing request for this endpoint and not on all transmission requests over time.

### 3.5.4 Spectral Monitoring Approaches

One interesting approach for wormhole detection based on physical layers of the protocol stack is based on spectral properties of received signals [66]. This assumes the transmission of periodic link-state routing announcements under a protocol such as Optimised Link-State Routing (OLSR) [67], and requires low-level physical layer monitoring. The wormhole introduces a characteristic property into the measured power spectral density (PSD) due to the inherent delay introduced when forwarding remote packets over the wormhole link.

However, this may not be appropriate for protocols in which widespread link-state flooding is not required, as it proves wasteful of energy and bandwidth in a network in which nodes remain idle until activated as sources. Also, modifications to the transceivers to analyse the spectrum in precise detail would be necessary, which would be beyond the capability of present-day sensor nodes. Unless such spectral monitoring was also a sensory-level goal of the network (for example a hostile interference warning network to track and monitor spectral conditions) then it would be unlikely that such high-fidelity monitoring would be realistic.

## 3.6 Security Primitives and Resources

It is important to consider the security resources and primitives that are commonly deployed and available upon current and future WSN nodes. There is a heavy reliance upon cryptographic approaches, in order to protect the confidentiality and integrity of data messages transmitted [41]. However, it is important to remember that many attacks upon WSNs, particularly those that attempt to compromise availability, cannot be countered solely via cryptographic protection of the data packets. Cryptography can help through authenticating participating entities, but cannot guarantee that the links they are operating upon are free of threats, or protect network availability properties. For example, in the wormhole attack, encrypted packets are simply tunnelled over the wormhole link as normal.

### 3.6.1 Cryptography In WSNs

Encryption is often assumed to be a silver bullet in network technologies, and in well-resourced environments is often applied liberally. The processing power of general purpose computers enables conservative use of advanced algorithms such as the current Advanced Encryption Standard algorithm Rjindael [68] or public-key algorithms such as that developed by Rivest, Shamir and Adleman (RSA), both with large key sizes. Although hardware cryptoprocessing modules may allow this to be implemented without direct load upon the CPU of a node, physical limitations mean that any computational operation must necessarily absorb some power.

For sensor networking, simpler and less power-hungry cryptographic primitives are obviously preferred wherever possible. One lightweight protocol which offers this is the one-way hash chain idea used as a common building block for security technologies. It is discussed in more detail in Section 3.6.4, page 66.

### 3.6.2 Symmetric Cryptography

Symmetric cryptographic algorithms are mathematical algorithms which transform source data (the plaintext) using a key into an encrypted variant (the ciphertext). They employ a variety of mathematical operations to achieve this, but generally depend upon delivering a combination of confusion (to obscure the final ciphertext output symbols so they bear no relation to the initial plaintext symbols) and diffusion (to spread the entropy or influence of a cipher symbol around). The operations depend on a cryptographic key, which must be held secret by the communicating parties. The operations are designed for reversibility, so that the plaintext can be recovered from the ciphertext by the reverse decryption procedure.

A practical symmetric cipher can operate on a continuous stream of data of any length, producing a ciphertext of equal length. The standard notation for an encryption function F such as this is $F : \{0,1\}^* - > \{0,1\}^*$. However, for convenience and ease of analysis, the underlying cryptographic operations behind such systems are built on that of the block cipher, which operates only on fixed-size chunks. To deal with this disparity, a mode of operation is employed, which is a set of rules describing how the block cipher primitive is combined with previous ciphertexts and incoming plaintexts to operate.

The simplest mode of encryption is the Electronic Code Book (ECB) which merely splits a plaintext into fixed-size chunks and encrypts each separately. This scheme is easy to parallelise; however it has serious deficiencies in that each block is independent, which enables several attacks. For example, an attacker can attempt a dictionary attack by encrypting a block of zeros under all possible keys, and then if ever a message contains an all-zero block, the key can be discovered trivially by inspection. This is especially serious in sensor network systems if smaller keys are used, so a cracking dictionary can be built more easily on general-purpose computers.

A more sophisticated mode of encryption is the Cipher Block Chaining (CBC) scheme (Figure 16, page 64), which mixes in the ciphertext of the previous stage via a bitwise exclusive-or (XOR) operation before feeding into the encryption operation. On the first stage, it uses an initialisation vector to feed into the XOR. This strategy effectively applies some diffusion on the larger scale of the input stream, making the encryption of a block depend on all previous plaintexts and stopping the dictionary attack detailed previously.

### 3.6.3 Asymmetric Cryptography

Although symmetric cryptography is acceptable in situations in which trust permits keys to be freely exchanged in advance, a solution is needed which allows entities that have not previously interacted to exchange keys. Asymmetric cryptography primitives constitute a public key infrastructure (PKI), a cryptosystem which separates the keys required for different cryptographic operations, providing strictly

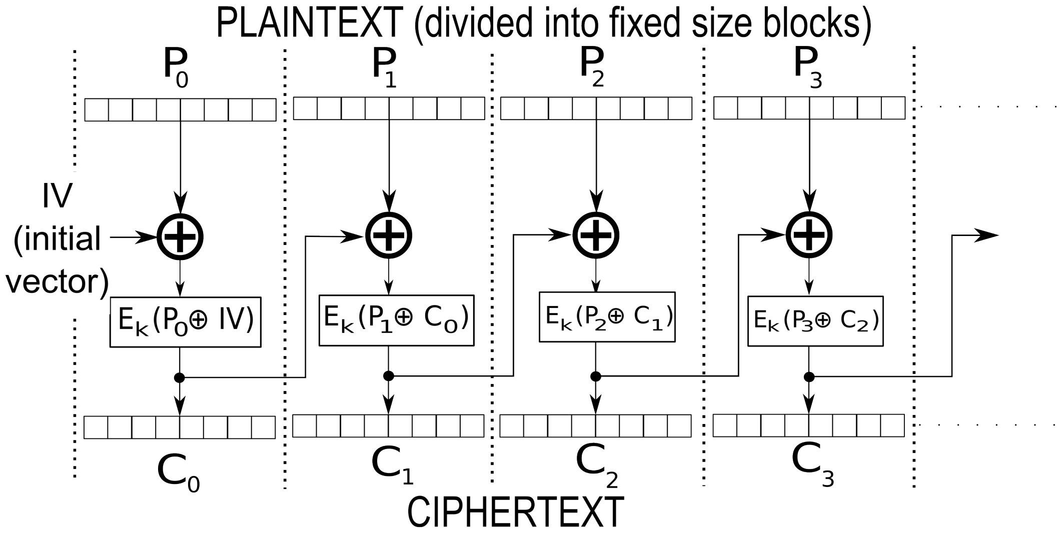

Figure 16: The use of cipher-block-chaining to convert a block cipher into a stream cipher

distinct keys for encryption and decryption of data. The key used for encryption only is known as the public key and the key used for decryption is known as the private key.

If a symmetric key algorithm could be represented as a safe, then a PKI system is representable as a mathematical padlock; opening it requires a separate process to closing it, and involves a distinct secret key. The names given to keys refer to the covertness they require; a public key can be globally disseminated, while a private key must be held confidential, as capture of it by any unauthorised party will lead to them acquiring the same privileges as the entity itself. Accordingly, asymmetric schemes are often referred to as public key cryptography.

The asymmetry inherent in these schemes therefore divides the key structure and the communicating principals, following the principle of least responsibility. In a symmetric scheme all entities, even if only performing encryption, must hold the valid symmetric key and therefore must be trusted, becoming viable targets for attack. In an asymmetric scheme the trust levels are much tighter; only the entities that must perform encryption require this level of trust.

Although these encryption technologies are often thought of in terms of confidentiality, they can also be used to protect message integrity as well. This is done by a digital signature - taking a random challenge from a requester and signing it by applying the decryption operation (using the private key). By then applying the public encryption function on this signed value, the requester can check it reproduces their original challenge. Only a holder of the private key could have produced a value satisfying this criteria, so the digital signature can authenticate its originator (assuming it can be trusted to have held its private key securely and not been compromised).

Examples of asymmetric protocols include [69], Diffie-Hellman [70] and elliptic-curve cryptography [71] [72]. The schemes are built on one-way functions which can easily be performed but require specialist knowledge (the private key) to invert. A typical example would be modular exponentiation operations, which rely upon the fact that arithmetic upon a cyclic group is difficult to invert without knowledge of the group structure.

The energy constraints of sensor nodes require a careful evaluation of the usage of public-key cryptography. Public-key algorithms typically involve discrete exponentiation in a cyclic group, which will require deep loops and lots of function calls to process on an 8-bit platform. Therefore, all but the most cursory uses of public-key encryption have traditionally been considered prohibitive on energy-constrained devices [41] [73] [74].

Watro et al. [75] provide an infrastructure utilising public key technology in sensor networks, to allow external entities like troops or supervisors to validate themselves to the network using a key shared with a trusted base station. The scheme uses an especially low prime modulus $e = 3$ in order to make the numerical operations viable under the constraints. However, notably their method takes advantage of the asymmetry in processing; since verification of authenticity via decryption is far less energy-intensive, the scheme does not perform any encryption operations upon nodes themselves, delegating that entirely to the external parties.

Malan, Welsh and Smith [76] claim PKI is viable for some occasional sensor network functions. They claim that elliptic-curve cryptography (ECC) is more viable than Diffie-Hellman, since it provides better attack resistance with a smaller prime modulus. This same result is supported by Piotrowski [77] with the discovery that a Mica2 nodes required nearly $360mJ$ to perform a RSA-1024 key generation, versus only $27mJ$ for ECC-160. Similar results for the energy costs for the server-side operations of key verification show that RSA is not feasible for general use between WSN nodes. They therefore leave open the possibility of using ECC sparingly, perhaps to bootstrap other security approaches.

It may be thought that ultimately the growth in processing power may nevertheless ultimately make public-key viable on commodity sensor hardware. However, the economic pressure is towards smaller and more energy-efficient devices and there is always an intrinsic energy cost to processing which drives it to be minimised [42]. Since smaller devices with a lower per-unit cost influence the scale and therefore data gathering utility of the deployment, the challenge is the provision of security under the resource constraints of an existing platform, expecting that the typical node platform will become smaller and cheaper but not necessarily better-resourced.

### 3.6.4 One Way Hash Chain

The one-way hash chain (OHC) is a computationally lightweight and elegant authentication technique which forms a key component of many security architectures, such as Secure Network Encryption Protocol (SNEP) (Section 3.10, page 70) and $\mu$TESLA (Section 3.10.1, page 71). The approach allows two parties to establish a trust relationship so that the claimant can later prove to the verifier that it is indeed the originally authorised entity and not a malicious peer injecting fraudulent messages. It was originally intended [78] for generation of one-time passwords capable of use over an insecure channel. The importance of the technique for sensor networking is that it allows arbitrary nodes which have some existing relationship to establish an arbitrary number and length of authentication sessions, using only computationally cheap operations.

In Figure 17, page 67, the OHC technique is demonstrated by a scenario in which a base station can authenticate itself to a local peer node N. Node N would require authentic knowledge of the initial value $v_N$, either by receiving a packet authenticated with a pair-wise symmetric key (known to the BS and N), or perhaps sending it authenticated by a digital signature. With a long session in which the chain length $N$ is high, it may be acceptable to use a less-intensive public-key technique such as ECC for this occasional session setup. The core of the technique consists of an operation involving a hash function on $n$ bits. This function on a bit string, denoted $f : \{0,1\}^n \rightarrow \{0,1\}^n$, has the property that given a value $y$ such that $y = f(x)$, it is computationally infeasible to find the corresponding $x$ (referred to as the inversion of the function). This property can be used to authenticate that two messages, separated in time, come from the same source.

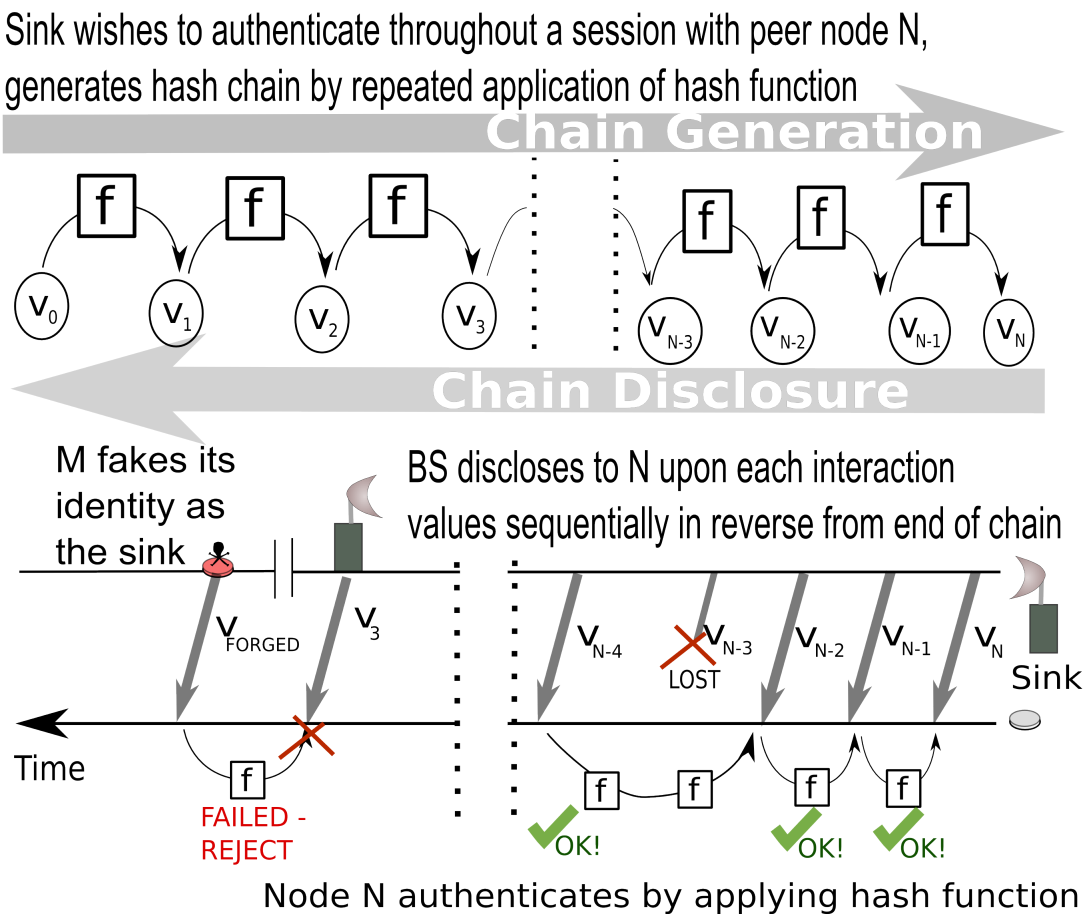

Sink wishes to authenticate throughout a session with peer node N,
generates hash chain by repeated application of hash function
Chain Generation
f
f
f
f
f
f
$v_0$
$v_1$
$v_2$
$v_3$
$v_{N-3}$
$v_{N-2}$
$v_{N-1}$
$v_N$
Chain Disclosure
M fakes its identity as the sink
BS discloses to N upon each interaction values sequentially in reverse from end of chain
$v_{FORGED}$
$v_3$
$v_{N-4}$
$v_{N-3}$
LOST
$v_{N-2}$
$v_{N-1}$
$v_N$
Sink
Time
f
FAILED - REJECT
f
f
f
f
OK!
OK!
OK!
Node N authenticates by applying hash function

Figure 17: The one-way hash chain (OHC) technique, used to authenticate entities, in this case between a base station and its peer node N

Suppose an authority such as a WSN sink wishes to authenticate itself to a node. Before deployment, it computes an initial value $v_0$ and a sequence $v_1 \ldots v_N$ such that $v_k = f(v_{k-1})$. Therefore, the sequence (chain of) elements are related by forward application of the hash function. The base station then issues a commitment to the sequence, by issuing $v_N$ with its initial message.

In every subsequent communication with the target, the sender works backwards along the chain, issuing $v_{N-i+1}$ with the $i$th message (numbered from one). By applying the hash function, the target can check that the hash values arrive at the commitment $v_N$, or any previously checked value in the sequence that has been authenticated. An outsider attacker cannot forge a message, as even if they eavesdrop, they cannot invert the hash function to find sequence elements that have not yet been disclosed by the sink.

The one-way hash chain approach is further extended into Merkle hash trees in the SECTOR protocol [79] which allow nodes to establish a unique time of interaction, and a dual directional hash chain (DDHC) to establish time windows for interaction

[80]. It will be applied to approaches in this thesis to provide authentication of reverse replies in routing protocols.

## 3.7 Key Infrastructure and Management

### 3.7.1 Key Management Introduction

Although the security primitives can establish the security priorities of confidentiality, integrity and authenticity between the channel established between arbitrary node endpoints, they require the existence of appropriate cryptographic keys at the endpoints. It is worth considering that end-to-end encryption schemes in which intermediate nodes cannot access or modify the message preclude aggregation to suppress redundant messages and therefore impose a capacity and energy burden on the network. Therefore, nodes having an individual key shared only with the base station on deployment is impractical for most situations, as it precludes the required interaction and collaboration. In many WSN situations, groups must dynamically form and adapt to deal with changing situations; perform distributed signal processing, comparing and aggregating sensor readings, together with other inherently distributed tasks.

There are three separate problems in the management of a key infrastructure:

**Key storage** How many keys must be held on board nodes

**Key distribution** How are keys transmitted between communicating parties?

**Key maintenance** How is refreshing of keys (rekeying) dealt with, and how do protocols deal with changing membership?

Two non-viable strategies for key sharing are identified by Roman in [49] as global keying and pairwise keying. Global keying (Figure 18a, page 69), the use of a single network-wide key, lacks resilience as compromise of the key at any node will invalidate it network-wide. Pairwise keying (Figure 18b) requires a unique key per peering, which squanders scarce memory on keys and energy on key generation. This is unacceptable when the majority of possible end-to-end peerings are unlikely to ever be used for active communication. A trade-off is clearly required, and Eschenaur and Gligor's work [81] provides the starting point. In their system, a network-wide keypool is generated, and every node holds a random subset of these keys. Nodes which wish to communicate must hold a single key from the pool in common, therefore nodes which cannot communicate directly must do so through an intermediate which shares one key with the first party and another with the second.

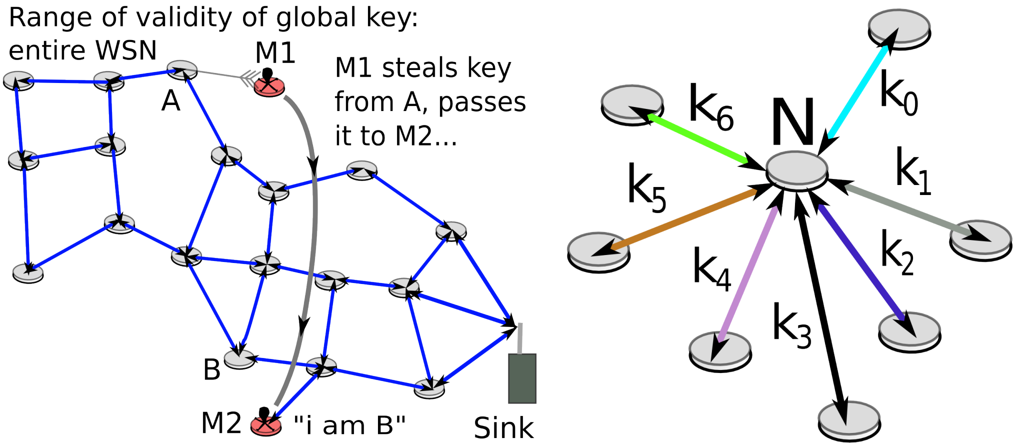

(a) Global keying (b) Pairwise keying

Figure 18: The problems with both global and pairwise keying strategies

#### 3.7.1.1 Key Distribution Through Physical Contact

As regards key distribution, Stajano and Anderson [59] provide an interesting alternative for secure key distribution, through close physical contact. This would normally require preloading of the keys before deployment, but the solution proposed by the authors is to lower the transmission power to the minimum limit. The nodes are brought extremely close together so as to prevent reception by eavesdropping adversaries. Using an extremely-low power channel and bringing or touching devices to their coordinator together during early deployment allows the key to be sent over the power-limited channel. Devices added later can be brought into close range of a security coordinator temporarily to initialise their keys.

## 3.8 Integrated WSN Security Solutions

This section considers previous integrated solutions that have been explored to provide some combination of security properties to a sensor network: confidentiality, authentication, and the solutions chosen for provision of security in existing WSN technologies.

## 3.9 LEAP

The Localised Encryption and Authentication Protocol (LEAP) [82] is a protocol which attempts to make key management more flexible, relating it to the requirements of a particular communications relationship. Since keys have fundamentally different requirements depending on their communications intent, number of involved parties, persistence of relationships, a multi-level keying scheme is required, tailored to each class of traffic.

LEAP features four classes of keys; individual (shared only with the base station), group (network-wide key), cluster keys (for a node and all its reception peers) and pairwise (for one-to-one relations between node pairs). The scheme allows a node's individual key to be generated by the base station running a secure hash function on a node's identity. Pairwise keys can be generated by interchanging a pseudorandom challenge and encrypted response message between the two intending nodes, and are secure as long as a node master key has not fallen into attacker hands. The larger-scale keys are bootstrapped similarly, using a TinyOS-inspired routing protocol to set up the group key.

## 3.10 SNEP

SNEP (Secure Network Encryption Protocol) is a protocol which provides encryption, authentication, integrity, and guarantees of data freshness between a pair of communicating nodes that hold a shared symmetric key, while requiring only an 8 byte increase in packet header size. SNEP uses a symmetric master key $\kappa$ to derive encryption key $\kappa_{encr}$ and authentication key $\kappa_{MAC}$. A key establishment and distribution scheme must ensure that $\kappa$ is held privately between the communicating pairs and not disclosed or revealed to outsiders. Nodes also hold a frame counter for the unique interaction with the peer.

Consider SNEP operating between transmitter A and receiver B. With a single message from A to B, SNEP can provide confidentiality, authentication, and replay protection (protection against later retransmission of data). A takes the data and encrypts it using the RC5 block cipher in counter mode (using the cipher to generate keystream by encrypting the counter using the key, and then using the XOR operation to combine plaintext with the keystream). This provides confidentiality protection. Then a MAC is created with a secure hash function of the counter concatenated with the encrypted ciphertext. The ciphertext and the MAC contents are concatenated and sent to the recipient.

$$A \rightarrow B : D_{<K_{encr},C>}, MAC(K_{MAC}, C|D_{<K_{encr},C>})$$

A malicious node cannot observe frame contents as $K_{encr}$ is unknown to it, being shared pair-wise between communicating principals. It cannot alter message contents as this would invalidate the MAC at the receiver. If a message was repeated to attempt a replay attack, then the expired counter would not match with the recipient's monotonically increasing counter and it would be thrown away. The receiver checks the MAC using the next expected counter. If a message has been lost in between, it may have to check a few additional counters.

There is a potential performance problem in that if bursts of errors cause sequential delivery failure, then an entire end-to-end counter reset must be performed, which requires considerable overhead. The number of forward counters tried must be sufficient to provide a margin of error based upon the expectation of packet loss in the network. However, too many will increase the latency before rejection, so for optimal performance SNEP must be tuned carefully according to network statistics.

### 3.10.1 $\mu$-TESLA

$\mu$-TESLA is a lightweight version of the Timed Efficient Stream Loss-Tolerant Authentication [83], which allows authenticated multicast streams to be delivered. $\mu$-TESLA eschews the PKI approach of digital signatures for the one-way hash chain approach, which was discussed in Section 3.6.4, page 66. To deal with the timing issues and the potential of a rushing attack, the system only discloses hash values in separate packets with a delay, which reduces the intolerance of delay or latency. The security condition now only requires that a data packet is not received after the corresponding key disclosure packet, which gives a much larger tolerance of packets requiring delays or retransmissions.

### 3.10.2 INSENS

The Intrusion Tolerant Routing Protocol For Wireless Sensor Networks (INSENS) protocol [84] aims to provide an intrusion-tolerant routing scheme. Routing is initiated by the base station, and provides a scheme for securely forwarding data back to the base station. It is effectively a form of one-time link-state routing in which computation is performed at the central coordinator. Accordingly, each node has a pre-configured pair-wise key shared only with the base station.

In the first stage, the base station forwards a request message to all nodes in the network, and in response to it all nodes return their local topology information to the sink node. The route request message is authenticated using the one-way hash chain technique of Section 3.6.4, page 66, in which the route request must carry a hash which ultimately hashes to a chain endpoint pre-configured before deployment. The requests are extended hop-by-hop to include a MAC of keys and identifiers of the intermediate forwarding node, which uniquely identifies the forwarding path. The replies use MACs which are dependant on the MAC of the parent in the forwarding tree.

The base station, having received topology information for the entire network, can then compute multipath forwarding trees for the network and relay them back to the original recipient, protected by the key and the path-specific MAC to prevent tampering on the way.

### 3.10.3 TinySec

Karlof, Sastry and Wagner present TinySec [41], which attempts to provide a high-performance, easy to use security extension for the TinyOS embedded operating system. The main goal is to provide a resource-efficient security architecture which does not extend message headers too much with over-conservative security.

Security is provided at the link-layer, which allows full in-network processing, and is transparent to application developers, meaning that they do not have to worry about correctly handling the low-level details of security implementations. TinySec provides authentication and integrity via cipher-block chaining message authentication code (CBC-MAC) [85] and optional confidentiality.

The encryption is optional to allow protection to be traded off for energy saving when the explicit confidentiality is not required. The authors mention the example of an alarm message which, although urgent, may not require explicit confidentiality protection as long as it reaches the sink unaltered.

## 3.11 Security Attacks Considered In This Thesis

This thesis will consider several security attacks. The philosophy it will incorporate will be relying upon routing away from potential threats, or securing the physical layer against them. It will therefore only focus upon timing-related issues when it is necessary for the transmission of data within beamforming.

The wormhole attack is the main attack that will be considered, being featured extensively within Chapters 5 and 6. As demonstrated in Section 3.5, page 56, the wormhole attack is interesting for study since it cannot be countered cryptographically and involves an attacker with the advantages of heterogeneity. This is normally relied upon by the deployment authority to implement a reliable network, and the previous approaches to detect it all either suffer scalability problems or are impractical for deployment in realistic network conditions.

Signal jamming attacks will also be considered in Section 4.9, page 101. Jamming attacks are interesting for study as they are very low-effort, given that almost any inexpensive device can inject interference into publically available communication bands like the ISM band upon which many network devices depends. Since they have the potential to disable the network completely, it is vital to explore them and determine the extent of their influence.

The sybil attack will be studied due to its potential to compromise distributed systems that depend upon effective collaboration, particularly the supernode. As discussed in Section 3.3.3, page 53, the sybil attack is difficult to detect using entirely distributed approaches when there is the possibility of a significant proportion of sybil nodes vouching for the fraudulent identities of their malicious peers. An approach to detecting the sybil attack and routing away from beamforming clusters affected by it is considered within Chapter 7.

## 3.12 Conclusion

This chapter has provided a consideration of the importance of security in WSN technologies, and the problems imposed by computation under such a resource-limited environment. The limited resources on board 8-bit nodes, and sparse availability of nodes frequently give an advantage to the attacker, whether it is in regard to low-power transceivers being swamped with interference on the wireless channel, or cryptography being restricted to small key-spaces due to energy constraints.

Under the WSN scenario, any individual device introduced by an attacker can often access resources beyond the capabilities of an individual node, such as the heterogeneous links used in the wormhole attack. Current countermeasures have been shown to have many problems in mitigating these approaches in real systems. Chapters 5 and 6 explore the use of novel routing techniques in order to mitigate against one particular attack, the wormhole attack.

Having considered the security threats to which a sensor network may be subjected, it is important to thoroughly consider how to analyse performance of systems in a real sensor network. The following chapter will analyse the mechanisms of data transmission within a WSN to discover their inherent robustness, and how the impact of particular techniques on performance and energy efficiency can be measured.

# Chapter 4

# Wireless Sensor Network Modelling

## 4.1 Introduction

In order to derive conclusions regarding principles and techniques for the design and implementation of a WSN, it is important to have methodologies which accurately reflect essential details of the systems being studied. This allows evaluation of the resilience and security characteristics of WSN data transmission methodologies such as multihop routing versus distributed beamforming. This chapter presents models for how these mechanisms operate that will be employed elsewhere in the thesis. The performance of multihop routing versus distributed beamforming in the presence of jamming attacks is studied.

A variety of low-level communication modalities have been employed in sensor networking research, including acoustic [86] and optical via infra-red [87] as well as radio communication. When using exotic deployment scenarios such communications methodologies may integrate more naturally into the scenarios. For example, underwater environments naturally favour acoustic communication due to the high attenuation experienced by radio waves in this environment [86]. For MEMS technologies such as Smart Dust, space for antenna deployment and power limitations for analogue antenna hardware favour the use of optical communication over radio [87].

In current practical examples for above-ground deployment on centimetre-scale hardware, radio communication is the most common transmission modality for WSN systems [15]. This results from the mature and inexpensive transceiver technology, the ability to communicate without a direct line of sight, and the favourable licence-free regime of communications bands such as the ISM band.

The intent of this chapter is to explore how to engineer a viable sensor network, emphasising the importance of simulation and analytical approaches for the effective design of WSN systems. It will develop models for assessing the reliability of end-to-end radio communication to the sink via either multihop routing transport or via distributed beamforming in the presence of distributed signal jamming attacks. Finally, specific topologies representative of real deployments will be presented.

## 4.2 Difficulty Of Hardware Implementation

The highest fidelity approach to investigating a phenomenon scientifically is to perform the actual experiment under the intended conditions in the physical world. This principle indicates that the most valid design strategies and performance conclusions are those obtained not by modelling and simulation but by building and deploying the physical hardware in the target environment and testing its performance [88].

However, it is unlikely to be economical to design a network architecture and devise suitable protocol design environments entirely through in-field hardware deployments, and simulation must be the first stage of testing a protocol idea. In WSN protocol development, the design of a functional and stable protocol requires a degree of iteration, whether to test ideas, tune parameters for the desired performance characteristics, or to assess the emergent behaviour of a protocol. In addition to the difficulties of engineering a protocol that functions effectively on its own in a live system, protocols developed entirely in isolation can often need modification to function as part of an integrated protocol stack, and therefore a more holistic approach is favourable to produce a complete system [89].

Therefore, when testing a complex distributed system such as a WSN iteratively in a real environment, it may be difficult to isolate performance variations resulting from modifications to protocol design, as opposed to a consequence of variations in the environment between experiments. Studies of WSNs have found that subtleties in the deployment environment can have far-reaching effects upon the performance experienced, requiring significant performance monitoring and debugging once a system is deployed [90]. However, it is still important to use modelling and simulation as a first stage in the development of viable protocols.

The deployment of a full-scale sensor network trial may require several hundred nodes, which will amount to a significant expense. It is possible that a fraction of nodes would be recoverable once their batteries are exhausted, and therefore a proportion would be available for battery replacement and reuse. Nodes may be difficult to locate for recovery and reprogramming. Schemes also exist for nodes to be remotely reprogrammed via special reprogramming protocols [91] [51], which may help to perform in-network maintenance and resolve bugs that are discovered upon initial deployment. However, if nodes become unreachable for communication due to the failures the upgrade is designed to repair, manual intervention to recover them may be the only option.

Therefore the most feasible strategy for implementing a viable sensor network solution for a real-world problem is to rely upon simulation for the early phases, in order to define viable protocols that show stability and good performance under any threats the system is likely to experience. A series of trials escalating in complexity and fidelity, for example, starting with a simple test-bed with a smaller topology, will then be required to uncover any unhandled discrepancies between protocol behaviour and hardware characteristics, and to make any necessary adjustments to protocol behaviour. Through this iterative approach combining simulation with a series of phased deployment tests leading up to live deployment, it will be possible to engineer a stable WSN system.

The following sections provide models for distributed communications in a WSN system both through multihop routing and distributed beamforming, based upon empirical performance characteristics measured for typical WSN radio channels.

## 4.3 Simulation Software

### 4.3.1 Introduction

In order to analyse the models and protocols considered in this thesis, simulation software has been developed. Although all Turing-complete programming languages are equally expressive in terms of the algorithms they can compute and therefore the problems they can analyse, some have features that make them more suitable for deployment than others. For example, scripting languages such as Tcl are suitable for development of operating system scripts and other tasks which are not performance-critical, while compiled languages such as C or C++ are generally applied to performance critical tasks.

This section considers the languages used to construct the software used for simulations, their advantages and limitations, and motivates the decisions made.

### 4.3.2 Objective Caml

Objective Caml (OCaml) [92] is a functional, object-oriented programming language which generates fast native code. It has been applied to programming language research, system administration and network programming. It is compatible with Windows and Unix platforms, and can be linked to external libraries to provide a graphical user interface.

The flexibility provided by OCaml is capable of modelling general system behaviour in any problem domain, and encapsulating complexity via its object system. This makes it a very appropriate fit for complex simulations with a number of active components. For example, individual protocol layers can be modelled as individual objects, encapsulating all their internal state to make development easier and allow the isolation of individual bugs. Or alternatively, simulation conceptual functions such as routing or energy analysis can be easily separated into distinct modules. This produces elegant and well-structured applications that are easily extensible.

The type system provided by OCaml provides for strong static typing, and type inference, which serves to eliminate a large proportion of errors by checking that data items only undergo meaningful operations. This elimination of a number of logic errors allows the later phases of testing to proceed more quickly, as many bugs have been exposed before compilation succeeds.

A further advantage of OCaml is that the native code generator allows the production of extremely fast code, with a typical benchmark speed between C and C++. In comparison to MATLAB, this allows faster development, by permitting iterations to test and generate new results. It also increases the size of result sets that can be generated, and allows larger topology sizes to be used. Furthermore, many tasks can be parallelised via the use of distinct processes and inter-process communication, allowing simulations to proceed in parallel on systems with multiple processors.

The external library interfaces available for OCaml allow the use of a graphical user interface through the Simple DirectMedia Layer (SDL), which provides an intuitive tool for system testing and analysis and validation of expected protocol behaviour in complex scenarios. This high-performance GUI provides for accessible inspection behaviour of protocols, and permits faster development than merely examining result outputs or event log files. For example, the emergent behaviour of the original dynamic disturbance protocol described in Section 5.4.2, page 121, which led to the development of the dual routing strategy was motivated by examining the behaviour of the protocols using the graphical interface.

There are several disadvantages to OCaml. Firstly, the standard library supplied lacks many convenient data structures, or useful operations upon them. This requires the programmer to reinvent many standard library operations. Secondly, due to the sophistication of the type system, errors can sometimes be cryptic and be caused by errors at a different location than that reported by the compiler. Although a top-level and debugger are provided which allow interaction with a running system, it is difficult to reliably debug a complex application which uses external libraries such as the GUI. Furthermore, parallelism is difficult, and increasing performance on multi-core processors requires the code to be divided into independent processes or to use inter-process communication, which sometimes makes development unnatural.

### 4.3.3 MATLAB

MATLAB is a programming language intended for fast vector and matrix processing for scientific programming. A wide range of toolboxes for specific tasks exist, and its extensive use in scientific computing ensures that a wide range of third-party code components and software modules are available. The primary advantage to MATLAB is that vector processing is a better fit for applications involving integrated numerical calculations that fit naturally into vectors or matrices, and as a result MATLAB is widely used in signal processing applications.

MATLAB offers an extensive set of libraries and toolboxes to allow code reuse rather than independent development. Its plotting tools allow the user to rapidly experiment with the best and most intuitive way of presenting the results for system testing and documentation. As a result, all topology diagrams produced as graphs in the thesis are generated from MATLAB, even if they are saved from OCaml code originally.

Another compelling advantage of MATLAB is its support for interactive modelling of a scenario, via the interactive command prompt environment, which speeds development and testing in prototyping situations. For example, topologies can be generated, plotted, connectivity tested and routing performed, allowing rapid development through continuous adjustment and debugging of the protocols during development. For example, prototypes of the simulator used in Chapters 5 and 6 were developed in MATLAB.

There are several disadvantages to developing simulation applications with MATLAB. The first is the performance which is notably poorer than OCaml. Attempts to compile the code using a MATLAB compiler did not succeed under the system configuration available, and interactive rendering made it preferable to run the code as normal under the standard environment. The data types available are less rich than OCaml, which makes it less suitable for tasks that do not naturally fit a vector paradigm. Also, MATLAB provides parallelism through its **parfor** (parallel for loop) constructs; however these are not entirely transparent as language features, and restrict the ways in which code within the parallel loops can operate.

### 4.3.4 Software Simulations For Thesis Results

The simulations in Chapters 4, 5 and 6 are implemented in OCaml, although results are exported to MATLAB for the production of result graphs. MATLAB is also used to provide additional validation in Section 5.6.4, page 127 and Section 6.4.4, page 151.

The reasons for building the earlier code components in OCaml are that these applications were developed as part of a flexible and extensible architecture, which was envisioned to fit generic multihop routing applications. As distributed beamforming concept was added, MATLAB proved a more natural fit which was easier to work with and debug interactively, especially in the presence of supernodes which may have statistical performance variations. Therefore, the simulator for Section 7, page 158 was implemented in MATLAB. The reduced performance of MATLAB relative to OCaml was compensated for with additional hardware, specifically a multi-core processor which permitted faster execution of the simulations in parallel.

## 4.4 Radio Communication Characteristics

Having established that it is too expensive to attempt to model protocol development completely via live deployments on a full-scale trial, it is important to investigate the characteristics of radio communication in the WSN environment. Through this, a suitably accurate model to use in simulations of system performance can be developed.

### 4.4.1 Theoretical Models Of Radio Propagation

In order to understand radio propagation in the typical scenarios encountered in WSN deployments, it is first necessary to understand propagation in the simplest possible physical environment, namely entirely free space without any interference from external devices, ground reflections, or obstructions to the signal path. Accordingly, this section will present a series of theoretical models for wireless communication of increasing fidelity, adding parameters to increase the resemblance between the scenarios modelled and reality.

#### 4.4.1.1 Friis Equation For Free-Space Path Loss

Consider a simple one-hop transmission between a source sensor node $N_{TX}$ and the sink node $S$. The gains of the antennas at the transmitting node and sink can be denoted $G_{TX}$ and $G_S$ respectively. The node is separated from the receiving sink by distance $D$ metres. The transmitting node is transmitting a signal with power $P_{TX}$ and wavelength $\lambda$. In this scenario, assuming both entities are within free space, the Friis formula (Equation 4.1, page 82) gives the linear signal power ($P_{RX}$) received at the sink:

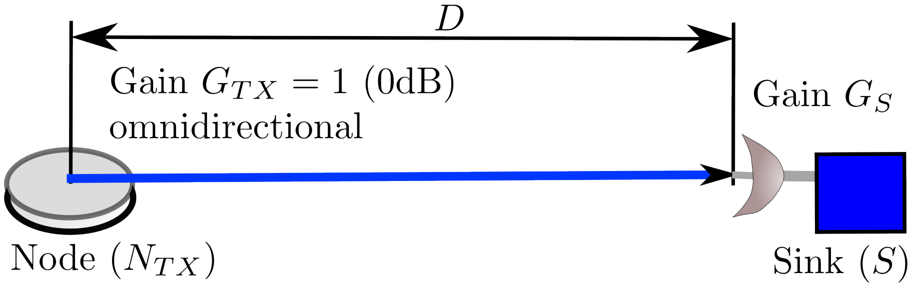

Figure 19: A simple scenario for one-hop transmission/reception in free space

$$P_{RX} = P_{TX} G_{TX} G_S \frac{\lambda}{4\pi D^2} \tag{4.1}$$

The Friis equation can be expressed logarithmically (Equation 4.2, page 82). In this form it consists of a term for transmission power, two terms for gains of transmitters and receivers respectively, a term depending on the wavelength of the transmission, and the distance-dependent term (path loss). It is clear from the structure of the equation that, for narrowband transmissions of equal or roughly equivalent wavelengths as occur in WSN channels, distance has the greatest influence upon received signal strength.

$$P_{RX}(dB) = P_{TX}(dB) + G_{TX}(dB) + 20log_{10}\left(\frac{\lambda}{4\pi}\right) - 20log_{10}(D) \tag{4.2}$$

#### 4.4.1.2 Two-Ray Model For Ground Reflection

The most notable divergence between the free-space model and real-world deployments is the presence of the ground. This is particularly acute for WSNs as in many applications it is anticipated that miniature nodes are to be deployed with integrated antennas lying very close to the ground. The ground has a significant impact upon radio propagation due to reflection effects introduced.

In most WSN scenarios it is assumed that nodes are very close to the ground, and therefore transmission and reception antenna heights are extremely small in comparison to the distance of signal travel $D$. For example, nodes typically lie within a few centimetres of the ground, while a typical communications distance is to the order of tens of metres. Accordingly, the rays produced meet the ground with glancing incidence, as illustrated in Figure 20 (not to scale vertically). The figure shows transmission from a node to the sink in a single hop, with node and sink antenna heights of $H_{TX}$ and $H_S$ respectively.

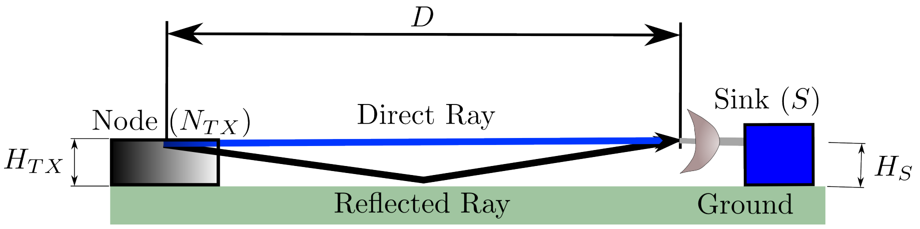

Figure 20: Two-ray model for one-hop transmission/reception in the presence of ground reflections

When a ray meets the ground and is reflected with glancing incidence, it undergoes a 180 degree phase shift [93]. The relative differences between the path lengths of the direct and reflected rays, together with the phase shift occurring from the ground produce either constructive or destructive interference depending on their relative path distances and the phase shift from the ground. In reality the ground surface is not a perfect reflector, absorbing some energy from the origin signal, and therefore the two rays never interfere perfectly destructively. At sufficiently large distances in which $D \gg \sqrt{H_{TX} H_S}$, this produces an overall inverse-fourth power rolloff of received signal power with distance [93] (Equation 4.3):

$$P_{RX} = P_{TX} G_{TX} G_S \left( \frac{{H_{TX}}^2 {H_S}^2}{D^4} \right) \tag{4.3}$$

#### 4.4.1.3 Shadowing and Log-Distance Rolloff

The free-space and two-ray models do not include the presence of objects acting as obstructions between the sink and the receiving antenna. However, in reality many objects can interfere with the direct signal ray, by absorbing energy from a signal and therefore reducing its strength. Potential static obstructions that can contribute to shadowing include buildings and vehicles in urban areas, and trees, hills and landscape features in environmental monitoring scenarios.

Since the impact upon any particular link is complex and depends on the exact shape and distribution of objects within the environment, shadowing is typically treated statistically [94]. Shadowing is conventionally modelled as a log-normal distribution with zero mean and a fixed variance. Equation 4.4, page 84 gives the structure of a log-distance loss equation featuring shadowing, in which a decibel value sampled from the shadowing distribution $X_\sigma$ is added to a distance-based path loss. $k$ is a constant representing the one-metre loss. Although the two-ray model predicts an inverse-fourth power rolloff with distance, the equation uses a customisable parameter $\gamma$ for rolloff rate. This allows the effect of the environment and any obstructions within it, which may alter mean loss characteristics, to be accounted for. $\gamma = 2$ represents the conventional inverse-square free space model, and $\gamma = 4$ represents the inverse-fourth loss predicted by the two-ray model.

$$L(dB) = G_{TX} + G_S + k(dB) + 10\gamma log_{10}d + X_\sigma \tag{4.4}$$

In the next section, empirically sampled values for these parameters in typical environments will be presented, supporting the extension of this model into two discrete distance regions (a near-field and far-field) with distinct parameters and characteristics.

### 4.4.2 Empirical Research On Propagation

Martinez-Sala et al. [95] performed empirical studies of the propagation losses for WSN communication in three different physical environments. They discovered that a two-slope log-distance loss model (separating the loss characteristics into near-field and far-field regions) with shadowing provides a good model within flat plain, urban, and outdoor park environments. The two-slope model is defined by the following pair of equations. Equation 4.5, page 84 applies to all distances within the transition region (breakpoint) and defines the near-field region behaviour, and equation Equation 4.6, page 84, applies to distances greater than this and defines the far-field.

$$L(d)(\mathbf{dB}) = L_{01} + 10\gamma_1 log_{10}d + X_{\sigma 0} \text{ if } d < d_r \tag{4.5}$$

$$L(d)(\mathbf{dB}) = L_{02} + 10\gamma_2 log_{10}d + X_{\sigma 1} \text{ if } d \gg d_r \tag{4.6}$$

Empirically measured parameters are provided in Table 1, and demonstrate the best fit (smallest statistical variables) in outdoor and rural environments. These parameters indicate that the most uniform channels are found in physical environments with the least environmental variation and without obvious obstruction.

It is notable that the breakpoint in Martinez-Sala's two-slope model is particularly close in all environments, particularly for sparsely deployed topologies. In the further work in this physical-layer modelling, the far-field environment will be considered, as this range is more realistic given the limited deployment densities in a sparse sensor network deployment. Although shadowing is a statistical phenomenon, it is possible

| Symbol | Parameter | Ground plain environment | University yard | Park |
|---|---|---|---|---|
| $\gamma_1$ | Near field exponent | 2.34 | 2.76 | 2.09 |
| $\gamma_2$ | Far field exponent | 3.73 | 4 | 4.01 |
| $\sigma_1$ | Near shadowing std. dev. | 0.6 | 2.98 | 0.28 |
| $\sigma_2$ | Far statistical std. dev. | 0.42 | 1.82 | 0.67 |
| $d_r$ | Breakpoint (m) | 6.2 | 3.2 | 0.95 |
| $L_{01}$ | One-metre intrinsic near loss (dB) | 37.8 | 63.24 | 72.1 |
| $L_{02}$ | One-metre intrinsic far loss (dB) | 26.79 | 44.5 | 41.9 |

Table 1: Parameters for the two-slope model for typical WSN channels in three environments discovered in [95]

to model it by including a shadowing distribution via which a logarithmic normally-distributed value is added to the loss output from the raw distance-based SINR model. By adding a conservative amount to the overall SINR requirement in the link budget, it is possible to develop a system which is resilient with high probability against temporary link changes brought about from shadowing and fading.

In the thesis, the far-field region of this model will be employed to analyse the communication properties of distributed beamforming (Section 4.5.2, page 89), for computation of the link properties and assessment of the transmission success. For short-range communication, given that the distance is shown to be the most significant factor in connectivity, the protocol model can be employed, which considers the closest interferers as significant.

### 4.4.3 The Protocol Model

The protocol model [33] is a simple model of connectivity which provides a static distance-based model of propagation success. It can be represented as a pair of graphs, the communication graph $C$ and interference graph $I$ defining communication and interference relationships [96]. Nodes constitute the vertices of these graphs and interactions between them, the edges.

Any nodes connected by an edge in $C$ can communicate without interference, as long as no node connected in $I$ to the receiver is also transmitting simultaneously.

Assuming a planar network in which loss is distance-based, this model defines a fixed connectivity range $c_r$ over which nodes can communicate, as long as no node within the receiver's interference range is transmitting concurrently. This situation is referred to as a collision. The interference range is $I_r = (1 + \Delta)c_r$, and so is larger than the connectivity range by an additional factor of $\Delta$. Typically values of $\Delta$ assumed to be significant for collision avoidance are in the range of 1.0 to 2.0, corresponding to significant interferers twice or three times further away from the further communications peer.

Figure 21, page 86 illustrates the protocol model of connectivity. Nodes A and C cannot ever communicate, since C is outside A's connectivity range. A and B can communicate, as long as any node in B's interference range is silent. Here, if I is transmitting to Z, A cannot simultaneously communicate with B under the protocol model. In this diagram, $I_r = 2c_r$, that is $\Delta = 1$.

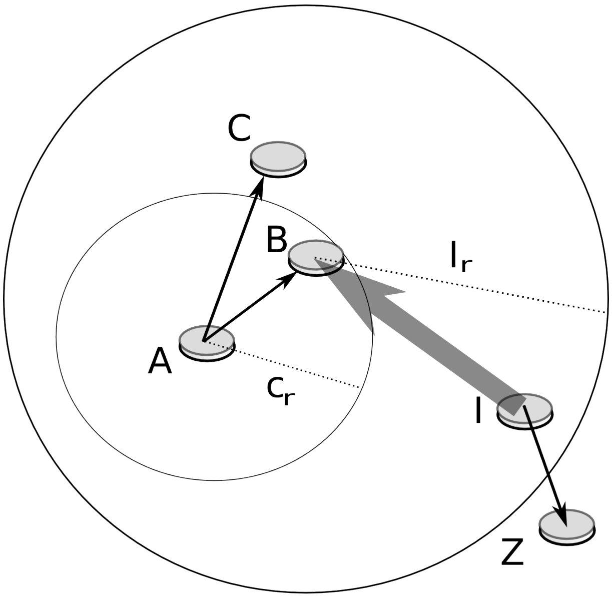

Figure 21: The protocol model of connectivity

#### 4.4.3.1 Protocol Model Validation

The intuition behind the protocol model is that transmissions from nodes outside of the interference range can be disregarded, given the high log-distance loss exponent assumed. For example, a node twice as far away as the furthest potential communication peer, under log-distance loss exponent $\gamma = 4$ experiences an additional distance-based loss approximately 12dB greater than the peer. With homogeneous WSN nodes transmitting with equal power, the contribution of sufficiently remote nodes to interference (and therefore to collision events) is typically assumed insignificant. This section analyses the physical-layer interference characteristics of transmissions to determine whether obeying the protocol model constraints produces reliable reception, using the empirically sampled model in Section 4.4.2, page 84.

Figure 22, page 88 presents a cumulative distribution function (CDF) of the signal-to-interference (SIR) ratio for 10000 trials in simple one-hop transmission-reception under the protocol model. A number of active interfering nodes are located between two and three times further away from a central receiver than its associated transmitter. This obeys the protocol model in the most permissive case of $\Delta = 1$, in which the closest interferer permitted is twice as far as the transmitter. Physical layer parameters are obtained from Martinez-Sala's two-slope log-distance loss model for the university environment (Table 1, 85), the most variable environment in which the greatest impact from shadowing is anticipated.

The results in the CDF show that in the presence of a single active interferer, 99.9% of test trials experienced a SIR greater than 3dB. In the presence of 3 active interferers outside of the interference range, 98.9% of trials still succeeded. With 5 interferers operating the figure is 96.6%. Therefore, only 3.4% of transmissions fail to deliver an SIR of 3dB or greater under the protocol model assumptions of interferer location, even in this rare case of local congestion. The presence of additional simultaneous interferers within this close a range would be rare, given that such interferers would require protocol model protection for their own transmissions.

This therefore validates the protocol model as a reasonable approximation to model connectivity in realistic physical-layer scenarios. Within this thesis, activity within the interference graphs will not be analysed as it is assumed that the MAC scheme provides sufficient collision protection to prevent these contending transmissions. The communication graph, and the range limits that generate it, will be analysed to determine connectivity properties of multihop routing topologies.

## 4.5 Supernode Communication Architecture

### 4.5.1 Introduction

Having considered the characteristics of direct short range communication between a single transmitter and receiver, this section explores an alternative communication

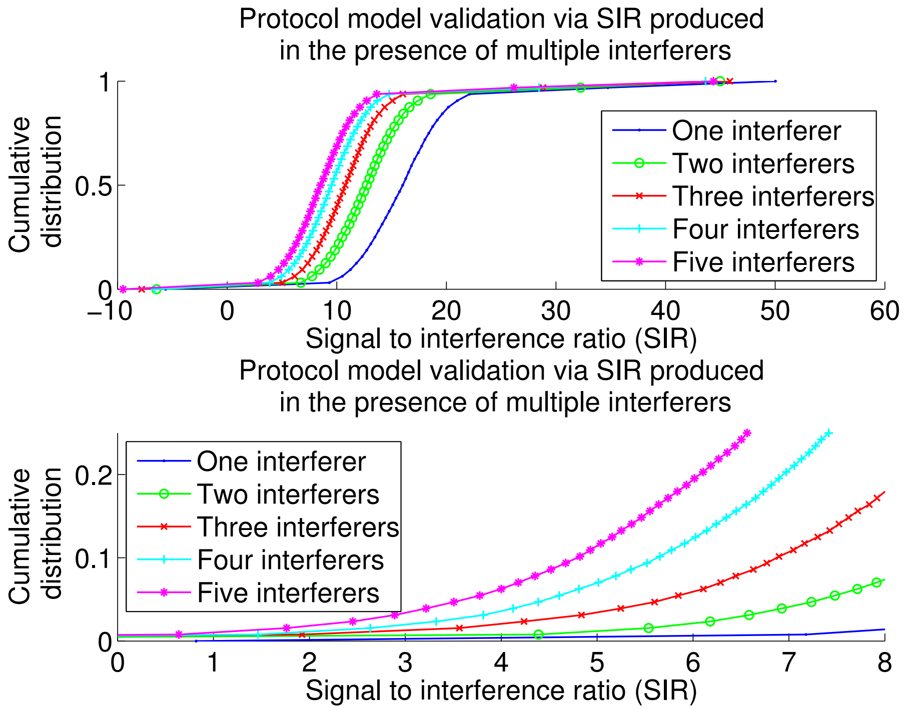

Figure 22: Physical SIR in the presence of interferers conforming to the protocol model

methodology. This employs distributed beamforming from a geographically close cluster of nodes (supernodes) in order to transport network data to the central sink. There exist a number of clear potential advantages to the use of supernodes for data delivery as compared to multihop routing:

**Restriction of coordination and key management** Although solutions for key management across an entire WSN exist (as explored in Section 3.9, page 70), key management is inherently easier and lower in overheads if it is highly localised and the only long-range communication is with a single highly-resourced, line-powered entity such as the sink.

**Location concealment of sources** In security-conscious environments an adversary may desire to reveal the location of transmitting entities. The supernode approach may be helpful to disguise a transmitting source from remote interception by spreading the power density of participating entities. This could potentially be useful to disguise the location of data originators in scenarios assumed to be subject to sophisticated physical-layer monitoring, such as military environments.

**The relaying burden presented by multihop routing is removed** The relaying burden leads to a per-node reduction in capacity as multihop networks scale

[33] due to the requirement for nodes to collaboratively forward their traffic over long distances. In particular, the greatest bottlenecks in a multihop WSN, those closest to the sink relaying more data for other nodes, are removed or relieved of some of their activity through this approach. Although there is the necessity for coordination amongst the supernode entities, the burden upon individual nodes is distributed more evenly. The complexity of coordination of remote entities is placed upon the sink, which, given its access to line power and directional antennas, is more capable of handling it.

### 4.5.2 Distributed Beamforming Fundamentals

In work upon the theory of random arrays it is established that the linear gain of $N$ transmitting antennas can be shown to be $N$, assuming perfect phase synchronisation amongst the transmitting elements [97]. A recent survey [98] covers current developments in beamforming, giving coordination approaches and options for organising their mutual communication and phase synchronisation process. This section introduces the supernodes as a fundamental communication primitive to be used by higher layer services, and outlines their mechanisms of operation.

Since sensor networks are normally energy-constrained due to their reliance upon limited batteries, it is vital to be aware of approaches which can improve performance and deliver energy efficiency advantages. Beamforming technologies can provide compelling improvements in energy efficiency [99]. Typical energy efficiency advantages over routing protocols occur from the removal of the overheads brought about by route formation protocols, together with the relaying burden during data delivery, with the removal of a requirement for idle listening, reception and retransmission at intermediate hops. Although a beamforming transmission may require many nodes making a simultaneous transmission, the transmitting group are typically spatially close and thus easily coordinated, thus reducing the energy impact of their transmissions.

As with any distributed systems technique, beamforming is dependent upon close cooperation between the participating nodes. A coordination process is presented [100] through which a pair of beamforming nodes can establish timeslots for transmission, with the aid of a central coordinator. Since the beamforming process is dependent upon close cooperation and tight time synchronisation between nodes, it is important to establish its robustness to timing or phase synchronisation errors. Deng et al [101] provide a performance analysis of the error tolerance of distributed beamforming technologies, and concludes that RMS phase errors within 0.5 radians lead to less than 3dB degradation of the peak beamforming gain in 95% of cases. Therefore, as long as the coordination protocol can deliver this approach, then supernode performance should be within a 3dB limit of the intended value.

### 4.5.3 Beamforming Architecture

In the beamforming approach considered in this thesis, collaborative transmissions are made from a cluster of geographically close nodes (a supernode) to relay information directly to the sink node in a single hop. Supernodes were proposed for location concealment of sources as part of a Ministry of Defence Competition of Ideas project conducted in the Communications Group of the Department of Electronics in York [43].

Using dynamically formed beamforming clusters to perform a long-range relaying task is implicitly difficult to place within the standard layer model. Essentially, long-range physical links are dynamically formed from lower-layer interactions, solving problems that would normally be solved at the routing layer through a combination of physical-layer and media access techniques requiring small-scale time synchronisation. A local collaboration is required to form supernodes, but multihop routing is only required for an initial flood to inform the sink of their identity.

The model assumes a cluster of beamforming nodes, the supernode members (SNMs) closely distributed around a coordinator (Figure 23), which assists the nearby nodes to perform beamforming. This single cluster is termed a supernode, and those that participate in its collaborative transmissions, including its coordinator, the *supernode normal members* (SNMs). These supernodes transmit to a sink employing directional antennas, and are organised by a network-wide media access scheme so as not to interfere with each other, as described in Section 4.5.4, page 92. The following section presents an architecture for transmission from the supernode to the sink node is arranged via the following stages:

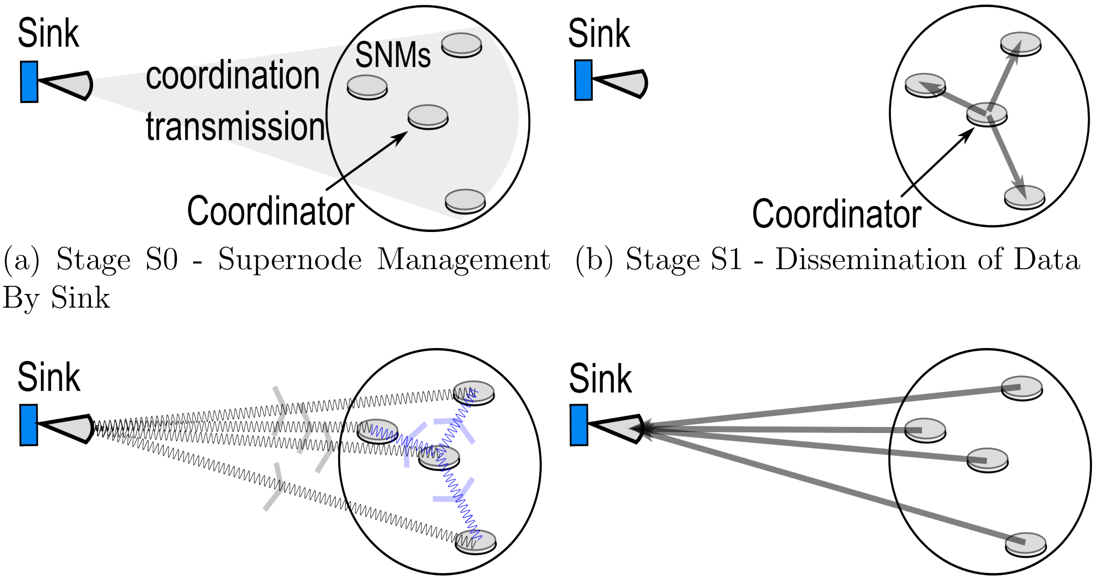

(a) Stage S0 - Supernode Management By Sink

(b) Stage S1 - Dissemination of Data

(c) Stage S2 - Phase Adjustment

(d) Stage S3 - Supernode Transmission and Sink Reception

Figure 23: The supernode and the phases of data transmission using distributed beamforming to relay information

#### 4.5.3.1 S0 - Supernode Management By Sink

During stage S0 (Figure 23a), a periodic transmission is made to carry control information to a supernode coordinator. For example, performance statistics such as the SINR delivered by previous transmissions from this supernode are periodically updated. It will act as a master time coordinator, informing the supernode coordinator of any timing constraints affecting its transmission, and give timing at which phases S2 and S3 must be performed.

#### 4.5.3.2 S1 - Dissemination of Data

During stage S1 (Figure 23b), data for transmission is sent from the data originator to the coordinator. The coordinator disseminates this transmission to all SNMs. Here it is assumed that all originating nodes are within range of a supernode, or can form a multihop route to reach one (via mechanisms explored in Chapter 7). This transmission may be unicast, but it is anticipated to be broadcast from the coordinator since it distributes identical data to all surrounding nodes. An acknowledgement from the nodes to the coordinator is expected, and retransmissions may be performed if the nodes do not correctly receive the data.

#### 4.5.3.3 S2 - Phase Adjustment

During stage S2 (Figure 23c), phase adjustment is made to allow the beamforming transmission to occur successfully. Phase adjustment is assumed to follow a master-slave architecture [100] [102] [103]. In this process the sink transmits a known frequency reference carrier, which is compared with a carrier broadcast from the coordinator to the supernode members. Through measurement of the relative timing offset, the coordinator can determine an appropriate phase offset for transmission. It is expected that this phase will occur less than 100 milliseconds before stage 3.

#### 4.5.3.4 S3 - Supernode Transmission and Sink Reception

During stage S3 (Figure 23d), the supernode member nodes (SNMs) perform their transmission, using the synchronisation information established. A known preamble is added to the data to allow the sink to synchronise upon the beamformed data and determine its start, compensating for any delay introduced by the channel. The previous stage S2 is used to determine the phase offset to apply to transmission. It is anticipated that this stage will occur less than 100 milliseconds after phase S2, to minimise oscillator drift in the meantime and meet the criterion in Section 4.5.2, page 89, for signals arriving at the sink with sufficient phase synchronisation to obtain the beamforming gains.

During this stage, the sink begins reception of the beamformed data. The phase offsets established allow the transmitted signals to arrive constructively, increasing their SINR and permitting the sink to receive the data. The SINR for reception is measured and used to update statistics for the supernode, which are delivered back to in the next S0 phase.

### 4.5.4 Supernode Formation and Media Access

It is possible to form supernodes either statically or dynamically. Static formation refers to nodes being preassigned with identities as supernode coordinators or members, with the attendant disadvantages of requiring manual involvement and configuration of nodes before deployment. This requires the same type of manual configuration of a relaying backbone as discussed in Section 2.2.1, page 36. It would be desirable if supernode formation could be dynamic, to permit self-organisation.

In order to form supernodes dynamically, it is necessary for nodes to discover their local neighbourhood, to avoid the problem of too many supernodes forming. A node which wishes to join a supernode first waits to see if any supernode formation broadcasts are received within a randomly selected time interval. If none are received, it begins formation as a coordinator with a restricted flood, which serves to both suppress supernode formation at nodes receiving it, and update a gradient pointer giving the location of the supernode to other nodes that may wish to reach it via multihop routing. This process effectively partitions the network regions into supernodes, in a similar manner to the cluster head selection of LEACH [104].

Newly formed supernodes then make a one-off multihop routing flood in order to inform the sink of their identity and node membership. The address assigned to a supernode is determined by the identity of its coordinator. Upon this the coordinator directs all nodes in the supernode to listen continuously, in anticipation of their first coordination broadcast for stage S0. The sink, upon receiving this broadcast, maintains a timing schedule for the supernodes in order to divide network capacity between them. Since this information is held centrally, it is easy to make a fair division of network capacity across all supernodes. Supernodes which do not reply for a fixed interval are removed from the allocation. Depending on hardware available at the sink, as discussed in Section 4.5.5.2, page 94, it may be possible to use space-division multiplexing in order to share capacity amongst the nodes.

### 4.5.5 Hardware Aspects of Supernode Communication

#### 4.5.5.1 Node Oscillators

It was noted that delay between stage S2 and S3 must be limited in order to minimise oscillator drift between the different stages and a consequent reduction in beamforming gain. In order to improve flexibility of this aspect, low-phase noise oscillators may be helpful [22]. It is expected that as WSN technology matures, low-phase noise oscillators will allow phase synchronisation to be held over longer time periods.

#### 4.5.5.2 Requirements For The Sink

Two possibilities present themselves for sink antenna management for the reception in the phase S3 above. The simplest possible option would be an omnidirectional antenna, in which all gain is delivered by the supernode beamforming process. The advantage of this is the lowest implementation costs and complexity due to its simplicity, with no requirement for antenna alignment or multiple antennas to receive simultaneously from a variety of nodes. The disadvantage is the reduction in capacity involved, since only a single supernode can be transmitting simultaneously throughout the network. This would represent a more significant capacity bottleneck than the use of conventional bottlenecks around the sink in multihop routing.

A more productive alternative is to apply a set of highly directional antennas to divide the network into angular sectors, as in the sectorisation approach in a cellular system. The advantage of the directional antenna approach is to increase capacity by allowing spatial reuse, through providing rejection of interference from other supernodes in other sectors of the network.

## 4.6 Hybrid Approaches

### 4.6.1 Routing To Reach Supernodes

It is possible to employ multihop routing in order to reach a supernode. The advantages of doing so include a reduction in the requirement for every node to be within range of a coordinator, which allows supernodes to be formed opportunistically. This allows for more flexible integration of supernodes into a network.

The flexibility of this strategy lies in its implicit fallback and failure tolerance, in that if a supernode cannot be reached, it is always possible for nodes to form a multihop route directly to the sink as in the conventional case. By providing a variety of transmission methodologies, nodes have more options for finding a viable transmission methodology in the presence of diverse attacks. Chapter 7 presents a routing algorithm, physical reputation-based routing (PRBR) that finds routes through high-performance supernodes.

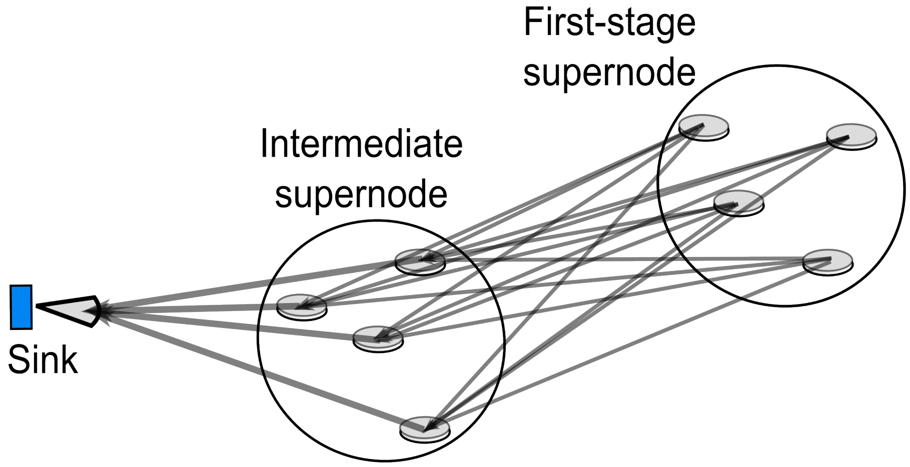

Figure 24: A hybrid supernode relaying strategy in which nodes relay their data through at least one other supernode before it reaches the sink

### 4.6.2 Hybrid Routing To Supernodes

It is also possible to perform transmissions from a supernode for reception at an intermediate relaying supernode, for further retransmission. In this approach, the destination of the beamforming transmission of the first-stage supernode would itself be a supernode. This is illustrated in Figure 24, page 95. This would provide much greater diversity through the number of possible independent channels generated, and therefore resilience against fading of any individual link between a single sender and receiver. However, the complexity of these algorithms is likely to increase unacceptably, together with problems at a system integration perspective.

There are several problems that limit the applicability of this approach. Supernodes are implicitly distributed and thus disparate entities. Since their presence is transitory, it would be difficult to devise a practical and scalable scheme to communicate between them their initial locations for route formation. Also, the use of directional antenna transmission in order to initially coordinate supernodes (i.e. to inform their presence and parameters) would be difficult without the presence of some single heterogeneous device, the sink which can serve to organise their initial communication. As a result, the supernode cases considered in this thesis all use the sink as an endpoint and not another supernode.

## 4.7 Topologies and Network Scenarios

This section will present three standardised models for node placement which are used in various models throughout the thesis. In order to provide a fair comparison between networking methodologies, it is important that the network topologies which are studied are sufficiently well-connected to allow all nodes to be reachable from the sink. For example, a topology in which the sink was not reachable from some nodes would be excessively vulnerable to a wormhole attack, and inherently unable to implement wormhole avoidance as the wormhole would be required in order to connect the topology. Therefore, this section analyses the connectivity behaviour of various topologies.

## 4.8 Topology Models

In some scenarios, it is possible to control the physical placement of nodes very precisely. This is referred to as deterministic coverage [105]. In networks in which nodes will be deployed manually in unobstructed terrain, deterministic coverage may be viable. However, this approach does not capture the impact of variability in placement, which may arise from physical obstructions in the deployment region, vulnerabilities in physical security limiting activity, or the inherent variability resulting from large-scale placement of devices such as aerial scattering of nodes. This leads to stochastic coverage [106], in which the placement of nodes is not fully deterministic, but incorporates variability.

Three topology placements are used throughout the thesis. If the sink can be centrally placed, a radial ring arrangement can be employed, with nodes upon each ring at a progressively greater distance from the central sink. However, this approach does not capture the impact of variability in placement, which may arise from physical obstructions in terrain, or automated placement such as aerial scattering of nodes. Accordingly, this thesis incorporates other topology models which serve to represent a realistic range of coverage strategies. These are the uniform random and grid-based Gaussian variation models.

If connectivity is sufficiently deterministic and follows the protocol model, it is possible to extrapolate local connectivity properties to the whole network. This

| | |
|---|---|
| Radial ring separation distance | $s$ |
| Arc length per node in ring $r$ | $k_r$ |
| Number of rings | $R_{max}$ |

Table 2: Parameters for the radial ring topology

can be done by considering the network itself a graph with each link as a vertex, determining from the behaviour of individual links whether nodes are reachable via any path within the topology. Computing the transitive closure upon this network graph starting from the sink, and measuring the number of nodes included, is able to determine whether nodes are reachable from the sink. Connectivity properties are therefore important since they set constraints on the number of devices that must be deployed to engineer a stable network.

As shall be investigated in Section 4.8.2, page 99, the connectivity of a network strongly depends on the density of nodes deployed, or upon their communication ranges relative to separation distance. Once a sufficiently large number of nodes is deployed, a multihop routing network suddenly passes the point of being disconnected islands and a high proportion of nodes become reachable from the sink. This is called the network connectivity phase transition [107]. Therefore, studying connectivity is able to predict whether a network will be sufficiently robust to fulfill its intended application goals, even without the presence of malicious attack.

### 4.8.1 Radial Ring Based

The radial ring topology consists of a single central sink node, surrounded by nodes arranged in concentric circles. It is assumed that the sink node possesses an out-of-band channel, or wired link allowing it to relay its information out of the sink. This topology structure is entirely deterministic, in that the location of each node can be determined precisely.

An advantage of the radial-ring topology is that by arranging the sink node to lie at the centre of concentric circles, routes from a particular distance away from the sink all have consistent hop lengths. The connectivity of the topology can be easily determined, and as will be be demonstrated, is highly consistent. The radial-ring based topology is structured according to the parameters in Table 2. The circumference of ring index $r$ is $2\pi sr$, and if $N_r$ nodes are placed around it, each with an equal angular separation $\theta_r$, then $N_r\Theta_r = 2\pi$.

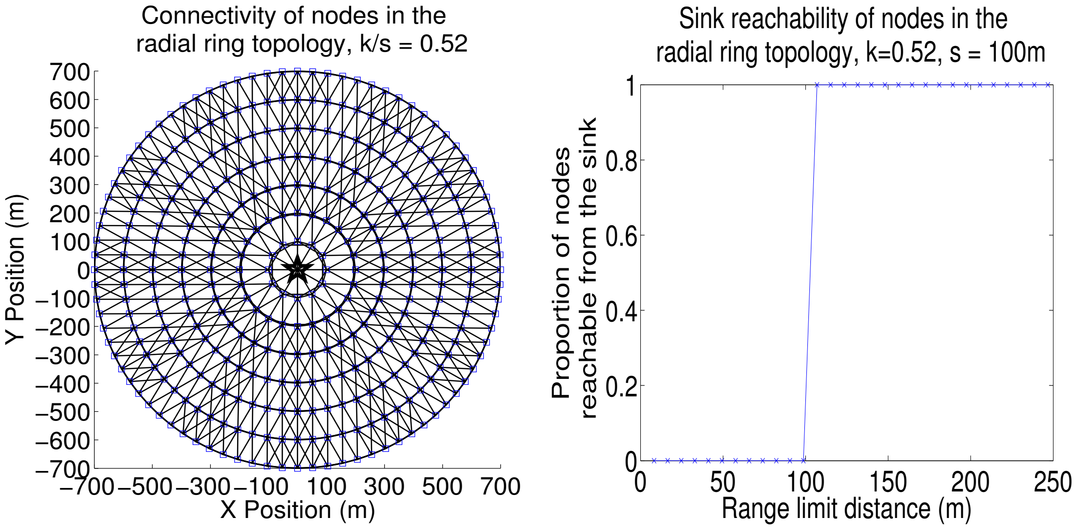

(a) Topology structure

(b) Proportion of nodes reachable from the sink

Figure 25: The radial ring topology and its connectivity (sink reachability)

In order to maintain connectivity between adjacent nodes in all radial rings, the arc-length is equalised across all radial rings, so for all $r$: $\forall r.k_r = k$. The integer number of nodes that can be placed around this ring, producing an arc-length between them of less than $k_r$, is:

$$N_r = \left\lfloor \frac{2\pi s r}{k} \right\rfloor$$

Therefore the corresponding $\theta_r$:

$$\Theta_r = \frac{2\pi}{N_r} = \frac{2\pi}{\lfloor \frac{2\pi s r}{k} \rfloor} \tag{4.7}$$

Therefore, in ring $r$ there exist $N_r$ nodes, $\{N_{r,0}, N_{r,1} \dots N_{r,N_r-1}\}$. The location of node index $n$ in ring $r$ in polar coordinates $(R_{r,n}, \theta_{r,n})$, is defined by Equation 4.9.

$$R_{r,n} = rs \tag{4.8}$$

$$\theta_{r,n} = \Theta_r \frac{(n-1)}{N_r} \tag{4.9}$$

A sample of the radial ring topology is presented in Figure 25, page 98, for parameter values $k = 0.52$ and $s = 100m$. The connectivity of the topology is analysed using a transitive closure algorithm. The transitive closure is found by starting at the sink, finding all nodes reachable from it, and iterating until all nodes connected to a reachable node are found. All nodes within the transitive closure of the sink will be able to find a viable route from the sink.

Figure 25b, page 98 illustrates the proportion of network nodes reachable from the sink. The reachability shows a very clear transition around the ring separation $s$. This is as expected, illustrating that the topology is highly regular. This topology will be used in Section 4.9, page 101 in the analysis of the performance of supernode and multihop relaying.

It is notable from the link structure depicted that some irregularities exist in which nodes are connected to adjacent peers in surrounding rings offset at an angle, while others are disconnected. Although the topology structure attempts to attain a consistent spacing around all radial rings, the restriction to an integer number of nodes within any ring makes this unattainable in all cases, which leads to situations in which some nodes have different peer counts dependant on their positions around the ring. Therefore, some nodes have better connectivity to the inner and other rings than others.

### 4.8.2 Uniform Random

The uniform random topology features entirely stochastic placement [106], in which both axes of the nodes Cartesian coordinates are uniformly distributed across the topology region, a square of side $S$ centred upon the origin. This may correspond, for example, to aerial deployments from high altitude, or the results of initially mobile nodes settling e.g. following mobility or drifting, or others with no a priori information about node placement other than a uniform density across the topology. The coordinates of uniformly randomly distributed node $N_i$, $(UX_i, UY_i)$ are defined as the result of drawing two independent samples from a pair of uniform distributions spanning axes along side of the deployment region.

One realisation of the uniform random topology is illustrated in Figure 26, page 100, showing a phase transition change in the connectivity pattern for a deployment of 100 nodes. In Figure 26a, page 100 the range cutoff for communication $D_{MAX} = 56m$ limits the nodes to disparate islands, but in Figure 26b, page 100, with $D_{MAX} = 110m$ the topology is now fully connected. The sink reachability of the nodes is presented in Figure 26c, page 100. Compared to the radial ring model, the uniform random topology model shows a gradual increase in sink reachability with maximum communications range, as the link lengths involved are more variable. It is notable that the link length that connects the topology fully with some redundancy is

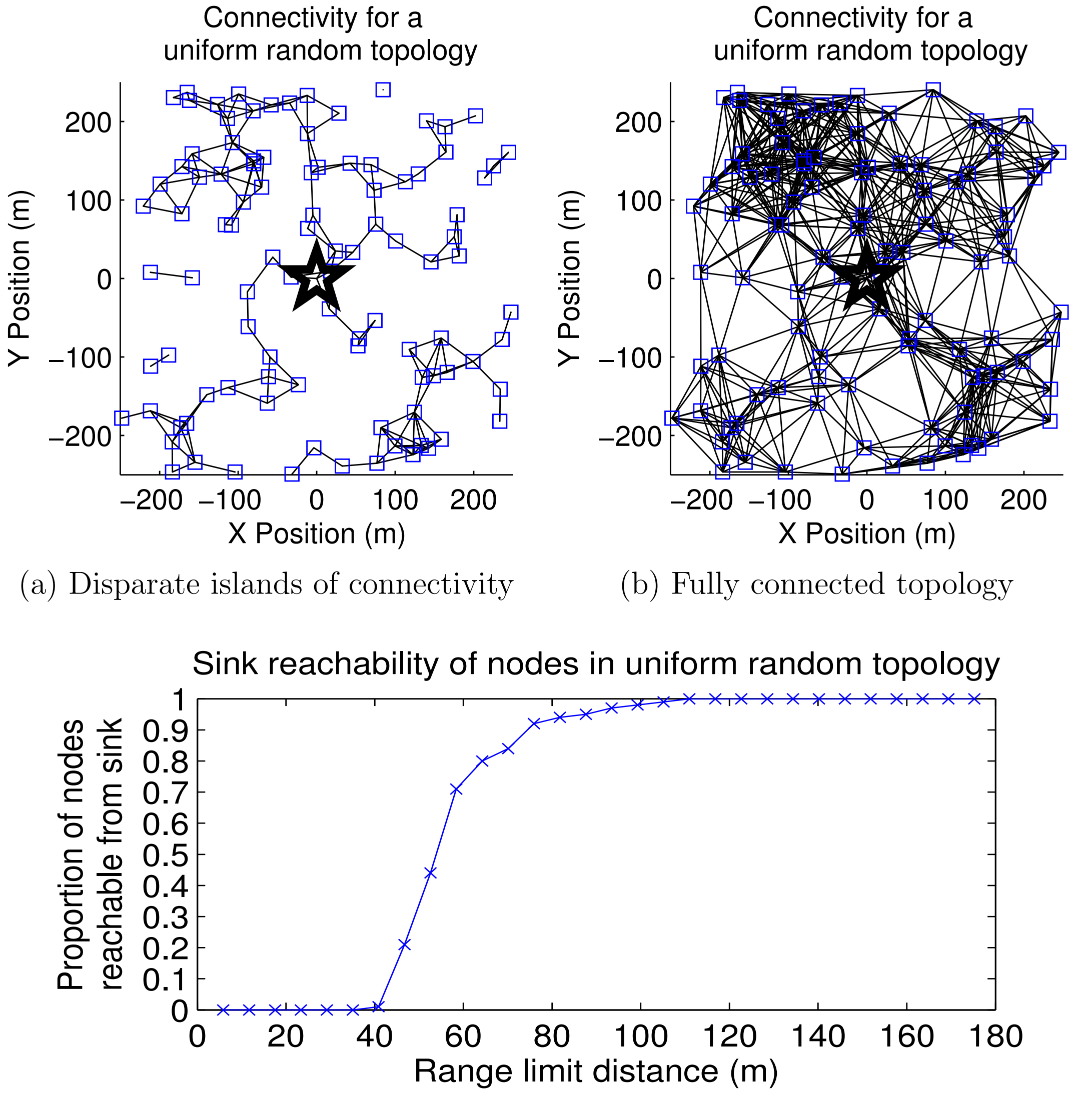

(a) Disparate islands of connectivity

(b) Fully connected topology

(c) Proportion of nodes reachable from the sink

Figure 26: The uniform random topology and its connectivity (sink reachability)

approximately double the connectivity of the mean link length (for this realisation $60m$).

#### 4.8.2.1 Grid-Based With Gaussian Variation

A grid topology consists of nodes placed precisely upon a regular grid. This is a standard topology model, the intuition behind which is to make sure that phenomena are covered by a subset of multiple sensors [108]. It also helps to ensure topology connectivity by giving each node a fixed number of neighbours, so if some links are broken due to link variability such as shadowing or slow fading, then the node is still reachable from other peers. The grid-based Gaussian variation topology (Figure 27,

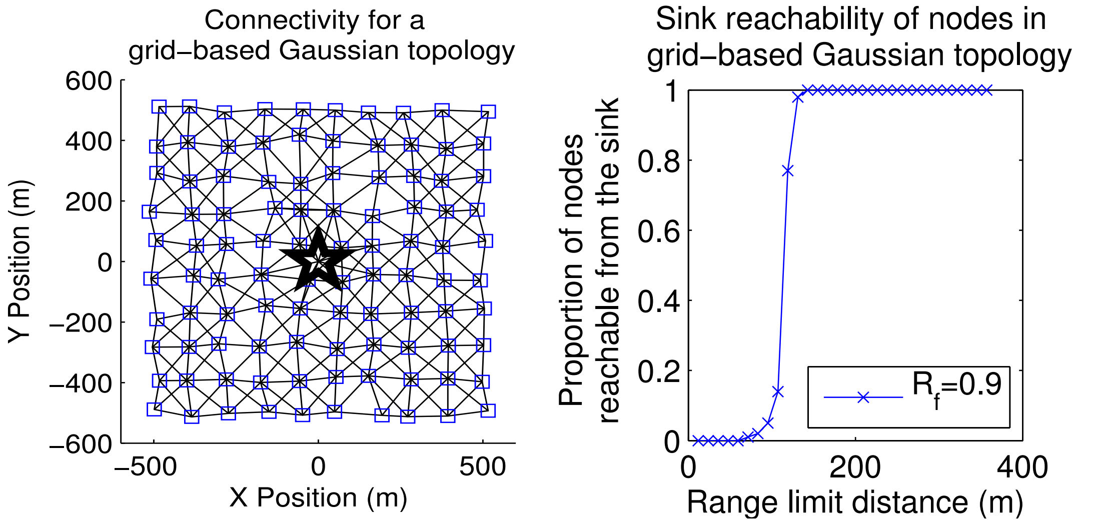

(a) Fully connected topology

(b) Proportion of nodes reachable from the sink

Figure 27: The grid-based Gaussian topology and its connectivity (sink reachability)

page 101) model incorporates an element of stochastic variation in coverage into the grid-based topology. It occurs in a square topology of side S, and the basis grid has a separation distance $D_P$ between nodes on one axis. Define the integer nodes on side $S_N$, where total node count $N = {S_N}^2$. Peer distance can be defined as $D_P = \frac{S}{S_N - 1}$. $\mathbf{G}(\mu, \sigma^2)$ defines sampling a Gaussian distributed random variable with mean $\mu$ and standard deviation $\sigma$.

Equation 4.11, page 101 defines the Cartesian coordinates of node $N_i$, $(N_X, N_Y)$ under the grid-based Gaussian model. The regularity factor defines the regularity of the topology, by controlling the variance of the Gaussian variation around the grid positioning. The special case $R_f = 1$ corresponds to a purely grid-based topology.

$$\begin{aligned} N_X &= D_P \left( i \mathrm{mod} S_N - \frac{S_N - 1}{2} + \mathbf{G}(0, (1 - R_f)^2) \right) \\ N_Y &= D_P \left( \lfloor (i/S_N) \rfloor) - \frac{S_N - 1}{2} + \mathbf{G}(0, (1 - R_f)^2) \right) \end{aligned} \tag{4.10}$$

## 4.9 Signal Jamming Impact Upon Data Delivery

### 4.9.1 Introduction

The previous models for transmission success have been developed for networks in which all nodes are operating in accordance with their expected behaviour. However, if malicious nodes exist which are are failing to fulfill their obligations under the protocol, it is likely that failure rates for end-to-end routing will be considerably higher. This section explores the success rates of multihop routing and beamforming in the presence of signal jamming attacks.

A signal jamming attack is one of the easiest attacks for an adversary to deploy in a WSN. Jamming is a particularly low-effort attack since the only equipment required is a transceiver capable of generating a null carrier or interference, which is conceptually simple and easily deployed. Furthermore, given the power limitations assumed upon sensor nodes, it is possible for jamming attacks to radiate considerably more power than any individual transceiver. Since the attacker may be deploying only a small number of devices, economics favour the attacker, in that it is possible for them to have transmitters capable of radiating greater power, and more interference, than a typical wireless sensor network node.

This section analyses the impact of signal jamming attacks upon the data delivery mechanisms in a WSN, explaining fundamental assumptions, providing a model of the performance of both multihop routing and distributed beamforming relaying mechanisms under interference. It then provides simulation results to demonstrate their performance, and discusses the conclusions obtained.

### 4.9.2 Scenario and Modelling Assumptions

The model assumes the fully deterministic radial topology Section 4.8.1, page 97. This is located within a circular region of radius $R = 800m$ with a central sink. An advantage of a deterministic topology such as this is that when no attack is present in the network, the supernode can always be formed, there are no failure modes due to insufficient supernode membership to transmit the necessary data. It is assumed that an out-of-band channel or wired link serves to transport data from the sink out of the network, and therefore no additional interference is contributed.

The radial rings in which the nodes are arranged are spaced $D_P = 100m$ apart. In specific tests $J_C$ jammers are distributed uniformly throughout the topology. Data sources (and supernode coordinators) are located on the outer ring of the topology at radial distance $D_S = 600m$. The log-distance loss exponent $\gamma = 4.01$ is assumed in this propagation environment, as corresponding to the far-field region of Martinez-Sala's empirical propagation model (Table 1, 85).

The scenario explored in this section is that all jammers considered in this work are equipower jammers, considered to radiate power equal to a standard network node. This case of attack is suitable to consider for attacks implemented by compromised nodes, in which malicious nodes are assumed to have all the the public decryption keys available to the node but not able to impersonate the sink due to the lack of resources. The jammers are assumed to be intermittent jammers, which do not block routing packets but instead block data delivery. This improves the stealth delivered by their attack and prevents the protocols from routing around them.

Regarding reception at the sink, it is assumed phase synchronisation using a local coordinator and the sink immediately before beamforming achieves negligible synchronisation error given the oscillators available. It is assumed that the sink's reception antenna is physically steerable, aligning towards the supernode during reception with high directivity, with a beamwidth $B_\theta$ radians that spans twice the radius of the supernode cluster, and that sidelobes are not significant for interference collection.

### 4.9.3 Multihop Routing

Jammers transmit with the same power as a node. Assuming a transmitter in the routing chain is spaced at $D_P$ from a receiver, and the closest jammer is $D_J$ from the receiver, the requirement for minimal reception at $SIR = SIR_{min}$ is:

$$\frac{{D_P}^{-\gamma}}{{D_J}^{-\gamma}} = SIR_{min} \tag{4.11}$$

The circle around the receiver at radius $D_J$ is the vulnerable area per multihop node $V_M = \pi {D_J}^2$. Rearranging Equation 4.11 for $D_J$ gives $V_M$:

$$V_M = \pi {D_P}^2 (SIR_{min})^{2/\gamma} \tag{4.12}$$

Without loss of generality, assume nodes lie in a straight line. Since these vulnerable areas partially intersect under typical parameters, total route vulnerable area $V_R$ on a route of $R_L$ nodes can be approximated using the cylinder and end semicircles (shown in Figure 28, page 104) containing them. This applies regardless of the relative angle between two nodes in the forwarding chain, since due to rotational symmetry, if two

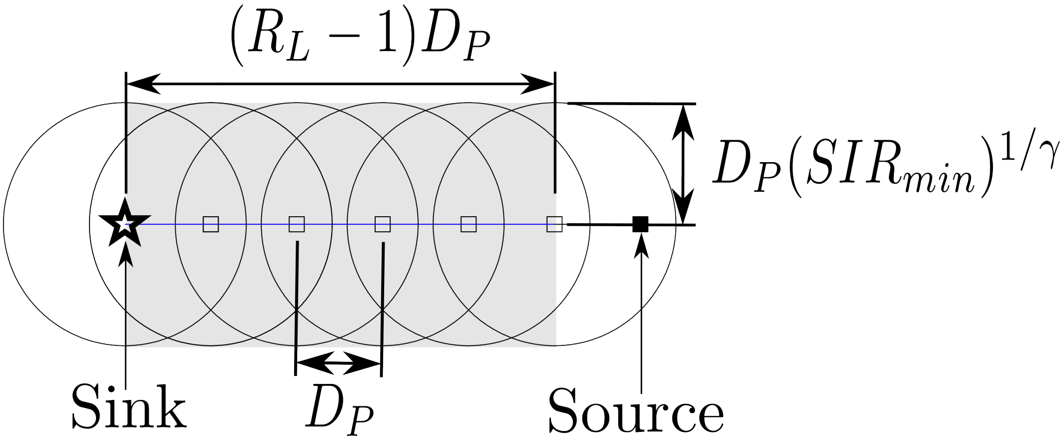

Figure 28: Modelling multihop routing vulnerable area as a cylinder and attached semicircles

circles are offset from one another, then the overlap area is constant regardless of the angles involved.

$$V_R \approx \pi \left( D_P SIR_{min}{}^{1/\gamma} \right)^2 + 2(R_L - 1)\left( D_P{}^2 SIR_{min}{}^{1/\gamma} \right) \tag{4.13}$$

If a jammer lies within the vulnerable area $V_R$, data delivery will fail. Therefore the probability of successful delivery via multihop routing $P_{MR}$ can be approximated from a binomial term giving the probability that none of $J_C$ jammers are located within the vulnerable proportion of the overall topology:

$$P_{MR} \approx \left( 1 - \frac{V_R}{\pi R^2} \right)^{J_C} \tag{4.14}$$

### 4.9.4 Supernodes

Using supernodes, two steps in the data delivery protocol are vulnerable to jamming; the hop-by-hop data distribution and synchronisation phase, and then the beamforming transmission back to the sink.

Any adjacent nodes within the cluster must be able to mutually communicate in order to synchronise their clocks and any phase offsets, and exchange data for the transmission. We assume that all nodes for the supernode lie in a single hop communication range of each other at range $D_P$. Therefore, the vulnerable area $V_{SNODE}$ is entirely localised around the supernode coordinator, and is the same as the single node multihop case in Equation 4.12:

$$V_{SNODE} = \pi D_P{}^2 (SIR_{min})^{2/\gamma} \tag{4.15}$$

For correct data delivery, the sink must also receive successfully, which requires the incoming signal to be above the SIR threshold. The use of a directional antenna gives a vulnerable area as a truncated sector (reduced radius) of the topology. At the axis of the antenna alignment, the receiving antenna amplifies both the signal and jamming interference equally, so the outer radius of this partial sector $R_{SLICE}$ can be derived from the supernode linear gain $G_S$ and distance from the sink to the supernode centre $D_S$ as:

$$R_{SLICE} = D_S \left( \frac{SIR_{min}}{G_S} \right)^{1/\gamma} \tag{4.16}$$

Therefore, the area of the vulnerable partial sector $V_{SINK}$ is determined from the receiving antenna beamwidth $B_\theta$ as a proportion of the area of the circle with radius $R_{SLICE}$:

$$V_{SINK} = \frac{B_\theta}{2} {R_{SLICE}}^2 \tag{4.17}$$

The final supernode success probability $P_{SN}$ is obtained using the binomial distribution, assuming none of $J_C$ jammers are located in either $V_{SNODE}$ or $V_{SINK}$:

$$P_{SN} = \left( 1 - \frac{V_{SNODE} + V_{SINK}}{\pi R^2} \right)^{J_C} \tag{4.18}$$

### 4.9.5 Simulation Methodology

The simulation is implemented using a simulator in the OCaml language [92]. To begin a simulation run, a radial ring test topology is generated, with sources at $600m$ radial distance from the sink. A gradient based routing algorithm is executed to construct the shortest path routes to the base station. Within this topology, $J_C$ jammers are generated, uniformly distributed. An ensemble of topologies is considered, incorporating variation in jammer placement.

To simulate multihop routing, routes are tested hop-by-hop in sequence from the source to their final destination at the sink. Jamming linear interference power from all jammers at the receiver's location is computed and summed. The received SIR is computed determine whether the transmission to the receiver of each hop could overcome the aggregate jamming interference. If any hop fails to meet the interference constraint, the routing request is considered subject to jamming interference, and recorded as such in the statistics.

For simulation of supernode delivery, a cluster of $N = 4$ nodes is considered, with each data source the coordinator of the data. This represents a pure beamforming scenario with no multihop routing involvement. Firstly, transmission for the data dissemination phase S1 is tested, by testing SIR over aggregate jamming interference from the coordinator to member nodes. Then the reverse direction (sink to candidate member) is tested in the same manner. Bidirectional communication must succeed for a minimum of N nodes for the S1 phase to be considered free of jamming.

Then phase S3 is modelled, testing SIR upon reception at the sink with the supernode gain applied. If the SIR meets the constraint, then this phase succeeds also. If both phases S1 and S3 succeed, then the delivery of this packet is considered a success.

### 4.9.6 Simulation Validation

This section considers the validation of the simulation against the analytic model. Although validation of the complete scenario is implicit in the close match between simulation and analytic results presented in the full scenario results (Section 4.9.7, page 109), validation tests employing simplified scenarios will be presented to demonstrate the conformance more clearly. In particular, activating only one single jammer per simulation, and plotting the jammer locations which lead to data delivery success allows the shape of vulnerable areas to be defined, validating the output of the simulations against the analytically predicted values.

#### 4.9.6.1 Single-Source Multihop Routing Validation Against Analysis

In order to perform this validation test, a special case of the deployment scenario was considered. In these validation tests, a single source is activated, with a single jammer present within each topology. The intent of this is to establish the geometric regions of vulnerability to a specific jammer, via repeated trials of jammer deployment at different locations. Consider a single multihop routing chain, as depicted in Figure 29, page 107. The active source $S$ is located at the end of this chain, and the sink at $(0, 0)$ is the destination of the routing requests. Areas surrounding intermediate receivers which are vulnerable to jamming are indicated by the circles.

Within a series of validation simulations, a single jammer is uniformly distributed within a circular region of radius $700m$. The validation test proceeds by computing

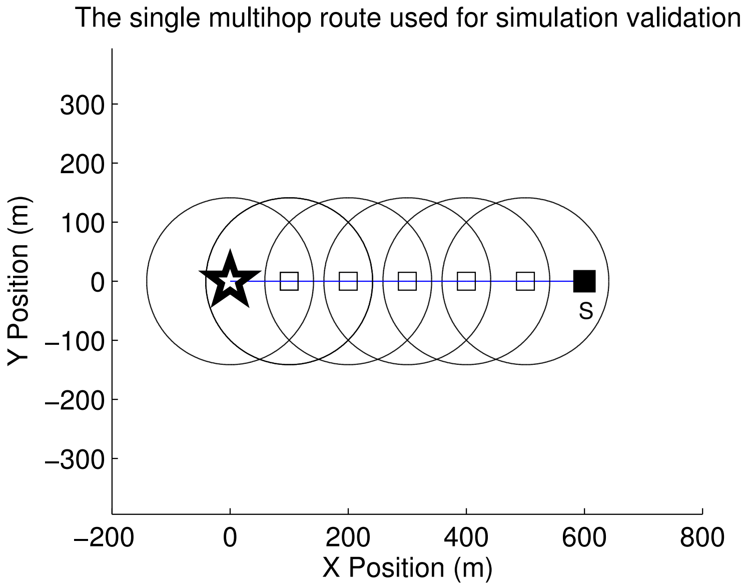

Figure 29: A simple multihop routing chain used in simulation validation

hop-by-hop the physical SIR at all intermediate receivers, taking interference from the jammer into account. Success is reported if the multihop transmission was able to reach the sink without jamming at any stage. The proportion of successful transmissions can be contrasted with the analytical prediction for vulnerable area (Equation 4.13, page 104. Since the jammers are uniformly distributed, the vulnerable area can be estimated from the proportion of simulation cases that fail, and the non-vulnerable area to jamming, $1 - V_A$, can be estimated from the cases that succeed.

Figure 30, page 108 illustrates the conformance between simulation and analysis for the single-source multihop routing chain, for $SIR_{min} = 0dB$. The circles and rectangle define the analytically predicted vulnerability regions for these parameter values. The dots define simulation trials in which the jammer location did not prevent successful delivery. In total 100000 trials of jammer placement were conducted.

It can be seen that the only locations in which the simulation did not conform to the analytically predicted vulnerable area $V_R$ is in the areas between the circles at the edges of the tubes, in which the tube model of Equation 4.13, page 104 assumes a failure. The simulation however respects the vulnerability circles surrounding each individual receiver, as illustrated in Figure 29, page 107. The proportion of topology vulnerable area is computed analytically as 0.915, and the proportion of simulation trials that succeed is 0.916.

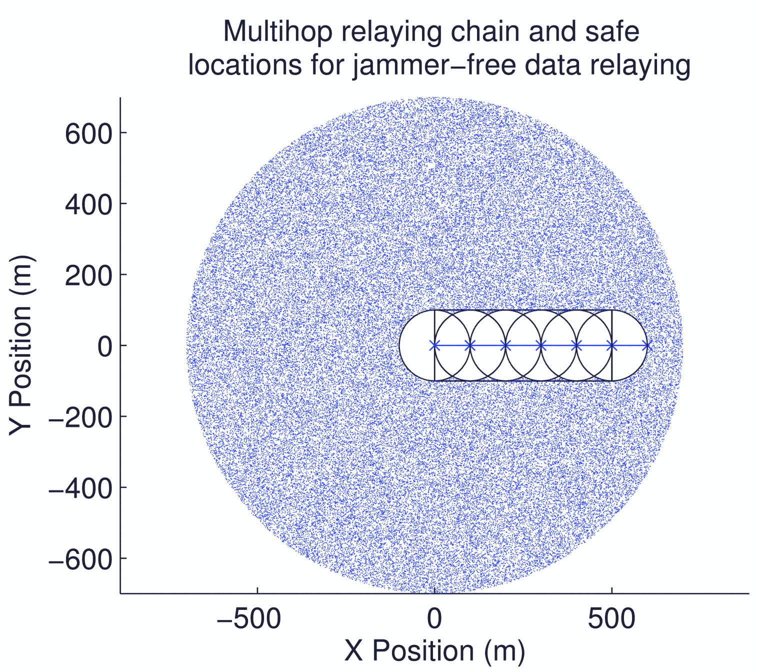

Figure 30: Simulation trials of multihop relaying in the presence of a single jammer

#### 4.9.6.2 Single-Source Supernode Validation Against Analysis

In this section the validation methodology of the previous section is applied to supernode data delivery. A single jamming model is investigated in which a single source is activated at $(600, 0)$. This source acts as a supernode coordinator and recruits other nodes to participate in distributed beamforming. The simulation models the success of this process both in finding the required number of members free of jamming to participate, and secondly in a successful jamming transmission to the sink free of interference.

The analytic supernode model predicts the existence of two vulnerable regions, firstly a circle located around the supernode coordinator, and secondly a sector around the sink reception antenna. Figure 31, page 109 shows the structure of this in the case of $SIR_{min} = 0$, in which the areas are disjoint. The figure clearly illustrates in the simulation trials the presence of a circle of vulnerable area around the coordinator, which under these parameters has the predicted radius of $D_P = 100m$. The sector around the sink is aligned towards the sink and with the predicted half-beamwidth of 18 degrees specified in the simulation parameters, and maximum $D_{SLICE} = G_S^{-1/\gamma} = \frac{600}{\sqrt{2}}$. The analysis predicts a vulnerable area of 0.942 while the proportion of simulation trials successful is 0.941.

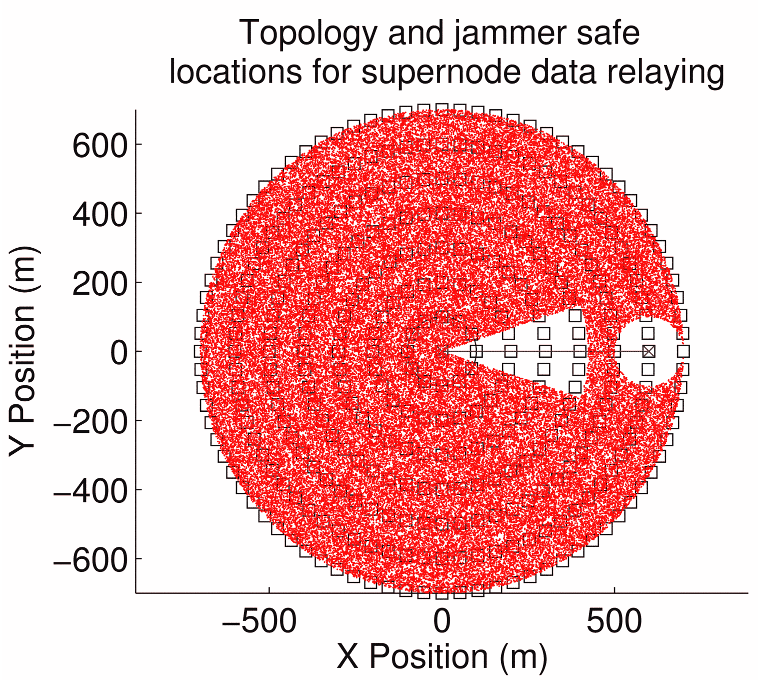

Figure 31: Simulation trials of supernode data delivery in the presence of a single jammer

### 4.9.7 Results

Figure 32, page 110 contrasts simulation results with the analytic models for multihop and supernode reception shown in $P_{MR}$ (Equation 4.14) and $P_{SN}$ (Equation 4.18) respectively.

The first purpose of these results is to demonstrate the close agreement between the analytic models and simulation for both multihop and supernode delivery. Especially with smaller number of jammers $J_C < 10$, the agreement is extremely close. When the number of jammers increases, the analytic model is further from the simulated result. This results from simulations which feature aggregate interference from all jammers in the network, in contrast to the analytic model which features only interference for a single jammer. It is notable that a closer match between simulation and analysis is exhibited for multihop routing compared to supernode delivery. For multihop routing, the absolute error in delivery proportion is less than 3% of data generated, although for multihop delivery the analytic model over-estimates delivery success by around 5%. This can be explained by the assumption that only a single jammer is significant in construction of the model. This assumption is likely to hold when jammers are located close to receivers, but given the greater distances in sector vulnerable area in the supernode model, the additional interference terms from other jammers are likely to be more significant.

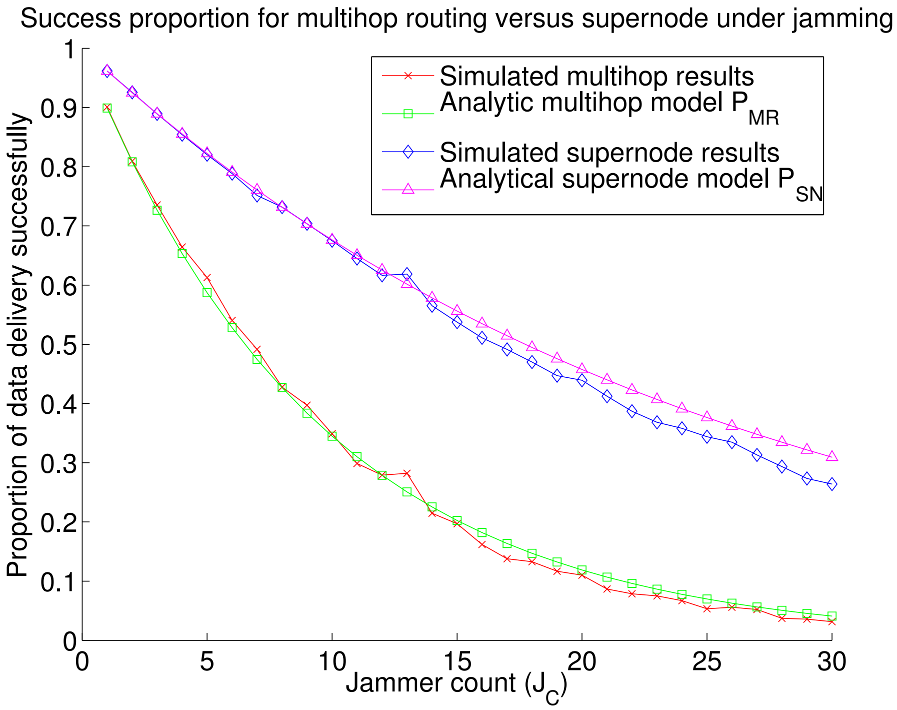

Figure 32: Results showing improved performance of the supernode approach versus multihop routing

Contrasting the supernode delivery scenario with multihop routing, both simulation and analysis indicate that the supernode approach provides significantly better performance under heavy jamming. For $J_C < 10$, it is possible to delivery approximately twice as much data successfully without jamming incidents using supernodes as opposed to multihop routing. For $J_C = 30$ approximately six or seven times as much data can be delivered without jamming using supernodes as opposed to multihop routing. A key factor in the vulnerability of multihop routing concerns the geographical distribution of its vulnerable areas throughout the radial ring topology, explored in Section 4.9.6, page 106. Multihop routing must communicate its data hop-by-hop towards the sink, in which the inner ring of relaying nodes is vulnerable to jamming. The placement of a single jammer sufficiently close enough can disable any multihop routes using this node as a forwarder, which is extremely likely to happen when a large number of jammers are introduced. However, by contrast with supernode delivery, jammers close to a source only disable it from participating as a supernode coordinator. For example, if a single jammer is close enough to be disruptive to some potential supernode members on one side of the coordinator, the coordinator is likely to be able to compensate by recruiting other members upon the other side of its communication range, far enough from the jammer to communicate successfully. This limits the impact of jamming upon the collaboration phase of the beamforming process.

In terms of vulnerability to failure and jamming tolerance, the result graph illustrates that supernode routing has considerably better jamming tolerance. Supernode jamming can tolerate in excess of 20 jammers network-wide before exhibiting delivery proportion of less than 0.4. By contrast, the multihop network reaches a delivery proportion less than 0.4 with only 9 jammers present. Again, the reduced tolerance of multihop routing in comparison to supernode delivery can be explained due to the presence of the single point of failure in the region of the sink in multihop routing, in which a single jammer can hamper delivery for a large proportion of the network.

## 4.10 Conclusion

This chapter has explored methodologies to implement practical WSN systems, and motivated simulation as important for the development of new network protocols, resulting from the high costs of deployments and the need for a consistent environment for testing. It has then explored the models of radio communication that will be presented throughout the thesis in order to perform comparisons of different data transmission methodologies.

The distributed beamforming transmission has been introduced and an architecture provided for coordinating transmission to the sink from supernodes. Finally, standard topologies have been specified and their connectivity properties analysed. An analysis has been made as to the impact of jamming interference upon multihop routing versus distributed beamforming, showing that the distributed beamforming approach provides superior jamming resistance. The following chapter will consider a particular security attack in sensor networks, the wormhole attack, applying novel routing metrics to avoidance of the wormhole attack.

# Chapter 5

# Wormhole Avoidance Using Disturbance Based Routing

## 5.1 Introduction

This Chapter presents and analyses routing metrics that can defend against subtle topology distortion attacks such as the wormhole attack (Section 3.5, page 56). This attack is important in that it cannot be countered directly by cryptographic means. The distortion of the topology provides control to the attacker, through a long-distance link which they can temporarily or permanently disrupt. Therefore, it is important (in addition to other security mechanisms) to prevent routes from using the wormhole if possible.

This chapter presents a multihop routing technique, disturbance-based routing, which uses custom metrics to defend against the wormhole attack by routing preferentially around wormholes. Through this approach, characteristics introduced by the wormhole, either in static connectivity of the topology, or during operation, allow it to be detected and penalised. This reduces the probability of multihop routes using the wormhole link. Through this approach the control which the attacker can gain, and therefore their capacity to disrupt network operation, is greatly reduced. The approach is entirely distributed, and builds upon a well-established protocol for Ad-Hoc On-Demand Distance Vector (AODV) routing [109]. Unlike the other techniques covered in Section 3.5, page 56, the disturbance-based routing approaches do not depend on details of timing, consume excessive system resources, or otherwise exhibit prohibitive computational complexity.

## 5.2 Analysis Of Wormhole Threat

As covered in Section 2.2.1, page 36, the deployment of heterogeneous entities, such as long-distance backhaul relaying links, is often used to enhance performance in real sensor network deployments, through the significant advantages it offers in maintaining connectivity across sparse regions. Therefore, an attacker introducing their own heterogeneous entities with greater capabilities such as a long-range out-of-band channel linking a pair of entities, will obtain an equivalent gain in resources and therefore a significant advantage. This section extends the consideration of the wormhole in the literature in Section 3.5, page 56, and develops a distinction between types of wormhole attack in regard to the level of intelligence and packet inspection exhibited.

### 5.2.1 Passive Wormhole Case

In the simplest wormhole case (the passive case) a malicious attacker deploys one or more pairs of energy-rich external devices that utilise a private low-latency channel (assumed out of band so as not be visible as an interferer) between the paired endpoints. An operating wormhole of this type is illustrated in Figure 33, page 114. Each wormhole endpoint listens to the channel in promiscuous mode and intercepts any packets heard locally, tunnels them across the private channel to the other wormhole endpoint, and rebroadcasts them at this remote endpoint. The passive wormhole merely intercepts all transmissions on a detected frequency and rebroadcasts them without any knowledge of their contents. This is the simplest type of wormhole to implement for an attacker as it can operate using any hardware platform capable of monitoring the radio spectrum, and does not require any protocol inspection or extraction of keys through compromise of an existing device.

During the update phase of next neighbour discovery, this effectively distorts the physical topology by causing network nodes within range of the endpoints to consider themselves as direct neighbours. If the wormhole provides a shortcut across a long range region, then under routing protocols which reward shortest paths, the wormhole link will feature prominently in routes eventually formed. This transfers control over network availability to the attacker, who is then free to mount any one of a number of further attacks depending on their objectives. Denial of service can now be implemented by suddenly severing the wormhole link, and a partial and a more stealthy denial of service (greyhole, as examined in Section 3.3.2, page 52) can be implemented via selective traffic dropping.

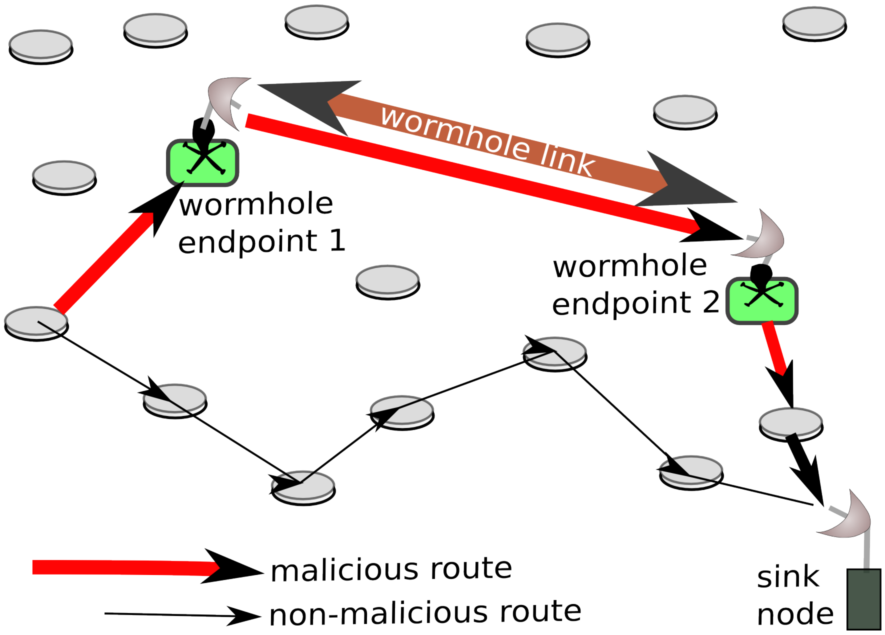

Figure 33: The structure of a wormhole attack in a WSN

Even if cryptography (discussed in Section 3.6.1, page 62) protects confidentiality and prevents direct inspection of the intervening data, elementary traffic analysis, such as waiting for surges in transmitted data rate may reveal a critical moment for an attacker who has successfully mounted a wormhole attack to disrupt the link. This attack strategy is particularly insidious as it gives network operators the impression that the network is still operating as intended, due to the continued availability of maintenance traffic or other ordinary traffic over the link.

### 5.2.2 Active Wormhole Case

Within this thesis the active wormhole is assumed to refer to one in which a device originally introduced by the deployment authority (or a compatible device equipped with stolen network keys if using a standard platform) has been modified via the addition of the private channel hardware and appropriate software to fulfil a role as a wormhole endpoint. The key distinction of the active wormhole from the passive case is that this type of wormhole is assumed to have more selectivity in choosing traffic from particular layers of the protocol stack to tunnel and rebroadcast.

An active wormhole is assumed to only tunnel packets from the network layer and above, that is, packets relevant to the routing protocols it wishes to disrupt, or (until severing the link) application layer data. Packets related to MAC layer activities such as schedule formation or neighbour discovery would be discarded. From the viewpoint of the attacker, this would be desirable, as reserving the private channel for packets relevant to its attack maximises the benefit it gains, while minimising any spurious effects upon the topology that may reveal its attack.

## 5.3 Disturbance-Based Routing

This section will describe a mechanism to counter the previously described wormhole attacks through a novel routing protocol, disturbance-based routing, a pair of approaches in which routing decisions take into account either the number of peers affected by transmissions, or potential congestion resulting from transmissions in order to assist in wormhole avoidance. Performance of the disturbance-based protocols will be evaluated via simulation in a series of topologies.

### 5.3.1 Philosophy behind Disturbance

#### 5.3.1.1 Philosophy behind Static Disturbance

There is a notable feature of topologies that assists detection of any passive wormholes that may be operating within them. In the passive wormhole case, a wormhole which forwards neighbour discovery packets can convince nodes surrounding a pair of endpoints that they are all mutually peers of each other. As illustrated in Figure 34, page 116, this arises as neighbour discovery requests are tunnelled across each wormhole endpoint, receiving replies from their recipients on the other site that convince the nodes surrounding the endpoints of their peer relationship. An active wormhole which is a modified network device will not usually have this effect upon connectivity, as it has packet inspection capabilities and can therefore mount a more sophisticated attack by ensuring that it only broadcasts the routing packets. The end result in the passive wormhole case is that the connectivity degree of nodes in the region is inflated, producing what appears as a well-connected set of nodes. This will appear as a static feature of the network topology when routing begins.

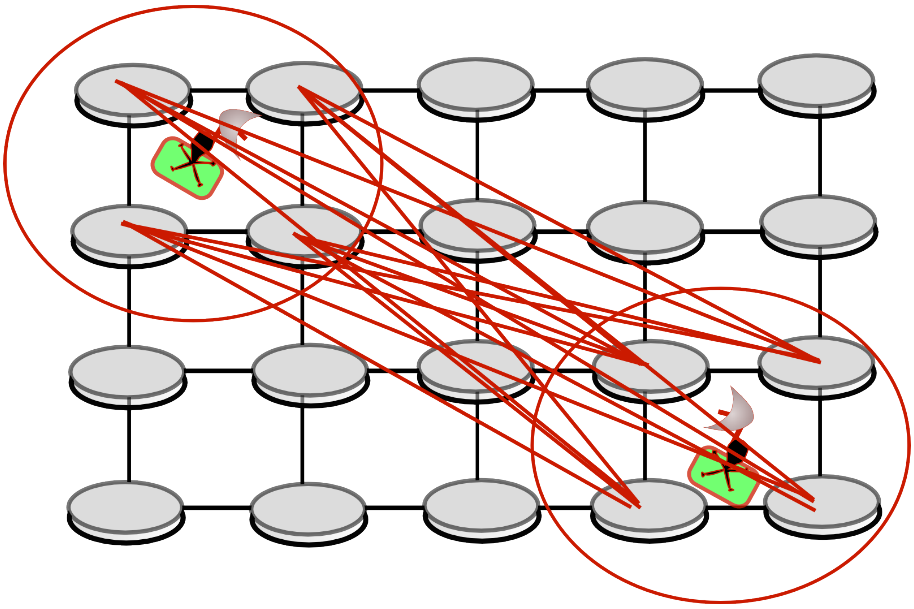

Figure 34: Connectivity changes caused by a passive wormhole, in which remote nodes consider themselves neighbours

This feature motivates an approach which can help in wormhole avoidance for passive wormholes. Avoiding the overhead of centralised computation to reconstruct this topology structure, discovery of these potential spots of improved connectivity can be integrated with the route discovery phase by routing based upon a static disturbance metric. This metric defines the cost of a link by the number of peers reachable from it, and thus rewards routes of low disturbance in which the path of nodes involved is surrounded by the fewest peers. In this view of avoidance, a wormhole is avoided as a consequence of the disturbance its tunnelling function would create to nodes around the endpoint, and this is used as an indicator of its potential presence to route away from the affected region. It is notable that with stochastic topologies such approaches may not reveal a wormhole perfectly; depending on the degree of irregularity in the topology, regions with dense connectivity may be perfectly natural, and wormholes may be falsely detected. This would be a false positive detection if the shortest safe path is considered optimal, leading to a suboptimal routing decision and increased hop count. However, depending on the network objectives it can potentially still be a good idea to route around these regions for the sake of performance, as using these densely connected areas would involve burdening a wireless medium in these areas and reducing the capacity available for others.

#### 5.3.1.2 Philosophy behind Dynamic Disturbance

The most notable dynamic feature of an ongoing wormhole attack will be the concentration of routes around the active endpoint, as a consequence of its attempts to draw in traffic by tunnelling routing requests across the network as a shortcut path. However, since the non-malicious homogeneous nodes surrounding the endpoint have no extra resources to match the out-of-band channel of the wormhole, then under load there will be a rapid exhaustion of available capacity in the region. This provides a detection framework that can be applied to high-risk regions for routing, by detecting this clustering of traffic that may indicate the presence of a wormhole in the region. It is also the case that this route clustering exposes poor routing choices from a performance point of view, and therefore the network does not suffer extensively from a decision not to route around a suspected wormhole but instead may obtain a performance benefit.

Consider a wormhole operating as an attacker intended, causing concentration of routes around the furthest endpoint. In this case, the wormhole is both a security threat and a potential performance problem. It is logical that as a region becomes increasingly heavily loaded with traffic, it becomes a progressively poorer choice for further routing, especially when used with contention-based MAC protocols under which queue build-up and traffic dropping under heavy load are possibilities.

To a certain extent, physical constraints of the surrounding medium limit the network's dependence on a wormhole link, and therefore the control it can exert over the network. Under heavy contention, collisions, build-up of MAC layer queues or slot exhaustion in time-scheduled schemes would serve to limit the wormhole's success at forwarding route discovery floods. However, this only applies under heavy instantaneous loads as would be seen in synchronised bursts of traffic, and if the duty cycle of these routes is low, a large number of routes may form through the wormhole before it can be detected. A more proactive approach which attempts to detect a concentration of developing routes by observing routing responses is needed, and the dynamic disturbance approach provides this.

A naive approach to constructing a dynamic disturbance metric is based upon nodes overhearing a route request from their peers, which serves as an indication of increased route density in a region. This would be used to update an activity factor which is used as an indication of the expected activity level in a region. The concentration of these activity requests gives a low-cost approximation of general routing-level activity under shortest path protocols in a region, which is useful to reveal the location of any operating wormholes. It must be pointed out, however, that if naively constructed an avoidance scheme may negate its own success, reaching a steady state in which there is a stable flow of traffic through the wormhole. This arises via a negative feedback loop in which a perfect avoidance scheme would negate the disturbance build-up that is integral to its own detection strategy.

Two approaches to avoiding this feedback problem exist. The first approach is to separate routing operation into distinct phases, a shortest path phase followed by a disturbance-based phase. During the shortest path phase, non-critical traffic would be submitted for routing, and used to accumulate disturbance around the endpoints. It is accepted that during this phase, the network would not be secure against wormhole attack. On expiry of a timer, the network would switch into disturbance-based routing mode, in which the dynamic disturbance metric gathered in the earlier phase would be used as the routing metric. On expiry of a further timer, network nodes would switch back into shortest path mode, and thus the cycle would repeat throughout the network's operation. However, this simple phased approach would lead to a number of significant problems. Changing protocols network-wide upon a timed interval required scheduling the transition between phases globally, and carried a possibility of the phases becoming unsynchronised without the intervention of external time synchronisation. It would be an advantage for simplicity if the network could operate without the requirement for an external time synchronisation protocol. Therefore, a more sophisticated alternative to this phased approach has been chosen, in which dual routing is employed to form both a disturbance and shortest path route simultaneously. The details and protocol implementation of this scheme are described in Section 5.4.2, page 121.

Therefore, these two static and dynamic anomalies point to viable mechanisms for potential wormhole avoidance via multihop routing. They add resilience at the network layer by directing data away from a potential threat, contributing to the important security engineering principle of defence in depth. This holds that an effective security infrastructure should be multi-layered to protect against failures in any one component, and a strategy that structures network routing to avoid not just potential wormholes but the performance problems they comprise is a useful constituent of this.

### 5.3.2 Metric Definition

#### 5.3.2.1 Static Metric

The static disturbance metric $SDYN_{i,j}$ for the link between a pair of nodes $N_i$ and $N_j$ is defined in Equation 5.1, page 119. The metric is static as it takes into account only a fixed geometric feature, the number of peers $P_i$ of the transmitting node $N_i$. Here, a peer is defined as any adjacent node the current node is connected to and able to communicate intelligible messages to, negating those that lie within the interference range and would be merely interferers under the protocol model. This does not make any connectivity or localisation assumptions about the nature of the topology, and may be obtained empirically upon deployment from packet exchanges for neighbour discovery.

$$SDYN_{i,j} = P_i^{\alpha} \tag{5.1}$$

The exponent $\alpha$ used in static disturbance is a tuning factor which controls sensitivity of the metric to densely connected regions. Higher values of $\alpha$ lead to the algorithm routing more aggressively around denser regions. In a network of approximately constant density which exhibits a high degree of regularity (such as the grid-based Gaussian topology), this will favour routing through the sparser regions at the edges of the network, penalising central regions in which peer count is greater. Figure 35, page 119 shows an example computation of the static disturbance metric in a route across a multihop network, for the case in which $\alpha = 1$. The end-to-end metric for the three-hop route from $\{N_0, N_1, N_2, Sink\}$ is 7.

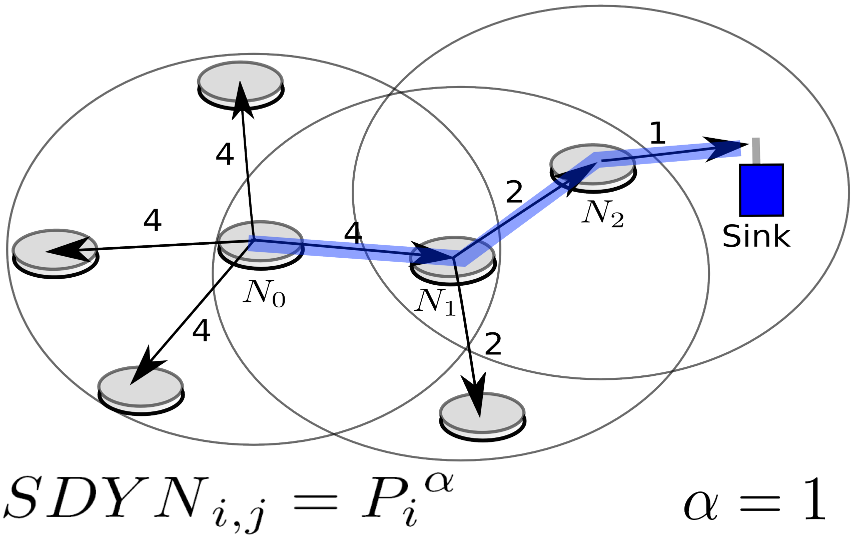

Figure 35: Computation of the static disturbance metric from local peer counts

#### 5.3.2.2 Dynamic Metric

In the dynamic disturbance case, the disturbance level to which a particular node would be subject (as a result of shortest path routing) is tracked using a parameter stored upon each node, the shortest path activity factor (SPAF). The SPAF at node $N_i$ is defined $SPAF_i$, and is incremented in response to shortest path traffic passing through this node.

In a network in which no QoS information is available, SPAF increments can be computed through the dynamic traffic properties. This is the approach taken in the simulations. Whenever traffic is sent upon a shortest path route, a counter of total data transmitted is incremented, and the $SPAF_i$ is computed as a proportion of the total traffic observed on shortest path routes at node $N_i$ divided by the total network capacity on that channel since activation. Therefore, $0 \leq SPAF < 1$, since it is computed as a proportion of total overall channel capacity.

It may fit application and scenario requirements to use Quality of Service (QoS) [110], in which a route typically represents a reservation of a certain maximum traffic level. If this information on the peak traffic demand of a route is transmitted in the route request header, then this information can be used to increment the SPAF level upon route establishment.

The metric for dynamic disturbance-based routing is defined in Equation 5.2, page 120, and uses an exponential function in which $DDYN_{i,j}$ becomes the basis $\beta$ at full $SPAF_i$. The structure of the expression is different from that employed in the static disturbance case, as the values employed must typically be much larger than the values used in the static scheme, as they must influence end-to-end total metrics even when $SPAF_i$ is accumulating in only a small portion of the network.

$$DDYN_{i,j} = \beta^{SPAF_i} \tag{5.2}$$

## 5.4 Protocol Logic and Implementation

### 5.4.1 Static Disturbance Routing Logic

The static disturbance scheme is intended to build upon an existing reactive routing protocol such as AODV [109], in which the static disturbance metric $SDYN_{i,j}$

replaces a unit value as the per-link metric from $N_i$ to $N_j$. The path that minimises the aggregate total end-to-end metric is selected by the destination (anticipated to be the sink) as the reverse reply.

In this protocol, nodes which did not have a route to the destination rebroadcast the request, until it reaches either the destination or a node with a sufficiently fresh active route to the destination. Then, a route response is delivered unicast to the requester, which allow the originating node to extract the route.

### 5.4.2 Dynamic Disturbance Routing Logic

The dynamic disturbance scheme performs a more sophisticated process, known as the dual routing strategy. This is to overcome the feedback loop problem discussed in Section 5.3.1.2, page 117. The protocol finds a pair of routes to a desired endpoint for every route request. Firstly, a shortest-path route is discovered using a conventional routing protocol such as AODV to form a sacrificial route. These routes are not designed for the transit of application-level data but during the reverse reply delivered from the sink, they increment load for the dynamic disturbance metrics. Since the wormhole would concentrate traffic sent under a shortest-path protocol, its location will be revealed from its presence in these shortest-path routes.

Therefore, in this security-focused scenario, dynamic disturbance technically refers to a hypothetical disturbance that would occur in the naive case if all application traffic was to be sent over shortest path routes. It may be possible to make profitable use of these sacrificial routes, perhaps for carrying encrypted application traffic, as this would be a source of a redundant multi-path flow that exploits some possible heterogeneity provided by the wormhole. Since routes controlled by an attacker are inherently unreliable, if higher guarantees of performance are required, it would be advisable to either ignore them for data transmission or inject plaintext disinformation (the exact nature of which would be application-specific) along these routes, thus confusing an attacker who was monitoring the traffic along these routes.

The second stage of dynamic disturbance routing is the stage which obtains the actual dynamic disturbance route. The logic of the protocol sums $DDYN_{i,j}$ along every possible path, to find the total cost incurred end-to-end upon a hypothetical route. The protocol finds these routes via a modified AODV protocol, in which an outgoing broadcast accumulating two metrics serves as a route request.

## 5.5 Scenario Description

### 5.5.1 Scenario Introduction

The intent of this section is to provide an application case for a security-critical deployment scenario and specify assumptions about topologies, sources and detection logic used in investigation of the disturbance-based schemes. The chosen deployment scenario is a military network as might be used surrounding a base or command station for the monitoring of the movements and behaviour of enemy troops (the phenomenon of interest) in the area.

The sink node represents a base or headquarters. The scenario assumes that the defender has set up a static network over a fixed area of terrain in which detection nodes are deployed. As is required of a sensor network deployment, the detection nodes are equipped with sensors capable of picking up indications of enemy presence such as sonic or thermal emissions. Nodes are deployed according to the topologies specified in Section 4.8, page 96, which allows the investigation of the schemes considered under topologies with a range of regularities.

When a phenomenon (the enemy troops on patrol) passes close to a source, these notifications trigger the sensors, which then enter a reporting phase, initiate routing to establish a long-lived route back to the sink node, and generate continuous data on any phenomena in the local region that might be ongoing. This is a useful example case as the routing protocol used fits the traffic dynamics of a security sensitive scenario: on first detection of a potential anomaly, the nodes establish a persistent route to the base station, proactively scanning for any further threat and reporting continuously along the route all further information that may arise for detailed central analysis at the sink.

As the intent of this case study is to model avoidance strategies for the wormhole attack, the scenario also features a wormhole installed by the malicious enemy. The enemy has freedom to place wormhole endpoints anywhere within the topology, but would be anticipated to position its endpoints in a position of maximum advantage, specifically within the central radial region to capture as much traffic as possible. The intent of the defender at their military base is to obtain as many wormhole-free routes to deliver as much accurate information as possible on enemy activity. The intent of the attacker is to ensure their troops can roam as widely as possible over the area, and ensure that as many of the reporting flows use the wormhole as possible so they can disrupt or otherwise disable this single point of attack. Dependence on the wormhole delivers control over network data to the attacker.

### 5.5.2 Traffic Model and Source Activation

The mobility of the sources used in the scenario is a simple model. The enemy troop clusters which initiate route discovery at sensors in their region are assigned an initial patrol velocity. Their speed remains constant throughout but their direction changes, in that they change direction upon boundaries. Enemy troop clusters passing within range of a sensor trigger activation, if it does not currently have an active route.

### 5.5.3 Topologies For Simulation

The three topologies employed for testing the disturbance-based routing scheme are those described in Section 4.8, page 96, namely the grid-based Gaussian, uniform random and radial ring topologies. The use of these topologies gives an assessment of the performance of an avoidance scheme in a variety of realistic deployment conditions. A description of example topologies follows. Topologies generated in this scenario for testing the disturbance schemes are referred to as malign topologies.

#### 5.5.3.1 Grid With Gaussian Variation

For the grid-based Gaussian topology, the region is a square of side $2S$ with the headquarters (sink node) located midway upon the northern edge at coordinates $(0, S)$. Homogeneous sensor nodes are positioned purely regularly upon the grid. The grid was chosen for investigation here in order to produce a regular topology.

In this topology, as defined originally in Section 4.8.2.1, page 100, the homogeneous sensor nodes have a grid-based component and a Gaussian variation. The base position for a node is placed upon a regular square grid spanning the scenario region. The variation is controlled by the regularity factor $R_f$, which adds in a Gaussian distributed variation for both axes, according to Equation 4.11, page 101. This attempts to account for realistic situations in which periodic placement cannot be guaranteed due to irregularities such as scattered placement, geographic features or other obstacles within the terrain, mandating a uniformly distributed choice of optimal deviation from the pure grid position. The special case when $R_f = 1$ corresponds to the network forming a regular, deterministic grid.

#### 5.5.3.2 Uniform Random

In the uniform random case, the geometry of the region and wormhole placement parameters are identical to the grid-based Gaussian case, although nodes are distributed uniformly randomly across the topology and not according to any regular placement. This topology is useful for testing avoidance behaviour in situations where the connectivity is highly irregular and there are wide variations in connectivity of individual nodes.

#### 5.5.3.3 Radial Rings

In the radial ring topology, the sink is centrally located at the origin, with a wormhole endpoint located within one hop of it. The remote wormhole endpoint for traffic gathering is distributed uniformly randomly across the topology in different realisations. This fully deterministic topology is useful for testing avoidance behaviour in situations where the connectivity is highly uniform.

### 5.5.4 Wormhole Placement Parameters

Topologies generated for testing disturbance-based routing schemes are referred to as malign topologies, in that they contain an attacker with a wormhole. In the malign topologies, it is important to consider placement of the wormholes. It is assumed that the attacker aims to maximise their influence, by obtaining control over as many routes as possible. This motivates them to attempt to place one of their wormhole endpoints close to the sink to maximise wormhole usage, since the sink is a privileged endpoint as a destination of all transmissions in a WSN scenario involving delivery out of the network. The scenarios explored all feature a single wormhole delivery endpoint located close to the sink. However, options for placing the other endpoint are very varied and at the discretion of the attacker, who could place their random wormhole endpoint (the pickup endpoint) in any arbitrary region they have a strategic interest in.

This motivates the use of a random strategy for pickup wormhole placement in simulations, since it is best to attempt to secure the network for an ensemble of all possible wormhole placements when the exact one chosen depends on the intentions of the attacker. It would be expected from their point of view that in the majority of simulations the attacker, expecting to draw in a majority of routes, would place their wormhole within the central region of the network.

Another approach is edge positioning, which may be a priority target to defend against as the attacker would have more opportunities to install a wormhole unobserved at the network boundaries out of the control of the deployment authority. Edge positioning scenarios include modelling of wormhole pickup endpoints midway along the West, East and South borders of the network, at coordinates $(-S, 0)$, $(S, 0)$ and $(0, -S)$ respectively. Edge positioning and its effect for avoidance will be explored within the results in Section 5.7.5, page 140.

## 5.6 Simulation Methodology and Validation

### 5.6.1 Simulation Introduction

To assess the benefits of the disturbance-based scheme, simulations of the given scenario was performed using a custom simulator written in the OCaml language [92]. Input parameters for the simulator include a disturbance-based metric (selecting a static or dynamic scheme and the associated metric value), a count of topologies to generate, and the set of scenario definition parameters governing, amongst other factors, topology generation and source behaviour. The names and explanations of simulation parameters are specified in Table 3. Upon execution the simulator produces an output metric to indicate the relative wormhole avoidance success of the given disturbance-based routing strategy, compared to pure shortest-path routing. The simulation can be run in both active and passive wormhole modes, modelling the avoidance provided for different classes of wormhole endpoints.

### 5.6.2 Simulation Process

The simulator generates an ensemble of topologies. In each topology, connectivity between nodes is modelled according to a standard protocol model (as described in Section 4.4.3, page 85), assuming bidirectional binary connectivity within a given connectivity range, the peer distance threshold $P_R$. This assumes that a link is connected if its endpoints lie within the range $P_R$, and disconnected if they are outside of this. For simplicity, the maximum sensing range $S_R$ within which the nodes will detect troops, is set equal to this maximum peer distance threshold $P_R$. Periodically, at the new flow interval during simulation, the fresh position of each troop cluster is recomputed using their known velocity, previous position, and the time delay. The simulator checks for idle sources surrounding each troop cluster within $S_R$, and proceeds to activate the nearest idle source that does not have an active route for reporting.

This chosen node executes the disturbance-based routing protocol to begin initiating data. Also, at this new flow interval, any expired flows (for which the time indicates that they have ended) will be removed and the nodes that originated them return to idle. At the route update interval aggregate statistics on packet flow are updated and the dynamic disturbance metrics, if they are in use, are recomputed, reducing $SPAF$ for any nodes around the completed flows. After a specified time limit, simulation is suspended and the avoidance advantage metric is computed.

### 5.6.3 Metrics Tracked By Simulator

#### 5.6.3.1 Avoidance Advantage

The simulator records a metric to assess the disturbance metric given for analysis. The avoidance advantage (ADV) is the additional proportion of all discovered routes throughout the simulation that successfully avoid the wormhole under the disturbance-based scheme as compared to shortest path. A value of zero corresponds to a state in which the disturbance-based scheme delivers no advantage, as precisely the same proportion of routes used the wormhole as in shortest path routing. In the unlikely case that the disturbance-based routes are actually more susceptible to use the wormhole, the value of ADV will be negative rather than positive. This could occur, for example, with a static disturbance metric in which avoidance preferentially routed on an edge pathway that happened to lead in that particular topology towards a wormhole.

### 5.6.4 Simulation Validation

This section presents the steps taken to ensure that the simulation results are reliable and representative of the system produced. The simulation validation proceeds using simplified topologies. Two test topologies are employed, a safe test topology and a binary test topology. In order to ensure the test topology is regular and deterministic, the safe test topology is purely grid-based, 10 nodes by 10, with $R_f = 1$. This provides regular peer counts without any of the Gaussian positioning variations in the grid-based Gaussian topology, which can alter the connectivity of each node.

Another test topology employed is the binary test topology. The binary test topology is a small topology with only two routing paths to the sink. The purpose of using these topologies is to provide a set of simplified test topologies and test correct operation of the simulator on regular topologies. In particular, optimal solutions in the binary test topology can be calculated analytically to verify simulator behaviour.

#### 5.6.4.1 Static Disturbance Routing Validation By Analysis

The logic behind disturbance-based routing protocols aims for the minimisation of the static or dynamic disturbance metric. In order to avoid the passive wormhole, static disturbance aims to route around denser regions of the topology. This routing effect can be analysed by routing within the binary test topology, a six-node topology, in which the analytic solution can be calculated. Figure 36, page 128 shows this test topology, with potential links $(i, j)$ towards the sink labelled with the peer counts of their originator $P_i$. The sink node is labelled $N_1$ since routing simulations require it to be assigned a numbered identity as a node.

Recalling Section 5.3.2, page 119, the static disturbance metric SDYN is defined for a link as $SDYN_{i,j} = {P_i}^{\alpha}$. Starting from the source node $N_2$, the shortest path route to the sink (in hop count) is through $N_3$. However, using static disturbance-based routing, an alternative route through $N_4$ and $N_5$ will become viable when $\alpha$

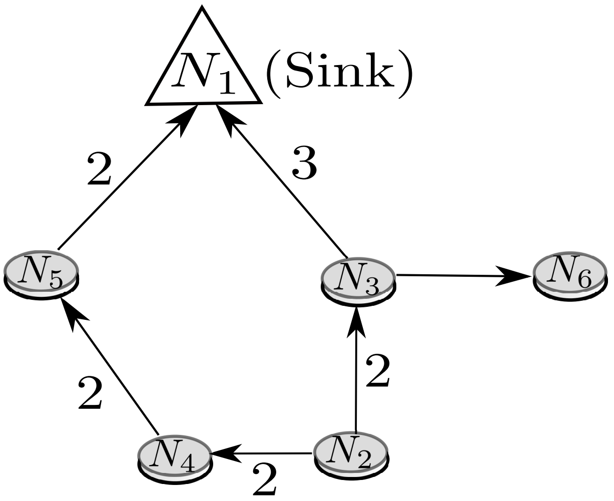

Figure 36: A binary topology for analytic testing of the simulator

is increased. The routing change will first occur when the following equation for aggregate metric is satisfied:

$$SDYN_{2,3} + SDYN_{3,1} = SDYN_{2,4} + SDYN_{4,5} + SDYN_{5,2} \tag{5.3}$$

Since $SDYN_{2,4} = SDYN_{2,3}$, given that the static disturbance metric is set by the originating node, subtracting $SDYN_{2,4}$ from both sides gives:

$$SDYN_{3,1} = SDYN_{4,5} + SDYN_{5,2} \tag{5.4}$$

Applying the static disturbance equation $SDYN_{i,j} = P_i^{\alpha}$ and the peer counts given in the diagram Figure 36, page 128 gives:

$$3^{\alpha} = 2^{\alpha} + 2^{\alpha} \tag{5.5}$$

Taking the natural logarithm of both sides and rearranging gives the $\alpha$ value, $\alpha_{CHANGE}$ at which the aggregate disturbance metrics for both routes are equal:

$$\alpha_{CHANGE} = \left(\frac{ln(2)}{ln(3) - ln(2)}\right) \approx 1.7095 \tag{5.6}$$

Figure Figure 37, page 129 shows the routing decisions made by both the MATLAB prototype and OCaml simulator in this test scenario. The figures show that the static disturbance route changes as expected from $\{N_2, N_3, N_1\}$ to $\{N_2, N_4, N_5, N_1\}$ when $\alpha > \alpha_{CHANGE}$.

#### 5.6.4.2 Routing Validation For Static Disturbance In Safe Test Topology

In order to validate the OCaml simulations on the safe test topology (a regular grid), an independent validation prototype was produced using MATLAB. This

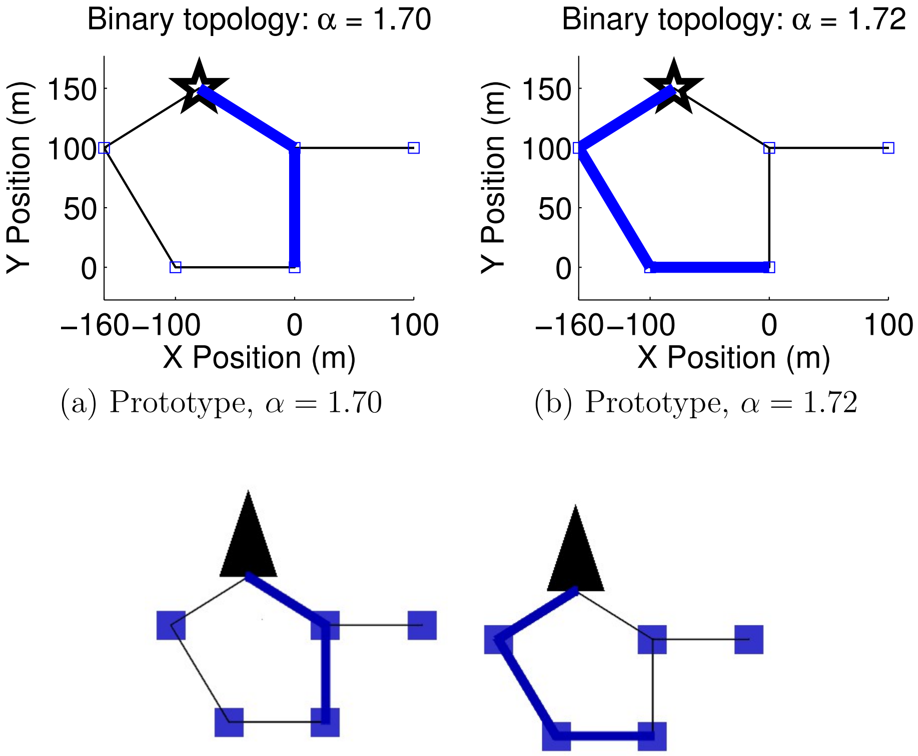

(a) Prototype, $\alpha = 1.70$ (b) Prototype, $\alpha = 1.72$

(c) Full simulator, $\alpha =$ 1.70 (d) Full simulator, $\alpha =$ 1.72

Figure 37: Static routing decisions in the binary test topology

prototype consists of MATLAB code encapsulating the topology generation, metric computation and routing phases, together with code to plot the generated topologies and the routes discovered.

The routing and metric computation was tested against the MATLAB prototype. Both simulators were set to generate an identical grid test topology and simultaneously generate routes for all nodes towards the sink. $\alpha = 2$ within the test network. Figure 38, page 130 shows the routing structure for routes leading to the sink from all nodes within the network, illustrating the paths taken by multihop routingx3 data. The validation test shows identical routing decisions made by both simulators.

#### 5.6.4.3 Dynamic Disturbance-Based Routing Validation By Analysis

The dynamic disturbance routing algorithm involves metrics that change in response to previous traffic activity, specifically traffic upon previous shortest path routes. In order to avoid wormholes, when activity occurs along shortest path routes, the dynamic disturbance protocol should route away from the nodes upon these routes.

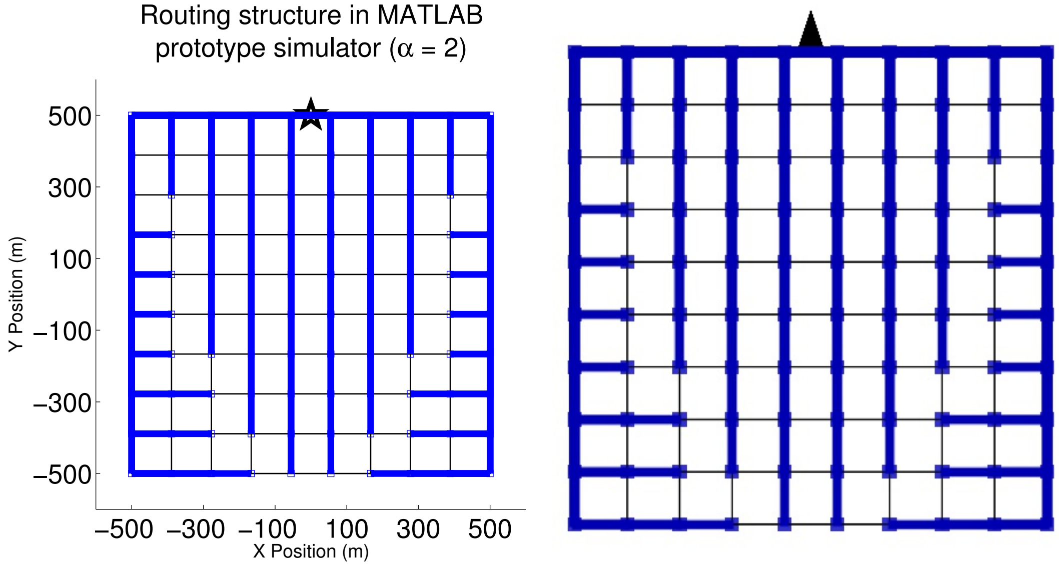

(a) Prototype simulator

(b) Full simulator

Figure 38: Metric validation for static disturbance in grid-based topology

Upon a simplified topology such as the binary topology, it is possible to validate the simulator by testing the routing decisions made by the protocol over time, and verifying that the dynamic disturbance routing decision changes at the appropriate time.

A variant of the binary topology will be used to implement this, in which a number of sources are connected directly to $N_2$. In order to validate the simulator, multiple route requests will be activated, from a source which must cross $N_2$ to reach the sink. In this topology, the shortest path route requests will follow the route $\{N_2, N_3, N_1\}$, and the early disturbance routes will also follow this shortest path route. However, as SPAF values upon intermediate route segments crossing $N_3$ increment, dynamic disturbance-based routing will reroute to use the alternative longer route $\{N_2, N_4, N_5, N_1\}$ which is free of dynamic disturbance. Only the route segment crossing the displayed region of the binary topology is considered in this analysis.

Considering the choices along the candidate route segment beginning at $N_2$, if a point in the simulation is reached at which the metric for both routes is equal then:

$$\beta^{SPAF_4} + \beta^{SPAF_5} + \beta^{SPAF_2} = \beta^{SPAF_2} + \beta^{SPAF_3} \tag{5.7}$$

Subtracting $\beta^{SPAF_2}$ from both sides, and assuming $SPAF_4 = SPAF_5 = 0$ due to the absence of any shortest path traffic along the route:

$$\beta^{SPAF_3} = 2 \tag{5.8}$$

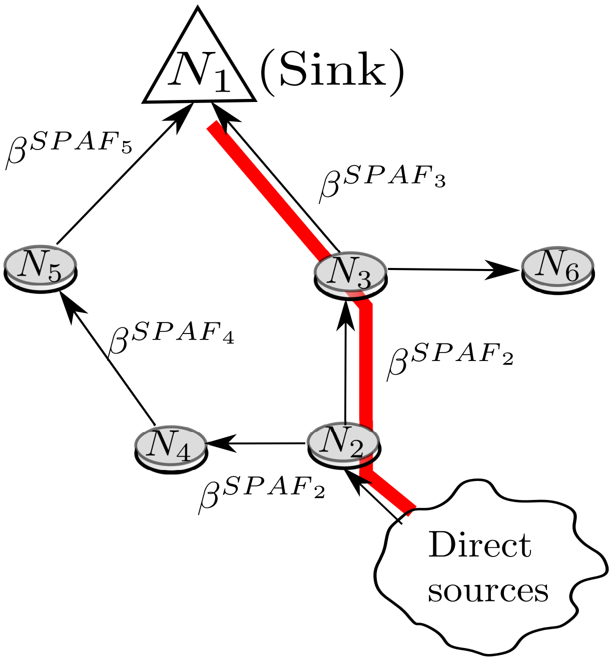

Figure 39: A binary topology for analytic testing of dynamic disturbance-based routing simulation

Taking the natural logarithm of both sides and rearranging gives an expression for the value of $SPAF_3$ (shortest path activity factor at $N_3$) necessary for dynamic disturbance-based routing to transition to the alternative route at various $\beta$ values:

$$SPAF_3 = \left(\frac{ln2}{ln\beta}\right) \tag{5.9}$$

Figure 40, page 132 shows the transition behaviour of dynamic disturbance-based routing. The horizontal axis shows the $\beta$ value, and the vertical axis the SPAF transition values. The result shows the theoretically predicted transition values according to Equation 5.9, page 131, together with the SPAF values before and after the transition. The range in SPAF occurs because it increases in discrete jumps between each new routing decision. The results show that the observed transition occurs within the predicted range, with the previous route found using $N_3$ while the subsequent route following the transition point uses $N_5$ as expected.

#### 5.6.4.4 Metric Validation At Baseline Values

There are several breakdown values for the disturbance-based routing metrics at which zero improvement over shortest path routing is expected. For example, using the SDYN equation $SDYN_{i,j} = P_i{}^{\alpha}$, when $\alpha = 0$, regardless of the local peer count $P_i$, $SDYN = 1$. Therefore, static disturbance-based routing is equivalent to shortest

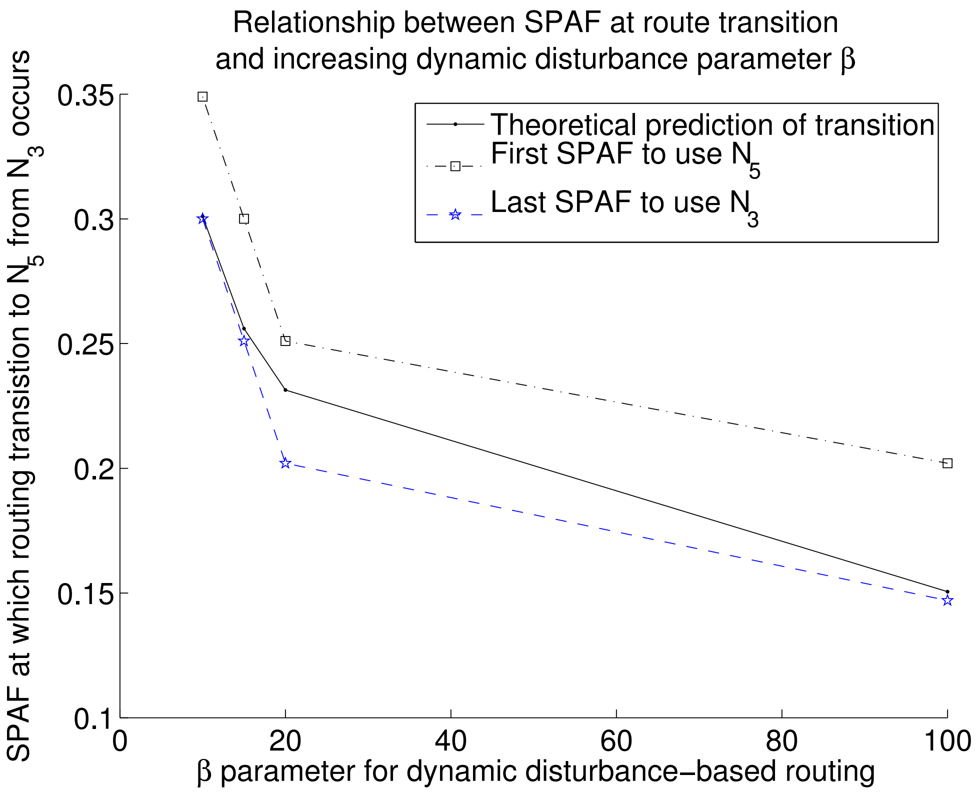

Figure 40: Transitions in dynamic disturbance-based routing to use $N_5$ rather than $N_3$ as a forwarding node

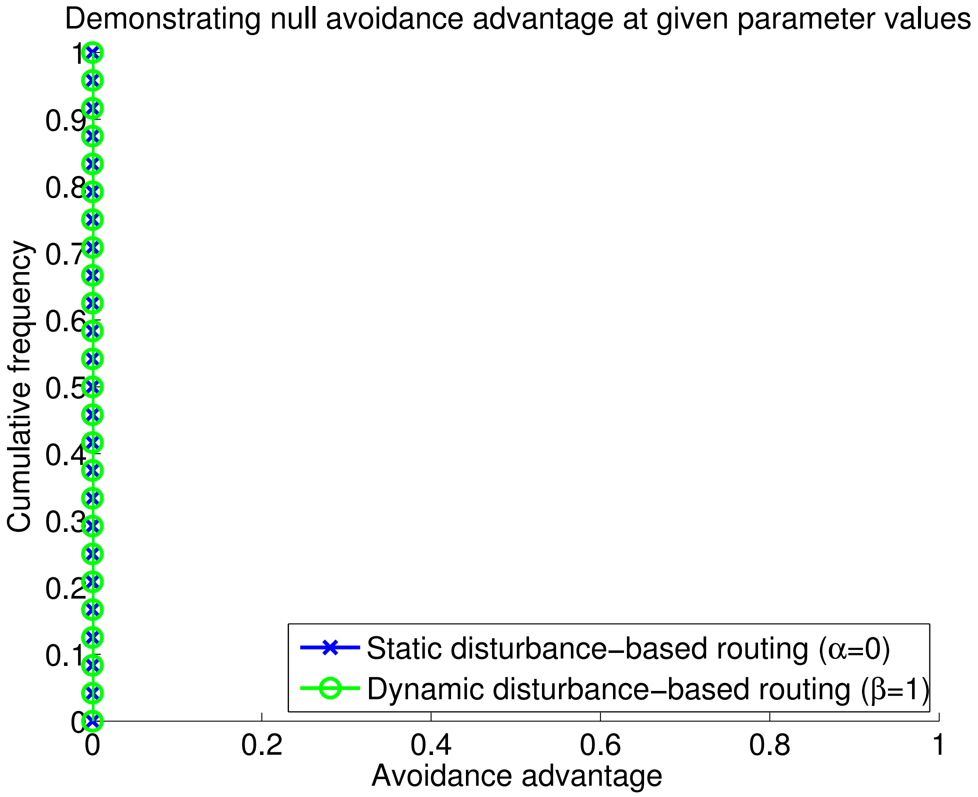

Figure 41: Metric validation for baseline values, showing zero avoidance advantage

path routing, and no avoidance advantage should be delivered. Equivalently, in the DDYN equation $DDYN_{i,j} = \beta^{SPAF_i}$, when $\beta = 1$, regardless of the value of $SPAF$ for the nodes upon the routes, the dynamic disturbance metric is unity for all hops. Therefore, if the simulator is performing correctly, there should be no avoidance advantage produced for these metric values. At these baseline points, the routing decisions of both protocols will be equivalent to shortest path routing.

Therefore, simulating disturbance-based routing in the safe grid topology across ensemble of topologies, with $\alpha = 0$ (for static) and $\beta = 1$ (for dynamic) provides an integrated test of both the metric generation and results analysis functions of the code. The CDF presented in Figure 41, page 132 shows an instantaneous rise at the zero point, indicating that all avoidance advantage results under this test are zero as expected. This validates correct behaviour of the simulator at these baseline routing metrics.

## 5.7 Results

In this section simulation results will be presented to verify the advantages in wormhole avoidance delivered by the disturbance-based routing protocols. In the following results, the avoidance advantage $ADV$ is presented as cumulative frequency distributions across an ensemble of topologies, which can incorporate variation in the node placements, wormhole placements and any other topics which may be specified as non-deterministic in the scenario.

The ADV metric is computed across an ensemble of topologies so the conclusions obtained are not tailored specifically to a single generated topology, but to the ensemble with its variability. This ensures that the results incorporate all variability of the attacker's wormhole placement strategy, and the variation inherent in the topology structure, instead of being merely specific to some particular node or wormhole arrangement. Table 3 shows the values of any default parameters which are assumed in the following result sets.

### 5.7.1 Default Parameters For Results

The parameters used in the simulations for computation of disturbance are given in Table 3.

| Parameter | Explanation | Default Value |
|---|---|---|
| Topology count | The number of custom topologies generated for an experiment | 100 |
| Simulation runtime | The number of time spent running a particular simulation before it ends | 6000 seconds |
| Route interval | The interval at which routing metrics are updated | 120 seconds |
| New flow interval | The interval at which the position of enemy troop clusters is updated and new flows generated | 20 seconds |
| Node count | The number of ordinary data transmission nodes in grid-based Gaussian or uniform random topologies | 100 |
| Regularity factor | The regularity factor applied in grid-based Gaussian topologies | 0.9 |
| Radial ring count | The number of radial rings in a radial-ring topology | 6 |
| Radial ring separation | Separation between radial rings | 100 m |
| Grid based Gaussian $P_R$ | Peer threshold range in a grid-based Gaussian topology | 150 metres |
| Uniform random $P_R$ | Peer threshold range in a uniform random topology | 200 metres |
| Radial ring $P_R$ | Peer threshold range in a radial ring topology | 120 metres |
| Topology side | The side length of the deployment region | 1000 metres |
| Maximum channel rate | The channel data rate of the transceivers used upon the nodes | 250 kbits |
| Rate per flow | The mean data rate assumed on each route that is initiated | 5 kbits |

Table 3: Default parameter values as used in the simulations of disturbance-based routing performance

### 5.7.2 Selection of Static Disturbance-Based Metric Exponents

The static disturbance equation (Equation 5.1, page 119) features an exponent which controls how strongly the disturbance metric routes away from regions of high connectivity. This section presents results and assesses how this metric should be tuned in order to provide workable wormhole avoidance. The results are presented using cumulative distribution functions of the avoidance advantage, to show the properties of avoidance across the ensemble of topologies. The advantage of presenting the full cumulative distribution is that it presents the full distribution of performance delivered and not just aggregate statistics. This is important for planning worst case performance of these security-oriented schemes.

### 5.7.3 Grid-Based Gaussian Topology

Figure 42 shows the variation of a static routing exponent $\alpha$ in a grid-based Gaussian topology. In these realisations, the remote wormhole endpoint is located arbitrarily within the radial region, which corresponds to an attacker with flexibility to place their wormhole within the central region. The active wormhole case (Figure 42a, page 136) shows that higher values of $\alpha$ produce improved avoidance performance. For example, for $\alpha = 1.25$, 80% of topologies exhibit an ADV value less than 0.19, but for $\alpha = 10$, 80% of topologies exhibit $ADV > 0.5$ which indicates that more than half the routes that would have otherwise used the wormhole under shortest path avoid it under the static disturbance-based protocol.

Since the active wormhole is free of topology distortion by peer inflation characteristics, the avoidance advantage delivered is due to the wormhole favouring routing through edge regions of the topology in which the wormholes are less likely to be located. With a regularity factor $R_f = 0.9$ used in the calculations, the grid is generally highly regular with distinct edges which the static disturbance protocol favours routing towards. Wormholes which have been centrally placed by the attackers to try to capture traffic will therefore be rejected by the protocol in favour of these alternative edge routes.

In the passive wormhole case (Figure 42b), static disturbance shows high avoidance performance, and this performance is less dependent on the precise $\alpha$ value employed.

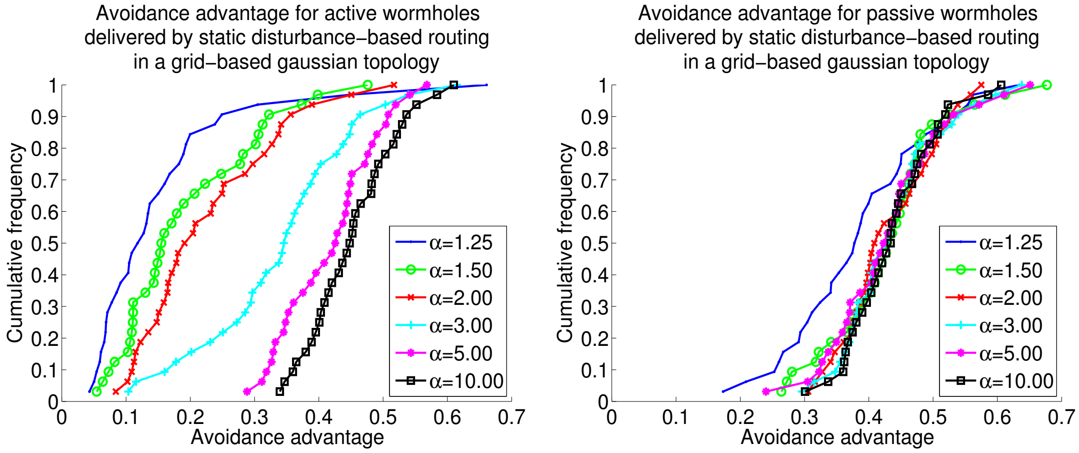

(a) For active wormholes

(b) For passive wormholes

Figure 42: CDFs of avoidance advantage for static disturbance in grid-based Gaussian topologies

For all $\alpha$ values, an avoidance advantage of 0.45 to 0.5 is generated in 80% of topology realisations.

This reduced dependence on $\alpha$ can be explained through a consideration of a transition value. For avoidance of a wormhole, the disturbance-based route must offer a lower-cost metric than the shortcut path the wormhole provides. The peer count increase for nodes around both endpoints of a passive wormhole creates strongly connected regions in the network graph, and therefore a large amount of static disturbance around them. The consistency and close match between these results shows that static disturbance-based routing protocol favours routing strongly away from such regions at $\alpha \geq 1.25$. Therefore, in the more conventional case of a passive wormhole, the peer inflation effect is highly revealing of wormholes located nearby. It is notable that $\alpha > 1.25$ provides marginally higher performance than $\alpha = 1.25$, with an increase in the median ADV of 0.05. This is possible due to the fact that increasing $alpha$ exponent penalises the strongly connected regions more strongly, increasing slightly the range of the topology in which avoidance will occur.

#### 5.7.3.1 Uniform Random

The results for the uniform random topology (Figure 43) show a similar effect as in the grid-based Gaussian, with a general tendency for increases in the avoidance advantages with increasing $\alpha$ values. However, in the active wormhole case (Figure 43a, page 137) the variation is less distinct due to the inherent variability of the

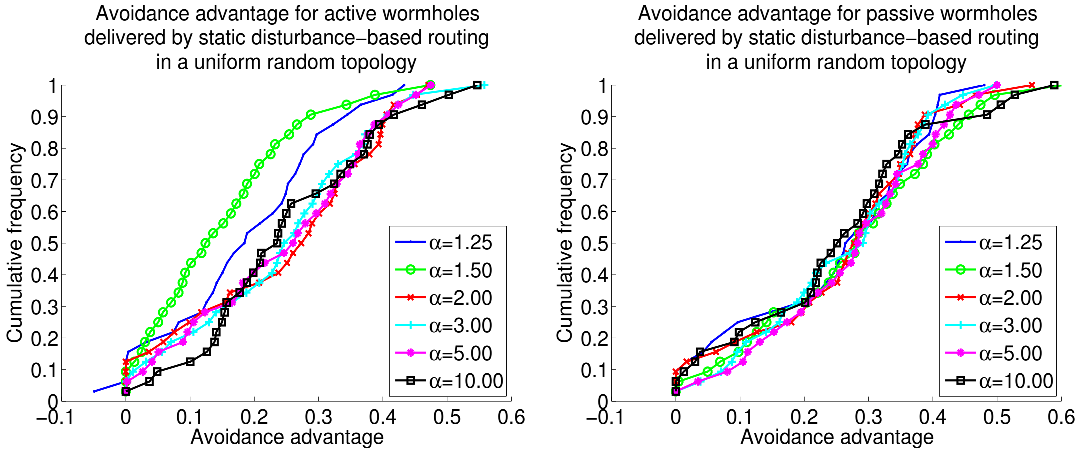

(a) For active wormholes

(b) For passive wormholes

Figure 43: CDFs of avoidance advantage for static disturbance in uniform random topologies

topologies. With an active wormhole in the grid-based Gaussian case, an edge effect was observed in which safer regions towards the edges are favoured. In uniform random topologies, the edges produced are less consistent, and placement variations can lead to nodes within the centre of the topology having lower connectivity. Therefore the regions of reduced threat on the outside of the topology are more difficult for the protocol to detect, and increasing $\alpha$ will not favour edge routing as strongly. This accounts for the lower variation with different $\alpha$ value compared to the grid-based Gaussian topology case.

In the passive wormhole case (Figure 43b, page 137), avoidance advantage is again shown to be largely independent of the value of $\alpha$ chosen for the metric. With these topologies, the uniform random variation gives a wider spread in peer count for ordinary nodes. However, the peer inflation effect is still noticeable, as on average it results in a doubling of the connectivity degree around these nodes. Increasing $\alpha$ therefore does not add any additional incentive to route away from the wormhole, and there is no consistent increase in median avoidance advantage with increasing $\alpha$.

#### 5.7.3.2 Radial Ring Topology

For the radial ring topology in the active wormhole case, results (Figure 44a, page 138) demonstrate that performance of the scheme for active wormholes is highly dependent upon the $\alpha$ value selected, with around $\alpha = 3$ being a critical value at

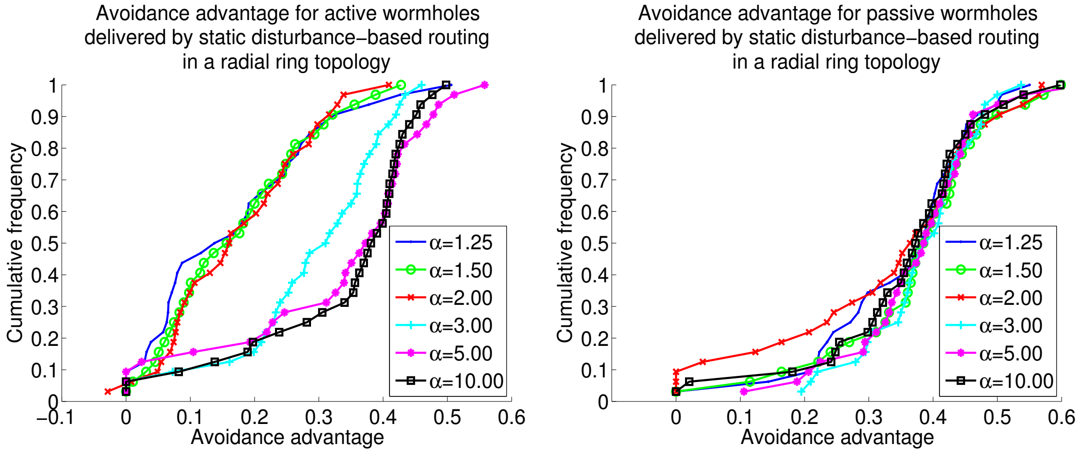

(a) For active wormholes

(b) For passive wormholes

Figure 44: CDFs of avoidance advantage for static disturbance in radial ring topologies

which performance begins to increase. The performance for $\alpha < 2$ is relatively consistent, with approximately 80% of simulation runs producing an avoidance advantage less than 0.25. In this case, the poorer performance is due to the weaker edge routing incentivised by the protocol at lower $\alpha$ values. For $\alpha = 3$, median avoidance advantage increases by 0.15 to 0.31, and at $\alpha = 10$, median avoidance advantage increases to 0.38. Since the radial ring topology has sharp and consistent edges, then the edge routing effect can easily find the edges at higher $\alpha$ values.

For the passive wormhole case, 80% of topology realisations experience avoidance advantage under 0.45, corresponding to just under half the routes avoiding the wormhole successfully. This performance is independent of the $\alpha$ value, as would be expected in a highly regular topology in which the peer inflation effect of a passive wormhole is highly detectable. It is in the lower quartile of simulation executions in which there is some dependence on the $\alpha$ parameter, with the spread increasing between the simulation links. Notably the case in which $\alpha = 2$ has slightly reduced performance. This motivates the choice of high $\alpha$ for good performance in general topologies.

### 5.7.4 Selection of Dynamic Disturbance-Based Metric Basis

Figure 45, page 139 shows the performance of dynamic disturbance-based routing for avoidance of active wormholes in a grid-based Gaussian topology and a radial ring topology. In dynamic disturbance routing, $\beta$ values must be considerably higher

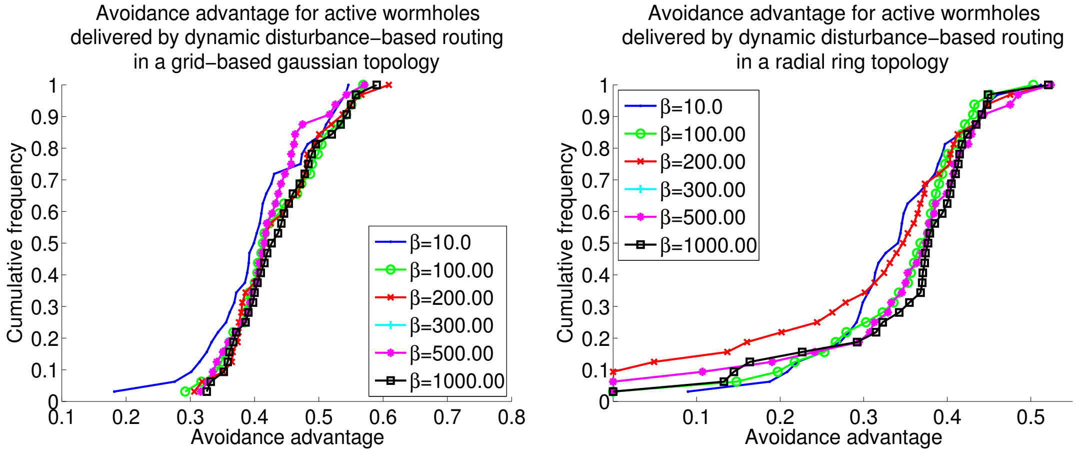

(a) For grid-based Gaussian topologies

(b) For radial-ring topologies

Figure 45: CDFs of avoidance advantage for dynamic disturbance metrics

than those used for $\alpha$ in static disturbance-based routing for dynamic disturbance to match the results previously obtained for static disturbance, and provide an initial avoidance when the $SPAF$ is low during the early phases of network establishment. Therefore the range $10 \leq \beta \leq 1000$ is considered.

The need for increased $\beta$ arises due to the structure of the equations. In static disturbance-based routing $\alpha$ is used as the exponent, but $\beta$ in dynamic disturbance-based routing is used as the basis. When $\beta = 1$, dynamic-disturbance routing reduces to shortest-path. For dynamic disturbance-based routing to perform well, the wormhole must be disadvantaged by the concentration of shortest-path routes around its endpoints which form the bottleneck. Therefore the basis $\beta$ values considered must be higher than the corresponding values used for $\alpha$ previously, to make alternatives a better choice. Correspondingly values of $\beta > 10$ are used.

In both figures with sufficiently high $\beta$ values (comparable to the number of nodes that the wormhole spans across the topology) the dependence of avoidance advantage on basis parameter $\beta$ is minor, even over a wide range of $\beta$ values. In the grid-based Gaussian topology (Figure 45a) there is an increment from 0.39 to 0.42 in median avoidance advantage with increasing $\beta$. In the radial ring topology (Figure 45b median ADV increases from 0.35 to 0.37.

### 5.7.5 Static Versus Dynamic Disturbance For Fixed Wormhole Locations

It was noted in Section 5.7.2, page 135 that static disturbance-based routing frequently obtains avoidance advantage via an edge routing effect, through incentivising routing towards the edges of the topology where the peer count was lower. However, in cases in which the wormhole is located upon an edge, such an approach will not lead to wormhole avoidance.

It is important to consider the performance of static versus dynamic disturbance-based routing in cases in which the wormhole is located upon the edge of the topology. This may arise, for example, in scenarios in which the attacker is known to control a certain region of the topology, in which they would have the ability to place their wormhole without detection. An active wormhole (the most challenging type for detection) in a fixed location is tested across an ensemble of topologies. Metrics values found to perform well in previous sections ($\alpha = 5.0$ and $\beta = 300$) are used in this comparison.

Figure 46, page 140 shows that for fixed wormhole location scenarios, the dynamic disturbance protocol obtains better performance than the static protocol, with static disturbance providing negative avoidance advantage in some cases, due to its tendency for edge routing which leads towards the wormhole in this scenario. In the case in which the wormhole is located upon the southern edge, selecting dynamic disturbance-based routing as opposed to static increases median avoidance advantage from 0.21 to 0.29. In cases in which the wormhole is located upon the

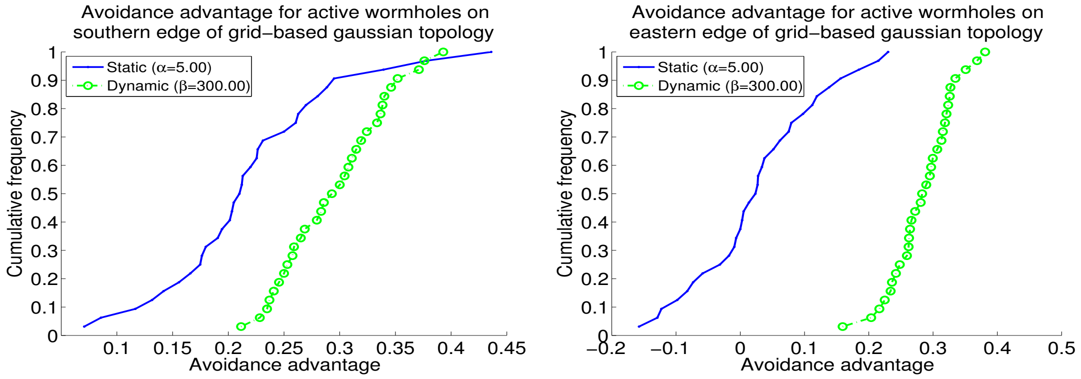

(a) Wormhole on southern edge

(b) Wormhole on eastern edge

Figure 46: Edge routing and the performance of static versus dynamic disturbance

eastern edge, the performance increment is more considerable. Static disturbance-based routing obtains a zero median avoidance advantage, while dynamic is able to obtain $ADV = 0.28$. The performance of dynamic disturbance-based routing is also more consistent than static, with a narrower range of possible avoidance advantages indicated on the CDF plot.

It is important for a security-conscious deployment that secure protocols perform better than a baseline solution, in this case shortest-path routing. However, when the wormhole is placed on the eastern edge (Figure 46b), static disturbance-based routing achieves a negative avoidance advantage in 35% of cases. By contrast, the important feature of dynamic disturbance-based routing demonstrated here is its stability and consistently positive avoidance advantage. This illustrates the ability of the dynamic disturbance protocol to locate active wormholes through their inherent bottleneck effect. Therefore, dynamic disturbance-based routing is especially favourable for stable performance in cases in which the attacker is known to control a particular region of the topology in which their wormhole would be anticipated for deployment.

## 5.8 Securing Dynamic Disturbance Against Followup Attacks

#### 5.8.0.1 Preventing Dropping Of Shortest Path Replies

A potential security vulnerability of the dynamic disturbance approach is its reliance upon the wormhole faithfully delivering reverse unicast replies for the shortest path routes. Since the attackers deploying the wormhole have an interest in attempting to defeat the protocol, it is possible for the wormhole to prevent disturbance from accruing along earlier points in a path by dropping the first response seen. This is only an advantage for the attacker if it is known that this disturbance scheme is being used, since in its absence, dropping route responses would be likely to reduce its exposure to traffic, preventing the wormhole from taking any part whatsoever in routing.

If the attacker knows that the disturbance-based protocol is in use, then an extra security measure can be implemented. This approach involves dispatching a periodic flood from the sink node. This route update consists of a single packet containing the largest node identities and their corresponding aggregate increments in SPAF for nodes on all routes found to that destination during that interval. The nodes and their peers apply these disturbance increments for the duration given in the packet.

This route update flooding mechanism serves to ensure the propagation of the most significant disturbance changes to all network entities, regardless of attempts by the wormhole to interfere by traffic-dropping. Since there are typically very few destinations in a sink-oriented sensor network relative to nodes themselves, this occasional flooding approach would not impose an excessive burden.

#### 5.8.0.2 Authenticating Disturbance Increments

In order to prevent spoofing of shortest path route replies, or other protocol updates from the sink, mechanisms can be used to authenticate them. A digital signature could be employed, but as discussed in Section 3.6.3, page 63, if routing is particularly frequent, the energy impact of the computation associated with the public key operations could be excessive. Since all the route responses originate from a common endpoint in a WSN (the sink) it is possible to use the one way hash chain approach (Section 3.6.4, page 66) to authenticate route responses as part of a consistent series delivered from the sink. This could distinguish any spoofed responses that try to generate spurious disturbance, as malicious nodes could not generate an authentic response as a result of not knowing the originally generated sequence number presented by the sink.

## 5.9 Conclusion

This chapter has presented and analysed two distinct disturbance-based routing protocols that can provide benefits for wormhole avoidance in WSNs; static and dynamic disturbance-based routing. Although a variety of schemes already exist to provide wormhole detection, they suffer many drawbacks, such as requirements for centralised communication, unreasonable algorithmic complexity, inability to integrate with realistic MAC schemes, and requirements for hardware that may not always be available. Overall, the continuous usage of such wormhole detection schemes imposes an energy burden in energy-constrained networks designed for long-term deployment.

The disturbance-based approaches presented in this chapter, by contrast, provide a way to embed awareness of possible wormhole locations into decisions made by a distributed routing protocol based upon the standard AODV protocol. Routing away from a wormhole reduces its exposure to network traffic, and therefore its ability to aggregate traffic flows and therefore compromise or otherwise interfere with ongoing network behaviour. Therefore, although these schemes cannot guarantee isolation of the wormhole from the network, integrating wormhole avoidance into a routing function that multihop networks must carry out anyway as part of its operation makes the system more stable and secure by an additional layer of protection. If data never reaches the wormhole, or uses it in reduced quantities, then its ability to disrupt network activity is correspondingly reduced.

The static disturbance-based scheme presented has been shown to be capable of avoiding both passive and active wormholes. This protocol uses a metric which takes the topology structure and peer count of each hop into consideration along the route. Passive wormholes are avoided based upon their peer inflation effect, in which the wormhole creates strongly connected components. These are penalised by the tendency of static disturbance to favour less densely connected network regions. Active wormholes are avoided based upon the tendency to route to the edge of the network. With a suitably tuned $\alpha = 10$ value, static disturbance based routing can produce an avoidance advantage of 0.5, corresponding to an additional 50% wormhole-free routes.

Dynamic disturbance-based routing locates wormholes by forming an additional shortest-path route which flows through them, and then using this route to accumulate dynamic disturbance. The route itself flows through regions of low dynamic disturbance. The dynamic disturbance-based protocol has been shown to be capable of locating the wormhole through the bottleneck effect it generates in operation, and delivers stable performance particularly in simulation scenarios in which the wormhole is located upon the edges of the topology. In these situations, dynamic disturbance-based routing is recommended for deployment.

Therefore, these approaches are suitable for deployment in existing networks, in which energy or hardware constraints mean that no conventional wormhole detection is permissible. They provide for continued network operation with wormhole-free routes if the wormhole link is severed, and the ability to continue to provide network service if the link is severed. These approaches provide a valuable complement to the existing detection schemes and are capable of delivering defence in depth for the overall network, by directing traffic away from regions in which a wormhole is suspected or detected from topological or traffic flow characteristics.

# Chapter 6

# Wormhole Avoidance Using Reputation-Based Routing

## 6.1 Introduction

The previous chapter introduced a novel routing concept, disturbance-based routing, as a countermeasure against the wormhole attack in sensor networks. This chapter presents an alternative wormhole avoidance approach, reputation-based routing (RBR), which is viable in topologies in which attackers will take time to deploy their wormhole. A logarithmic reputation metric is demonstrated to create long-term memory in the network that encourages reuse of nodes and links traversed earlier, favouring the use of wormhole free paths even after a shortcut across the network is introduced by a wormhole attacker. Simulation results are presented to verify the performance of the reputation-based routing approaches.

Reputation-based routing is chosen to provide a viable wormhole avoidance approach in scenarios in which it can be assumed that a stabilisation interval free of attack exists. This is likely to be the case, for example, in scenarios in which the attacker is assumed to be poorly resourced, or a deployment is spontaneous. The reputation-based routing approach has the advantage of not requiring tunable parameters such as the $\alpha$ and $\beta$ values involved in the disturbance-based routing schemes. This absence of parameters simplifies deployment by removing the requirement to consider tuning the scheme to specific topology characteristics, which therefore improves the simplicity of deployment. This chapter motivates the intuitions behind the novel reputation-based routing approach [3], defines its metric and logic of operation, and presents simulation results to demonstrate its performance characteristics for standard topologies.

## 6.2 Overview of Reputation-Based Routing

The nature of the novel idea, reputation-based routing, presented in this chapter is to provide routing that is resilient against the future introduction of a wormhole attack via a conceptually simple and persistent reputation metric, updated and reinforced by the dynamic traffic patterns at a particular node. In this section the nature of the idea and its protocol operation will be defined and design consequences explored. The goal of the approach is to introduce long-term hysteresis into routing decisions, in which even though particular routes have expired, their constituent nodes remain favoured candidates for later routing by the rest of the network.

The key idea is that in many attack scenarios there can be expected to be a stabilisation interval from early deployment, during which the network will remain free of threats. In a newly deployed network, before implementing a wormhole attack, the attacker would be required to scan the topology, locate the sink, determine the goals of the network, realise that a wormhole is the desired attack vector to gain control of network routing, and implement their attack.

It can be assumed that this stabilisation interval will form a safe operational window during which the network can operate unhindered, particularly if node deployment is a gradual process and nodes self-organise to discover routes from their individual activation. Within this interval, the nodes will perform their routing and data dissemination along wormhole-free paths, loading the reputation metrics such that these nodes become preferential nodes for inclusion in routes.

The protocol depends entirely on local calculations using overheard information as part of the normal routing process. As a result, it does not impose any additional overheads as seen in other wormhole detection mechanisms. Potential overheads include sentry packets as in packet leashing (Section 3.5, page 56) or watchdog packets for collaborative behaviour checking [53]. The underlying logic of the routing protocol can operate using a standard and well-tested routing protocol for end-to-end metric minimisation such as AODV [109]. This assists integration of the protocol into existing sensor network operating systems, allowing it to use similar routing logic but with a custom metric.

## 6.3 Philosophy Behind Reputation-Based Routing

Consider the case in which an attacker deploys a wormhole some time after the network begins operation. Previously, it can be anticipated that routing protocols carrying traffic to the sink would have taken relatively direct routes. However, when the wormhole is introduced, the topology is suddenly changed dramatically, with the wormhole presenting a shortcut across several hops. If a routing metric can be devised in which the previous usage of those hops creates a sufficiently powerful incentive to continue using them in the presence of the sudden topology change, then the wormhole attack will fail to draw significant traffic. Figure 47, page 148 illustrates this, demonstrating the accumulation of reputation in the early phases of operation that later leads those nodes to be preferred over a newly introduced wormhole shortcut with no reputation.

The intuition behind the reputation routing protocol is to create suspicion regarding topology changes and a resulting disincentive to use the newly available shortcut route that a wormhole would introduce. The reputation metric is structured so that even though the original routes have expired and the wormhole now provides a shortcut route to the destination, the newly established wormhole and its surrounding nodes do not have sufficient reputation to be selected. Thus, the reputation-based routing protocol will treat these new routes with suspicion and will favour the routes featuring trusted nodes until the alternatives are exhausted.

Figure 6.2, page 146 presents an overview of the reputation-based routing metric. During the stabilisation interval, reputation levels have incremented upon nodes on the route shown at the start of the sink. When the wormhole is introduced, the nodes around its endpoint do not have sufficient reputation for the route through the wormhole to be chosen for routing. Therefore, the safe route continues to be located.

### 6.3.1 Reputation Metric Definition

Given a particular multihop route in the network, successful delivery of data to an endpoint requires retransmission at all intermediate nodes along the route. If a

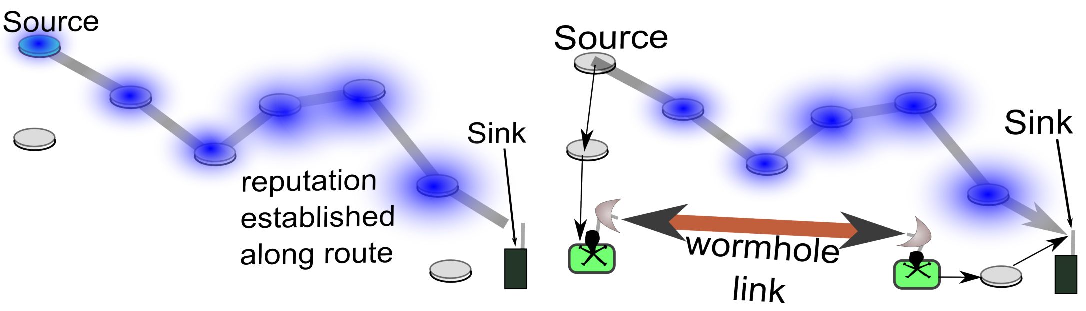

(a) During stabilisation interval (b) Following stabilisation interval

Figure 47: Operation of reputation based routing, preferring long-established routes

node is malicious and refuses to forward, or is subjected to destructive jamming interference or the presence of a wormhole, then the route carries an increased probability of failure. The challenge for an avoidance protocol is to determine the probability that a wormhole or other security threat is located within a region.

It is possible to explore the use of an analytic approach, in which a priori information about the structure and nature of an attack is explored to the individual link probabilities. This approach was considered in Section 4.9, page 101 in an analysis of signal jamming attacks.

However, in order to make the best selection of routes in an operating network in which the precise form of the attack is unknown and no statistical assumptions about the placement of wormholes help to structure the attack, a more robust mechanism will use empirically sampled past performance to approximate these probabilities. Therefore an estimate of the likelihood of routing success can be obtained from historical information, using the concept of a per-node reputation level $RLEVEL_i$. This represents the reputation, and an aggregate of the trust placed in a node from its successful forwarding. RLEVEL itself is bounded to one, a state that represents complete trust of a particular node. Complete trust occurs when the bandwidth demand of the route replies received is equal to the node response.

The reputation level of a single node is increased on each successful routing response unicast back from the sink by $RLEVEL\_INC$, which is defined for new route $R$ by Equation 6.1 in terms of the bandwidth demand of the particular route $BW_R$ (its data rate request carried in a routing header) and the data rate $DR_i$ of the transceiver at $N_i$.

$$RLEVEL\_INC(R) = \frac{BW_R}{DR_i} \tag{6.1}$$

The reputation metric of a single link between nodes $N_i$ and $N_j$, $RM_{i,j}$ is defined as a function of the reputation level of the originator at that particular time $t$, $RLEVEL_i(t)$, in Equation 6.2, page 149. The reputation metric is initialised to a nominal reputation null constant (RNK) upon activation of the protocol. Therefore for formation of the first route (before any reputation increments are received) the behaviour of the protocol is effectively equivalent to shortest-path routing. The nature of the logarithmic function employed is that as $RLEVEL_i$ tends to one, the reputation metric of the nodes upon the path to the sink goes to zero.

$$RM_{i,j}(t) = \begin{cases} RNK & \text{if } RLEVEL_i(t) = 0 \\ -ln(RLEVEL_i) & \text{if } RLEVEL_i(t) > 0 \end{cases} \tag{6.2}$$

A node with data to transmit that does not have an active route to the sink, broadcasts a RBR-RREQ, which is retransmitted at intermediate nodes, incrementing the aggregate reputation metric stored in the packet as it travels. Upon receiving a new reputation-based routing request, the sink chooses the end-to-end route with the lowest aggregate reputation metric (representing the highest reputation levels and thus the best choice), and unicasts the reply along the reverse route which serves to increment the reputation level.

From this, routes featuring nodes with a high RLEVEL (which have previously carried large amounts of traffic) will be rewarded strongly. The effect of this is to make the reputation algorithm very cautious, biasing it heavily towards the use of previously explored nodes, with a high reputation level, wherever possible. This is precisely the effect desired to engineer a secure network.

## 6.4 Simulation Methodology and Validation

### 6.4.1 Scenario Definition

This section defines the simulation scenarios, which are designed to model a security-critical hypothetical military deployment. The scenarios considered consist of a fixed region of terrain, within which the network operator seeks to defend their territory and track the motion of hostile enemy troop groupings. Homogeneous detection nodes are arranged within this region, using the standard topologies defined in Section 4.8, page 96. This ensures that topologies employed are representative of a wide variety of network situations, in which terrain prohibits an optimal regular deployment.

For the grid-based scenarios, the sink is located at the military headquarters upon the northern edge of the topology. For the radial ring topologies, the sink is located centrally. The malicious attacker chooses to deploy one of their wormhole endpoints within a one-hop distance from the sink. The remote pickup endpoint of the wormhole is located upon the midpoints of either the southern edge of the topology.

In this scenario it is assumed that, immediately following the stabilisation interval, the attacker activates their wormhole. This could either occur by the deployment of the endpoints, or the activation of the link between them. Following this, future routing packets and responses are tunneled through the wormhole, which allows allow it to control routing as usual in the case of an attack.

Armies move in a randomly selected direction, reflecting of the boundaries of the southern half of the deployment region. At the new flow interval on approach of an army within detection range of an idle detection node, routing to the sink is initiated according to the defined protocol. Network routing is updated at each routing interval, and flows remain active at their given flow rate for their specified route lifetime. During simulation, the wormhole is activated after the stabilisation interval, and then begins to propagate traffic as intended. The simulation is implemented as a custom program in the OCaml programming language [92].

### 6.4.2 Simulation Methodology

The simulator generates an ensemble of topologies. In each topology, connectivity between nodes is modelled according to a standard protocol model (as described in Section 4.4.3, page 85), assuming bidirectional binary connectivity within a given peer distance threshold $P_R$. This assumes that a link is connected if its endpoints lie within the range $P_R$, and disconnected if they are outside of this. For simplicity, the maximum sensing range $S_R$ within which the nodes will detect troops, is set equal to the communication range. Periodically, at the new flow interval during simulation, the fresh position of each troop cluster is recomputed using their known velocity, previous position, and the time delay. The simulator checks for idle sources surrounding each troop cluster within $S_R$, and proceeds to activate the nearest idle source for reporting. Reputation level increments are applied to the route with the lowest aggregate metric.

### 6.4.3 Success Metric Definition

The metric employed to analyse reputation-based routing is the avoidance advantage ADV. The simulator records a metric to assess the success of reputation-based routing with the given topology properties. The avoidance advantage (ADV) is the additional proportion of all discovered routes throughout the simulation that successfully avoid the wormhole under the disturbance scheme as compared to shortest path. A value of zero corresponds to a state in which the disturbance-based scheme delivers no advantage, as precisely the same proportion of routes used the wormhole as in shortest path routing.

### 6.4.4 Simulation Validation

This section considers validation of reputation-based routing simulations. The core of reputation routing simulation is based upon the software developed for disturbance-based routing (Chapter 5), and therefore inherits the tests for the routing and results generation demonstrated in Section 5.6.4, page 127.

#### 6.4.4.1 Single Circle Topology For Reputation-Based Routing Validation

This section will consider a simple single circle topology, and the behaviour of the reputation-based routing protocol within it. Simulation behaviour will be compared against an analytic model to verify correct computation of the reputation-based routing metrics with additional routes, and correct routing decisions according to the protocol logic.

Consider a simple topology as depicted within Figure 48, page 152. This circular test topology contains $C = 16$ uniformly spaced nodes around the circle, with the sink node as one of them with index $N_1$. The connectivity of the topology is sufficient to connect all adjacent nodes within the circle. Node $N_2$ is originally disabled. As a result the data transmissions from node $N_3$ at the start of network activation must form a multihop route counter-clockwise all the way around the circle.

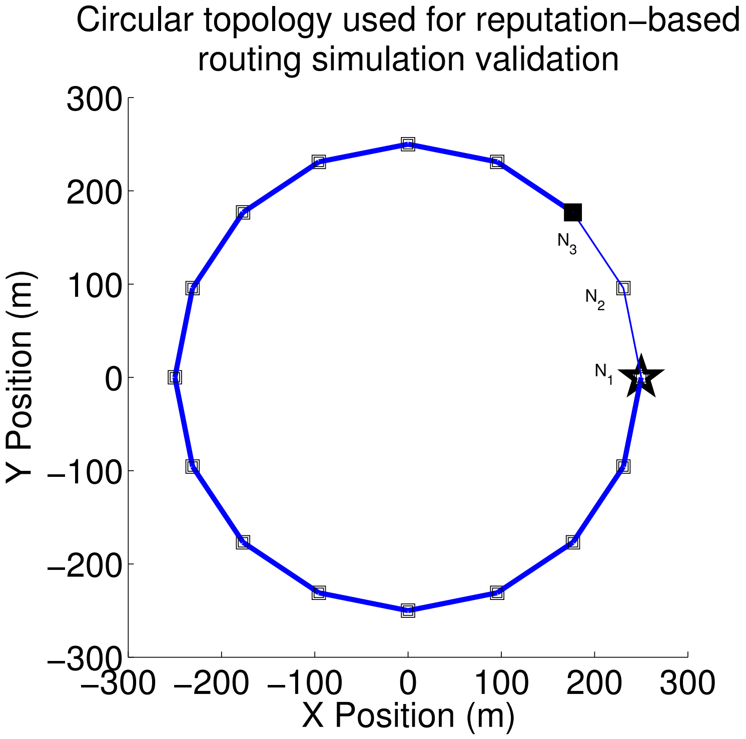

Figure 48: The circular test topology

#### 6.4.4.2 Validating Reputation-Based Routing Against Analysis

After a given time interval $T_{change}$, disabled node $N_2$ is activated. This models the process by which a wormhole changes the connectivity properties of the system. A potential shortcut is now available in which node $N_3$ is connected to the sink via an intermediate clockwise hop through $N_1$. In order to provide wormhole avoidance, reputation-based routing should however choose to reject the shortcut in favour of the previous counterclockwise route. This occurs when sufficient reputation has accrued for the route to have a lower overall reputation metric, despite its overall increased length.

Upon its initialisation, the node $N_2$ upon the newly introduced shortcut does not have any reputation, and therefore the metric for the hop using it is the reputation null constant $RNK$ (Equation 6.2, page 149). Since only the intermediate hops and not the originator itself contribute to the reputation metric, the shortcut route metric only contains the contribution from the link leaving $N_2$. For a reputation level $RLEVEL_{min}$ at which the previous counterclockwise route will be equal in aggregate metric to the shortcut, the following must hold:

$$RNK = -\sum_{i=4}^{C} ln(RLEVEL_{min}) \tag{6.3}$$

The reputation upon all previously used nodes will be a constant, due only a single source $N_3$ being previously activated. Therefore the summation can be replaced with the number of nodes contributing to the reputation. This gives the following relationship between the parameters:

$$RNK = -(C-3)ln(RLEVEL_{min}) \tag{6.4}$$

In order to verify this relationship, the simulation results were contrasted with this analytic prediction. The simulation proceeded by generating the previously described circular topology, with $N_2$ adjacent to the sink disabled. Given a reputation level target and a particular value of the null constant RNK, initial routes were formed until the reputation level equalled this value. At this point, the disabled node was reactivated to offer a shortcut route. Success was recorded for the trial if the counter-clockwise route was used, and failure if the shortcut was used. Figure 49, page 153 shows an example of failure and successful cases during this routing operation. In the successful avoidance case, $K = 10$ and $RLEVEL = 0.5$, which is, as predicted analytically, sufficient reputation to continue using the counter-clockwise route. In a failure case, $K = 10$ and $RLEVEL = 0.4$.

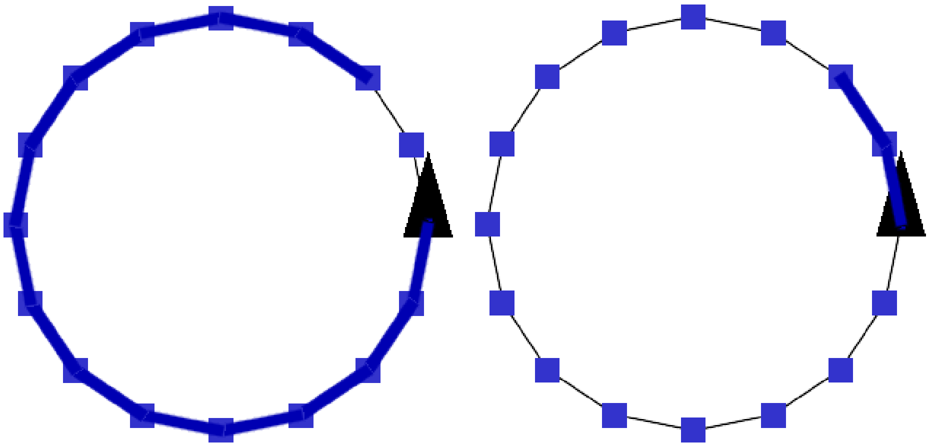

(a) Avoidance success case (b) Avoidance failure case

Figure 49: Simulation of reputation-based routing in the simulation test topology

Figure 50, page 154 demonstrates a match of simulation performance with the analytically predicted values. This validation test is conducted in a single circle topology consisting of $C = 16$ nodes (including the sink as $N_1$). The figure shows the minimal value of RNK which allowed the reputation-based routing protocol to successfully use its original route in the presence of the shortcut. This was found using a bisection method, beginning with a range of RNK values from 0 to 50.

This range was iteratively bisected and the midpoint tested, to discover the smallest value of RNK that produced successful avoidance of the shortcut. It is clear that the simulation results for minimal required $RNK$ are precisely as predicted by the equation. This serves as validation of the simulator logic for route establishment and computation of the reputation metrics.

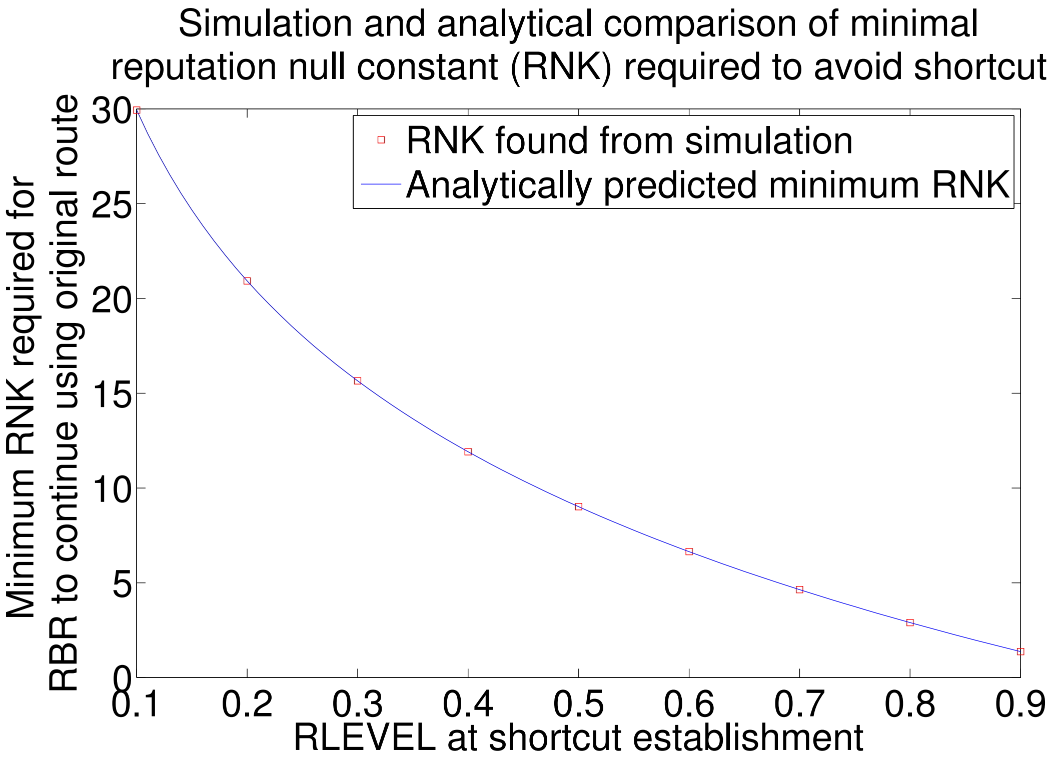

Figure 50: The relationship between RNK and RLEVEL

### 6.4.5 Default Parameters

Unless otherwise specified, the parameters displayed in Table 4 are employed to generate the full simulation results for this chapter. The topologies employed are those standard topologies as specified in Section 4.8, page 96.

## 6.5 Results

This section describes and analyses the performance of reputation-based routing in ensembles of grid-based Gaussian, radial ring and uniform random topologies (Section 4.8, page 96). The results use a stabilisation interval of $S_i = 200$ seconds,

| Parameter | Symbol | Default Value |
|---|---|---|
| Simulation run topology ensemble size | | 50 |
| Simulation runtime | | 3000 seconds |
| Stabilisation interval | $S_i$ | 200 seconds |
| Routing interval | | 10 seconds |
| Route lifetime | | 100 seconds |
| Bandwidth demand | $BW_R$ | $5kbit/s$ |
| Channel data rate | $DR$ | $250kbit/s$ |
| Grid based Gaussian regularity factor | $R_f$ | 0.9 |
| Topology edge size | $S$ | 1000m |
| Peer communication distance | $P_R$ | 150m |
| Grid based Gaussian node count | N | 100 |
| Radial topology ring count | $R_{MAX}$ | 6 |
| Radial topology ring separation | s | 100 (m) |
| Radial topology radian separation | $k_r$ | 0.9 |

Table 4: Default parameters employed in simulation results

corresponding to the lifetime of 20 routes. Following the stabilisation interval, the wormhole is deployed and activated by the attacker. The wormhole remote pickup endpoint is located at a fixed location in the midpoint of the southern edge or eastern edges of the topology. These correspond to the cases in which the attacker controls a fixed edge region of the topology far from the sink and is able to install their wormhole in this region.

Figure 51, page 156 illustrates the avoidance advantage provided by the reputation-based routing scheme in the described scenario across an ensemble of 50 topologies. These results are presented as a cumulative distribution function to allow the range of avoidance advantage values across the ensemble of topologies to be examined and any outlier results identified. The performance for the highly regular topologies is very consistent. For the wormhole located upon the southern edge in grid-based Gaussian topologies, the median avoidance advantage is 0.97, and for the radial ring topology it is 0.87. Reputation-based routing always delivers an avoidance advantage above 0.8 in the case of southern wormhole placement in the grid-based and radial topologies.

The grid-based Gaussian topology result is considerably better than that achieved by the dynamic disturbance-based routing scheme in Section 5.7.5, page 140. With edge wormhole placements, the best avoidance advantages generated in the grid-based Gaussian topology were below 0.4. Therefore, reputation-based routing can deliver twice the avoidance advantage of dynamic disturbance in this regular topology. This

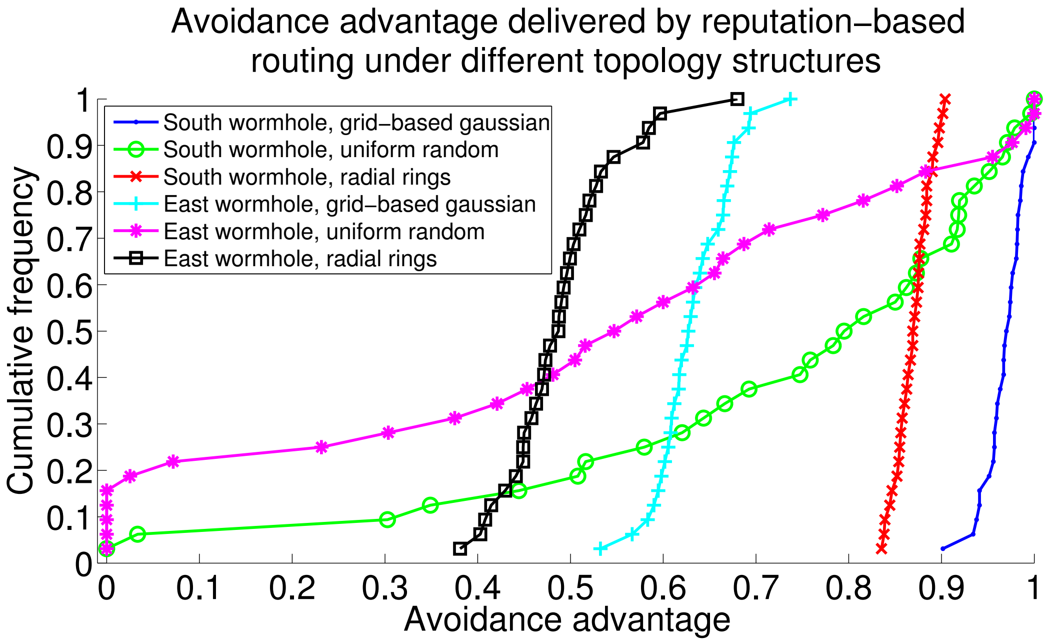

Figure 51: Distribution of avoidance advantage for reputation routing, under various topology ensembles

is due to the reputation buildup during the stabilisation phase across these highly regular topologies, which create tendencies to use these stable routes again from any nodes in the network.

For both wormhole placements, in the uniform random case there are some cases in which reputation-based routing fails to deliver such consistent performance. These have been investigated and shown to be those in which the local connectivity properties disadvantage the wormhole under the metric chosen. For example, the avoidance advantage metric is defined relative to how many routes would use the wormhole anyway under shortest path. If the wormhole placement site is poorly connected within the topology graph and thus offers an unfavourable shortcut, it may not achieve an advantage since it may be unreachable under either shortest path or reputation-based routing. This is not however a security failure, as the attackers will fail to achieve a significant gain from their wormhole.

This highlights a potential issue for deployment of reputation-based routing in irregular topologies. If the topology is sufficiently irregular that all traffic is bridged under a single link, then it is likely that introducing a wormhole next to this link could hijack its reputation. Therefore a condition for deployment of the scheme is that, if randomly deployed, the topology must guarantee sufficient connectivity along a variety of redundant paths (beyond the requirement for mere reachability of all nodes from the sink) to ensure an effective flow of reputation to the sink.

## 6.6 Conclusions

This chapter has introduced reputation-based routing, the motivation behind its introduction, and the logic that allows it to successfully avoid wormhole attack introduced after a given stabilisation interval, via its hysteresis which causes it to favour previously established routes for future routing following their expiry.

Simulation results have demonstrated the performance of reputation-based routing, showing a high avoidance advantage in topologies in which wormholes exist at a fixed location. It has been shown that the scheme is capable of operating successfully at schemes with a short stabilisation value. As long as the network as deployed can achieve full connectivity across a variety of diverse paths, implying that the topology must be sufficiently regular, reputation-based routing can avoid wormholes with high probability.

# Chapter 7

# Sybil Avoidance Using Hybrid Multihop and Supernode Routing

## 7.1 Introduction

Chapter 4 introduced the fundamental relaying concepts for supernode data transfer, and analysed the vulnerability of supernode routing relative to multihop routing for attacks such as homogeneous signal jamming. However, it is important to consider the supernode data delivery methodology not as a complete replacement for multihop routing, but instead as a complementary element that fits within a multihop routing topology. Accordingly, it is valuable to consider how routing technologies can accommodate supernodes to deliver good network-wide performance and reliable end-to-end routing. This chapter introduces the integration of physical-layer information to support reputation routing in the presence of supernodes, defining the physical reputation-based routing (PRBR) protocol.

Given the fluctuations in deployment density in stochastic topologies, together with the necessity for central coordination to manage these supernodes, it is likely that nodes will not always be able to reach a supernode coordinator, or that supernode data delivery will not always succeed, requiring retransmissions which will lead to capacity reductions. Therefore, a requirement for robustness suggests that multiple data relaying mechanisms should be made available, and that the choices between them should be dynamic if possible.

Furthermore, a multitude of issues, from temporary obstructions of nodes due to shadowing from mobile obstructions, time-dependent changes such as slow fading

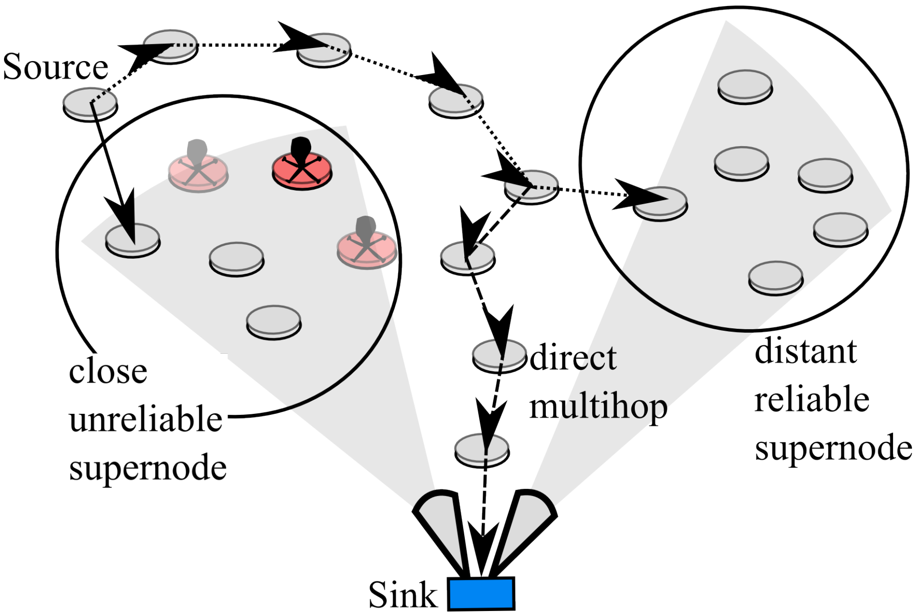

Figure 52: Options for routing in the presence of intermittently reliable supernodes

[95], to malicious jamming attacks from external devices (Section 4.9, page 101) can change network conditions and thus complicate supernode data delivery. Therefore, even if a node is close to a particular supernode, it is possible that alternative mechanisms may provide better performance for data delivery. Figure 52 illustrates options for data relaying, illustrating a node adjacent to an unreliable supernode (following malicious attack) but with the options of relaying via a more reliable supernode at a greater distance (illustrated dotted line), or using a pure multihop route to the sink (dashed line).

## 7.2 Overview of Physical Reputation-Based Routing

This chapter considers a hybrid routing model in which multihop routing is used by data originators to reach a supernode coordinator. Reputation-based routing, introduced in Chapter 6 is modified to use cross-layer information from the physical layer, forming physical-reputation-based-routing (PRBR). This protocol takes into account physical layer information, using the SINR of any supernodes comprising the final link in the route. As the supernode is the final limiting factor in delivery success, this is a critical parameter for assessing future data delivery success. By assessing these physical-layer parameters, the PRBR protocol can progressively during network operation learn the performance characteristics of these supernodes and distribute this knowledge throughout the network as part of route formation. If a supernode consistently delivers high performance at the physical layer, then it is reinforced and becomes more likely to feature in multihop routing from other sources.

The advantages of this approach include increased robustness. Should a supernode fail to deliver the idealised physical layer gain, as a result of physical-layer issues such as channel changes (brought about by obstruction), or local oscillator instability, then this will be reflected in a poorer performance as determined by the sink upon reception. In this case, it is likely that alternative supernodes should take over, allowing those suffering from impaired performance to relay a reduced amount of traffic.

This fits the security principle of using a diverse series of fallback mechanisms, and graceful degradation. An important part of forming a robust network is adaptation to observed performance characteristics. Using physical reputation-based routing, nodes do not automatically route through the closest supernode coordinator, but attempt to discover the most stable routes with the highest SINR for the relaying phase, in turn updating reputation metrics in accordance with their decision. This approach provides stability by directing traffic away from supernodes where performance may be intermittent, whether through malicious attack or connectivity problems. One particular malicious attack which may impair supernode performance is the sybil attack, discussed in Section 3.3.3, page 53.

Upon initiating routing for a new source, selection of the forwarding path depends upon relative performance of the network's supernodes, so those which are likely to be less reliable in delivery and require increased retransmissions will see the load that they are carrying reduced quickly. A final aspect of resilience provided is the ability for participating nodes to form a multihop route direct to the sink, which constitutes fault tolerance, in which the network reverts to a conventional multihop network with data delivery to the sink in cases of supernode failure. Through this mechanism it is always possible to fall back to multihop data delivery if performance of all available supernodes is poor.

## 7.3 Sybil Attack

### 7.3.1 Sybil Attack In Multihop Networks

The sybil attack, discussed in the literature review (Section 3.3.3, page 53) is an identity spoofing attack in which nodes fabricate additional identities. These false identities allow them to participate multiple times in protocols, thus compromising distributed voting or other protocols that depend upon distributed decisions or consensus. The sybil nodes may compromise the diversity of multihop routing, by creating unexpected single points of failure. In a similar manner to the wormhole attack where multiple paths converge on a link under the control of the attacker, multiple routes converge at a single physical node. This leads to a network in which the attacker can very easily implement a selective forwarding or complete denial of service attack, subverting the normal diversity of intermediate forwarding nodes and links that would normally limit the control a single node can obtain. An example is illustrated in Figure 53a, page 163. From the perspective of sources $S_0$, $S_1$ and $S_2$, traffic is sent along several diverse multihop routes that do not share a node in common. However, since one of malicious node M's sybil identities A, B or C is included on all three paths, M has defeated the diversity of multihop routing and controls all traffic in the network.

### 7.3.2 Sybil Attack in Distributed Beamforming Supernodes

The sybil attack has a different effect which impairs the performance of a beamforming network, through its inability of a sybil node to fulfil the level of commitment claimed. In the event that one of the nodes participating in a supernode to perform beamforming is actually a sybil node, phase S3 (the distributed beamforming transmission phase to the sink) does not include as many SNMs as the coordinator anticipated from the acknowledgements received in dissemination phase S1.

This is because some of the participating nodes from the perspective of the coordinator are merely sybil identities, and ultimately underlying these virtual identities there is only one single physical node, with a single transceiver. Therefore the true number of SNMs participating in the beamforming transmission must be lower than expected by the coordinator. This leads to a lower possible theoretical peak SINR at the sink node receiving the beamforming transmissions, and therefore the probability of successful reception is reduced.

The motivation of the attacker in performing a sybil attack may not be to compromise beamforming intentionally; their motivation could be the desire to compromise other distributed services such as data aggregation schemes, or key establishment. In this case, it can be considered that the attack is implemented by code modification as a custom module of malicious code deployed onto conventional network nodes, which otherwise function undisturbed as intended by the defender. In this case, the sybil node will still make a beamforming transmission from its single authentic physical identity.

Given that the sybils in the network are malicious, if they are aware of the beamforming architecture in use, performance can be reduced further. One power-efficient example would be selective forwarding: participate in the first phase of the beamforming protocol, giving agreement to participate to the coordinator in phase S1, and then fail to make the transmission as agreed. In this case, the received SINR at the sink would be as if only the non-malicious nodes participated, as it will not include any contribution from the sybil nodes. This is the pessimistic case considered in the model employed in this chapter. Figure 53b, page 163, demonstrates this with a sybil node M around supernode coordinator C, which has two additional false identities $MS_1$ and $MS_2$. Although the coordinator expects six nodes including itself to participate, only three nodes make the transmission since M declines to transmit.

The PRBR protocol is shown to penalise supernodes subject to the sybil attack as candidates for routing. In addition to the benefits that routing over a supernode with a high SINR offers for resilience, this also draws traffic away from the sybil nodes, which being malicious nodes are under the control of the attacker and thus should be given as little exposure to network traffic as possible.

## 7.4 Physical Reputation-Based Routing Protocol

This section presents and explains the physical reputation-based routing protocol (PRBR), its foundational logic, equations and parameters. It operates by analogy to reinforcement learning, in that it rewards relaying supernodes with desirable

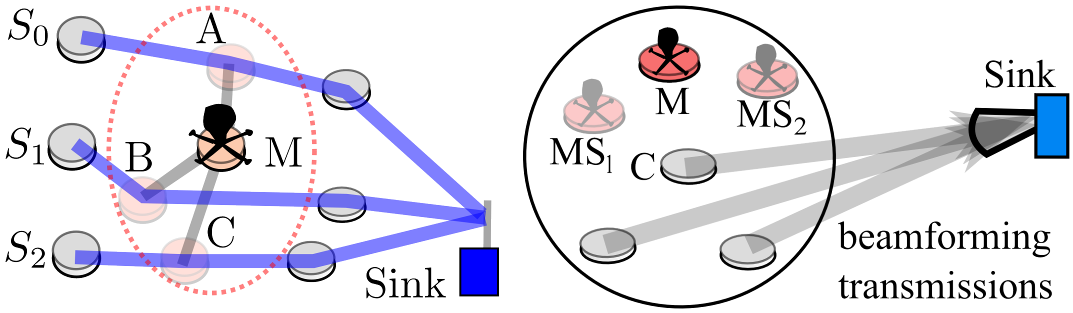

(a) Multihop routing (b) Beamforming

Figure 53: The interaction of the sybil attack with multihop routing and beamforming

characteristics, in this case a consistently good physical layer performance. One difference in philosophy compared to conventional reinforcement learning is that the protocol does not use reputation decrements, which during development were found to decrease performance. The protocol does contain a mechanism for allowing reputation to expire, which enforces a relatively short lifetime, maintaining continuous pressure towards exploration over the long term.

### 7.4.1 PRBR Introduction

Although the supernode provides a direct physical link to the sink node via a single hop, it may not be possible for every node in the network to make direct beamforming transmissions, whether due to insufficient deployment density of participating nodes around a coordinator, or malicious attack such as presence of sybil nodes in a region (Section 3.3.3, page 53). Therefore, it is necessary for these nodes to use multihop routing, either to reach a supernode coordinator or directly to the sink node.

Reputation-based routing [3] (Chapter 6) has demonstrated advantages in avoiding late-established wormhole threats in a multihop network, by prioritising routes established during the early threat-free period. A modification of RBR to form PRBR is shown to have utility in finding reliable supernodes for routing.

The PRBR protocol operates upon each node that is not a supernode member. Supernode members use their local supernode to relay their traffic, passing it to the coordinator for dissemination during stage S1. The protocol for PRBR performed by nodes that are not supernode member nodes (SNMs) is based on conventional reputation-based routing (RBR) for multihop networks (Chapter 6). It modifies the routing request phase so the sink selects the highest reputation metric, which is set by the physical-layer SINR value of the last hop, not the traffic load of the newly initiated route as in RBR.

A difference between the RBR and PRBR presented in this chapter is that PRBR stores reputation values for links and not merely individual nodes, and computes aggregate metrics upon a set of links traversed and not merely the nodes upon the route. The tasks for which the two protocols are applied is different, in RBR it is for wormhole avoidance, while PRBR is required for link selection and therefore benefits from the ability to select on the basis of link reputation values. The use of link metrics rather than node metrics has been shown to provide the best empirical performance.

### 7.4.2 PRBR Protocol at Nodes Not Supernode Members

A metric assesses the quality of links for routing based upon their physical-layer characteristics. Initially, reputation level $RLEVEL_i$ is initialised to zero for all nodes. This causes the reputation metric $RM$ to take the value of the reputation null constant $RNK$, which is initialised to a nominal high value. Effectively, in this case with a null reputation level as exists at initialisation, the protocol is equivalent to shortest path routing.

From this the reputation metric $RM$ is used in end-to-end routing, as defined in Equation 7.1, page 164. The logarithmic nature of $RM$ allows the end-to-end values to respond rapidly to changes, in which reliable routes quickly become favoured for forwarding. The best route, chosen for data delivery, is that with the lowest end to end $RM$ sum.

$$RM_{i,j}(t) = \begin{cases} RNK & \text{if } RLEVEL_i(t) = 0 \\ -ln(RLEVEL_i) & \text{if } RLEVEL_i(t) > 0 \end{cases} \tag{7.1}$$

Any node which wishes to route to the sink begins the PRBR protocol. A node which is not a supernode member broadcasts a request packet (PRBR-RREQ), which is rebroadcast at intermediate receivers not with a sufficiently fresh route, until it reaches the sink. These intermediate receivers include the supernode coordinators, which perform a beamforming transmission (via the mechanisms in Section 4.5.2, page 89) to deliver their data to the sink. The sink measures the incoming SINR of the transmission of the RREQ and uses its values relative to the historical SINR information for all supernodes in the network to determine a reputation increment, using the strategy given in Section 7.4.3, page 165.

A conventional multihop route response from the sink is also received, and can be used as a fallback if the supernode route formation process fails. This transmission is assigned a nominal SINR equal to the minimal detection or decoding threshold of the modulation scheme employed.

The sink then assesses the received routes, chooses the one with the highest reputation metric, and delivers a route response (PRBR-RREP) which propagates along the reverse path. If multiple PRBR-RREP packets have the same aggregate metric, then the selection is made based upon the physical SINR of the supernode that delivered the final hop to the sink. The reply PRBR-RREP from the sink is transmitted during the next S0 period of supernode control and establishment. From the supernode coordinator, it is unicast along its reverse path and propagates back to the route originator. If the sink chooses to apply a reputation increment, then the PRBR-RREP packet triggers increments to reputation level RLEVEL values upon the nodes that it passes on the reverse reply. Upon reaching the originator, this node uses the route contained in the packet to begin transmitting its data.

Therefore a supernode which is transmitting intelligible packets with high SINR is continuously reinforced, encouraging its used for transmissions from nodes all over the network, in addition to future transmissions from the current originator. In the language of reinforcement learning, this represents a very strong reinforcement of routes and partial route sections which have shown desirable performance characteristics for relaying data.

### 7.4.3 Determining Reputation Increments

Upon successful reception of the RREP, the sink may, if the route is of sufficient quality, apply a reputation level increment to the route through the best supernode. RLEVEL is incremented by $RLEVEL\_INC$ upon the nodes along the chosen route, to a maximum of one. The magnitude of this increment is specified in Equation 7.2, page 165. All signal-to-interference ratios employed are in logarithmic units.

$$RLEVEL\_INC = \frac{SINR_r - SINR_{min}}{SINR_{max} - SINR_{min}} \tag{7.2}$$

The magnitude of reputation delivered for a chosen route featuring a supernode is governed by the measured SINR of the beamforming transmission of the PRBR-RREQ to the sink, $SINR_r$, relative to the best $SINR_{max}$ and worst $SINR_{min}$ received at the sink over the course of the network operation. These function as high and low water-mark values, adjusting dynamically to the measured performance as the network runs. These include the current SINR samples $SINR_r$ from the route request under consideration. As a result, supernodes that perform very well receive a high increment in reputation.

An important characteristic inherent in the supernode delivery is that transmissions must meet a certain minimal reputation reward threshold $SINR_{thresh}$ for any reputation increment to be applied. Below this, routes are considered insufficiently low quality to receive any reputation increment. PRBR uses a dynamic strategy in which a fixed proportion of the best performing supernodes in the network receive the reward.

To track supernode routes that should be rewarded, the sink maintains history of supernode performance values per route request, and ranks the SINR of incoming requests relative to each other. If a supernode transmissions SINR is not in the highest $P_{BEST}$ proportion, the current route does not receive a reputation increment. A hard minimal cutoff $SINR_{cutoff}$ is also defined, below which no reputation increment is received regardless of relative performance. This is anticipated to be set to the decoding threshold for a particular scenario, plus a certain margin to account for link change or other performance problems. Therefore, even if a supernode is in the highest $P_{BEST}$ proportion of performers, if all performers are poor it does not receive increments. This is a static constraint that prevents the system from delivering reputation increments to supernodes performing below a predefined physical limit. This ensures that the network would prefer multihop routing over potentially unreliable supernodes, or supernodes suffering the presence of lots of sybils in their vicinity.

Upon network initialisation and the setup of the sink for data reception, the minimal $SINR_{min}$ and maximal $SINR_{max}$ tracking values are initialised based upon the reputation reward threshold value $SINR_{cutoff}$:

$$\begin{aligned} SINR_{min} &\leftarrow SINR_{cutoff} \\ SINR_{max} &\leftarrow SINR_{cutoff} + 1(dB) \end{aligned}$$

### 7.4.4 Gradual Expiration of Reputation

Information gathered about local performance frequently reflects transient behaviour. For example, in multihop routing protocols, links may intermittently fail and reactivate before routing protocols can compensate for this [40]. This can be expected to be even more true for supernodes, given their collaborative transmissions and the necessity for phase stability for a successful transmission. Therefore, it is useful for ensure reputation information remains current, via a mechanism in the protocol which removes old reputation information. By doing so, initial decisions (such as an exploratory choice of a poor supernode) will be automatically reversed if not continually refreshed by other reputation increments. By contrast, well-performing supernodes will be reinforced continually through the ongoing traffic that they contain, encouraging not just their continual use from the same sources but from other nodes.

The mechanism chosen to implement this is exponential decay of reputation values. Accordingly, unless an increment is applied the reputation level at each link is exponentially decreased, each time intervals $t_{INT}$ by a constant decay factor $D_f$, as illustrated in Equation 7.3. A decay factor value of $D_f = 0.99$, when $t_{INT}$ is equal to the average route lifetime, gives a half-life to the data of approximately 70 route requests.

$$RLEVEL_i(t + t_{INT}) = D_f RLEVEL_i(t) \tag{7.3}$$

## 7.5 Simulation Methodology and Validation

### 7.5.1 Simulation Methodology

The simulation is implemented in MATLAB. Firstly a topology realisation is generated and supernode clique memberships established. The source activation model is random, with three sources activated per routing interval. Routes are computed to all potential supernodes coordinators using the reputation level values for the network graph to calculate $RM_{i,j}$ for all links and the route with the lowest aggregate reputation metric is chosen and reinforced with an increment. The reputation increment received for these routes depends upon the appropriate sink SINR for the simulated supernode transmission, which takes into account supernode transmission with a specified level for the aggregate transmission. Exponential decay is applied to the all route level values to according to Equation 7.3.

### 7.5.2 Simulation Validation

This section considers validation of the simulations for physical reputation-based routing (PRBR). The simulation software for this chapter is implemented using MATLAB. The routing engine is based upon the prototype which was developed for disturbance-based and reputation-based routing, and successfully validated against an independent implementation in OCaml in Section 5.6.4, page 127.

#### 7.5.2.1 Fixed-Supernode Topology For Simulation Validation

In order to validate the simulations, a simplified topology was employed, the fixed-supernode topology, in which supernodes are considered as abstract entities whose performance was hard-coded into the simulation topology. This simplifies the simulation by removing issues of supernode member recruitment and resulting performance variations, and helps in validating the simulations by making anticipated behaviour analytically tractable. Figure 54, page 169 shows an example topology, with a single source and three candidate supernodes with sink SINRs performances of 12dB, 0dB and $-4$dB. All three supernode coordinators are reachable from the source node $S$ through a member node on their boundary.

#### 7.5.2.2 Validating Selection Of Best Candidate Supernodes

PRBR routing makes its selection of supernodes as a result of the reputation metric values. When no reputation is applied at the beginning of the simulation, all link metrics are equal to the reputation null constant (RNK). In this case, PRBR-RREQ packets will be flooded through the possible supernodes and reach the sink with equal reputation metric, but a decision will be made between them on the basis of physical SINR. The route with the highest SINR will be reinforced. From then, its repeated reinforcement will cause it to be chosen for all subsequent routing requests from $S$. For example, in Figure 54, the supernode with a 12dB SINR will be consistently selected for future requests.

Figure 55, page 170 shows this, illustrating the SINR for all routing requests across 100 trials of supernodes with fixed performance. 20 sequential routing requests were made from the source, with a new routing request after the expiry of the

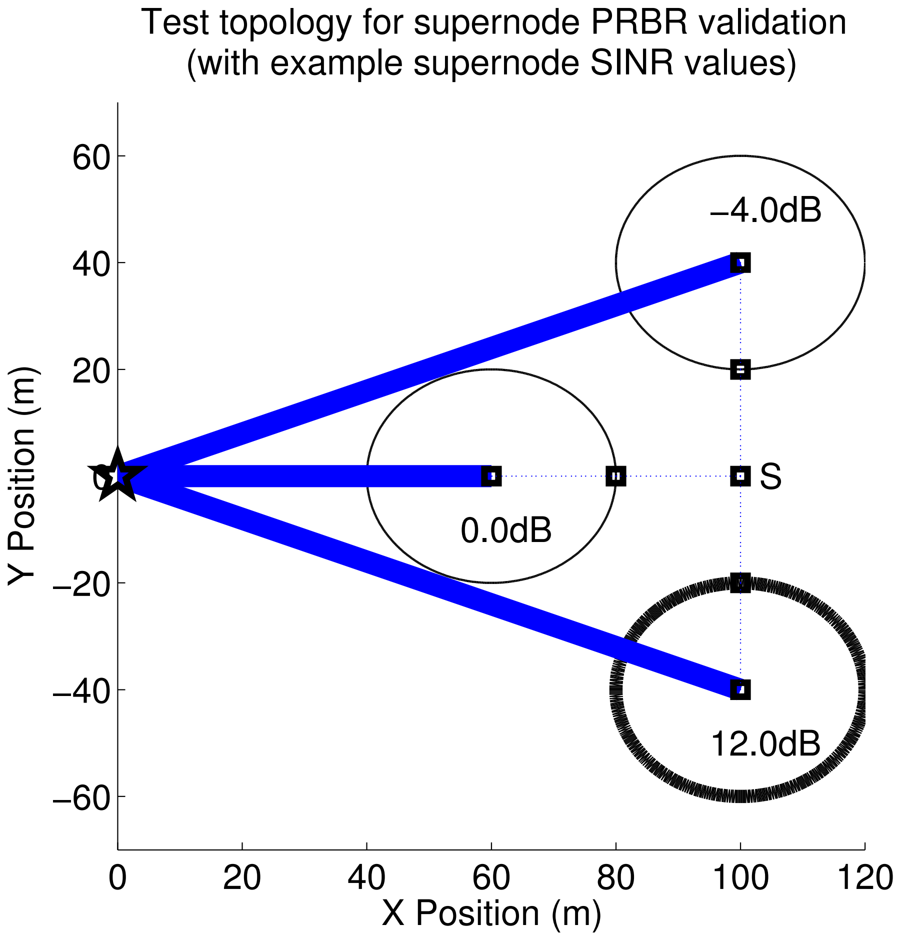

Figure 54: The fixed-supernode topology with a single source

previous. The supernode SINR performance was uniformly distributed between $0dB$ to 12dB, but filtered to contain at least one supernode with performance above 4dB (which according to the protocol logic is the minimal threshold $SIR_{thresh}$ to receive a reputation increment). Results are shown sorted by their SINR of the best performing supernode available in that trial. The modal SINR across all routing requests is shown to be precisely equal to the highest SINR available in the topology, indicating the choice of the best performing supernodes from the initial route request. This validates the simulator by showing the correct behaviour of the reputation routing increment, and its sensitivity to the SINR characteristics of the supernode.

#### 7.5.2.3 Validating Reputation Expiration and Route Change

Simulation validation tests in the previous section showed that PRBR is able to choose the best performing supernode following an initial PRBR-RREQ flood. However, it is also important for the protocol to be flexible and able to respond to changes in supernode performance. Validation of this property consists of allowing

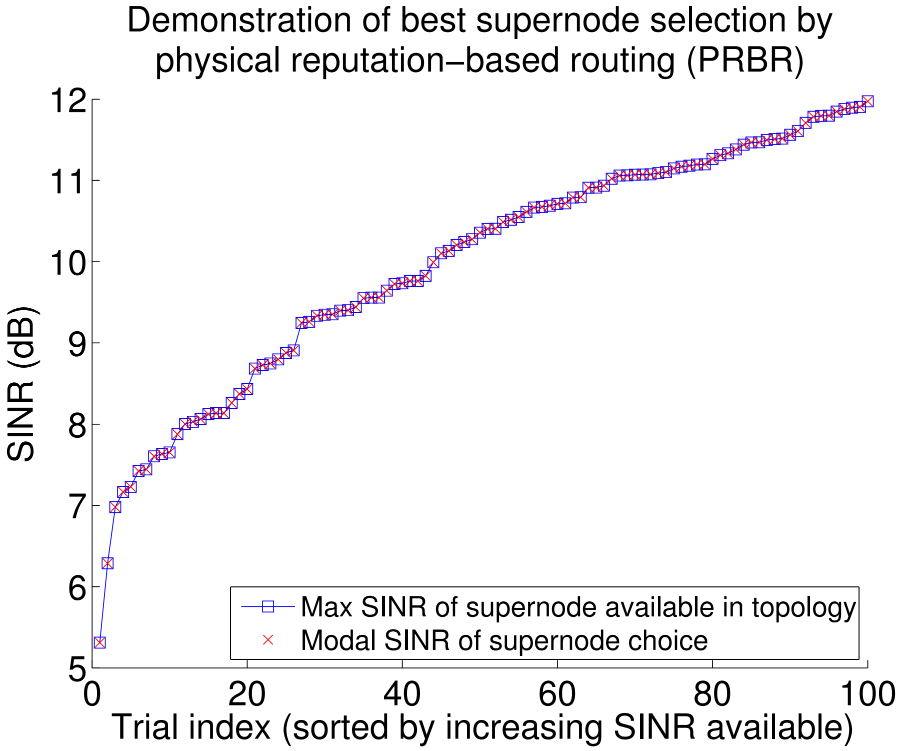

Figure 55: Supernode SIR selection for a single-source fixed-supernode topology

reputation to decay, in the presence of supernode performance change, and validating that the simulator respects analytically predicted behaviour in selection of a new supernode.

Consider the situation in which the performance of supernodes has changed, due to node failures, the introduction of sybil nodes, or physical-layer factors such as slow fading. From the structure of Equation 7.2, page 165, since the SINR of the best supernode will by definition by equal to $SINR_{max}$ (the best SINR the sink has seen over network operation), the reputation metric delivered will be unity along the route to that supernode. Since reputation levels are bounded to unity, the reputation levels upon this route will remain at this value until the exponential decay according to Equation 7.3, page 167 reduces the metric sufficiently to make an alternative route the better choice.

According to the protocol logic for reputation expiry (Section 7.4.4, page 167), upon every decay time interval $t_{INT}$ the reputation level at a node is multiplied by a decay factor, $D_f$, where $0 < D_f < 1$. Assume that the metric at a certain time is unity, and that no further reinforcement is delivered after this. In the fixed-supernode topology all possible routes to a supernode are of equal length, due to the source S being two hops from all supernode coordinators. Therefore if $(i, j)$ is a link on the route with existing reputation, after a time $T_{change}$ after the last request, the optimum route will change when the reputation metric upon the previously used link $i, j$ is equal to the null constant $RNK$ offered by the alternative route:

$$RM_{i,j} = -ln(D_f^{T_{change}/t_{INT}}) = RNK \tag{7.4}$$

The time at which the routing change is anticipated under this analysis, $T_{change}$, can be computed from the PRBR parameters by rearranging the equation:

$$T_{change} = \frac{-RNK.t_{INT}}{ln(D_f)} \tag{7.5}$$

The simulation was validated against the analytic equation given by the following methodology. The original scenario before the supernode performance change is depicted in Figure 56a, page 171. A single transmission is made with this scenario, which establishes reputation levels upon the route chosen as unity. After the first routing request is finished, supernode performance changes, as depicted in Figure 56b, page 171. Notably, the lower supernode declines from 12dB to 5dB, at which point performance is marginal and it would be advantageous to use another. The best decision in terms of physical-layer performance for future routes would be to use the upper supernode which obtains 12dB SINR.

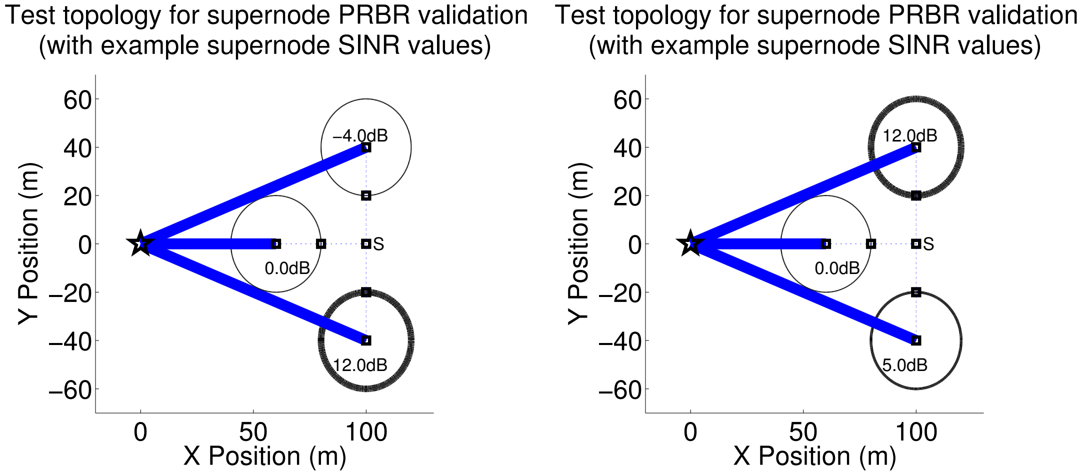

(a) Before SINR performance change (b) After SINR performance change

Figure 56: A fixed-supernode topology in the presence of supernode SINR performance change

After a given delay to allow reputation to expire (during which no routing requests are performed), another routing request is made. If reputation has decayed sufficiently, the upper supernode, with performance of 12dB, will be chosen for routing. If this process does not succeed, then the simulation is repeated with an increased

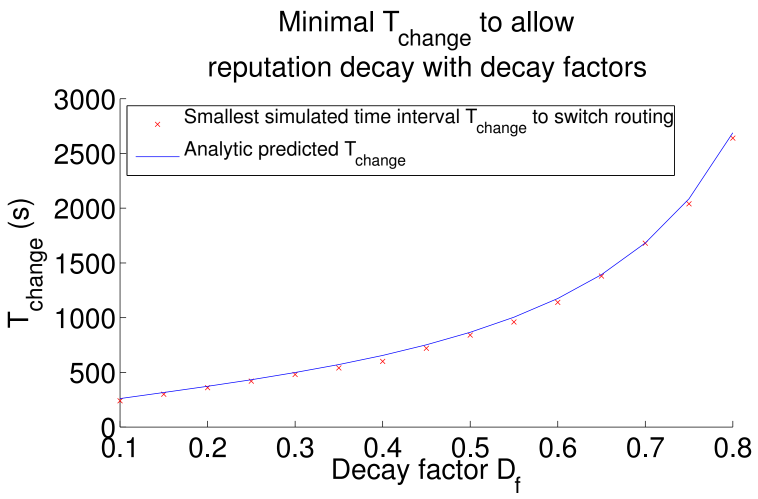

Figure 57: The relationship between required reputation decay time and reputation decay factor

delay attempt. The smallest delay that allows the routing to succeed is recorded as the empirical value of $T_{change}$. Figure 57, page 172 shows the predicted and actual change times $T_{change}$ for different values of the decay factor $D_f$. The reputation null constant $RNK = 10$, and $t_{int} = 60s$. The results show a close match between the analytically predicted time interval $T_{change}$ and the recorded transition times required for reputation to decay from simulation.

## 7.6 Topology Structure

The topology is a uniform random topology, square with side $1000m$, and contains three supernodes as well as the multihop relaying nodes. The density of node deployment is set so that the expectation of nodes within a supernode relaying is equal to minimal clique size $K$. The sink is located centrally, using an external out-of-band channel or wired link in order to transport its data out of the network for processing or analysis. The supernodes are located at polar coordinates $(400m, -\pi/2), (400m, -\pi/3), (400m, -2\pi/3)$. One realisation of this topology is depicted in Figure 58, page 173.

It is assumed that a fixed proportion of participating nodes are sybil nodes, with the distribution of sybils uniform across the topology. This corresponds to a case in which there exists a well-resourced attacker capable of manual insertion of malicious nodes throughout the network, or the ability to remotely reprogram a significant proportion of network nodes. During neighbour discovery sybils respond multiple

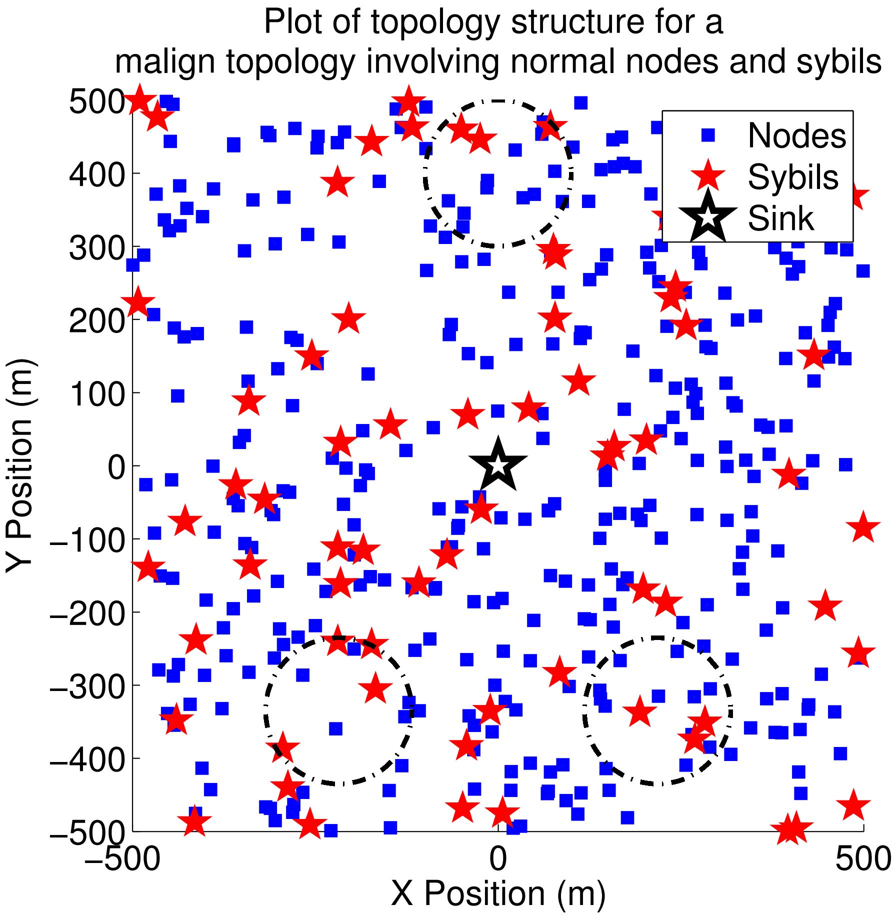

Figure 58: The structure of a standard topology containing malicious sybils

times with additional faked identities, although they fail to make the anticipated contribution to the beamforming transmission. Therefore, as discussed in Section 7.3.1, page 161, the performance of the supernodes around sybils will be lower than anticipated due to the failure of these nodes to fulfil their obligations and contribute to the transmission to the sink.

## 7.7 Results

In this section, results will be presented to examine the performance of PRBR routing in the presence of sybil nodes. The parameters used in the simulations are as presented in Table 5, page 174. The level of instantaneous variation in supernode performance is approximated as a log-normal variable with a standard deviation of $0.6dB$. This corresponds to a figure that arises from oscillator drift of less than 0.5 radians, giving less than 3dB reduction of the beamforming gain in 95% of cases (Section 4.5.2, page 89).

| Symbol | Parameter | Value |
|---|---|---|
| $T$ | Topology ensemble size | 20 |
| $D_P$ | Supernode communication radius | 100m |
| $AG$ | Sink Antenna gain | 40 (dB) |
| $k_{dB}$ | One-metre loss constant | 35 (dB) |
| $\gamma$ | Log-distance rolloff exponent | 4 |
| $K$ | Supernode membership including coordinator | 13 |
| $p$ | Sybil proportion | 2/12 |
| $S_I$ | Sybil total identities | 3 |
| $P_{TX}$ | Max transmission power | 0 (dBW) |
| $Itot_{dBW}$ | Interference/noise floor | -100 (dBW) |
| $SINR_{thresh}$ | Minimal threshold SINR for reception | 4 (dB) |
| $RNK$ | Reputation null constant | 100 |
| $D_f$ | Reputation decay factor | 0.99 |
| $P_{BEST}$ | Best supernode reputation reward proportion | 0.3 |

Table 5: Simulation parameters for topology and routing protocol

Figure 59, page 175 shows the progression over time of the supernode SINR, generated by recording the SINR per route request across an ensemble of uniform random topologies. The results are presented as cumulative distribution functions. The packets delivered by conventional multihop routing receive a nominal SINR of $SINR_{cutoff} = 4dB$. The initialisation state of PRBR and its early route discovery is represented by the series for route requests 1-10. At this point, the median SINR is only slightly above the minimal routing, with approximately 30% of traffic delivered by supernodes in SINR under 4dB. Approximately 15% of traffic is delivered by multihop routing, which can be seen from the vertical rise in sudden jump illustrated at 4dB in the series for route requests 1-10.

The next CDF series shows that by route requests 90 to 100, approximately 70% of the requests are being delivered by the high performance supernodes (achieving SINR of 8dB or above). Less than 25% of routes are using the supernodes with SINR less than $SINR_{cutoff}$. The absence of any vertical rise at 4dB indicates that multihop routing has been replaced entirely by supernode delivery. This illustrates the rapid convergence of the algorithm towards higher performance supernodes over the first hundred route requests.

The simulation was continued for longer in order to investigate the long-term behaviour, to discover whether further performance improvements occur. The increasing closeness of the CDF series indicates that as the system converges towards higher performance, further improvements are achieved more slowly. One interesting aspect is in the presence of a small vertical step at 4dB between route requests 290 to

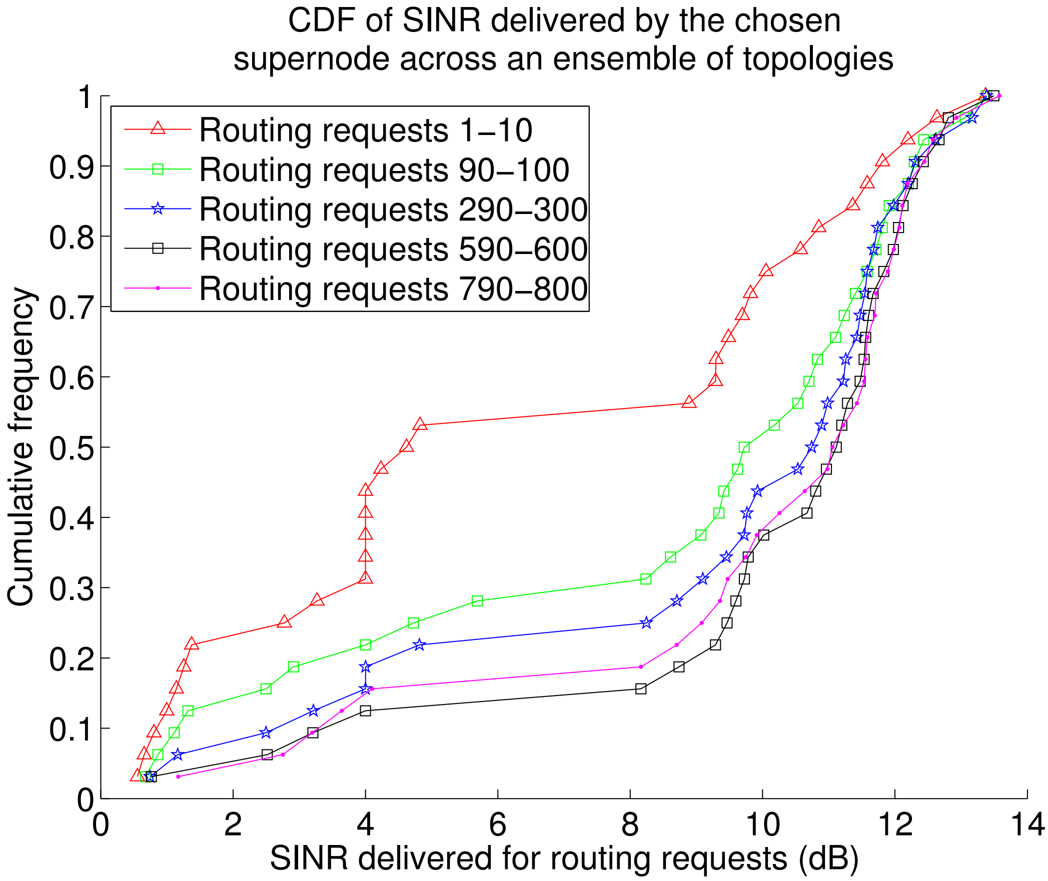

Figure 59: Simulated SINR for an ensemble of topologies in the presence of sybil nodes

300. This indicates that the algorithm's exploration has resorted to multihop routing instead of using one of the lower performance supernodes. This routing decision is temporary however, since the vertical step disappears in the next CDF series.

By route requests 590-600, only around 10% of transmissions are still made by poor performing supernodes. One aspect that explains this is the exploration inherent in the algorithm, via the decay applied to the reputation levels. The expiry of reputation creates a pressure to retest supernodes to discover if performance improvement has occurred. In some cases this continuous expiration leads to temporary minor reductions in performance. This is illustrated in the CDF series for route 790-800. Although the distribution is unchanged from the series for 590-600 above the median, the lower quartile exhibits a minor reduction in performance due to these exploratory decisions.

Figure 60, page 177 displays the proportion of supernode routed traffic carried over supernodes with certain characteristics. These results are taken at the end of simulation over an ensemble of 20 topologies, and disregard any data that was transmitted over multihop routing. Figure 60a, page 177 demonstrates that PRBR shows a strong preference for the best performing supernodes for relaying. The best performing supernodes with SINR in the range of 11 to 14dB typically receive over 40% of the network traffic. By contrast, the supernodes which produce less than 4dB gain typically carry less than 25% of network traffic. The notable outliers on the left (delivering high proportions with performance under 4dB) arise from cases in which topology characteristics of that uniform random topology left only the poor performing supernode viable. Figure 60b, page 177 demonstrates PRBR's avoidance of sybil nodes, by illustrating the relationship between sybil count in a supernode and the traffic using it. Sybil-free supernodes are carrying from 44% to 79% of the network traffic to which they are exposed. The tendency visible from the scatter plot is a reduction in traffic carried with increasing sybil count. The variability is quite high since often topologies have multiple good candidate supernodes, and therefore traffic from these supernodes is divided amongst them.

The scatter plot demonstrates that when four sybils are clustered in a region, the eventual proportion of traffic using each of them is less than 30%. This typically encompasses the nodes close to that particular supernode, together with other nodes experimentally testing it to discover if any performance change has occurred. These results show PRBR shows a strong incentive for sybil avoidance in cases in which multiple sybils are clustered together sufficiently to impair the SINR produced by supernodes.

## 7.8 Implementation Issues

One positive aspect of PRBR is that no specific complexity is added to sensor node behaviour, beyond the computation of reputation metrics. In comparison to the use of distributed decision protocols for sybil detection, this protocol provides sybil avoidance through the routing process. The particularly troublesome case is the existence of multiple sybil nodes in a region, given that the more sybils exist, the more of a potential threat they pose, given their ability to compromise distributed protocols increases as they are clustered more densely in a region. If clusters of sybils exist around a beamforming supernode, then PRBR is capable of reducing their exposure to traffic. Although it does not provide complete rejection of the sybils, it serves to limit the influence of these attacking nodes on the network, by reduction of the level of traffic to which they are exposed.

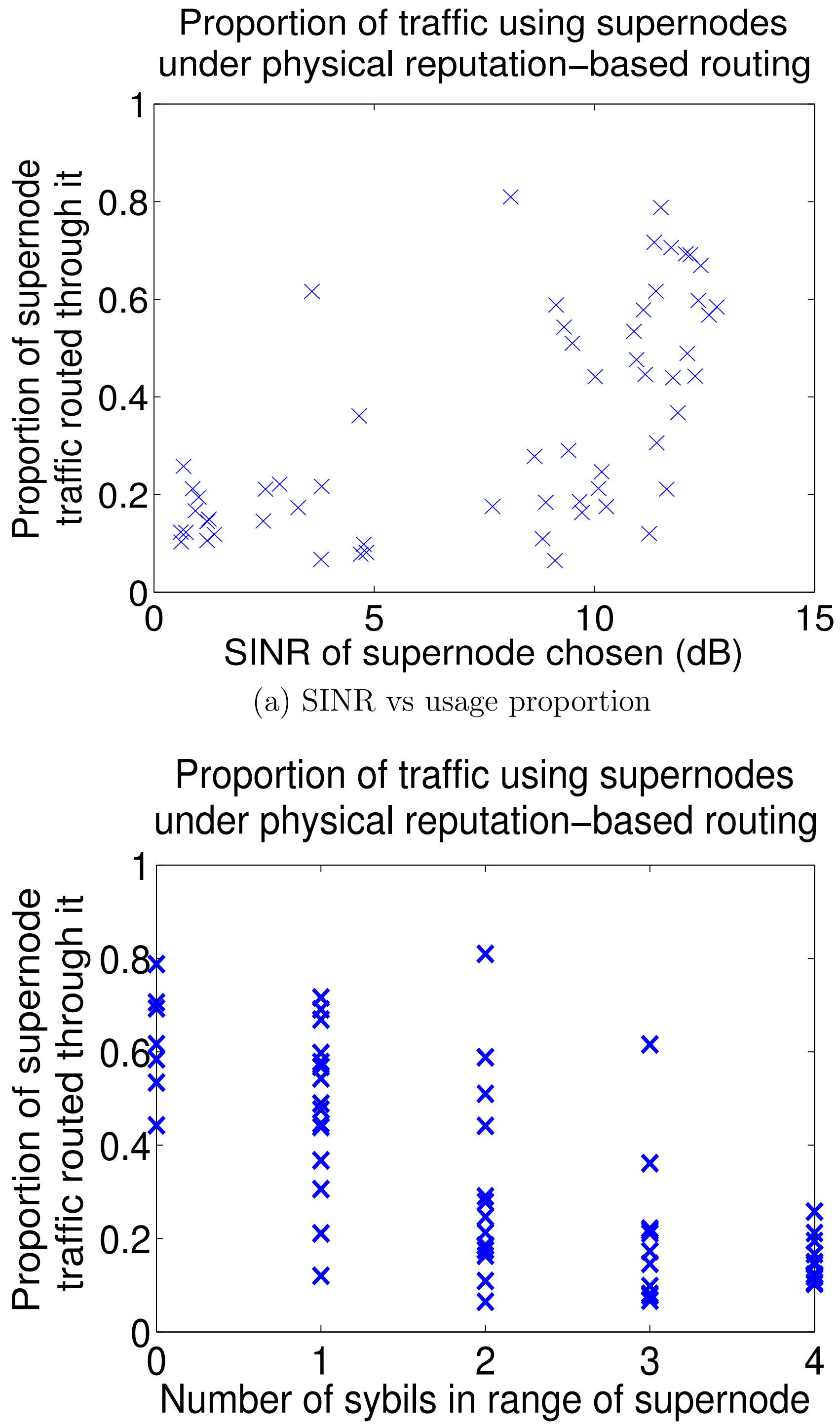

(a) SINR vs usage proportion

(b) Sybil count vs usage proportion

Figure 60: Supernode proportions used by reputation-based routing

In addition to its requirements under the beamforming protocol as described in Section 4.5.3, page 90, the sink is required to determine the SINR of the combined signal received. This can be done via mechanisms such as energy detection or waveform detection [111] with a known preamble on the beamformed packets.

It is possible to envisage extension of the protocol to multiple sinks. A mechanism would be required using fast communication between sinks (via their out-of-system connectivity) to ensure that only one sink replied to a particular route request, and that reply was based on the best $RM$ system-wide at any sink. The $SINR_{min}$ and $SINR_{max}$ parameters, and the historical record of all SINRs would also need to be tracked globally across the network.

## 7.9 Security Issues In PRBR Implementation

In order to protect against fraudulent updates of the reputation values, it is necessary to use a one-way hash chain to protect against forgery of their values, via the process described in Section 3.6.4, page 66. The PRBR-RREP can be authenticated to prove that the sink produced it, and receiving nodes can easily authenticate the reputation updates and discard any updates that appear fraudulent.

## 7.10 Conclusion

This chapter has introduced a modification of reputation-based routing, physical reputation-based routing (PRBR) which incorporates empirical SINR performance characteristics of distributed beamforming clusters (supernodes) used as final-stage relays into the routing process multihop routing network. The protocol has been introduced, its logic, operation procedures and equations presented, together with the presentation of simulation results in a malign topology subject to attack from malicious sybil nodes. The scheme has been demonstrated to avoid the supernodes subject to sybil attack, sending the majority of its traffic through sybil-free supernodes.

It has been demonstrated that the reputation routing strategy has the capability to adapt to specific topologies and their SINR characteristics, discovering with high probability the locations of the best performing supernodes for relaying. The reputation routing protocol is shown to be responsive to the empirical SINR characteristics a particular supernode can deliver, penalising poorly performing supernodes. The system is also shown to be resilient to the presence of sybil nodes, implicitly via their impact on supernode relaying. This is delivered as part of the beamforming without the overheads of additional sybil detection algorithms.

# Chapter 8

# Further Work

## 8.1 Introduction

The previous chapters have presented security techniques intended to defend against single attacks in particular fixed scenarios. For example, disturbance-based routing (Chapter 5) and reputation-based routing (Chapter 6) protocols are designed for scenarios consisting of a single attack (the wormhole attack) and in which multihop routing is used for data transfer. However, in the deployment case studies presented in the Introduction (Chapter 2), it is likely that real-world deployments will be more heterogeneous and include additional complexity. Given the variations in potential attacker motivation and resources, it is likely that the practical attacks introduced will also require more complex adaptive responses.

The challenge for system integrators attempting to secure a WSN is that the advantage frequently lies with the attacker, given the energy economics of a power-limited deployment. In order to disable a network or compromise a security policy focused on availability, the attacker only has to perform one single successful compromise. Adding multiple layers of protection through defence in depth, for example routing away from areas in which threats exist, in addition to running conventional threat detection algorithms (such as the sybil detection algorithms explored in Section 3.3.3, page 53) is one way to reduce the likelihood of such compromises. However, the energy impact of continuously running all the proactive countermeasures that would be required to secure the network against all possible attacks would likely prove prohibitive of both energy and channel capacity, limiting the usage of WSNs in power-limited, security-conscious environments.

This chapter presents further work on developing a system to respond flexibly to attacks, or to combat multiple attacks ongoing contemporaneously within the network. This architecture is termed cognitive security, in which the network shows a holistic, cross-layer awareness of ongoing threats, and can adapt its behaviour and protocol selections in order to cope with dynamically changing threats. This response is provided through observation, decision and action phases which progressively adapt to developing network conditions.

## 8.2 Cognitive Security For Dynamic Optimisation

The previous chapters have considered security techniques which operate in a static scenario and environment, containing implicit assumptions about threats to which the network may be subjected. Although these assumptions are designed to combat standard attacks commonly analysed in the literature, every WSN scenario is unique and therefore so will be the intent and nature of the attack presented. For example, multiple attacks may be combined to attack weak points simultaneously, necessitating a response from multiple protocol layers (such as rerouting, channel changing and then refreshing keys) in order to mitigate the threat successfully. Following the strict layering of the protocol model, a single security-oriented protocol, such as a routing protocol, would not have the authority to order the discarding of current keys in response to anomalous behaviour.

This section presents an implicitly cross-layer security architecture in which nodes attempt to understand their security environment, and considers its application to mitigate attacks using the defensive techniques explored within the Literature Review (Chapter 3) and the novel techniques developed within this thesis.

### 8.2.1 Cognitive Security Architecture

#### 8.2.1.1 Introduction and Motivation

The architecture proposed for a cognitive security system is shown in Figure 61, page 181. This architecture assumes a cross-layer security module operating continuously or periodically upon each individual network node, taking local decisions to optimise

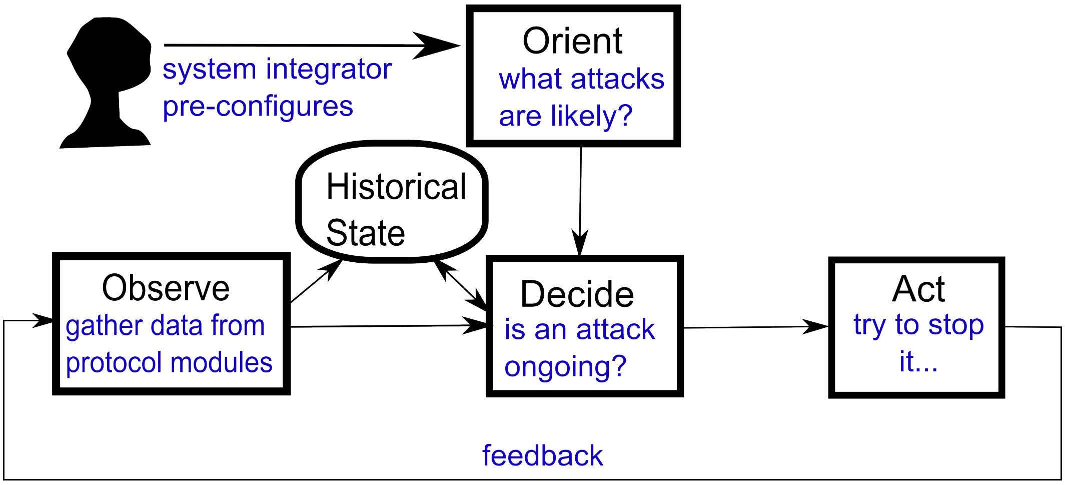

Figure 61: The structure of the architecture for cognitive security

the security situation (although collaborative decisions are also permitted). Its intention can be defined by analogy to cognitive radio [112]. Cognitive radio seeks to obtain an awareness of the spectral situation and utilise currently free spectral holes in order to make the most effective use of available capacity. By analogy, cognitive security seeks to comprehend the threat environment and respond to changing conditions to best uphold a given security policy. The basic structure of a cognitive security architecture is modelled upon the military concept of an OODA loop and its constituent phases of activity: *observe, orient, decide, action.* This concept originated in military analysis, and is intended to deepen analysis of the thought processes of an adversary, and thus obtain a tactical advantage. The loop operates continuously as a security module upon individual nodes, except for the orientation phase, which in cognitive security is supplied upon system initialisation by the deployment authority. The system uses feedback, in which the actions performed influence the environment and therefore the future observations and decisions of the current node and other nodes. The phases of the OODA loop are described in detail in Section 8.2.2, page 182, and summarised below:

- Observe: examine behaviour at all layers of protocol stack
- Orient: using prior knowledge of deployment environment and normal protocol conditions
- Decide: is an attack anticipated or currently ongoing?
- Action: engage a countermeasure or countermeasures to defend against potential attack

The primary advantage cognitive security offers is the potential for flexible and energy-efficient responses to an evolving threat. The solutions focused upon in the Literature Review concentrate upon the solution of a unique threat normally by the addition of inter-node communication (such as packet leashing to combat the wormhole attack in Section 3.5.1, page 57), or by encryption in network security architectures such as TinySec (Section 3.10.3, page 72). However, the energy burden of running defensive techniques continuously during network operation may only be acceptable in a network designed for the highest threat levels.

Therefore, in conventional security engineering in a resource-constrained environment the advantage lies with the attacker, who only has to find a single unhandled vulnerability to defeat the security policy. The flexible responses enabled by cognitive security techniques instead allow a WSN system to increase its level of paranoia and therefore activate increasing levels of countermeasures in response to potential attack. One example, considering the dynamic disturbance-based routing protocols of Section 5.3.1.2, page 117, involves activating conventional wormhole detection approaches in a region once the shortest path activity factor (SPAF) at a node crosses a given threshold indicating a potential wormhole. This approach is capable of both extending network lifetime by avoiding unnecessary countermeasures during network operation, while assisting with quicker detection and isolation of the wormhole endpoints. Specific case studies indicating how the cognitive security architecture would operate in the presence of specific threats will be explored later in Section 8.3, page 185. The nature of the phases of operation of the OODA loop will now be examined.

## 8.2.2 Cognitive Security Phases and Processes

### 8.2.2.1 Observation Phase

Following the implicitly cross-layer nature of cognitive security, the observation phase involves the collection of data potentially relevant to security from all layers of the protocol stack. The data collected depends on the application requirements and anticipated attacks, but may potentially include:

- Measured interference levels and SINR of previous packets

- Collision rates over time and timing irregularities, ACK failures
- Route lifetime, route refreshing rates, local routing tables contents
- Rekeying or key refresh events, decryption failures and failure to follow key establishment protocols by peer nodes
- Metrics values for disturbance-based routing e.g. $SPAF$ or reputation-based routing $RLEVEL$ values
- Application data traffic timing

This data is assumed to be obtained by querying interfaces available within individual protocol layers, which may necessitate modifying them for cross-layer use to expose the needed function calls. The node operating system is presumed to grant sufficient privileges to the cognitive security engine that it can obtain this data on demand. Once data is collected, it is timestamped and stored so that later decisions can be made based upon these historical values, or by comparison of historical values to current ones to detect relative changes.

#### 8.2.2.2 Orientation Phase

In order to make security decisions, the engine must have a model of behaviour that constitutes potential attacks, and such a model must be sufficiently mature and discriminating to be able to respond to transient failures brought about during deployment. Such a model constitutes an orientation for the cognitive security engine, providing a context within which its decisions are made. The orientation phase provides this context.

In human military application of the OODA loop, the orientation phase proceeds from the implicit knowledge and intuition of the entity making the decision. However, requiring the engine to form or infer this model entirely locally from observed behaviour without guidance from system developers and integrators aware of its environment and the complexities of deployment would likely lead to a brittle system which is not robust against any unexpected changes in its environment. This arises as attacks generally have subtle and sometimes counter-intuitive consequences which are difficult to locally detect. For example, the wormhole attack proceeds through an attacker adding a heterogeneous link which is later severed. This wormhole link delivers a benefit to the network in its initial phases, and any system that rejected new links as potential threats would likely reject new links that became available as a result of network or topology change.

As a result, the orientation phase of the cognitive security model proposed here utilises prior human comprehension of the network and attacker motivations in its definition of attacks. This orientation is provided in the form of several decision rules supplied in advance to the cognitive security engine, before or during deployment. The orientation comprises a characterisation of attacks, the network behaviours and activities that constitute attacks in progress, and the countermeasures that are appropriate for them.

#### 8.2.2.3 Decision Phase

The decision phase executes logical rules to determine whether any aspect of current behaviour indicates an attack is ongoing, and if so, the countermeasures to activate to defend against the attack. This is done by interpreting data gathered from observation within the context of the supplied orientation. The decisions are therefore the link between observation and action.

The decision phase can be modelled as the sequential processing of a number of rules, each of which contains a trigger condition, and a set of associated actions. The trigger condition of each rule is tested against the current observations and historical state, and if it evaluates to true, the associated actions given in the rule are invoked. An example rule is presented in Figure 62, page 185 which presents a rule to assist with interference avoidance. It changes the channel used for communication when the current state (the last interference level) or the past link layer status (historical state) indicates delivery failure. It also manipulates a state variable for paranoia, increasing it to represent an occurrence that represents a potential threat (interference that may represent an ongoing jamming attack).

It is anticipated that the decision rules will not be hard-coded as compiled code within the cognitive security engine but programmed as bytecode for evaluation using some form of lightweight interpreter. The advantage of this is to allow flexibility for learning and rule modification in future cognitive security research, as discussed in Section 8.4.3, page 191.

```
R1: change channel on interference
Trigger: ((phy_interference ()) > MAX_THRESHOLD)
         or (last_ack_status == FAILED)
Actions:
   engage_action PHY_SWITCH_CHANNEL;
   paranoia = paranoia + 0.1;
```

Figure 62: Pseudocode for a sample cognitive security rule for responding to interference

#### 8.2.2.4 Action Phase

The action phase of the cognitive security engine engages any countermeasures selected by the decision phase. Actions consist of operations performed upon a particular protocol layer or system component. Potential actions that could be productive as countermeasures include route refreshing to route around compromised regions of the topology, shifting to a different physical layer channel, or launching a sybil node detection process such as radio resource testing (Section 3.3.3.2, page 54). Actions can also be taken at the operating system level, such as switching protocols entirely, for example replacing supernode data delivery with multihop routing or vice versa.

Actions consist of operations performed upon a particular protocol layer or system component, such as route refreshing to use a different region of the topology, or the selective activation of entire protocol modules. This provides, for example, the ability to transition from multihop to supernode data delivery upon the detection of a wormhole attack. Since they are triggered upon different protocol layers, these actions proceed asynchronously. For example, if rerouting is requested, other security engine actions and protocol functions can proceed in parallel while this process is performed at the routing level.

## 8.3 Case Studies For Cognitive Security

### 8.3.1 Jamming Detection

An example case study for cognitive security in the avoidance of intermittent signal jamming attacks in a multi-channel scenario is illustrated in Figure 64, page 187.

Originally the situation is as depicted in Figure 63a, page 186, with the presence of a malicious intermittent jammer around an active route. Following the operation of the cognitive security engine and the execution of associated rules, an alternative route is formed to avoid the jammer as depicted in Figure 63b.

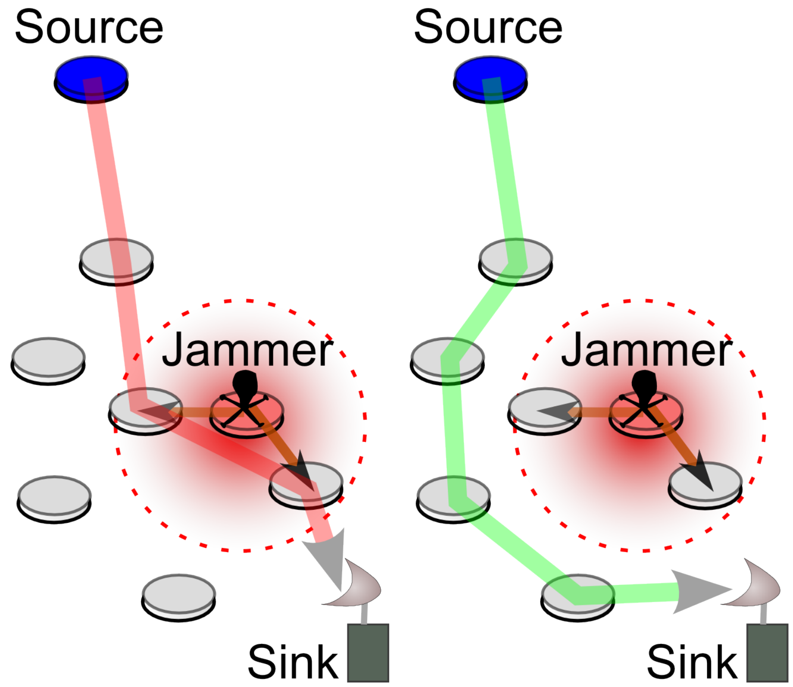

(a) Jamming scenario at start (b) Jamming scenario after rule J3

Figure 63: Cognitive security routing around a malicious jammer

Four cognitive security rules are provided to mitigate the jamming attack: J1, J2, J3 and J4, presented in Section 64, page 187. The first rule J1 is triggered by observations of physical layer parameters, namely the physical interference level recorded during the last packet, or the acknowledgement status of the last packet. If the interference level is excessive, or an acknowledgement was not received, then J1 is activated. The action associated increased the paranoia level.

Rule J2 is activated when the paranoia level rises, that is, when a significant number of interference events have occurred. The action associated with this rule changes the channel used in the region (following the MAC protocol to request access upon the new channel and notify the surrounding nodes as normal). The intent of this rule is to improve performance in the presence of transient non-malicious interference, or to avoid a narrowband jammer.

```
J1: change channel on interference
Trigger: ((phy_interference ()) > MAX_THRESHOLD)
         or (mac_ack_status == FAILED)
Actions:
   paranoia = paranoia + 0.1;

J2: switch to a different channel
Trigger: (paranoia > CHANGE_THRESHOLD)
Actions:
   engage_action PHY_SWITCH_CHANNEL;

J3: engage cross-layer responses
Trigger: (paranoia > DANGER_THRESHOLD)
Actions:
   engage_action SEC_REFRESH_KEYS;
   engage_action REROUTE_EXCLUDE(current_node);

J4: become less paranoid over time
Trigger: Periodic
Actions:
   paranoia = paranoia * FORGET_FACTOR;
```

Figure 64: Cognitive security for jamming detection

Rule J3 is activated when the paranoia level crosses the next threshold, indicating that jamming is likely or communications are otherwise disrupted. It triggers two cross-layer countermeasures, firstly requesting the refreshing of keys in the region. Given the likely presence of malicious nodes in a region, keys should be discarded and regenerated, in case existing keys have been compromised or intercepted by the malicious attackers. The second countermeasure is a routing layer response, in which the routes crossing this node are refreshed to exclude the present node. The intent of this is to exclude the node suffering intermittent jamming from data distribution. Therefore traffic is directed away from this node, and towards safer areas of the network. If system integrators wished to increase the paranoia of the system, this approach could be extended to isolate the node and all its peers from routing, or, if geographic information is available, to isolate an entire region from routing temporarily or permanently.

Rule J4 is a rule to maintain security state, which decreases paranoia over time. This rule is always triggered periodically. The associated action multiplies the paranoia level by a given forgetting factor, which leads to an exponential decrease in the paranoia level over time. This allows the system to forget isolated suspicious events over time, which is useful as some failures detected during J1 are likely to be transient interference unrelated to jamming. This rule gives the system more tolerance of sporadic jamming or delivery failures.

### 8.3.2 Sybil Node Detection

The scenario for detection of sybil nodes, and associated rules is presented in Figure 65, page 188. The sybil node detection algorithm operates in a hybrid beamforming network using protocols described in Section 4.5.3, page 90, in which the normal course of action is to use the distributed beamforming supernode to deliver data to the sink (Figure 65a). The outcome of the protocol is depicted in Figure 65b, in which the network falls back to multihop routing when potential sybil nodes are detected in the beamforming cluster. A multihop route has been formed to the sink, and the sybil nodes detected by the coordinator by the execution of the SEC_DETECT_SYBIL action. The rules presented in Figure 66, page 189 are run upon the coordinator of the cluster. Throughout the operation of a beamforming cluster, rule S1 is invoked whenever the SINR reported from the sink is less than some critical threshold. In this case, the first response selected is a physical layer response; changing the channel used for the beamforming transmissions in an attempt

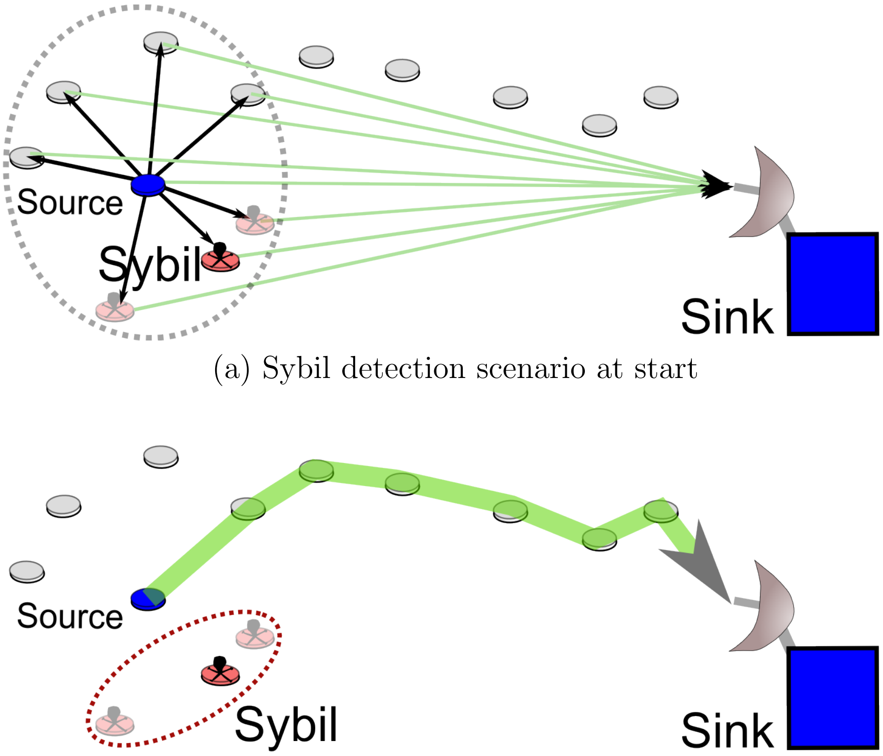

(a) Sybil detection scenario at start

(b) Sybil detection after rule S3

Figure 65: Cognitive security suspending beamforming in the presence of sybil nodes

```
S1: check the SINR on receipt of sink messages
Trigger: ((phy_beamforming_sinr() < MIN_SINR)
Actions:
   engage_action PHY_CHANGE_BEAMFORM_FREQ
   failure_count = failure_count + 1;

S2: begin sybil node detection
Trigger: (failure_count > 3)
Actions:
   engage_action SEC_DETECT_SYBILS;

S3: give up beamforming, switch to multihop
    delivery
Trigger: (failure_count > 10)
Actions:
   engage_action CANCEL_BEAMFORMING;
   engage_action ROUTE_TO(sink_id)
   failure_count = 0;
```

Figure 66: Cognitive security rules for handling sybil nodes in beamforming networks

to improve performance. This also updates a state variable of failure count in order to keep track of how many packets failed in transmission, to use with future rules.

Rule S2 is employed when the number of failures exceeds three. In this case, a sybil detection algorithm such as radio resource testing (Section 3.3.3.2, page 54) is invoked to detect sybils in the region, and exclude them from beamforming. This process may take some time to complete, or may fail to detect the sybils if they mutually vouch for their fake identities. In the meantime, if the number of failures passes 10, then the actions of rule S3 are invoked. These actions perform a protocol switch, replacing beamforming with multihop routing, by cancelling the beamforming process and removing nodes from their responsibilities under it, and forming a multihop route to the sink. In this case study the cognitive security engine has acted not just to increase security but also system performance, by switching to a fallback protocol after the repeated failure of data delivery.

## 8.4 Research Issues To Investigate For Cognitive Security

The architecture as presented in the previous section is capable of solving security issues according to the fixed rules provided in the orientation. However there are several interesting areas for research on this topic which offer the potential for productive future work. This section defines four particular areas: varying the rules assigned to particular nodes, employing collaboration and joint detection, allowing nodes to learn and modify their own rules in response to changes in circumstances, and the involvement of human intervention in cognitive security decisions. This section introduces and discusses these research issues.

### 8.4.1 Using Paranoid Versus Tolerant Nodes

In the case studies presented above, the nodes have all operated using a common set of rules, and therefore the behaviour decisions they make will be common. It may be productive to allow some nodes to be more paranoid than others, for example, discarding keys earlier than expected, or otherwise changing their behaviour. One advantage to the use of especially paranoid nodes is that they could serve as sentries to warn others of potential attack earlier than expected. In addition, making a proportion of nodes more tolerant of misbehaviour could allow service to continue in the presence of normal non-malicious failures, which paranoid nodes could reject as evidence of an attack.

### 8.4.2 Collaboration Between Nodes

The present architecture for cognitive security makes its decisions entirely based upon local information, which is a low overhead strategy that does not impose any distributed communication requirements. By making security decisions locally, it is also secure against bad-mouthing in which nodes fraudulently claim their neighbours are malicious. However, it is worth experimenting with adding a level of collaboration between the cognitive security engines of different nodes. In the previous example of using paranoid nodes as well as normal nodes, the paranoid nodes could be used as sentries to warn of potential attacks. Alternatively, allowing nodes to collaborate over longer distances, and share metrics or other local information, could allow earlier detection of topology distortion attacks such as the wormhole attack.

### 8.4.3 Self-Modification Of Decision Rules

In the examples provided above, the nodes all follow identical rules, supplied as part of the orientation phase. However, it is possible using machine learning techniques for nodes to discover entirely new strategies via their own exploration, in addition to exploiting the results of past successes. One strategy for this is reinforcement learning, in which nodes explore multiple behaviours and keep records of performance. This approach has already been applied to the problem of channel partitioning in the presence of interference [113]. A reinforcement learning security engine would track the performance of possible security strategies and reward those which perform well, for example maintaining continuous delivery, while penalising those approaches that lead to a reductions in performance metrics: for example, additional dropped packets.

Other approaches may permit deeper customisation or more flexibility in node responses. For example, genetic algorithms [114] offer the potential for nodes to explore different sets of cognitive security rules under an evolutionary framework, with incremental modification from previous successful strategies and combination of rules from past successful rule-sets. Over the long term, nodes could evaluate the fitness of their strategies according to predefined security metrics, such as end-to-end delivery rate, and discard strategies that appear to impair performance or security.

Under a genetic algorithm framework for cognitive security, nodes would begin with the decision rules provided by their orientation, but add additional rules to strategies in response to their environment. The original strategies would be allowed to mutate and survive if they prove effective in their environment. For example, one node may decide to change channels periodically, and may retain that rule if it permits it to stay ahead of potential eavesdropping attacks. Alternatively, if a rule that changes in response to interference never provides any benefit against potential jamming, cognitive security engines using a genetic algorithm approach could decide that the jamming suffered is most likely wideband and eventually delete this rule in favour of more direct countermeasures.

The ultimate but ambitious goal of this approach is the development of cognitive security engines that can learn effective responses to novel attacks without human assistance. It is likely however, given that many attacks will be distributed and require global knowledge or widespread communication to detect, that cognitive security research will have to advance incrementally towards this goal.

### 8.4.4 Involvement Of Human Operators

Many sensor networks provide some form of centralised interface upon the sink node to their human operators, such as the vineyard monitoring system example studied in the Introduction (Section 2.2.1.2, page 38). It can be envisaged that metadata on network performance and security will also be highly relevant and of interest to the operators. For example, the network could report its overall energy status and aggregate performance condition, in order to warn its operators of any likely impending failures.

In a similar manner, a cognitive security engine, with its awareness of security-related state from all across the protocol stack, could give information on security status and potential security events to the human operators, and allow them to participate in the decisions. This effectively changes the OODA loop to incorporate human operators in the decision phases as well as orientation. For example, if new nodes are being deployed, then the operators could choose to temporarily override any security-related alerts that may be generated from the topology change. Alternatively, operators could choose to control directly the system's level of paranoia. They may also wish to introduce new decision rules to a subset of nodes, or nodes in certain regions.

## 8.5 Conclusion

In order to implement a high-performance WSN capable of handling the security challenges of the future, it is necessary for the participating nodes to have the advantage over an attacker in terms of energetics. Rather than the network using all countermeasures proactively from the beginning of deployment, cognitive security permits countermeasures to be activated gradually in response to indications that a threat may exist. This permits the more intelligent usage of energy, together with a potential to learn responses and define new decision rules. It also permits the involvement of human operators in security decision making.

Cognitive security presents a future work area for providing flexible and energy-efficient responses to changing threats, and ultimately for allowing networks to develop their own countermeasures to novel threats. This chapter has proposed an architecture for its implementation, case studies to illustrate how such a system would operate and several directions in which research can focus in order to develop the potential of this emerging field.

# Chapter 9

# Conclusion

Wireless sensor networks offer compelling advantages over manual data gathering, presenting new opportunities for economically efficient and high-resolution data gathering. They offer amongst other applications the potential to enable new applications for environmental monitoring, provide high-resolution analysis of scientific phenomena, lower costs in logistical tracking, and provide advance warning for military and border control applications.

However, careful consideration of security threats and potential attacks is required in order to ensure that systems do not exhibit unintended failure modes. In order for public acceptance of WSN deployments not to be hindered by malicious attacks and outside subversion, it is essential to consider the impact of common security threats upon their data relaying methodologies, and to develop defence in depth in which routing technologies assist in avoidance of threats within the network.

The analysis of past deployments in the Introduction (Chapter 2) showed that particular deployments have undergone extensive customisation, with variations in node capabilities and performance. Examples include the use of heterogeneity for the XSS aggregation nodes in the ExScal system (Section 2.2.1.3, page 39), or the backhaul links in the Great Duck Island project (Section 2.2.1.1, page 37). A key characteristic of these deployment examples is that they contain regions or clusters of homogeneous nodes, modifying this model as necessary to meet their application constraints most economically. These deployments have been generally very ad-hoc, and therefore the security analysis must also be tailored to particular applications. The thesis has concentrated upon general attacks as referenced in the literature, as these attacks have been heavily studied by other researchers. However, these attacks and relevant countermeasures have been studied in a variety of representative topologies to examine the impact of topology variation. Accordingly, the results of this thesis provide valuable protocol options to consider in the selection of specific security strategies for a real-world deployment.

The conventional approach to security engineering is to rely upon cryptography for the protection of message confidentiality and integrity. The energy implications of public key cryptography generally render it prohibitive for anything other than bootstrapping other encryption schemes. Lighter weight authentication technologies such as the one-way hash chain provide an economic way for entities to establish longer-lasting, authentic relationships. However, a more serious set of objections to cryptographic schemes is that they cannot protect network availability in the presence of attacks that modify or distort the topology, such as signal jamming or the wormhole attack.

The wormhole attack is a troublesome attack to which multihop wireless networks are vulnerable. In this attack a malicious attacker introduces a pair of nodes with a heterogeneous link that provides a shortcut across the network, and leads to the centralisation of routing around its endpoints. By severing the wormhole link at a convenient time the attacker can abruptly disconnect the network, thus defeating the redundancy expected by routes across a diverse field of multihop nodes. The wormhole attack is most likely to be mounted by an attacker with greater resources, such as heterogeneous antennas and the ability to align them. Wormhole detection in the literature has explored a variety of approaches, such as timing and direction analysis via packet leashing, and central topology reconstruction. However, the difficulties of implementing these in a busy, realistic network motivate an alternative routing strategy.

The thesis provides two alternative mechanisms for routing-layer avoidance of potential wormhole attacks, introducing the static and dynamic disturbance-based routing protocols. Disturbance-based routing provides a complement to the direct wormhole detection techniques analysed in the Literature Review. In the conventional passive wormhole attack, the static disturbance-based routing protocol can avoid wormholes based on a local topology property, the peer inflation effect, which leads to the creation of a strongly connected region around the endpoints. Dynamic disturbance-based routing by contrast is capable of directing a high proportion of traffic around even wormholes free of this peer inflation effect, deployed upon the edge of the topology. By routing around the suspected threat locations, data is directly along safe routes and therefore less likely to encounter the wormhole threat. The disturbance-based routing strategy is therefore a viable addition to the security options, assisting in delivering the defence-in-depth strategy favoured in security engineering.

In many scenarios, the attacker will take time to analyse the structure of the network and deploy the hardware necessary to launch the wormhole attack. Therefore it can be expected that there will exist a stabilisation interval during which wormhole-free routes can be formed. In this situation, reputation-based routing is a viable alternative, which favours the routes formed early on during network development and provides stability against the topology changes introduced by the wormhole.

Distributed beamforming is a novel technology which offers the potential to greatly increase capacity by avoiding the overheads of multihop routing. By using this distributed physical-layer technology (termed supernodes within the thesis), nodes collaborate with precisely timed simultaneous transmissions that are received constructively by a distant sink node. This beamforming architecture also reduces the requirements of coordination to communicating only with nodes in the local area. This removes the trust requirement implicit in requiring distant nodes to forward data, as required by multihop routing. With the likely evolution of oscillators upon a WSN towards greater phase stability and precision, it offers a potential alternative data relaying mechanism. This thesis has analysed the security performance against signal jamming attacks and found that it offers the potential to increase resilience. In the multihop routing case, a chain of dependencies is created, in which nodes must sequentially forward packets, resulting in vulnerability to jamming around every potential candidate receiver. Since jamming is a low-effort attack, particularly when performed with homogeneous nodes such as the disposable nodes of the network itself, distributed beamforming relaying offers the ability to secure the network against jamming by reducing the total areas of vulnerability in the network.

It is likely that distributed beamforming will be integrated as part of a hybrid approach to support multihop routing, as this approach would only require sporadic beamforming clusters forming to support the general multihop network. In this approach physical-reputation based routing protocols (Chapter 7) can be employed to improve system performance by discovering beamforming clusters with high SINR performance to use for relaying. The PRBR protocol also provides avoidance of regions subject to the sybil attack, in which malicious nodes increase their influence by creating additional false identities. Since beamforming success depends on multiple nodes collaborating successfully, the sybil attack reduces received SINR since the virtual sybil identities cannot participate in simultaneous transmissions. As a result, the PRBR protocol which rewards high SINR supernodes, rapidly converges to avoid supernodes featuring multiple sybil nodes. This sybil avoidance is provided along with the discovery of routes featuring beamforming clusters which will be most robust in the presence of link change. Therefore, the sybil avoidance is delivered alongside a routing feature which improves network performance in the presence of unreliable beamforming clusters. This is in contrast to the other approaches in the literature for sybil detection, such as resource testing which requires the injection of additional traffic, in the form of several iterations with challenge packets in order to detect the malicious nodes.

Although this thesis has explored techniques for securing data delivery within the network, a full security analysis considering the likely motivations and sophistication of any attackers will have to be performed before deployment, taking into account any unique characteristics of the scenario and its intended usage. If the application task depends on distributed agreement or aggregation, a sybil attack is likely. If the attackers are known to have time and resources to activate their own heterogeneous links and control a region of the topology, wormhole attacks are likely within the region they control. Performing a full security analysis allows system integrators to choose the techniques from the thesis to deploy. If a wormhole attack is likely and the attacker is anticipated to have their attack ready and in operation when the network is activated, the best strategy would be a disturbance-based routing protocol. Alternatively, if the network is in a regular topology and will have time to begin operating first and stabilise upon trusted wormhole-free routes, reputation-based routing is the best choice. If the sink antennas are available to support beamforming and nodes are deployed with sufficient density, then PRBR also permits defence against the sybil attack.

As part of this thorough security analysis, the access network through which data leaves the WSN will also be an important consideration before deployment. This thesis has concentrated upon in-network threats affecting the individual wireless nodes, but a more complete denial of service effect could be achieved, for example, by severing or interrupting a wired link connecting the network to the monitoring station. Attacks upon the wireless channel such as signal jamming, and upon the topology such as the wormhole attack, can be mitigated using the techniques provided in this thesis. However, if an attacker can provide their own insider within a monitoring or command centre, or can compromise the access link to the network, then they can disable the system even if the WSN itself is invulnerable to attack. Therefore, best practices of conventional security engineering must be followed, including a consideration of the environment surrounding the WSN and any dependencies it introduces, and an analysis of any threats to which it could be subject.

However thorough the security analysis, it is not possible to anticipate ahead of time precisely which attacks will be launched. The Further Work chapter proposes a remedy in the form of a cognitive security architecture, in which individual nodes scan the network for potential indications of misbehaviour from all layers of the protocol stack. As potential indications of misbehaviour change, indicating the likelihood of attack, nodes engage countermeasures such as changing their data relaying methodology, rerouting or discarding keys, or running the more energy intensive sybil detection and wormhole detection strategies mentioned in the Literature Review. This approach permits some flexibility in the security analysis before deployment, as the network can adapt the countermeasures it employs to spend its scarce energy in regions at which a threat is detected.

Therefore, the content of this thesis makes a valuable contribution to security within WSNs, by providing new approaches that enable defence in depth in the routing layer to protect against wormhole and sybil attacks, and study of the security implications of distributed beamforming technologies. Within the context of an application-specific security analysis, these techniques can form valuable components of the toolbox of a system integrator or security administrator. The Further Work chapter also shows how the presented techniques can be extended as part of an adaptive strategy that integrates them with work by other researchers to meet future evolving threats, and provide a sensor network engineered to meet the complex design challenges of the future.

## 9.1 Novel Contributions

The novel contributions contained in this thesis are summarised below:

### 9.1.1 Supernode and Multihop Routing Vulnerability Analysis

A distributed beamforming (supernode) architecture (Section 4.9, page 101) has been analysed to determine its vulnerability to the deployment of homogeneous distributed signal jammers. The supernode scheme has been shown via simulation and analysis to perform better in the the presence of signal jamming attacks than multihop routing.

### 9.1.2 Disturbance-Based Routing For Wormhole Avoidance

Two novel routing techniques are introduced, static and dynamic disturbance-based routing. Static disturbance-based routing is sensitive to connectivity characteristics, and avoids wormholes as a consequence of the increased connectivity they generate within the network, and by choosing safer edge routes rather than the shortest path in which wormholes are more likely to be deployed. Dynamic disturbance-based routing uses an additional sacrificial route through the shortest path protocol to discover the wormhole and incentivise the dynamic disturbance-based route away from it. These techniques have been shown to route away from wormhole attacks based upon their geometric properties, or by the ongoing traffic patterns that they introduce under a custom dual-routing protocol. The performance of these schemes has been analysed under a variety of representative topologies.

### 9.1.3 Reputation-Based Routing

A novel routing technique, reputation-based routing (RBR) (Section 6.2, page 146) has been introduced. This protocol is suitable for deployment in networks with a regular topology, in which an early stabilisation interval exists before wormhole activation. The protocol logic allows it to successfully avoid wormhole attacks introduced after this stabilisation interval, via its hysteresis which causes it to favour previously established routes for future routing following their expiry. Simulation results have presented favourable avoidance advantage.

### 9.1.4 Physical Reputation-Based Routing

Physical reputation-based routing (PRBR) (Section 7.2, page 159) has been introduced. This protocol integrates with the distributed beamforming (supernode) architecture described in Section 4.5.3, page 90, and directs multihop routing to use the best performing supernodes as the final stage for traffic relaying. This provides a viable approach for avoiding the sybil attack in WSNs, given the reduction in beamforming performance they generate. Simulation results are presented to demonstrate the performance of the PRBR protocol.

# Definitions

**ADV** Avoidance Advantage

**AODV** Ad-Hoc On-Demand Distance Vector

**CBC-MAC** Cipher Block Chaining Message Authentication Code

**CBC** Cipher Block Chaining

**CPU** Central Processing Unit

**DARPA** Defence Advanced Projects Research Agency

**DDHC** Dual Directional Hash Chains

**DDYN** Dynamic disturbance metric

**DID** Defence In Depth

**DSSS** Direct Sequence Spread Spectrum

**DoS** Denial of Service

**ECB** Electronic Code Book

**ECC** Elliptic Curve Cryptography

**GPS** Global Positioning System

**IEEE** Institute of Electrical and Electronics Engineers

**INSENS** Intrusion-Tolerant Routing Protocol For Wireless Sensor Networks

**ISM** Industrial, Scientific and Medical

**JTAG** Joint Test Action Group

**LEAP** Localised Encryption and Authentication Protocol

**MAC** Media Access Control

**MEMS** Micro-Electro-Mechanical Systems

**$\mu$-TESLA** $\mu$-Timed Efficient Stream Loss-Tolerant Authentication

**MoD** Ministry of Defence

**O-QPSK** Offset Quaternary Phase Shift Keying

**OHC** One-Way Hash Chain

**OLSR** Optimised Link State Routing

**OSI** Open System Interconnection

**PIR** Passive Infra Red

**PKI** Public Key Infrastructure

**PRBR-RREP** Physical Reputation-Based Routing Route Reply

**PRBR-RREQ** Physical Reputation-Based Routing Route Request

**PRBR** Physical Reputation-Based Routing

**PSD** Power Spectral Density

**QoS** Quality of Service

**RBR-RREP** Reputation-Based Routing Route Reply

**RBR-RREQ** Reputation-Based Routing Route Request

**RBR** Reputation-Based Routing

**RLEVEL_INC** Reputation Level Increment

**RLEVEL** Reputation Level

**RM** Reputation Metric

**RNK** Reputation Null Constant

**RSA** Rivest, Shamir and Adleman

**RTT** Round Trip Time

**SAM** Statistical Analysis of Multipath

**SDYN** Static disturbance metric

**SECTOR** Secure Tracking of Node Encounters

**SINR** Signal to Interference and Noise Ratio

**SNEP** Sensor Network Encryption Protocol

**SNM** Supernode Members

**SPAF** Shortest Path Activity Factor

**TDMA** Time Division Multiple Access

**TTL** Time To Live

**USB** Universal Serial Bus

**VANET** Vehicular Ad-Hoc Networks

**WSN** Wireless Sensor Network

**XOR** Exclusive OR

**XSM** eXtreme Scale Motes

**XSS** eXtreme Scale Stargate

# Glossary

**ADV - (Avoidance Advantage)** A success metric for wormhole avoidance protocols; the additional proportion of all discovered routes that successfully avoid the wormhole under disturbance-based routing, compared to under shortest path

**AODV - (Ad-Hoc On-Demand Distance Vector)** A well-established and commonly studied reactive routing protocol which can be adapted to use other metrics in addition to shortest path

**CBC-MAC - (Cipher Block Chaining Message Authentication Code)** A way of using the Cipher Block Chaining mode of a fixed-length block cipher in order to compute an integrity protection (MAC) code which depends upon an entire arbitrary-length message

**CBC - (Cipher Block Chaining)** The sequential execution of an encryption algorithm upon separate blocks of a longer message, such that encryption of previous blocks is used as an input to a current block

**CPU - (Central Processing Unit)** The core of a embedded or desktop computer, responsible for computation and interfacing with memory and input/output devices through interrupts and system buses

**DARPA - (Defence Advanced Projects Research Agency)** A US military research agency responsible for some fundamental networking and early sensor network research

**DDHC - (Dual Directional Hash Chains)** A pair of one-way hash chains (OHCs) operated simultaneously in alternative directions, allowing interactions at unique time windows to be established

**DDYN - (Dynamic disturbance metric)** The metric value computed in dynamic disturbance-based routing protocols, calculated from the shortest-path activity factor (SPAF) at the source node and a basis value $\beta$

**DID - (Defence In Depth)** The use of a layered set of independent countermeasures supporting a single system feature, to increase the minimal work the attacker must perform for a successful compromise

**DSSS - (Direct Sequence Spread Spectrum)** A transmission method which increases the transmission rate by using a spreading code, so as to expand the bandwidth of a signal and hide it beneath the noise floor

**DoS - (Denial of Service)** An attack in which a malicious entity attempts to disable a system and remove temporarily or permanently the functionality it provides

**ECB - (Electronic Code Book)** A simple encryption scheme involving the division of a message into fixed-sized blocks which are encrypted independently

**ECC - (Elliptic Curve Cryptography)** A public-key cryptosystem built upon the mathematical entity elliptic curves, which have advantageous properties for energy usage at a low modulus compared to other public-key system

**GPS - (Global Positioning System)** A system for accurate localisation of devices (and accurate time-keeping upon them) supported by satellites

**IEEE - (Institute of Electrical and Electronics Engineers)** A professional organisation responsible, amongst other activities, for engineering research, publication and standardisation

**INSENS - (Intrusion-Tolerant Routing Protocol For Wireless Sensor Networks)** A secure routing protocol built upon proactive link-state routing in which messages are authenticated by one-way hash chains and the topology centrally computed

**ISM - (Industrial, Scientific and Medical)** Radio transmission bands allowing license-free operation commonly employed in wireless sensor and ad-hoc network research

**JTAG - (Joint Test Action Group)** A standardised approach for in-circuit debugging of electronic systems with embedded processors or microcontrollers

**LEAP - (Localised Encryption and Authentication Protocol)** A key management architecture which features a hierarchy with multiple keys at different geographic levels

**MAC - (Media Access Control)** A sub-task of the data link layer in the OSI model, which involves managing access to a shared communications medium by multiple devices

**MEMS - (Micro-Electro-Mechanical Systems)** A micro-scale technology for extremely small physical technology such as sensors and actuators, which can be used in developing extremely small sensor nodes

**$\mu$-TESLA - ($\mu$-Timed Efficient Stream Loss-Tolerant Authentication)** A lightweight protocol which allows multicast streams to be delivered, for example from the sink to all nodes

**MoD - (Ministry of Defence)** The UK body for military strategy development, forces management, resource allocation and technology development

**O-QPSK - (Offset Quaternary Phase Shift Keying)** A modulation scheme providing two bits per symbol, in which the constellation points are rotated $\pi/2$ radians from standard QPSK

**OHC - (One-Way Hash Chain)** A lightweight scheme for authentication based upon a hash function, allowing an entity such as a sink to prove itself as authentic by releasing values that hash to a pre-released value

**OLSR - (Optimised Link State Routing)** A routing protocol which continuously scans adjacent peers for link connectivity and propagates this link information throughout the topology to allow routing

**OSI - (Open System Interconnection)** A model for characterising communication in terms of a hierarchy of abstract layers, communicating with their adjacent neighbours to separate protocol functions

**PIR - (Passive Infra Red)** A sensory device which detects heat emissions from an object in its field of view

**PKI - (Public Key Infrastructure)** Security architectures involving public-key cipher schemes and associated key establishment and management operations

**PRBR-RREP - (Physical Reputation-Based Routing Route Reply)** The response packet sent from the sink to the nodes along the reverse direction of the best candidate route

**PRBR-RREQ - (Physical Reputation-Based Routing Route Request)** The request packet broadcast by nodes to the sink in physical reputation-based routing (PRBR), in order to trigger route formation

**PRBR - (Physical Reputation-Based Routing)** A reputation-based routing approach covered in Chapter 7 which is sensitive to physical-layer SINR of relaying beamforming supernodes and thus avoids sybil attacks

**PSD - (Power Spectral Density)** The density of instantaneous energy in the frequency domain, used in spectral analysis of a signal

**QoS - (Quality of Service)** A characteristic of communication systems regarding guarantees of a certain level of performance, for example limits to latency (transmission time) or bandwidth demand

**RBR-RREP - (Reputation-Based Routing Route Reply)** The response packet sent from the sink to the nodes along the reverse direction of the best candidate route

**RBR-RREQ - (Reputation-Based Routing Route Request)** The request packet broadcast by nodes to the sink in reputation-based routing (PRBR), in order to trigger route formation

**RBR - (Reputation-Based Routing)** A reputation-based routing approach which is suitable for the avoidance of late-established wormholes

**RLEVEL_INC - (Reputation Level Increment)** The magnitude of the increment in reputation-based routing (RBR), computed from the bandwidth demand of an individual route and the channel capacity

**RLEVEL - (Reputation Level)** The reputation level recorded in RBR or PRBR and incremented at nodes upon a favourable route to indicate favouring of this node in future

**RM - (Reputation Metric)** The metric value computed logarithmically from the reputation level (RLEVEL) and aggregated along a route to establish its overall quality

**RNK - (Reputation Null Constant)** A constant value for the reputation metric when reputation levels are zero, therefore an initialisation value for the routing metric

**RSA - (Rivest, Shamir and Adleman)** A public key encryption algorithm involving modular exponents, featuring a secret key used for encryption and a public key which can be published

**RTT - (Round Trip Time)** The time taken for a reply to reach a remote endpoint and for a response to be received back from the original recipient

**SAM - (Statistical Analysis of Multipath)** An approach to detect wormholes by the statistical properties of multipath routes formed

**SDYN - (Static disturbance metric)** The metric value computed in static disturbance-based routing from the peer count at the transmitting node, and an exponent $\alpha$

**SECTOR - (Secure Tracking of Node Encounters)** A protocol for tracking node encounters and securely establishing the time of interactions between nodes using hash chains

**SINR - (Signal to Interference and Noise Ratio)** A measure of the strength of the intended signal relative to the combination of interfering signals from other transmitters and environmental radio noise

**SNEP - (Sensor Network Encryption Protocol)** A link-layer protocol for use in sensor networks, deriving separate encryption keys for confidentiality and integrity protection

**SNM - (Supernode Members)** Sensor nodes which participate in distributed beamforming in support of a coordinator which manages the beamforming process

**SPAF - (Shortest Path Activity Factor)** A dynamic parameter for dynamic disturbance-based routing, incremented in response to shortest path traffic passing through this node

**TDMA - (Time Division Multiple Access)** The separation of multiple contenting transmissions into different time allocations (such as slots) to avoid mutual interference from the devices

**TTL - (Time To Live)** A timing countdown applied to network packets to prevent routing loops, decremented at each intermediate forwarding point, and causing packet deletion when it expires

**USB - (Universal Serial Bus)** A standard for serial communication between a host, such as a developer's computer, and several devices, such as sensor nodes or storage devices

**VANET - (Vehicular Ad-Hoc Networks)** Networks comprised of vehicles such as cars and buses, and associated roadside equipment, or using vehicles for the relaying of traffic-related data

**WSN - (Wireless Sensor Network)** A distributed network of sensory and communication nodes, which conventionally have limited energy resources and communicate to perform sensing and relaying of sensed data

**XOR - (Exclusive OR)** A multiple-input boolean logic operation which outputs true if any of its inputs are true, but false if all or none of them are true

**XSM - (eXtreme Scale Motes)** The lowest level individual sensory device in the ExScal (Extreme Scale) wireless sensor network system

**XSS - (eXtreme Scale Stargate)** The aggregation level of the ExScal system, which manages communications from multiple lower-level nodes (XSMs)

# Bibliography

[1] J. Harbin, P. Mitchell, and D. Pearce, *Security Of Self-Organizing Networks: MANET, WSN, WMN, VANET - Secure Routing Architectures Using Cross Layer Information for Attack Avoidance: With Case Study on Wormhole Attacks*, ch. 19, pp. 465–492. Taylor and Francis Group (CRC Press), 1st ed., Dec. 2010.

[2] J. Harbin, P. Mitchell, and D. Pearce, Wireless sensor network wormhole avoidance using disturbance-based routing schemes in *ISWCS 2009: Proceedings of the Sixth International Symposium On Wireless Communication Systems*, (Piscataway, NJ, USA), pp. 76–80, IEEE Press, Sept. 2009.

[3] J. Harbin, P. Mitchell, and D. Pearce, Wireless sensor network wormhole avoidance using reputation-based routing in *ISWCS 2010: Seventh International Symposium on Wireless Communication Systems*, pp. 521 –525, Sept. 2010.

[4] J. Harbin and P. Mitchell, Reputation Routing To Avoid Sybil Attacks In Wireless Sensor Networks Using Distributed Beamforming *ISWCS 2011: Eighth International Symposium on Wireless Communication Systems*, Nov. 2011.

[5] R. Lacoss, Strawman Design of a DSN (Distributed Sensors Networks) to Detect and Track Low Flying Aircraft in *Proceedings of the Distributed Sensor Nets Workshop*, pp. 41–52, Dec. 1978.

[6] H. Abelson, D. Allen, D. Coore, C. Hanson, G. Homsy, J. Thomas F. Knight, R. Nagpal, E. Rauch, G. J. Sussman, and R. Weiss, Amorphous computing *Communications of The ACM*, vol. 43, pp. 74–82, May 2000.

[7] R. Jedermann, C. Behrens, D. Westphal, and W. Lang, Applying autonomous sensor systems in logistics–Combining sensor networks, RFIDs and software agents *Sensors and Actuators A: Physical*, vol. 132, pp. 370–375, Nov. 2006.

[8] L. Schwiebert, S. K. S. Gupta, and J. Weinmann, Research Challenges in Wireless Networks of Biomedical Sensors in *ACM MOBICOM: Proceedings of the Seventh Annual International Conference on Mobile Computing and Networking*, pp. 151–165, ACM, July 2001.

[9] W. Hu, N. Bulusu, C. T. Chou, S. Jha, A. Taylor, and V. N. Tran, Design and evaluation of a hybrid sensor network for cane toad monitoring *TOSN: ACM Transactions on Sensor Networks*, vol. 5, pp. 4:1–4:28, Feb. 2009.

[10] A. Mainwaring, D. Culler, J. Polastre, R. Szewczyk, and J. Anderson, Wireless sensor networks for habitat monitoring in *WSNA '02: 1st ACM International Workshop On Wireless Sensor Networks and Applications*, (New York, NY, USA), pp. 88–97, ACM, 2002.

[11] S. H. Lee, S. Lee, H. Song, and H. S. Lee, Wireless sensor network design for tactical military applications: Remote large-scale environments in *MILCOM 2009: IEEE Military Communications Conference*, pp. 1–7, IEEE, Oct. 2009.

[12] G. Simon, M. Maroti, A. Ledeczi, G. Balogh, B. Kusy, A. Nadas, G. Pap, J. Sallai, and K. Frampton, Sensor network-based countersniper system in *SenSys 2004: Proceedings of the 2nd International Conference on Embedded Networked Sensor Systems*, (New York, NY, USA), pp. 1–12, ACM, Nov. 2004.

[13] I. Akyildiz, W. Su, Y. Sankarasubramaniam, and E. Cayirci, A survey on sensor networks *IEEE Communications Magazine*, vol. 40, pp. 102–114, Aug. 2002.

[14] J. Yick, B. Mukherjee, and D. Ghosal, Wireless sensor network survey *Computer Networks*, vol. 52, no. 12, pp. 2292–2330, 2008. Elsevier B.V.

[15] K. Romer and F. Mattern, The design space of wireless sensor networks *IEEE Wireless Communications*, vol. 11, pp. 54–61, Dec. 2004.

[16] J. Hill, M. Horton, R. Kling, and L. Krishnamurthy, The platforms enabling wireless sensor networks *Communications of the ACM*, vol. 47, pp. 41–46, June 2004.

[17] M. Yarvis, N. Kushalnagar, H. Singh, A. Rangarajan, Y. Liu, and S. Singh, Exploiting heterogeneity in sensor networks *IEEE INFOCOM: 24th Annual Joint Conference of the IEEE Computer and Communications Societies*, vol. 2, pp. 878–890, Mar. 2005.

[18] R. Stoleru, J. A. Stankovic, and S. H. Son, Robust node localization for wireless sensor networks in *EmNets '07: Proceedings of the 4th Workshop on Embedded Networked Sensors*, (New York, NY, USA), pp. 48–52, ACM, 2007.

[19] E. Gaura, L. Girod, J. Brusey, M. Allen, and G. Challen, *Wireless Sensor Networks: Deployments and Design Frameworks.* 236 Gray's Inn Road, Floor 6, London, WC1X 8HB, UK: Springer Verlag, first ed., 2010.

[20] G. E. Moore, Cramming more components onto integrated circuits *Electronics Magazine*, vol. 8, Apr. 1965.

[21] S. Borkar, Getting Gigascale Chips: Challenges and Opportunities in Continuing Moore's Law *ACM Queue*, vol. 1, pp. 26–33, Oct. 2003.

[22] F. Sebastiano, L. J. Breems, K. Makinwa, S. Drago, D. Leenaerts, and B. Nauta, A low-voltage mobility-based frequency reference for crystal-less ULP radios *IEEE Journal of Solid-State Circuits*, vol. 44, pp. 2002–2009, July 2009.

[23] "Mica2 wireless measurement system datasheet." `http://bullseye.xbow.com:81/Products/Product_pdf_files/Wireless_pdf/MICA2_Datasheet.pdf`, Crossbow Technology, Inc., 2005. Doc No 6020-0042-08 Rev A.

[24] "Micaz wireless measurement system datasheet." `http://bullseye.xbow.com:81/Products/Product_pdf_files/Wireless_pdf/MICAz_Datasheet.pdf`, Crossbow Technology, Inc., 2006. Doc No 6020-0060-08 Rev A.

[25] P. Levis, S. R. Madden, J. Polastre, R. Szewczyk, K. Whitehouse, A. Woo, D. Gay, J. Hill, M. Welsh, and E. Brewer, TinyOS: An Operating System for Sensor Networks *Ambient Intelligence*, vol. 35, pp. 115–148, 2005. Springer Verlag.

[26] Wireless medium access control and physical layer specifications for low-rate wireless personal area networks IEEE Standard 802.15.4-2003, IEEE, May 2003.

[27] JN-DS-JN5148-1v6 Data Sheet Tech. Rep. JN-DS-JN5148-1v6, Jennic (NXP Semiconductors), 2010.

[28] M. Gad-el Hak, ed., *The MEMS Handbook.* CRC Press (Taylor and Francis Group), second edition ed., Dec. 2005.

[29] S. Roundy, P. K. Wright, and J. M. Rabaey, *Energy scavenging for wireless sensor networks: with special focus on vibrations.* Springer Netherlands, Nov. 2003.

[30] International Telecommunications Union (ITU-T), *Recommendation X.200 (07/94): Open Systems Interconnection - Basic Reference Model*, July 1994.

[31] I. Demirkol, C. Ersoy, and F. Alagoz, MAC protocols for wireless sensor networks: a survey *IEEE Communications Magazine*, vol. 44, pp. 115–121, Apr. 2006.

[32] J. Hill, R. Szewczyk, A. Woo, S. Hollar, D. Culler, and K. Pister, System architecture directions for networked sensors *ACM SIGPLAN Notices*, vol. 35, pp. 93–104, Nov. 2000.

[33] P. Gupta and P. R. Kumar, The capacity of wireless networks *IEEE Transactions on Information Theory*, vol. 46, pp. 388–404, Mar. 2000.

[34] T. Melodia, M. Vuran, and D. Pompili, The State of the Art in Cross-Layer Design for Wireless Sensor Networks in *Wireless Systems and Network Architectures in Next Generation Internet* (M. Cesana and L. Fratta, eds.), vol. 3883 of *Lecture Notes in Computer Science*, pp. 78–92, Springer Berlin, 2006.

[35] P. Skraba, H. Aghajan, and A. Bahai, Cross-Layer Optimization for High Density Sensor Networks: Distributed Passive Routing Decisions in *Ad-Hoc, Mobile, and Wireless Networks* (I. Nikolaidis, M. Barbeau, and E. Kranakis, eds.), vol. 3158 of *Lecture Notes in Computer Science*, pp. 630–644, Springer Berlin, 2004.

[36] S. Biswas and R. Morris, ExOR: opportunistic multi-hop routing for wireless networks *SIGCOMM Computer Communications Review*, vol. 35, pp. 133–144, Aug. 2005.

[37] S. Cui, R. Madan, A. Goldsmith, and S. Lall, Joint routing, MAC, and link layer optimization in sensor networks with energy constraints in *ICC 2005: IEEE International Conference on Communications*, vol. 2, pp. 725–729, IEEE, May 2005.

[38] J. Burrell, T. Brooke, and R. Beckwith, Vineyard computing: Sensor networks in agricultural production *IEEE Pervasive Computing*, vol. 3, no. 1, pp. 38–45, 2004.

[39] A. Arora, R. Ramnath, E. Ertin, P. Sinha, S. Bapat, V. Naik, V. Kulathumani, H. Zhang, H. Cao, M. Sridharan, S. Kumar, N. Seddon, C. Anderson, T. Herman, N. Trivedi, C. Zhang, M. Nesterenko, R. Shah, S. Kulkarni, M. Aramugam, L. Wang, M. Gouda, Y.-r. Choi, D. Culler, P. Dutta, C. Sharp, G. Tolle, M. Grimmer, B. Ferriera, and K. Parker, ExScal: Elements of an Extreme Scale Wireless Sensor Network *RTCSA 2005: 11th IEEE International Conference on Embedded and Real-Time Computing Systems and Applications*, vol. 0, pp. 102–108, Aug. 2005.

[40] Y. Choi, M. G. Gouda, H. Zwang, and A. Arora, Routing on a logical grid in sensor networks Tech. Rep. TR-04-49, Computer Science Department, The University of Texas, Austin, Texas USA, 2004.

[41] C. Karlof, N. Sastry, and D. Wagner, TinySec: a link layer security architecture for wireless sensor networks in *SenSys 2004: Proceedings of the 2nd International Conference on Embedded Networked Sensor Systems*, (New York, NY, USA), pp. 162–175, ACM, Nov. 2004.

[42] C. Karlof and D. Wagner, Secure routing in wireless sensor networks: attacks and countermeasures *Ad Hoc Networks*, vol. 1, no. 2-3, pp. 293–315, 2003.

[43] A. Burr, T. Clarke, D. Chen, J. Chen, Y. Deng, D. Grace, B. Han, P. Likitthanasate, Y. Liu, P. Mitchell, D. Pearce, A. Pomfret, and Y. Wang, Cognitive Routing for Tactical Ad Hoc Networks Tech. Rep. UOY/MODCOI/B990/FR/1, UK Ministry of Defence, Sept. 2008.

[44] R. Riem-Vis, Cold Chain Management using an Ultra Low Power Wireless Sensor Network *WAMES: Workshop on Applications of Mobile Embedded Systems*, 2004.

[45] M. Nekovee, Sensor networks on the road: the promises and challenges of vehicular ad hoc networks and grids in *Workshop on Ubiquitous Computing and e-Research*, 2005.

[46] P. Juang, H. Oki, Y. Wang, M. Martonosi, L. S. Peh, and D. Rubenstein, Energy-efficient computing for wildlife tracking: design tradeoffs and early

experiences with ZebraNet *ACM SIGPLAN Notices*, vol. 37, pp. 96–107, Oct. 2002.

[47] R. Anderson, *Security engineering*. Wiley New York, 2001.

[48] M. Stamp, *Information Security: Principles and Practice*, ch. 8, pp. 195–196. John Wiley and Sons, Inc., first ed., 2005.

[49] R. Roman, J. Zhou, and J. Lopez, On the security of wireless sensor networks *Proc. Int. Conference on Computational Science and its Applications (ICCSA 2005), LNCS*, vol. 3482, pp. 681–690, 2005.

[50] B. Randell, P. Lee, and P. C. Treleaven, Reliability Issues in Computing System Design *CSUR: ACM Computing Surveys*, vol. 10, pp. 123–165, June 1978.

[51] J. W. Hui and D. Culler, The dynamic behavior of a data dissemination protocol for network programming at scale in *SenSys 2004: Proceedings of the 2nd International Conference on Embedded Networked Sensor Systems*, (New York, NY, USA), pp. 81–94, ACM, Nov. 2004.

[52] N. R. Prasad and M. Alam, Security framework for wireless sensor networks *Wireless Personal Communications*, vol. 37, no. 3, pp. 455–469, 2006. 10.1007/s11277-006-9044-7.

[53] S. Marti, T. J. Giuli, K. Lai, and M. Baker, Mitigating routing misbehavior in mobile ad hoc networks in *ACM MobiCom 2000: Proceedings of the 6th International Conference on Mobile Computing and Networking*, pp. 255–265, ACM, 2000.

[54] J. Clulow and T. Moore, Suicide for the common good: a new strategy for credential revocation in self-organizing systems *ACM SIGOPS Operating Systems Review*, vol. 40, no. 3, pp. 18–21, 2006.

[55] J. Douceur, The Sybil Attack in *Peer-to-Peer Systems* (P. Druschel, F. Kaashoek, and A. Rowstron, eds.), vol. 2429 of *Lecture Notes in Computer Science*, pp. 251–260, Springer Berlin, 2002.

[56] J. Newsome, E. Shi, D. Song, and A. Perrig, The sybil attack in sensor networks: analysis and defenses pp. 259–268, ACM, 2004.

[57] B. N. Levine, C. Shields, and N. B. Margolin, A Survey of Solutions to the Sybil Attack tech report, University of Massachusetts Amherst, MA, 2006.

[58] C. Piro, C. Shields, and B. N. Levine, Detecting the Sybil Attack in Mobile Ad hoc Networks in *IEEE Securecomm: Third International Conference on Security and Workshops*, pp. 1–11, Aug. 2006.

[59] F. Stajano and R. Anderson, The Resurrecting Duckling: Security Issues for Ad-hoc Wireless Networks *IEEE Computer*, vol. 35, no. 4, pp. 22–26, 2002.

[60] Y. C. Hu, A. Perrig, and D. B. Johnson, Packet leashes: a defense against wormhole attacks in wireless networks vol. 3, pp. 1976–1986, Apr. 2003.

[61] D. Liu, P. Ning, A. Liu, C. Wang, and W. K. Du, Attack-Resistant Location Estimation in Wireless Sensor Networks *ACM Transactions on Information and System Security*, vol. 11, pp. 1–39, July 2008.

[62] L. Hu and D. Evans, Using directional antennas to prevent wormhole attacks in *Network and Distributed System Security Symposium (NDSS)*, pp. 131–141, The Internet Society, Feb. 2004.

[63] R. Poovendran and L. Lazos, A graph theoretic framework for preventing the wormhole attack in wireless ad hoc networks *Wireless Networks*, vol. 13, pp. 27–59, Jan. 2007.

[64] W. Wang and B. Bhargava, Visualization of wormholes in sensor networks in *WiSe 2004: Proceedings of the 3rd ACM Workshop on Wireless Security*, pp. 51–60, ACM New York, NY, USA, Oct. 2004.

[65] L. Qian, N. Song, and X. Li, Detection of wormhole attacks in multi-path routed wireless ad hoc networks: a statistical analysis approach *Journal Of Network and Computer Applications*, vol. 30, pp. 308–330, Jan. 2007.

[66] M. A. Gorlatova, M. Kelly, R. Liscano, and P. C. Mason, Enhancing frequency-based wormhole attack detection with novel jitter waveforms in *IEEE Securecomm: Third International Conference on Security and Workshops*, pp. 304–309, Sept. 2007.

[67] P. Jacquet, P. Muhlethaler, T. Clausen, A. Laouiti, A. Qayyum, and L. Viennot, Optimized link state routing protocol for ad hoc networks in *INMIC 2001: IEEE International Multi Topic Conference - Technology for the 21st Century*, pp. 62–68, Dec. 2001.

[68] J. Daemen and V. Rijmen, *The design of Rijndael: AES–the advanced encryption standard.* Springer Verlag, 2002.

[69] Public Key Cryptography Standards (PKCS) No 1 V2.1: RSA CRYPTOGRAPHY STANDARD Standard No 1. V2.1, RSA Data Security Inc, RSA Laboratories, 174 Middlesex Turnpike, Bedford, MA 01730 USA, June 2002.

[70] W. Diffie and M. Hellman, New directions in cryptography in *IEEE Transactions on Information Theory*, vol. 22, pp. 644–654, Nov. 1976.

[71] N. Koblitz, Elliptic curve cryptosystems *Mathematics of Computation*, vol. 48, no. 177, pp. 203–209, 1987.

[72] V. S. Miller, Use of elliptic curves in cryptography *CRYPTO 85 Proceedings: Advances in Cryptology*, pp. 417–426, 1986.

[73] A. Perrig, J. A. Stankovic, and D. Wagner, Security in wireless sensor networks *Communications of the ACM*, vol. 47, no. 6, pp. 53–57, 2004.

[74] A. Perrig, R. Szewczyk, J. Tygar, V. Wen, and D. Culler, SPINS: Security Protocols for Sensor Networks *Wireless Networks*, vol. 8, no. 5, pp. 521–534, 2002.

[75] R. Watro, D. Kong, S.-f. Cuti, C. Gardiner, C. Lynn, and P. Kruus, TinyPK: securing sensor networks with public key technology in *SASN '04: Proceedings of the 2nd ACM workshop on Security of ad hoc and sensor networks*, (New York, NY, USA), pp. 59–64, ACM, 2004.

[76] D. Malan, M. Welsh, and M. Smith, A public-key infrastructure for key distribution in TinyOS based on elliptic curve cryptography *IEEE SECON 2004: First Annual IEEE Communications Society Conference on Sensor and Ad Hoc Communications and Networks.*, pp. 71–80, Oct. 2004.

[77] K. Piotrowski, P. Langendoerfer, and S. Peter, How public key cryptography influences wireless sensor node lifetime in *SASN '06: Proceedings of the fourth ACM workshop on Security of ad hoc and sensor networks*, (New York, NY, USA), pp. 169–176, ACM, 2006.

[78] L. Lamport, Password authentication with insecure communication *Communications of the ACM*, vol. 24, no. 11, pp. 770–772, 1981.

[79] S. Capkun, L. Buttyan, and J.-P. Hubaux, SECTOR: secure tracking of node encounters in multi-hop wireless networks in *SASN '03: Proceedings of the 1st ACM workshop on Security of ad hoc and sensor networks*, (New York, NY, USA), pp. 21–32, ACM, 2003.

[80] Y. Jiang, C. Lin, M. Shi, and X. Shen, Self-healing group key distribution with time-limited node revocation for wireless sensor networks *Ad Hoc Networks*, vol. 5, no. 1, pp. 14–23, 2007.

[81] L. Eschenauer and V. D. Gligor, A key-management scheme for distributed sensor networks in *CCS '02: Proceedings of the 9th ACM conference on Computer and communications security*, (New York, NY, USA), pp. 41–47, ACM, 2002.

[82] S. Zhu, S. Setia, and S. Jajodia, LEAP: efficient security mechanisms for large-scale distributed sensor networks in *CCS '03: Proceedings of the 10th ACM conference on Computer and communications security*, (New York, NY, USA), pp. 62–72, ACM, 2003.

[83] A. Perrig, R. Canetti, J. Tygar, and D. Song, Efficient authentication and signing of multicast streams over lossy channels *IEEE Symposium on Security and Privacy*, vol. 5, 2000.

[84] J. Deng, R. Han, and S. Mishra, INSENS: Intrusion-tolerant routing for wireless sensor networks *Computer Communications*, vol. 29, no. 2, pp. 216–230, 2006.

[85] M. Bellare, J. Kilian, and P. Rogaway, The security of the cipher block chaining message authentication code *Journal of Computer and System Sciences*, vol. 61, pp. 362–399, Dec. 2000.

[86] I. F. Akyildiz, D. Pompili, and T. Melodia, Underwater acoustic sensor networks: research challenges *Ad Hoc networks*, vol. 3, pp. 257–279, May 2005.

[87] B. Warneke, M. Last, B. Liebowitz, and K. Pister, Smart Dust: communicating with a cubic-millimeter computer *IEEE Computer*, vol. 34, pp. 44–51, Jan. 2001.

[88] J. A. Stankovic, Research challenges for wireless sensor networks *ACM SIGBED Review*, vol. 1, pp. 9–12, 2004.

[89] S. Tilak, *Towards A Holistic Approach for Protocol Development in Sensor Networks*. PhD thesis, State University of New York, 2005.

[90] M. Ringwald, K. Romer, and A. Vitaletti, Passive Inspection Of Sensor Networks *Distributed Computing in Sensor Systems*, vol. Lecture Notes In Computer Science, no. 4549, pp. 205–222, 2007.

[91] S. E. Ha, S. Choi, B. Song, and H. S. Lee, A new data propagation scheme for WSN network reprogramming in a noise-full environments in *ICOIN: International Conference on Information Networking*, pp. 547 –552, Jan. 2011.

[92] E. Chailloux, P. Manoury, and B. Pagano, *Developing Applications With Objective Caml.* O'Reilly France, 2000.

[93] T. S. Rappaport, *Wireless Communications: Second Edition*, ch. 4, pp. 120–125. Upper Saddle River, NJ 07458: Prentice Hall PTR, 2002.

[94] T. S. Rappaport, *Wireless communications: Principles and Practice.* Prentice Hall, second ed., Jan. 2002.

[95] A. Martinez-Sala, J. M. Molina-Garcia-Pardo, E. Egea-Lopez, J. Vales-Alonso, L. Juan-Llacer, and J. Garcia-Haro, An Accurate Radio Channel Model for Wireless Sensor Networks Simulation *Journal of Communications and Networks*, vol. 7, Dec. 2005.

[96] T. Moscibroda, R. Wattenhofer, and Y. Weber, Protocol Design Beyond Graph-Based Models *Proceedings of the 5th ACM SIGCOMM Workshop on Hot Topics in Networks (HotNets)*, 2006.

[97] H. Ochiai, P. Mitran, H. V. Poor, and V. Tarokh, Collaborative beamforming for distributed wireless ad hoc sensor networks *IEEE Transactions on Signal Processing*, vol. 53, pp. 4110–4124, Nov. 2005.

[98] R. Mudumbai, D. Brown, U. Madhow, and H. V. Poor, Distributed transmit beamforming: challenges and recent progress *IEEE Communications Magazine*, vol. 47, no. 2, pp. 102–110, 2009.

[99] Energy Savings from Implementing Collaborative Beamforming for a Remote Low Power Wireless Sensor Network in *AusWireless (International conference on Wireless Broadband and Ultra Wideband Communication)*, Mar. 2006.

[100] D. Brown and H. V. Poor, Time-slotted round-trip carrier synchronization for distributed beamforming *IEEE Transactions on Signal Processing*, vol. 56, no. 11, pp. 5630–5643, 2008.

[101] Y. Deng, A. Burr, D. Pearce, and D. Grace, Distributed beamforming for cognitive radio networks in *Third International Conference on Communications and Networking in China - ChinaCom*, pp. 1206–1210, Nov. 2008.

[102] Y.-S. Tu and G. J. Pottie, Coherent cooperative transmission from multiple adjacent antennas to a distant stationary antenna through AWGN channels in *VTC 2002: IEEE 55th Vehicular Technology Conference*, vol. 1, pp. 130 – 134, Aug. 2002.

[103] I. Brown, D.R., G. B. Prince, and J. A. McNeill, A method for carrier frequency and phase synchronization of two autonomous cooperative transmitters in *IEEE 6th Workshop on Signal Processing Advances in Wireless Communications*, pp. 260 – 264, June 2005.

[104] W. B. Heinzelman, A. P. Chandrakasan, and H. Balakrishnan, An application-specific protocol architecture for wireless microsensor networks *Wireless Communications, IEEE Transactions on*, vol. 1, pp. 660 – 670, oct 2002.

[105] M. Haenggi, A. I. Reuther, J. I. Goodman, D. R. Martinez, A. Boulis, B. Warneke, A. E. Kamal, J. N. Al-Karaki, A. Loutfi, and P. Wide, *Handbook of Sensor Networks: Compact Wireless and Wired Sensing Systems*, p. 308. CRC Press, Florida, 2005.

[106] S. Meguerdichian, F. Koushanfar, M. Potkonjak, and M. B. Srivastava, Coverage problems in wireless ad-hoc sensor networks in *INFOCOM 2001. Twentieth Annual Joint Conference of the IEEE Computer and Communications Societies. Proceedings. IEEE*, vol. 3, pp. 1380 –1387 vol.3, 2001.

[107] H. M. Ammari and S. K. Das, Integrated Coverage and Connectivity in Wireless Sensor Networks: A Two-Dimensional Percolation Problem *IEEE Transactions on Computers*, vol. 57, pp. 1423–1434, 2008.

[108] K. Chakrabarty, S. S. Iyengar, H. Qi, and E. Cho, Grid coverage for surveillance and target location in distributed sensor networks *Computers, IEEE Transactions on*, vol. 51, pp. 1448 – 1453, December 2002.

[109] C. Perkins and E. M. Royer, Ad-hoc On-Demand Distance Vector (AODV) Routing in *IEEE Workshop on Mobile Computer Systems and Applications*, vol. 100, pp. 90–100, Feb. 1999.

[110] M. Younis, K. Akkaya, M. Eltoweissy, and A. Wadaa, On Handling QoS Traffic in Wireless Sensor Networks vol. 9, (Los Alamitos, CA, USA), pp. 90–95, IEEE Computer Society, 2004.

[111] T. Yucek and H. Arslan, A survey of spectrum sensing algorithms for cognitive radio applications *Communications Surveys and Tutorials, IEEE*, vol. 11, no. 1, pp. 116–130, 2009.

[112] S. Haykin, Cognitive radio: brain-empowered wireless communications *Selected Areas in Communications, IEEE Journal on*, vol. 23, no. 2, pp. 201–220, 2005.

[113] M. Yang and D. Grace, Cognitive radio with reinforcement learning applied to heterogeneous multicast terrestrial communication systems in *Cognitive Radio Oriented Wireless Networks and Communications, 2009. CROWNCOM'09. 4th International Conference on*, pp. 1–6, IEEE, 2009.

[114] D. E. Goldberg, *Genetic algorithms in search, optimization, and machine learning.* Addison-Wesley, Jan. 1989.

# Index